

**Part A. Synthesis of Second generation dillapiol and sesamol analogues;  
inhibition of Cytochrome P450 3A4**

**Part B. Synthesis of analogs of Z02; compounds with potential to help  
regenerate partially severed spinal cords.**

**Vikrant Raina**

Submitted to the Faculty of Science, University of Ottawa,  
in partial fulfillment of the requirements for the M.Sc. Degree in Chemistry

Candidate

Supervisors

---

Vikrant S. Raina

---

Professor Dr. Tony Durst  
Dr. Robert N. Ben

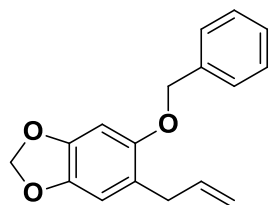
© Vikrant Raina, Ottawa, Canada, 2018

## **Abstract: Synthesis of novel second generation dillapiol and sesamol analogs; inhibition of Cytochrome P450 3A4**

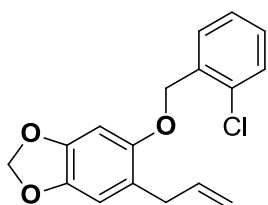
Dillapiol is a naturally occurring methylenedioxyphenyl (MDP) compound that acts as an insecticide synergist comparable in activity to the widely used piperonyl butoxide (PBO). More than thirty synthetic analogs of dillapiol and sesamol were prepared and evaluated for their inhibitory activity in a cloned human Cytochrome P450 3A4 (CYP 3A4) enzyme in order to assess their use as pesticide synergists and to determine the next generation of compounds. These compounds represent a second generation of analogs based on the knowledge gained from compounds prepared and evaluated by a former member of our group.

The choice of new structures was also influenced by the surprising and important observations by Dr. Suqi Liu that compound **21** inhibited not only CYP 3A4 but also glutathione-S- transferase (GST). A set of compounds related to **21** were sent to BASF (Durham NC) for evaluation of their synergistic activity, toxicity and persistence in soil studies. In a number of instances these analogs outperformed PBO as synergists even when given at 1:1 synergist: pesticide ratio compared to PBO at 5:1 when tested against a variety of resistant insects in BASF laboratories in the USA, Holland, India and Indonesia. All of the compounds were shown to be non-toxic to animal life. Their half-life in soils was typically less than 10 days. The results obtained form the basis of two BASF - University of Ottawa patent applications.

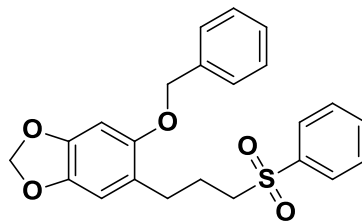
The most potent CYP3A4 inhibitors synthesized as part of this project are the sulfones **15** and **15a**. These compounds are 107 and 71 times more potent than dillapiol, respectively which has an IC<sub>50</sub> of 8.9 ± 0.3 μM. The *ortho*- chlorobenzyl ether **48** was shown to be 74 times more potent than dillapiol.



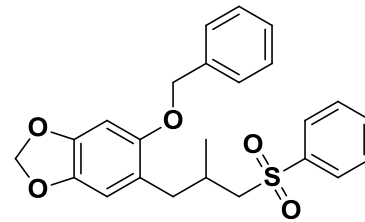
**21**  
1.8  $\mu\text{M}$



**48**  
0.12  $\mu\text{M}$



**15a**  
0.085  $\mu\text{M}$



**15**  
0.13  $\mu\text{M}$

**Abstract: Synthesis of Z02 analogs; compounds with potential to help regenerate partially severed spinal cords**

The synthesis of **Z02** analogs in which the NH and C (O) substituents of the B unit are in the *ortho*-, *meta*- and *para*-orientation compared to the *meta*-orientation of **Z02** is reported. The bioactivities of these compounds were compared with previously synthesized *meta*- substituted analogs to determine which of the three orientations, *ortho*-, *meta*-, or *para*-, resulted in the most potent compounds. In vitro bioassay results obtained by the Brown group allow us to draw conclusions on the effects of the structural characteristics necessary for optimization of activity. Results acquired thus far have suggested that both the *ortho*- or *para*- substituted analogs have reduced activity relative to the *meta*- substituted analogs. Replacement of the oxygen in the CD unit by a sulfoxide and sulfone gave compounds with slightly improved inhibition of SOX9 but with still lower activity relative to **Z02**. The SAR performed in this project did not result in compounds superior to **Z02**. Nevertheless, the results described in this thesis give guidance for future SAR studies. It is recommended that future synthetic efforts be concentrated on the *meta*-oriented analogs.

## Table of Contents

Abstract: Synthesis of dillapiol and sesamol analogs; inhibition of Cytochrome P450 3A4.....	ii
Abstract: Synthesis of Z02 analogs; compounds with potenaital to help regenerate partially severed spinal cords .....	iv
List of Abbreviations .....	vii
List of Figures .....	ix
List of Schemes.....	xi
List of Tables .....	xii
Acknowledgements.....	xiv
1.0 Introduction.....	1
1.1 Pesticides.....	1
1.2 Pesticide synergists and piperonyl butoxide (PBO).....	5
1.3 Dillapiol .....	6
1.4 Dillapiol as a lead compound for the development of pesticide synergists .....	7
1.5 Mechanism of action of insecticide synergists.....	8
1.6 Cytochrome P450 isoenzyme family .....	10
1.7 Inhibition of CYP P450 by Dillapiol .....	11
1.8 Sulfone analogs as CYP 3A4 inhibitors.....	13
1.9 GST assays.....	14
2.0 Objectives .....	17
3.0 Results and Discussion .....	19
3.1 Synthesis of analogs.....	19
3.2 Second generation analogs of 21, requested by BASF .....	24
3.3 Biological evaluation of second generation compounds.....	26
3.4 BASF studies .....	27
3.5 BASF results .....	28

3.6 Determination of CYP3A4 inhibition of additional analogs and other MDP compounds.....	29
3.6.1 CYP3A4 inhibition assay.....	29
3.6.2 Ethers.....	42
3.6.3 Amines and Amides.....	48
3.6.4 Sulfides and Sulfones.....	50
3.6.5 Miscellaneous MDP compounds.....	51
4.0 Conclusions and proposals for additional studies.....	53
5.0 References.....	56
6.0 Introduction.....	59
6.1 Spinal Cord Injury.....	59
6.2 Neuronal Regeneration Inhibition.....	61
6.3 Chondroitin sulfate proteoglycans and regulation pathway.....	62
6.4 SOX9 conditional knockouts improved neurological recovery.....	63
6.5 Z02, a small molecule inhibitor of SOX9.....	68
6.6 Synthesis of Z02.....	70
7.0 Objectives.....	71
8.0 Results and Discussion.....	72
8.1 Retrosynthetic analysis and potential analogs of Z02.....	72
8.2 Synthesis of Z02.....	77
8.3 Ortho and Para substituted analogs.....	87
8.4 Open chain vs cyclic A unit.....	89
8.5 NMR studies.....	91
9.0 Future Directions and Conclusions.....	101
10.0 References.....	102
APPENDIX A: Part A.....	105
APPENDIX B: Part B.....	201

## List of Abbreviations

PBO- Piperonyl Butoxide

CYP3A4- Cytochrome P450 3A4

GI- Gastrointestinal

IC<sub>50</sub>- Half maximal inhibitory concentration

<sup>1</sup>H NMR- Hydrogen-1 nuclear magnetic resonance

<sup>13</sup>C NMR- Carbon-13 nuclear magnetic resonance

C4- Carbon 4

C6- Carbon 6

QSAR- Quantitative structure activity relationship

GST- Glutathione-S-transferase

DEM- diethylmaleate

ECB- European Corn Borer

LD<sub>50</sub>- Lethal Dose, 50%

MDM- Methylenedioxyphenyl

*t*-butyl- *Tert*-butyl

TLC- Thin layer chromatography

UV- Ultraviolet

DCM- Dichloromethane

MeOH- Methanol

SCI – Spinal Cord Injury

CNS – Central Nervous System

CSPGs – Chondroitin Sulfate glycoproteins

GAG – Glycosaminoglycans

XT-I – Xylosyltransferase I

XT-II – Xylosyltransferase II

C4ST– chondroitin 4-sulfotransferase

BMS – Basso Mouse Scale

PNN – perineural nets

COTI– Critical Outcomes Technologies Inc

EDCI\*HCl – 1-Ethyl-3-(3-dimethylaminopropyl)carbodiimide

DCM – Dichloromethane

NaHCO<sub>3</sub>– Sodium Bicarbonate

mCPBA– meta-Chloroperoxybenzoic acid

HCl- Hydrochloric acid

NaOH- Sodium hydroxide

## List of Figures

<b>Figure 1.</b> Metabolism of insecticide incorporating phase I and phase II metabolism. PSMOs; poly-substrate monooxygenase, MFO: mixed function oxygenase, GSH: Glutathione-S-transferase .....	8
<b>Figure 2.</b> Methylene dioxyphenyl core used for the basis of all dillapiol analogs .....	11
<b>Figure 3.</b> Previously synthesized dillapiol analogues with high bioactivity: <b>AF31</b> , <b>AF53</b> , <b>AF59</b> and <b>AF70</b> .....	12
<b>Figure 4.</b> CYP3A4 IC <sub>50</sub> values, and activity of dillapiol and sesamol analogues. ....	12
<b>Figure 5.</b> IC <sub>50</sub> of DEM and compound 21 for inhibition in vitro of RS-CPB GST .....	16
<b>Figure 6.</b> Percent inhibition of CYP3A4 by dillapiol vs the log concentration (mg/ml) .....	31
<b>Figure 7.</b> Structure of compounds synthesized with varying Log P .....	33
<b>Figure 8.</b> IC <sub>50</sub> values (μM) of compounds tested for CYP3A4 inhibition. A Millipore Cytofluor 4000 Fluorescence Measurement System set to 485nm excitation filter (20nm bandwidth) was used to analyze each plate after 20 minutes with endpoint reading. Standard error is shown. C.I 95%, n= 3 .....	42
<b>Figure 9.</b> Miscellaneous MDP compounds and their relative CYP3A4 inhibition relative to <b>21</b> = 1 .....	52
<b>Figure 10.</b> mRNA levels of specific inhibitory enzymes in SOX9 conditional knock-out and control mice with healthy spinal cords .....	63
<b>Figure 11.</b> mRNA levels of specific inhibitory enzymes in SOX9 conditional knock-outs and control mice with T9 SCI .....	64
<b>Figure 12.</b> Assessment of locomotor functionality of SOX9 conditional knock-out and control mice after SCI .....	64
<b>Figure 13.</b> Model for how SOX9 ablation results in improved locomotor recovery after SCI .....	67
<b>Figure 14.</b> The expression of SOX9 and various regeneration-inhibiting enzymes after exposure .....	68
<b>Figure 15.</b> The expression of SOX9 and various regeneration-inhibiting enzymes after exposure to the dimerization-inhibiting molecule Z02 .....	69
<b>Figure 16.</b> Dimerization-inhibiting small molecule lead compound Z02 .....	70
<b>Figure 17.</b> Structure of Z02. Retrosynthesis to four distinct units (A,B,C,D) .....	70
<b>Figure 18.</b> Synthesis of Z02 analogs by combining AB units and CD units through amide bonds .....	72
<b>Figure 19.</b> Potential cyclic A units .....	73

<b>Figure 20.</b> Potential phenols as replacements for the D unit.....	73
<b>Figure 21.</b> Shape of the molecule changes with the no ortho substituent in the D unit to the isopropyl group from being in the same plane to a twist shape. ....	74
<b>Figure 22.</b> I. Hydrogen bonding between the 4-methoxy substituent and the amide nitrogen. II. Ring B twist out of the plane of the CD unit due to the steric interactions. III. The shape of the 4-unsubstituted derivative .....	75
<b>Figure 23.</b> <i>Ortho-</i> , <i>meta-</i> and <i>para-</i> contributes to the shape of compounds in ring B. ....	75
<b>Figure 24.</b> Difference in overall shape of <i>ortho-</i> , <i>para-</i> vs the <i>meta</i> isomer.....	76
<b>Figure 25.</b> <sup>1</sup> H NMR of <b>Z02</b> (synthetic <b>1</b> ).....	79
<b>Figure 26.</b> The first group of compounds featuring ring <b>B</b> derived from 3-amino benzoic acid. ....	81
<b>Figure 27.</b> <sup>1</sup> H NMR of compound <b>9</b> .....	82
<b>Figure 28.</b> Bioassay for the first four synthesized derivatives using ATDC5 cells that have been stably transfected with PGL4.11 SOX9 4x48bp. Compounds <b>12</b> ( <b>TD751</b> ), <b>9</b> ( <b>TD752</b> ), <b>10</b> ( <b>TD753</b> )and <b>11</b> ( <b>TD754</b> ) are compared to <b>Z02</b> .....	83
<b>Figure 29.</b> This is readily apparent from the overlays of the <i>ortho-</i> vs <i>meta-</i> and <i>para-</i> vs <i>meta-</i> structures reproduced below.....	88
<b>Figure 30.</b> N,N-dimethylformamide barrier to rotation. ....	92
<b>Figure 31.</b> Amide restricted rotation a). Restricted rotation in the aromatic to carbonyl carbon-carbon double bond b) .....	93
<b>Figure 32.</b> Axial and equatorial hydrogens in each case undergoing slow exchange of position. ....	94
<b>Figure 33.</b> 400 MHz <sup>1</sup> H NMR Spectrum in CDCl <sub>3</sub> .....	95
<b>Figure 34.</b> 100 MHz <sup>13</sup> C NMR spectrum in CDCl <sub>3</sub> .. ....	96
<b>Figure 35.</b> 600 MHz <sup>1</sup> H NMR spectrum in CDCl <sub>3</sub> .....	97
<b>Figure 36.</b> 600 MHz HETCOR spectrum in CDCl <sub>3</sub> .....	98
<b>Figure 37.</b> 400 MHz <sup>1</sup> H NMR Spectrum in CDCl <sub>3</sub> .....	99
<b>Figure 38.</b> 100 MHz <sup>13</sup> C NMR spectrum in CDCl <sub>3</sub> .....	100

## List of Schemes

<b>Scheme 1.</b> Synthesis of PBO from safrole .....	6
<b>Scheme 2.</b> Oxidation of MDP compounds by CYP P450 enzymes .....	9
<b>Scheme 3.</b> Metabolism of benzhydryl esters by insect esterases.....	13
<b>Scheme 4.</b> General preparation of analogs 21-28.....	19
<b>Scheme 5.</b> Preparation of analogs of sesamol via electrophilic aromatic substitution .....	20
<b>Scheme 6.</b> Preparation of compound 35 from dillapiol.....	21
<b>Scheme 7.</b> Preparation of compound 21 .....	24
<b>Scheme 8.</b> Preparation of amine 42 from safrole .....	26
<b>Scheme 9.</b> Preparation of compounds 56 and 57.....	46
<b>Scheme 10.</b> Preparation of sulfonamides .....	50
<b>Scheme 11.</b> Thionyl Chloride reaction.....	76
<b>Scheme 12.</b> Amide bond coupling with DCC .....	77
<b>Scheme 13.</b> Synthesis of Z02 analogs using EDCLHCl as coupling agent.....	77
<b>Scheme 14.</b> Synthesis of the A-B and C-D units required for the preparation of Z02, 1 .....	78
<b>Scheme 15.</b> Reduction of AB nitro unit into an amino group using iron fillings and ammonium chloride.....	79
<b>Scheme 16.</b> Halogenation of carboxylic acid into an acid chloride using oxallyl chloride then coupling with AB amino group to yield Z02 .....	80
<b>Scheme 17.</b> Synthesis of analog 25 .....	87

## List of Tables

<b>Table 1.</b> Major botanical products used for pest control .....	4
<b>Table 2.</b> IC <sub>50</sub> values relative to dillapiol. ....	22
<b>Table 3.</b> IC <sub>50</sub> values of CYP3A4 inhibitors and activity relative to dillapiol .....	26
<b>Table 4.</b> IC <sub>50</sub> values (μM) of compounds tested for CYP3A4 inhibition. Activity relative to 21 and (=1) and activity relative to dillapiol (=1). Standard error is shown. C.I 95%, n= 3. ....	34
<b>Table 5.</b> Bioassay data comparing compounds 9-21 .....	85

*Dedication,*

*To my father, Pritam Raina*

## Acknowledgements

Firstly, I would like to thank my supervisor Dr. Tony Durst for giving me the opportunity to pursue my Master's degree in his lab. His dedication, expertise, support and pleasant personality have all added positively to my graduate experience. I cannot express how thankful I am for his constant encouraging words, stories and intellect that have uplifted me even in times of difficulty. He always had my best interests, and was extremely considerate. I thank him for all the opportunities he has given me during my undergraduate and graduate studies; since COOP in my third year to my second year of masters. His ongoing passion and enthusiasm for chemistry has pushed me to my full potential. I cannot thank him enough for his guidance on my thesis, seminar and for making these past years very memorable. It will be hard to move on. I will never forget this amazing experience.

During my graduate studies, I have been fortunate to have worked alongside many inspiring people who have made coming into the lab much more enjoyable working environment. I would like to extend a special thanks to Amanda Saikaley who had my back in every aspect of the years we worked together. She has been an inspiration, and a wonderful friend. Rui for teaching me the biology side of my project. Adrien and Julien; for all the great laughs and sushi expeditions. To all the COOP, Master's, honours and summer students Anna, Salma, Karishma, Sandra, Mike Wazowski, Rowan, Lotty, Ashleigh, and Daniel, it has been a pleasure getting to know each and every one of you. Lastly, I am thankful for making friends with the Ben and Arnason group. In addition, I would like to acknowledge Dr. Robert N. Ben, for being my co-supervisor, Dr. John T. Arnason and Dr. Arthur Brown for being collaborators on my projects. I cannot thank you enough for your help and assistance during these years at University of Ottawa.

To my close friends, and everyone else who has shown me love and support at University of Ottawa, I appreciate every bit of push and the conversations we had. Firstly, to my mom, who has been an inspiration and positive attitude in my life. To my brother Kevin, who has always has my back. Finally, this is for my father, who has battled ALS for three long years and allowed me to continue on with this Masters program. He has taught me the value of life, perseverance and the will to fight. He stayed up at nights teaching me math, science and English, always putting education first and foremost. This one's for you.

# **PART A: Synthesis of novel second generation dillapiol and sesamol analogs; inhibition of Cytochrome P450 3A4**

## **1.0 Introduction**

### **1.1 Pesticides**

Pesticides are substances that attract, destroy or mitigate pests. In general, a pesticide is a chemical or biological agent such as a virus, bacterium, antimicrobial or disinfectant that kills pests.<sup>1</sup> Pests include mollusks, fish, nematodes, microbes and insects that destroy property or spread disease. Pesticides have many benefits; however, they can also have harmful effects such as potential toxicity to humans and other life forms.<sup>1</sup>

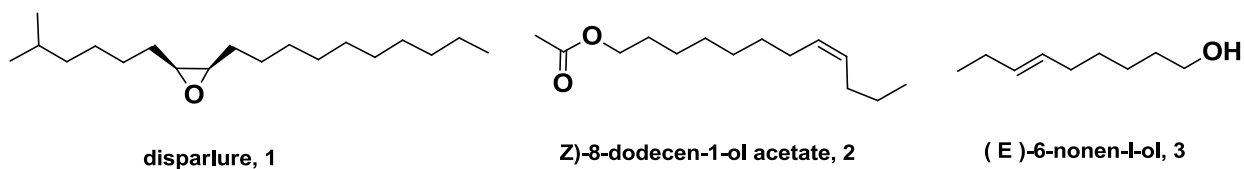
Millions of pounds of pesticides of various types (insecticide, fungicides etc.) are consumed by the United States every year.<sup>2</sup> Their value was more than \$ US3.5 B in 2012. These numbers increase in countries such as Brazil where they do not experience winter. These countries play an important role in the world food supply as they can harvest three times more than countries that experience winter season.<sup>2,3</sup>

Due to environmental and health concerns ranging from short term impacts such as headaches and nausea to chronic impacts like cancer, endocrine disruption.<sup>4</sup> Many synthetic carbamates and organophosphates were retracted from being used as pesticides.<sup>4</sup>

Pesticide synergists play an important role since insects can develop pesticide resistance quickly due to recurrent selection in succeeding populations. A synergist is a non-toxic compound that is added to insecticides to increase their effects against insect pests.<sup>12</sup> Synergists do not have pesticide activity on their own. Some insects in a population have the metabolic

machinery (enzymes) that metabolize, thereby detoxifying insecticides. This allows them to survive and pass on their genes to future progeny.<sup>12</sup> Due to recurrent selection, exposure to a particular insecticide evolves into a population that becomes highly resistant to a particular type of pesticide. In some instances farmers may apply increased doses of pesticides which lead inevitably to even greater resistance and more environmental damage.

With increasing concern about the use of toxic pesticides to control insects and other organisms it is important to look for other alternatives for pest management. Pheromones present a particularly effective and environmentally benign approach.<sup>13</sup> Pheromones are a class of chemicals that insects and other animals release to communicate with other individuals of the same species.<sup>14</sup> The behavioural chemicals leave the body from the first organism; pass through the environment and reach the second organism, which are detected by the receiver. In insects, these pheromones are detected by the antennae on the head.<sup>14</sup> Pheromones can be effective in attracting faraway mates, and in some instances, can be persistent, remaining active for days. Typical pheromones are small hydrophobic molecules, for example, disparlure, 1, *Z*-8-dodecen-1-ol acetate, 2 and (*E*)-6-nonen-1-ol, 3 the sex attractants of the gyps moth, the cabbage looper and the **Mediterranean fruit fly**, respectively.<sup>14,26</sup> These structures are shown below



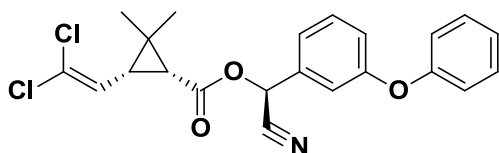
There are three main uses of pheromones in pest management. One important application is monitoring a population of insects to determine if they are present or absent in an area or to determine if enough insects are present to warrant a costly treatment.<sup>13,14</sup> For example, 3-(*Z*-

hexenol has been used to track the spread of certain major pests for example the spread of the emerald ash borer in the upper Mid-West states and Ontario during the past two decades.<sup>27</sup>

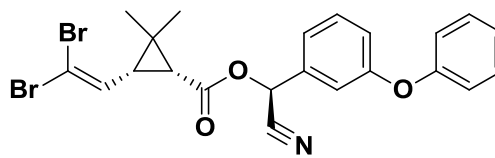
A second major use of pheromones is to mass trap insects to remove large numbers of insects from the breeding and feeding population.<sup>13, 14</sup> A third application of pheromones is in the disruption of mating populations of insects. Synthetic pheromones are dispersed into crops and false odor plumes attract males away from females that are waiting to mate. This causes a reduction of mating and reduces the population. In some instances this had lead to eradication of pests.<sup>13, 14</sup>

Botanical pesticides have been used by humans for thousands of years. They are toxic to the target insects but generally not detrimental to human health.<sup>4</sup> Botanical pesticides are extracted from plant material. Although, the use of botanical pesticides is considered safer and cleaner for the environment, there are some major limitations for use of these products which include lower efficacy, high cost and reduced lifetime duration compared to synthetically made pesticides.<sup>4</sup> Four main registered plants products are currently used for insect control. The structures of the active ingredients have been determined. They are shown below in **Table 1**. Before the development and use of synthetic pesticides, plant products were the major tools in pest control by farmers.<sup>21</sup> One of the major limitations for use of these products is lower efficacy and greatly reduced life-time compared to synthetically made products.<sup>21</sup> There is also a higher cost associated with some of them such as pyrethrins.<sup>21</sup> Since these factors render botanical products to be ineffective for large scale use it is important to develop synthetic products as these are more efficient. For example, the synthetic pyrethroids such as cypermethrin, **4** and deltamethrin, **5** are more potent and longer lasting in the environments than the natural compounds. A drawback of the synthetic pyrethroids relative to the natural materials is that the

synthetic compounds are used as single entities thus target insect develops resistance to the pure synthetic compounds much more rapidly than the mixtures present in the natural product.



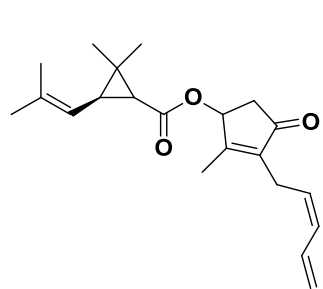
**Cypermethrin, 4**



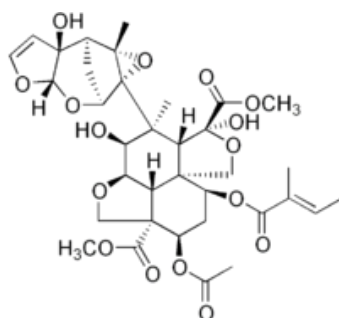
**Deltamethrin, 5**

**Table 1.** Major botanical products used for pest control.

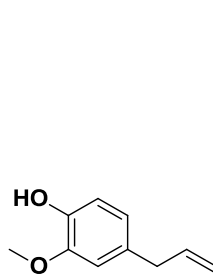
Botanical Product	Plant source/ Product
a) Pyrethrum	<i>Tanacetum cinerariaefolium</i> (Asteraceae)
b) Neem Tree	<i>Azadirachta indica</i> (Meliaceae)
c) Essential Oils	<i>Rosmarinus officinate</i> (Lamiaceae) and <i>Eucalyptus globus</i> (Myrtaceae) from Rosemary; Eugenol from clove oil; <i>Syzyglum aromaticum</i> (Myrtaceae); thymol from garden thyme; <i>Thymus vulgaris</i> (Lamiaceae)
d) Rotenone	Tropical legumes <i>Derris</i> , <i>Lonchocarpus</i> and <i>Tephrosia</i>
e) Ryanodine	<i>Ryania speciosa</i> (Salicaceae)



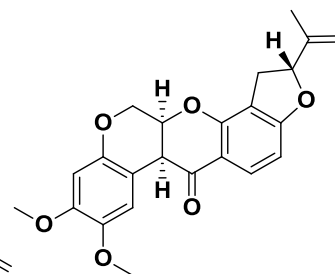
**A) Pyrethrin I, 6**



**B) Azadirachtin, 7**



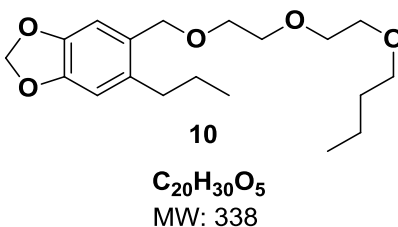
**C) Eugenol, 8**



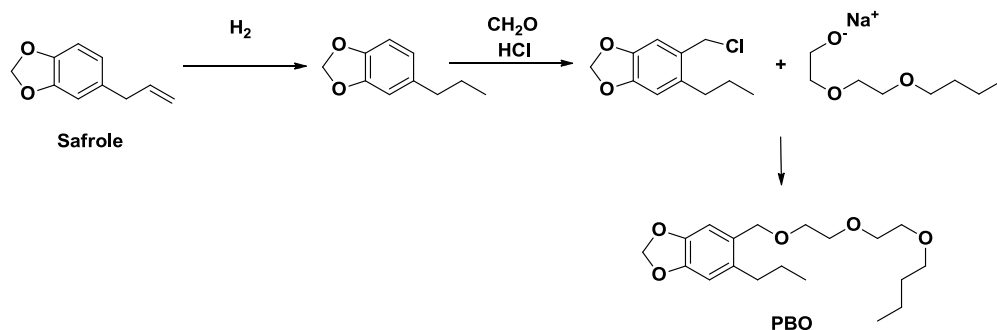
**D) Rotenone, 9**

## 1.2 Pesticide synergists and Piperonyl Butoxide (PBO)

Pesticide synergists can be either natural products or synthetic materials. Synergists increase the effectiveness of the pesticide thereby lowering the amount of pesticide required to control a particular pest. Insecticide synergists themselves have little or no toxicity towards insects. The most commonly used insecticide synergist is piperonyl butoxide (PBO), **10**, a man-made compound. PBO increases the effectiveness of insecticides by reducing the insects' ability to detoxify it.<sup>23</sup> PBO has low toxicity in humans, is non-toxic to birds, mammals, and bees; However, it is moderately toxic to fish.<sup>22</sup> PBO is currently the most widely used synergist for pyrethrins.



PBO is contained in more than 1,600 pesticide products. As mentioned before PBO was not designed to interfere with the insect's ability to detoxify some insecticides.<sup>23</sup> PBO inhibits the mechanism of action of the CYP enzymes. PBO acts by protecting the co-applied insecticide (e.g. pyrethrins, and other pesticides) from metabolic attack thus allowing them to reach their biochemical targets.<sup>24</sup> Since PBO inhibits an enzyme system which catalyzes oxidative processes in living systems, it also has an intrinsic toxic potential to arthropods.<sup>24</sup> PBO is relatively easy to synthesize. Its synthesis starting from the inexpensive natural product safrole is shown in **Scheme 1**.



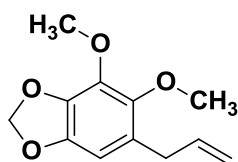
**Scheme 1.** Synthesis of PBO from safrole.

Despite its reputed low toxicity a number of concerns have recently arisen. Horton *et al.* have recently reported that PBO disrupts a biological signaling system that is critical in neurological development and that the disruption of this critical pathway may be the molecular basis for profound developmental defects in children exposed in *utero* to PBO.<sup>22</sup> Many current products also contain 5-10 times more PBO than the pesticide itself (ratio of 1:5) which means that there is large amount of PBO in the pesticide formulation.<sup>24</sup> Thus it is crucial to develop new pesticide synergists that have a lower ratio to pesticide and that are biodegradable, non-toxic and relatively easy to synthesize. The Durst lab in collaboration with Dr. Arnason lab has found a natural product with similar effects as PBO in the *Piperaceae* known as dillapiol.

### 1.3 Dillapiol

*Piper aduncum L.* (Piperaceae) is a tropical shrub native to Central America. This plant is used in traditional medicine for the treatment of stomach aches, trachoma and insect repellent.<sup>9</sup> It has been reported that the essential oil of *Piper aduncum L* obtained from the leaves and fruit of this plant has pesticide activity.<sup>10</sup> This plant contains a high concentration of dillapiol **11** with concentrations in the range of 37-98%, depending on the collection sites.<sup>10</sup> The plants grown in Brazil, Cuba and Costa Rica have the highest concentration of dillapiol.<sup>9</sup> It is reported<sup>21</sup> that the

essential oil obtained from the fruit and leaves collected in the Caribbean region of Costa Rica (Sarapiquí and Guapiles) consisted of close to 98 percent dillapiol. The material was considered sufficiently pure so that chemical reactions could be carried out without additional purifications. Due to high concentration of dillapiol in the leaves and especially the fruit of the plant growing in the region of Costa Rica could become a commercial source of dillapiol.<sup>9</sup>

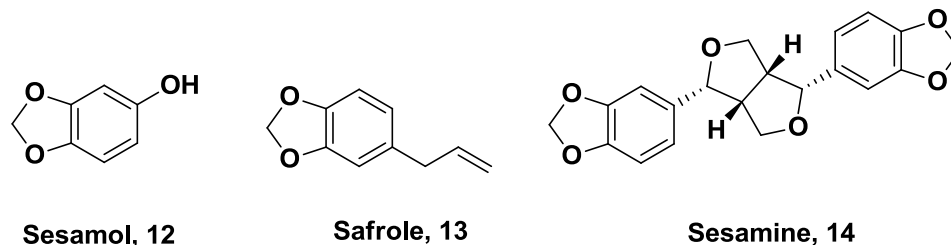


**Dillapiol, 11**  
**Mw: 222**

#### **1.4 Dillapiol as a lead compound for the development of pesticide synergists.**

Dillapiol is a MDP compound that acts as a synergist when combined with certain pesticides.<sup>12</sup> Pesticide synergist also play a very important role and potentially delays pesticide resistance.<sup>13</sup> Our group, worked on the development of a novel synthetic pathway for the preparation of dillapiol and other analogs. These dillapiol analogs showed synergistic activity with the insecticide  $\alpha$ -T.<sup>25</sup> Dillapiol itself had the highest synergistic activity. In 2000, our group<sup>18</sup> performed an *in vitro* evaluation of human CYP 3A4 inhibition by herbal extracts and pure herbal derived compounds. In his study, he found that dillapiol was the most potent inhibitor of this enzyme.<sup>25</sup> These results suggested an explanation of synergistic effect observed for dillapiol and its analogs as inhibitors of insect CYP enzymes. The inhibition of the CYP enzyme blocks the metabolism of other xenobiotic compounds present in the organism, therefore the exposure time to the compound is increased and the overall toxicity is enhanced.<sup>18</sup> In addition to dillapiol a number of other natural products which have the key methylenedioxyphenyl group

required for synergistic activity as part of their structure have been shown to synergize both natural and synthetic pesticides. Amongst these are sesamol **12**, safrole **13**, and sesamine **14**.



### 1.5 Mechanism of action of insecticide synergists

The metabolism of insecticides involves the conversion of compounds to more polar; less toxic and extractable products via enzymatic reactions.<sup>14</sup> There are two phases of metabolism: Phase I and phase II metabolism, **Figure 1**.

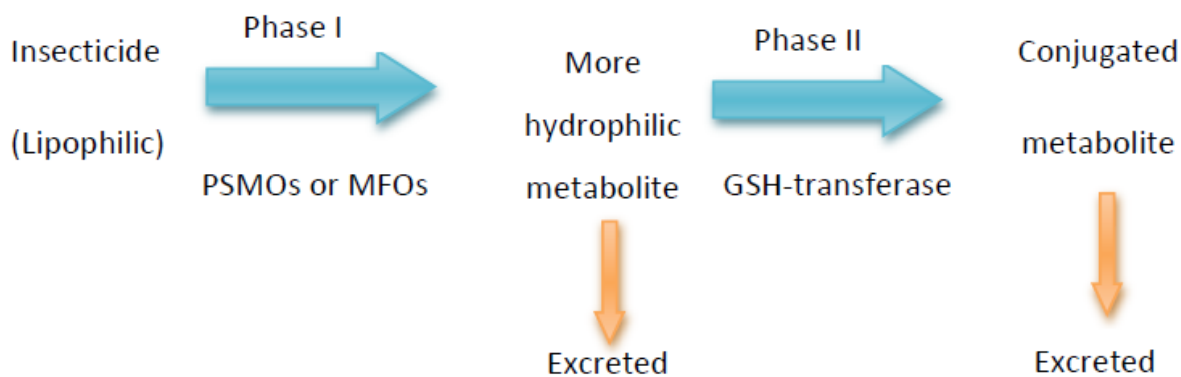
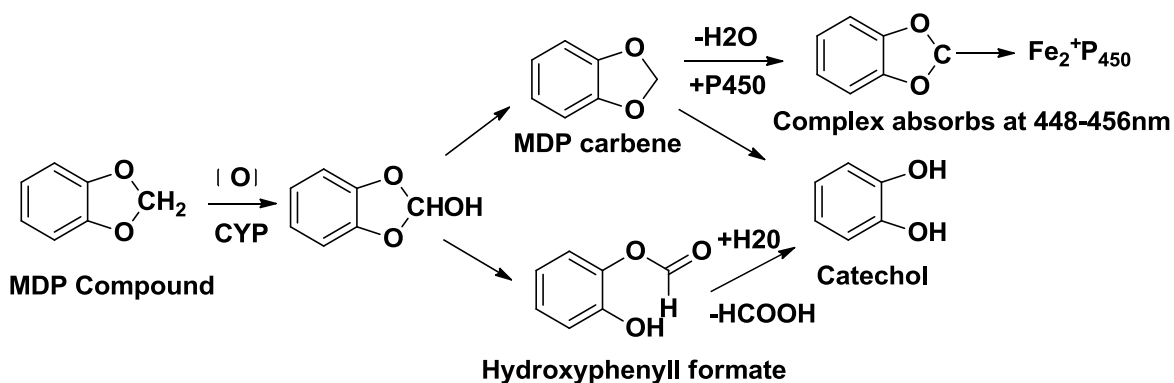


**Figure 1.** Metabolism of insecticides, incorporating phase I and phase II metabolism. PSMOs: poly-substrate monooxygenases, MFO: mixed function oxygenase, GSH: Glutathione-S-transferase,

Phase I metabolism is carried out by Cytochrome (CYP P450) dependent poly-substrate monooxygenases.<sup>15</sup> The up-regulation of the metabolism of the insecticide compounds via this system is a major cause of the development of pesticide resistance in insects. Through careful study it has been realized many compounds containing a methylenedioxyphenyl unit can act as

CYP P450 inhibitors.<sup>15</sup> Such compounds act as suicide inhibitors of CYP P450 enzymes and as a consequence the insect loses its ability to metabolize the pesticides and they remain in the insects hemolymph for a longer period of time. The inhibition mechanism is shown in **Scheme 2** below.



**Scheme 2.** Oxidation of MDP compounds by CYP P450 enzymes.

The combination of pesticide with methylenedioxyphenyl compounds enhances the activity of the pesticide. During this process, CYP oxidize methylenedioxyphenyl compounds to catechols. These catechols which are stable compounds can bind to the heme group causing inhibition of oxidation of the substance. The hydrophobic and electronic properties of methylenedioxyphenyl metabolite intermediates can be formed which are stable when the heme group is in the ferrous oxidized state. These can be displaced by lipophilic compounds, restoring the activity of CYP- methylenedioxyphenyl with electron donating groups on the aromatic ring and aliphatic side chains form stable methylenedioxyphenyl intermediates. Conversely, methylenedioxyphenyl with electron withdrawing groups on the aromatic ring induce the production of carbon dioxide and the catechol.<sup>16</sup>

## 1.6 Cytochrome P450 isoenzyme family

Cytochrome P450 (CYP P450) is a family of isoenzymes involved in the biotransformation of compounds, contains a heme cofactor and uses a large variety of substrates in enzyme reactions. CYP P450 enzymes are mainly present in the smooth endoplasmic reticulum of several tissues. CYP P450 enzymes are found in all forms of life, including plants, animals, fungi, protists etc. Only a handful of CYP P450 such as CYP2C1A2, CYP2C19, CYP2C9, CYP2D6, CYP2E1 and CYP3A4 enzymes play an important role in metabolizing xenobiotics via oxidation.<sup>16</sup> The hepatic CYP3A4 enzyme is responsible for significant first pass metabolism of orally administered drugs in the gastrointestinal tract (GI tract).<sup>17</sup> The inhibition of these enzymes may lead to prolonged metabolic elimination and higher bioavailability of drug, causing an increased potency/or toxicity. CYP P450 can undergo competitive or non-competitive inhibition the former being more likely. In competitive inhibition two drugs compete for the same receptor site on the isoenzyme and in non-competitive inhibitor occurs on the allosteric site. The more potent inhibitor will predominate thus reducing the metabolism of the competing drug. This reduced metabolism causes the drug to remain in the plasma for quite some time, increasing the toxicity and overall potency. There are potential positive effects and negative consequences of inhibiting CYP P450 enzymes. The inhibition of CYP P450 may be useful in increasing the potency of the drug, provided that the drug remains below toxic levels in blood. An increase in potency means a reduced dose of drug to be administered to induce therapeutic effects. In addition, dangerous drug interactions may result as a consequence of CYP P450 inhibition which results in reduced metabolism of drug until it reaches toxic levels.

## 1.7 Inhibition of CYP P450 by Dillapiol

Dillapiol extracted from *Piper aduncum L.* (Piperaceae), inhibits CYP 3A4, with a lower 50% inhibition concentration ( $IC_{50}= 9.2\mu M$ ) than most other secondary metabolites.<sup>18</sup> In a recent study, dillapiol was shown to be an effective synergist of pyrethrin in both sensitive and resistant strains of the Colorado potato beetle, *Leptinotarsa decemlineata* (Chrysomelidae).<sup>19</sup> In previous studies by Liu *et al.*, dillapiol, inhibited CYP P450 enzymes in the beetle, preventing the Colorado potato beetle from metabolizing the insecticide pyrethrin and increasing the bioavailability and efficiency by 9.1 fold in the resistant strains.<sup>19</sup> The synergistic activity of dillapiol can be enhanced by modifying the molecule as demonstrated by Belzile *et al.* in 2000. In this study, dillapiol analogues were tested with a botanical larvicide (phototoxin)  $\alpha$ -terthienyl and demonstrated synergistic activity against the mosquito larvae *Aedes atropalpus* (Ochlerotatus) with synergistic activity between 0.9 and 2.4.<sup>20</sup> Dillapiol was isolated from *P. aduncum* via using steam distillation. All analogues contained the key methylenedioxyphenyl core (**Figure 2**)

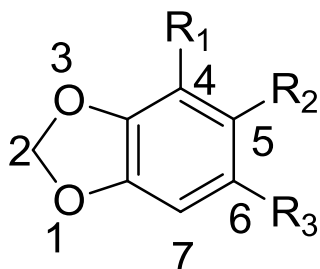


**Figure 2.** Methylenedioxyphenyl core used for the basis of all dillapiol analoge.

Amongst the group of more than fifty analogs that were prepared the compounds with the highest CYP P450 activity were **AF31**, **AF53**, **AF59** and **AF70** with  $IC_{50}$  values of 0.2, 0.36,

0.54, 0.47 $\mu$ M, respectively as shown in **Figure 3**. The most potent of these molecules, **AF31** was close to 50 times more potent as an inhibitor of CYP3A4 than dillapiol itself.

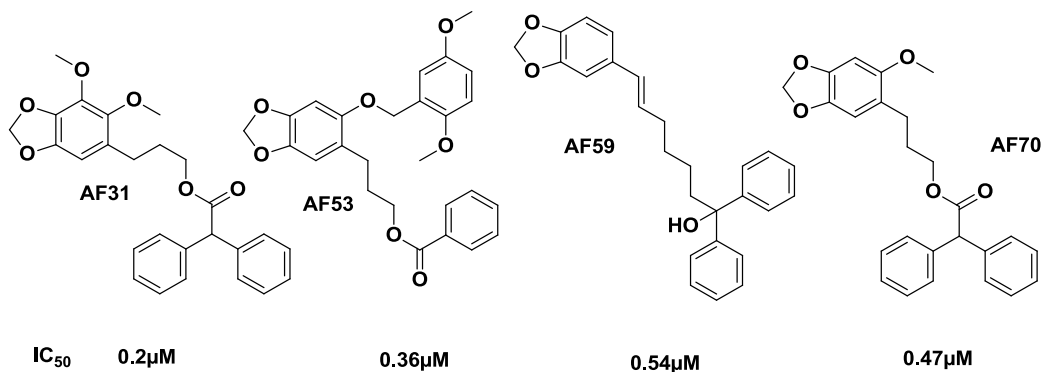


**Figure 3.** Previously synthesized dillapiol analogues with high bioactivity: **AF31**, **AF53**, **AF59** and **AF70**.

A structure activity relationship of the first generation dillapiol analogs showed that the methoxy group at C4 did not play an important role in bioactivity, whereas bulky substituents on C6 greatly enhanced the inhibitory activity. It was later determined that highly hydrophobic compounds showed greater bioactivity. Furthermore, based on these previous results, another set of dillapiol analogues was synthesized and showed a more potent inhibitory action against CYP3A4 as shown in **Figure 4**.

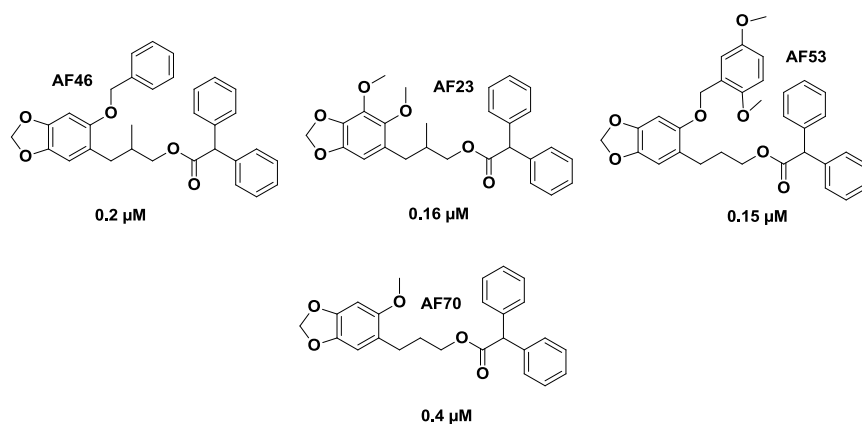
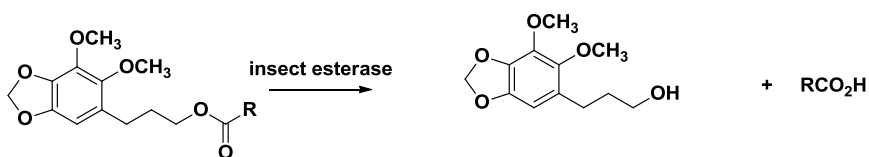


**Figure 4.** CYP3A4  $IC_{50}$  values, and activity of dillapiol and sesamol analogues.

Based on the above results, large substituent on dillapiol's R<sub>3</sub> attached at C6 enhance the inhibition of CYP3A4. The methoxy group (R<sub>1</sub>) at C4 on compounds **AF46**, **AF53** and **AF70** does not seem to have a large enough effect on activity as similarly demonstrated for **AF23** and compound **21**.

Interestingly, even though the molecules shown in **Figure 4** were very potent CYP3A4 inhibitors *in vitro*, they were no more effective than the much less potent ethers such as AF16 *in vivo*. Indeed, esters other than the benzhydryl esters above were less active than dillapiol itself.<sup>19</sup> It was realized that all of the esters prepared by Carballo were subject to insect esterases and were cleaved rapidly to the corresponding acid and the primary alcohol which had been shown by Carballo to be less potent in inhibiting the CYP enzymes than dillapiol.<sup>21</sup> Metabolism of the benzhydryl esters (**Scheme 3**) is relatively slow and therefore these compounds show reasonable *in vitro* activity.



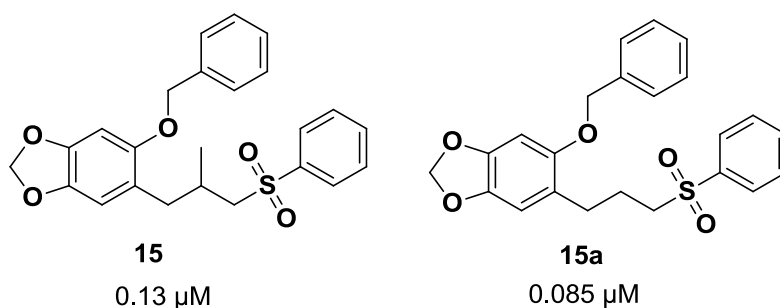
**Scheme 3.** Metabolism of benzhydryl esters by insect esterases

### 1.8 Sulfone analogs as CYP 3A4 inhibitors

Based on the above results and the QSAR model developed by C. Compadre<sup>28</sup> at the University of Arkansas we began to synthesize and determine the inhibition of CYP 3A4 of additional analogs of dillapiol and sesamol including those in which the C6 substituent carried a terminal phenyl sulfone group in place of the diphenyl acetate. This was carried out as part of the

author's undergraduate Honour's project. The goal was to generate compounds that inhibited CYP 3A4 at 1 $\mu$ M or less and were not subject to esterase metabolism.

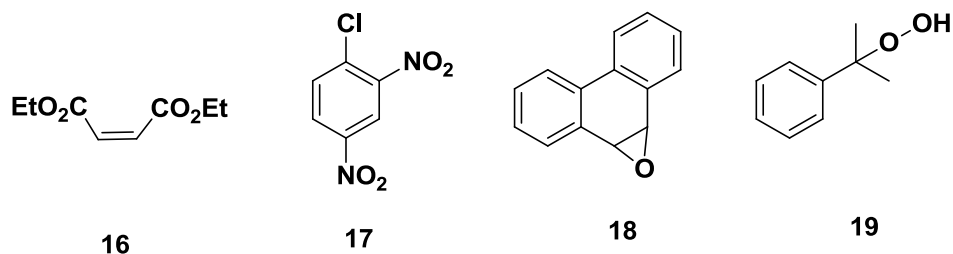
We were pleased that the two sulfones **15** and **15a**, prepared with the help of David Carranza, a visiting student from UNA, Heredia, Costa Rica, became the most potent inhibitors amongst all the compounds our Lab had prepared. These sulfones derived in six steps from sesamol inhibited CYP3A4 with IC<sub>50</sub>'s of 0.13  $\mu$ M 0.085  $\mu$ M, respectively. These compounds were 70 and 107 times more potent than dillapiol.



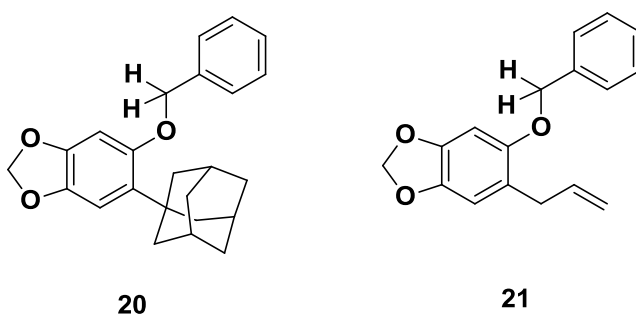
## 1.9 GST assays

Dr. Suqi Lui, decided to test these and some previously prepared compounds as potential inhibitors of insect GST.<sup>19</sup> GSTs are a family of enzymes important for phase II metabolism of lipophilic compounds where a glutathione group becomes attached to a reactive lipophilic compound making it more hydrophilic and ready for excretion from the body of insects. The observations that a number of these compounds were potent GST inhibitors was to us highly surprising and unexpected. Typical GST inhibitors are electrophilic compounds such as the Michael receptor diethyl maleate (DEM), **16**, a variety of  $\alpha,\beta$  unsaturated ketone and aldehydes, and 1-chloro-2,4-dinitrobenzene **17**. The very reactive epoxide derived from phenanthrene **18**, and has also been shown to be a potent GST inhibitor. Finally, cumene hydroperoxide **19** inhibits

GST by a reduction mechanism involving GSH which results in the formation of cumene and GS-SG. The first three compounds react with GSH to give adducts which bind to GST thereby inhibiting its ability to catalyze the GSH addition to other reactive xenophobic molecules.<sup>32</sup>



Compounds **20** and **21** are non-electrophilic and have no functional groups that would be considered obviously reactive to GSH. A reduction mechanism involving radical chemistry and the conversion of GSH into its dimer GS-SG is plausible since the weakest C-H bonds in these molecules, the benzylic C-H bonds have bond dissociation energies (BDEs) estimated to be approximately 340 kJ is comparable to that of the S-H bond in GSH (RS-H BDE is 344 kJ).<sup>29</sup> Another potential mechanism for GST inhibition by these compounds is a strong binding, either direct or allosteric, to the enzyme.



The  $IC_{50}$  for inhibition of the insect GST RS-CPB by **21** was determined to be  $0.23\mu\text{M}$ . This compound was shown to be 180 more potent than DEM a standard GST inhibitor whose

IC<sub>50</sub> was shown to be 42 μM. Compound **20** was subsequently shown to be five times more potent than **21**.

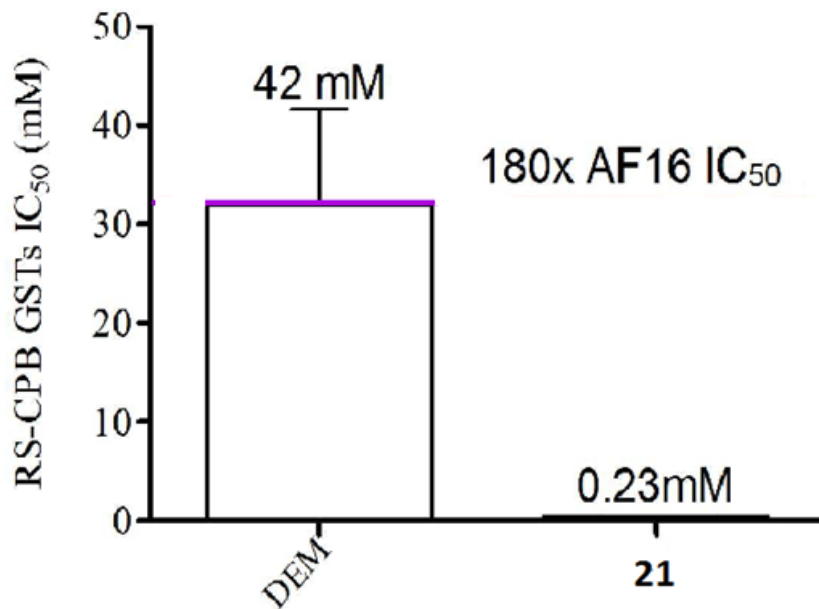


**Figure 5.** IC<sub>50</sub> of DEM and compound **21** for inhibition *in vitro* of RS-CPB GST

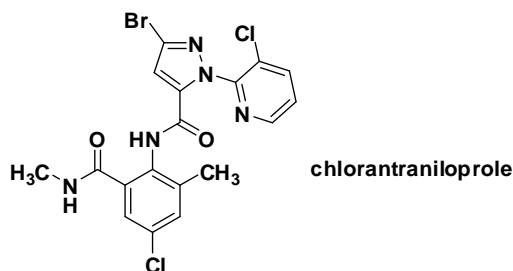
The GST inhibition activity was also determined on European corn borer (ECB) GST. The ether **21** inhibits GST with an IC<sub>50</sub> of 0.04 (0.034-0.044) mM which is 575 times lower than (DEM), a standard GSTs inhibitor (IC<sub>50</sub> =23 (18.6-27.2) mM. Neither dillapiol nor PBO affected significantly the *in vitro* GSTs activity at 1mg/mL.

These data show clearly that **21** and analogs such as **20** are potent insect GST inhibitors. This combined with their inhibition of CYP450s suggests a strong potential for use as a new class of pesticide synergists. Dr. H. Alejandro Arevalo, Global Insecticide-Biology Manager at BSAF, Durham NC, found these molecules to be sufficiently intriguing and offered to enter into a joint research project to investigate and develop additional analogs.

## 2.0 Objectives

As was pointed out in the previous page, renewed interest in dillapiol and sesamol analogs was to a considerable extent due to the observation by Liu that some of the compounds synthesized by Carballo-Arce inhibited not only CYP3A4 but also a variety of insect glutathione transferases (GSTs).

These data intrigued researchers at BASF to the extent that the company asked for a 2.5g sample in late 2016. Subsequently, they reported the following very promising data relating to controlling the tomato leaf minor *Tuta absoluta* (Gelechiidae) as the target insect using chlorantraniliprole as insecticide.



- i) Compound **21** alone was inactive
- ii) Chlorantraniliprole alone at 40g per hectare gave 72% control
- iii) The addition of **21** to chlorantraniliprole in a 1:1 ratio at 40 g of chlorantranilipole/hectare resulted in 94% control
- iv) The addition of **21** to chlorantraniliprole in a 3 :1 ratio at 40 g of chlorantranilipole/hectare resulted in 97% control

In a second set of experiments the activity of **21** alone and in combination with the above pesticides was studied with respect to preventing plant damage caused by the black diamond or cabbage moth *Putella xylostella*, (Noctuidae). The general conclusions were as follows:

- i) The tendency of the feeding damage followed the pattern observed with the insect mortality.

- ii) At 3 days after application, the addition of a 1:1 mixture of **21** and chlorantraniliprole [10g /hectare] significantly reduced the damage caused by the RYN resistant *P. xylostella*.
- iii) Longer time periods gave less definitive results

The first set of experiments indicated that **21** reduces the tolerance of insects with metabolic resistance to chlorantraniliprole, and pyrethroids

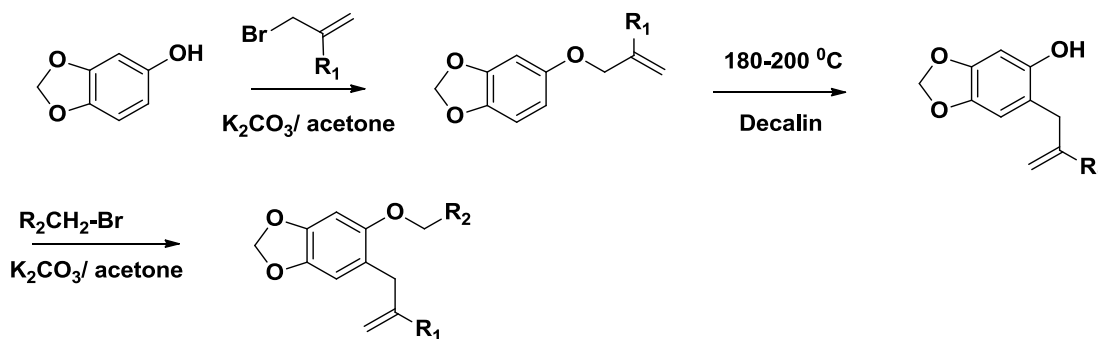
Based on these initial results, BASF initiated a joint project involving researchers both at the University of Ottawa and scientists at various BASF research facilities. The goal was to synthesize a set of analogs of compound **21** in sufficient quantity so that the BASF researchers could investigate their activity against a variety of insect pests in different parts of the world such as the US, Western Europe, India and Indonesia. The toxicity and persistence of these compounds in soils would also be determined. Such data is required by the Environmental Protection Agency in the US and similar agencies in other countries in order for these compounds to be registered as synergists in combination with different pesticide, whether organic such as the pyrethroids or synthetic such as the currently important nicotinoids.

This chapter describes the synthesis of the analog compound requested by the BASF research group in Durham NC lead by Dr. Alejandro Arevalo. Prior to this request we had prepared additional analogs and determined their inhibition of CYP 3A4. Also, during that time period, Dr. Liu evaluated the RS-ECB inhibition of seventeen compounds derived from dillapiol and sesamol. The data from the group of compounds shown below was used in discussions with the BASF researchers to decide on the set of targets for further evaluation by BASF.

## 3.0 Results and Discussion

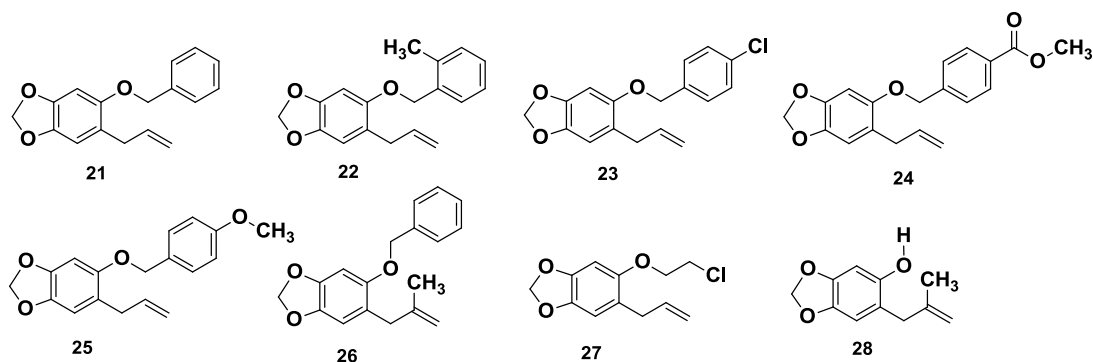
### 3.1 Synthesis of analogs

The following sets of compounds were either available from previous work in the group or prepared as shown below. Except for the sulfur compounds, all were obtained starting with sesamol as shown in the scheme below. All new compounds were characterized by their  $^1\text{H}$  and  $^{13}\text{C}$  NMR which were clearly consistent with the expected structures. Details dealing with compounds prepared by the author are given in the Experimental Section.

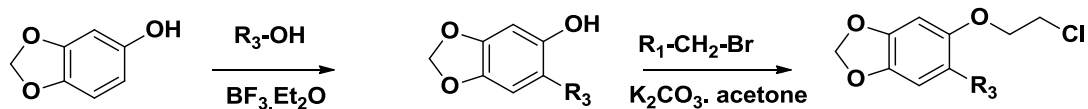


**Scheme 4.** General preparation of analogs **21-28**.

Analogues **21- 28** prepared via the **Scheme 4**.

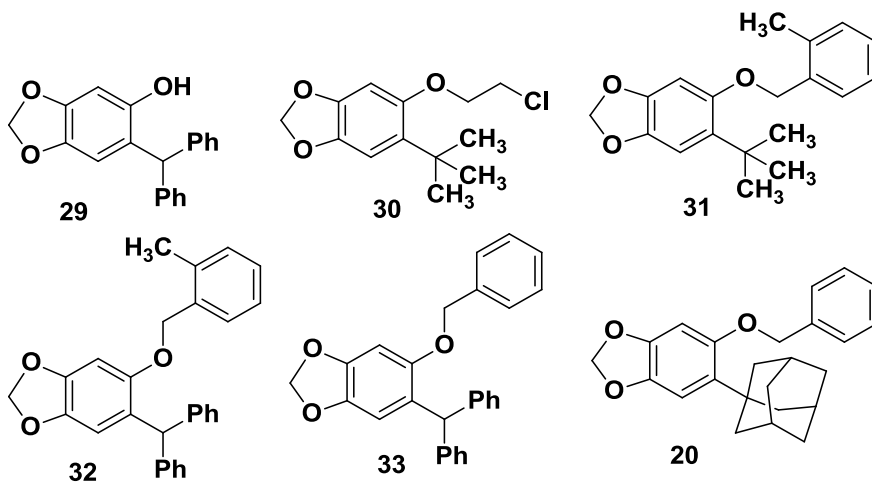


A further set was prepared by first *ortho*-alkylating sesamol by reaction with alcohols that can lead to relatively stable carbocations, for example *t*-butanol, benzhydrol and 1-adamantanol as shown in **Scheme 5**.

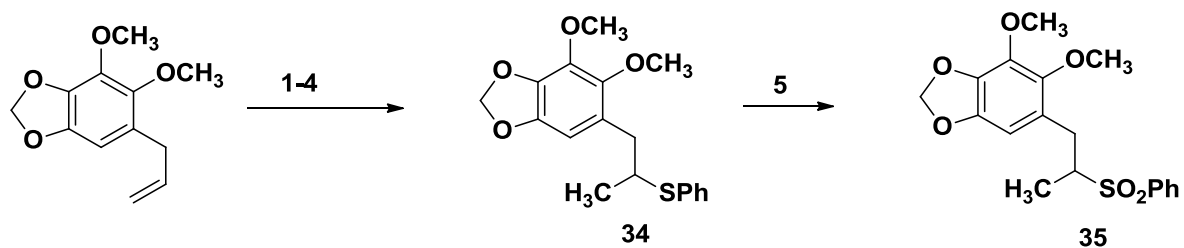


**Scheme 5.** Preparation of analogs of sesamol via electrophilic aromatic substitution

The above scheme yielded phenols such as **29**. Subsequent alkylation afforded the series, **20, 30-34**.



The two compounds, **34** and **35**, containing sulfur as part of  $R_3$ , position C6 in dillapiol were prepared in four and five steps, respectively, starting from dillapiol.



Reagents: 1.  $\text{BH}_3 \cdot \text{THF}$ ; 2.  $\text{H}_2\text{O}_2/\text{Ho}(-)$ ; 3.  $\text{Ts-Cl}$ . 4.  $\text{PhS}(-)$ ; 5. MCPBA

**Scheme 6.** Preparation of compound **35** from dillapiol.

The results of both the CYP3A4 and the RS ECB GST inhibition studies are shown in **Table 2**.

**Table 2.** IC<sub>50</sub> values relative to dillapiol.

Compound #	IC <sub>50</sub> μM. Inhibition of CYP3A4 <sup>1</sup> (Relative to dillapiol)	IC <sub>50</sub> μM Inhibition of RS-ECB <sup>2</sup> (Relative to dillapiol)
20	-	0.0083 (67)
21	1.8 (5.0)	0.040 (14)
22	2.34 (3.9)	0.011 (48)
23	1.6 (5.8)	0.0097 (58)
24	3.8 (2.4)	0.035 (16)
25	9.8, 8.5 (0.93, 1.1)	0.010 (56)
26	3.6 (2.5)	-
27	1.9 (4.2)	0.018 (32)
28	9.3 (0.97)	0.012 (37)
29	2.3 (4.0)	0.010 (52)
30	2.64 (3.4)	0.018 (32)
31	2.2 (4.1)	0.016 (35)
32	2.2 (4.1)	0.0098 (57)
33	8.3 (1.1)	0.14 (4)
34		0.027 (21)
35		0.025 (22)

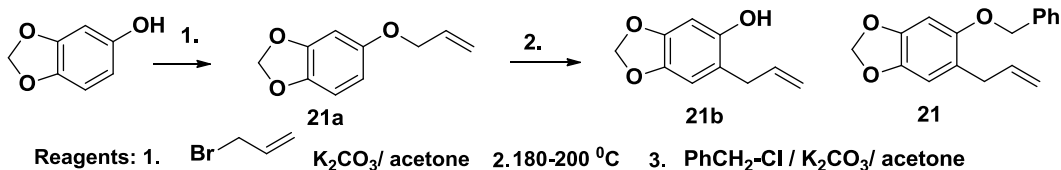
---

<sup>1</sup> Typical SE is 10 %. <sup>2</sup> Typical SE is 10%

Based on an analysis of the results in **Table 2** it was decided in discussions with BASF scientists that two gram quantities of about a dozen compounds would be prepared. Our group here at the University of Ottawa would not only carry out the synthesis but we would also determine their effectiveness as CYP3A4 inhibitors. Unfortunately, BASF was not willing to fund the determination of inhibition of insect GSTs by these compounds. BASF scientists at various research facilities would carry out *in vivo* studies of the synergistic activity of these compounds against important agricultural insect pests common in that region. In addition to this, BASF scientist at Durham NC would determine if these compounds pass Environment Protection Agency requirement which means that these compounds need to show little or no toxicity to different animal life and thus be deemed relatively harmless to the overall environment.

In making the decision about which compounds to pursue the ease and cost of preparation was also taken into account. This was crucial since any new commercial application would need to compete with the entrenched PBO. As was described in the Introduction PBO is prepared from safrole in a three step sequence. Safrole can be obtained by steam distillation of the bark and fruit of sassafras trees native and widely dispersed tree of Eastern North America. Because of the immense scale at which PBO is used worldwide PBO is an inexpensive, essentially a commodity chemical

The synthesis of compound **21** starts with the natural product sesamol. It too requires only three steps and involves simple chemistry and inexpensive reagents. The cost of preparing **21** or analogs relative to PBO will depend to a considerable extent on the cost of commercial amounts of sesamol compared to safrole. The other reagents used in the preparation of these two compounds should not result in a major cost differential.

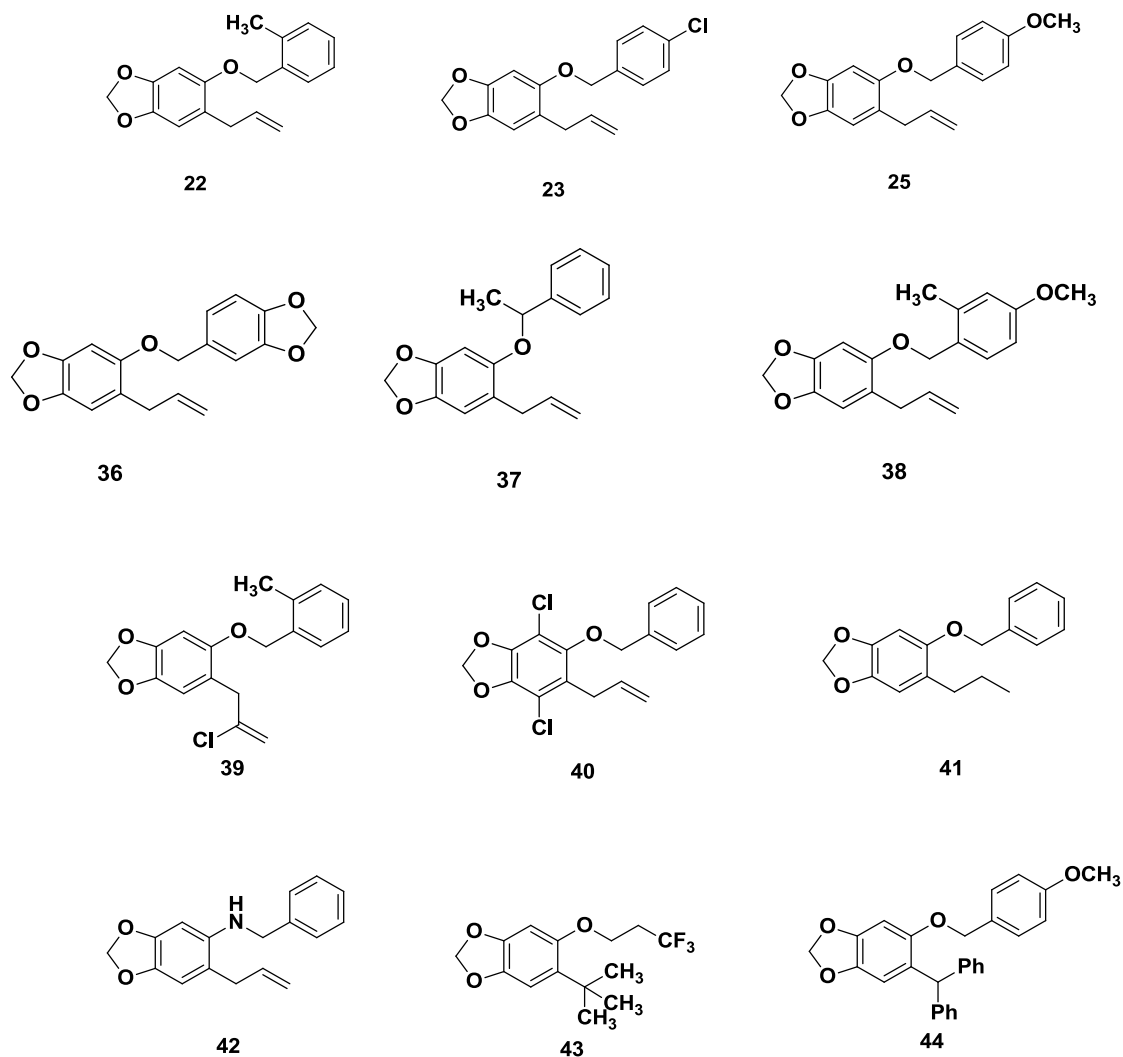


**Scheme 7.** Preparation of compound **21**

The first BASF experiments with **21**, as reported to us, suggest that it may be effective in as low as a 1:1 synergist to pesticide ratio. In contrast the PBO to pesticide ratio in most commercial preparations is 5:1. If the lower ratio for **21** and analogs were to be verified in other applications then a higher cost of preparing **21** could be justified.

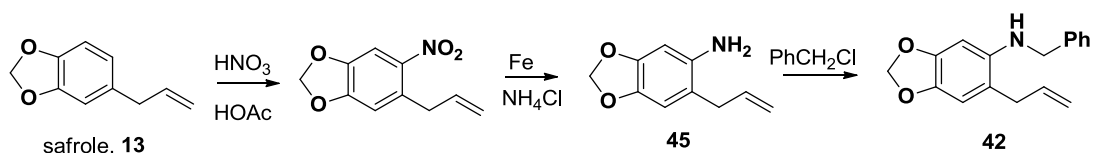
**3.2 Second Generation analogs of 21, requested by BASF.**

The following compounds were selected for synthesis and further evaluations. The majority are close analogs of **21** in which a variety of typical substituent such as  $-\text{CH}_3$ ,  $-\text{OCH}_3$ ,  $-\text{CO}_2\text{CH}_3$  and  $-\text{Cl}$  are introduced *ortho*- and *para*- on the aromatic ring attached to C5 of the methylenedioxy ring. The replacement of the benzyl ether in **21** by benzylamine as in **42**, the effect of removing the double bond in the ally side chain as in **41** would be evaluated. Finally, a few examples such as **43** and **44** in which the ally group at C6 was replaced by *t*-butyl and benzhydryl were also chosen. It was hoped that one or more of these compounds would give sufficiently promising results that they could be chosen for further development.



The synthesis of the above compounds on a more than two gram scale was for the most part uneventful. All products were appropriately characterized prior to submitting them for the *in vivo* assays. We were unsuccessful at the preparation of **40** and **43**. The alkylation of the *ortho*-, *t*-butyl phenol, and the precursor of **43** with  $-\text{CF}_3\text{CH}_2\text{CH}_2\text{Br}$  under typical alkylation conditions did not proceed probably due to steric hindrance. Attempted chlorination of **21** with *N*-chlorosuccinimide resulted in chlorination of the allyl side chain rather than electrophilic aromatic chlorination.

The synthesis of the amine **42** commenced with the nitration of safrole at C5. Subsequent reduction of the nitro group with iron filings in an ethanol-water solution containing NH<sub>4</sub>Cl yielded the intermediate amine **45**: benzylation gave **42**. The aniline **42** served as precursor of other derivatives which will be discussed later in this chapter.



**Scheme 8.** Preparation of amine **42** from safrole.

### 3.3 Biological Evaluation of Second Generation compounds.

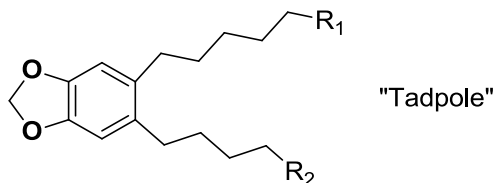
The CYP3A4 Inhibition studies for this group of compounds are summarized in **Table 3** below. Several compounds had activity roughly comparable to **21**, but none was more potent.

**Table 3.** IC<sub>50</sub> values of CYP3A4 inhibitors and activity relative to dillapiol

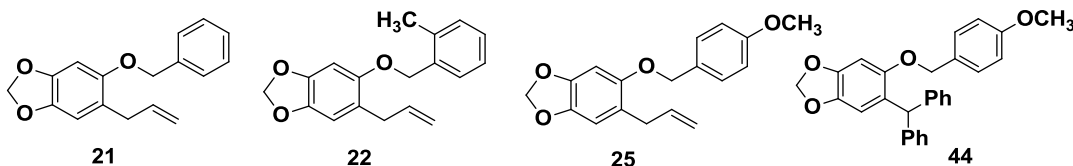
Compound # relative to dillapiol = 1	CYP3A4 inhibition; IC <sub>50</sub> (μM)	Activity
Dillapiol	9.2, 8.6	1
<b>21</b>	1.8	5.0
<b>23</b>	1.61	5.8
<b>25</b>	9.8, 8.5	0.93, 1.1
<b>36</b>	2.4	3.8
<b>41</b>	2.2	4.2
<b>42</b>	3.8	2.4
<b>44</b>	8.3	1.1

### 3.4 BASF studies

BASF chose the code name “tadpoles” (**Figure 19**) for this group of compounds. The MDP portion of the molecule can be imagined as the body and eyes and the two substituents as the legs of a tadpole



Environmental safety data and comparison to PBO was obtained for the following four tadpole molecules.



The LD<sub>50</sub> as a contact poison for bees was not accurately determined but found to be greater than 100 µg per bee for all compounds; for PBO this number is known to be 296 µg per bee. Similarly the oral LD<sub>50</sub> for each compound was greater than 90 µg per bee; the known value for PBO is 611 µg per bee. Acute toxicity to *Daphnia spp* which are a group of several small aquatic crustaceans, commonly called water fleas, was very low with EC<sub>50</sub> = 1200 µg/mL compared to 510 for PBO.

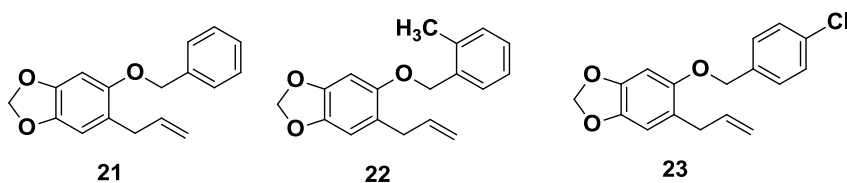
These compounds degraded under typical climate conditions in Durham, NC to 50% of the initial concentration in 7, 10 and 11 days for compounds **21**, **22** and **23**, respectively. Compound **44** had a half-life of about 41 and 59 days in two different soils. The conclusion is

that the persistence risk of the first three compounds is low and for **44** it is moderate. Leaching of these compounds from soils was determined to be low. Based on these data the company concluded that these compounds are assessed as registrable in the US. A variety of studies which demonstrated the effectiveness as synergists for different pesticides and against different insect pests in a number of BASF locations were also reported. A brief summary is given below.

### 3.5 BASF results

Fifteen molecules were synthesized. Testing is underway both for screening and semi field trials. So far, most tadpoles are at least as active as or more active than PBO at the same dose. The lowest ratio we recommend is 1:1 [ai: tadpole]. At lower ratios the efficacy starts to diminish. (vs. 1:5 [ai : PBO]) Increases in efficacy have been observed for: chlorantranilprole, spinosad, spinetoram, imidacloprid, pyrethroids, cyflumetofen and the commercial mixture Engeo Pleno. Insects tested include: *Frankliniella occidentalis* , BPH, stinkbugs, *Tuta absoluta*, DBM, and *Tetranychus* mites. Four molecules were selected molecules for regulatory profile, all show an excellent profile.

Based on the above, BASF instructed its Intellectual Property team to prepare two patent applications to cover potential uses of these compounds in various aspects of agriculture. These were filed as preliminary PCTs in February, 2018. Additionally, the BASF scientists chose the three compounds shown below from the 15 submitted in 2017 for further evaluations. As part of this we prepared approximately 10g of each and submitted these materials in the beginning of May 2018.



### **3.6 Determination of CYP3A4 inhibition of additional analogs and other methylenedioxyphenyl compounds available in our chemical inventory**

#### **3.6.1 CYP3A4 inhibition assay**

Enzyme inhibition assays were conducted with a cloned CYP3A4 isozyme (BD Gentest, ON, Canada). The method described by Budzinski et al. (2000) was adopted in the present study. Three different solutions were prepared: 1) a 100 mL Solution A containing distilled water, 43 mL, NADPH ( $\beta$ -nicotinamide adenine dinucleotide phosphate) (20 mM), 6 mL, DBF (dibenzylfluorescein) (200  $\mu$ M), 1 mL and potassium phosphate buffer solution (0.5 M, pH 7.4), 50 mL; 2) a 90 mL Solution B containing distilled water, 65 mL, CYP3A4, 1 mL, and a potassium phosphate buffer solution (0.5 M, pH 7.4), 24 mL; 3) a 90 mL Solution C was identical to Solution B except that the enzyme was heat denatured, and it acted as the reading background to adjust the active assay value. Assays were performed in clear bottom; opaque-welled microtiter plates. Wells were designated as either "Control," "Blank," "Test," or "Test-Blank." Control wells consisted of Solution A, B and methanol; blank wells consisted of Solution A, C and methanol; test wells consisted of Solution A, B and dillapiol analogs at a particular concentration; and test blank wells consisted of the Solution A, C and corresponding compounds. A volume of 100  $\mu$ L of solution A was added to all wells, and followed by 10  $\mu$ L of test wells, and the same volume of Solution C was added into the remaining half of the test wells. A Millipore Cytofluor 4000 Fluorescence Measurement System set to 485 nm excitation filter (20-nm bandwidth) was used to analyze each plate after 20 mins with endpoint reading. DBF, the substrate in the assay, contained a benzyl group on the fluorescein moiety which can be cleaved by CYPs and converted to fluorescein benzyl ester. The produced ester compound could be detected under 485 nm wavelength. When the CYP inhibitor is present, the production of

fluorescein ester is blocked, therefore no fluorescence can be detected. Percent inhibition calculations were based on differences in fluorescence between the control/blank wells and test/test blank wells. All assays were performed under gold fluorescent lighting. Methanol only served as the control. Ketoconazole at 10 µg/mL was selected as the positive control.

In order to clarify the relationship between molecular structure and the IC<sub>50</sub> values of CYP3A4 inhibition, analogs were selected and grouped by structural similarity based on dillapiol and sessamol as starting materials. Inhibition calculation and statistical analysis

Percent inhibition values were calculated based on differences in fluorescence between the control/control-blank wells and test/test-blank wells by the formula:

$$[1 - (\text{Test } t=X - t=0) - (\text{Test blank } t=X - t=0) / (\text{Control } t=X - t=0) - (\text{Control blank } t=X - t=0)] * 100$$

Where t=X and t=0 are the reading values of the control/control-blank/test/test-blank wells at the end and at the beginning of running 20 min, respectively. The median inhibition percent (IC<sub>50</sub>) of each analog was determined with linear curves plotted by different concentration and percent inhibition. The dillapiol-relative inhibition activity was obtained by the formula: IC<sub>50</sub> of dillapiol / IC<sub>50</sub> of tested compound. Statistical analysis was undertaken using Graphpad Prism 5.01 software. The significant differences between dillapiol and individual compounds were determined using one-way analysis of variation (ANOVA) and Bonferroni post-hoc tests.

A standard CYP P450 inhibition assay was performed on second generation dillapiol and sesamol analogues. The IC<sub>50</sub> was found based on the linear relationship between percent inhibition and logarithm of the concentration. Dillapiol concentrations of 0.01mg/ml, 0.002mg/ml, 0.0004mg/ml, 0.00008mg/ml, 0.00004mg/ml and 0.00002mg/ml were tested. The IC<sub>50</sub> calculated from the equation of the line was found to be 9.05µM. Ketoconazole (0.01mg/ml) was tested as a positive control and yielded an inhibition of 96.2%. Methanol (10%) was also

tested as a vehicle control. All inhibition values were taken as an average over three tests. The  $IC_{50}$  value of dillapiol of  $9.05\mu M$  found for pure dillapiol compares with the  $IC_{50}$  value found in Ana Francis' (PhD Thesis 2013) bioassay of  $9.18\mu M$ , with an error of 1.42%. These similar values validate the bioassay performed in this thesis, and allow for the comparisons to the  $IC_{50}$  values obtained in Ana Francis' thesis. The positive control ketoconazole yielded an average inhibition of 101% over all bioassays conducted and allowed for comparisons to the activities of dillapiol analogues. The background level of enzyme inhibition was measured from the vehicle control (methanol, 10%) and was taken into account in the  $IC_{50}$  calculation. New enzyme and reaction solutions were prepared for each experiment to account for any discrepancy between the tests. A total of three tests per compounds were conducted in order to have ample sample size.

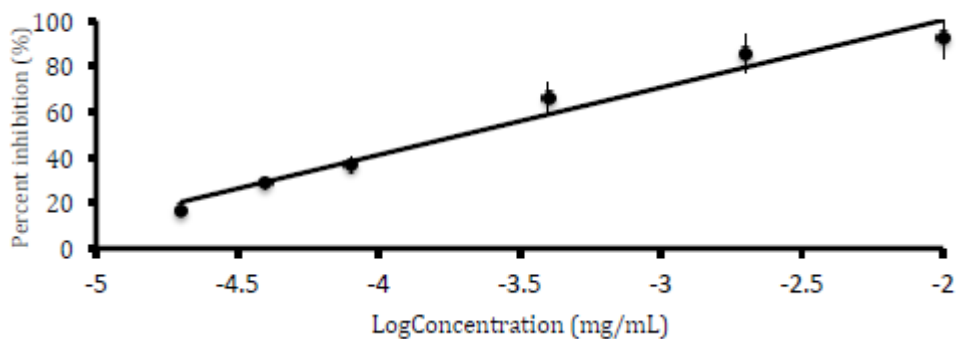
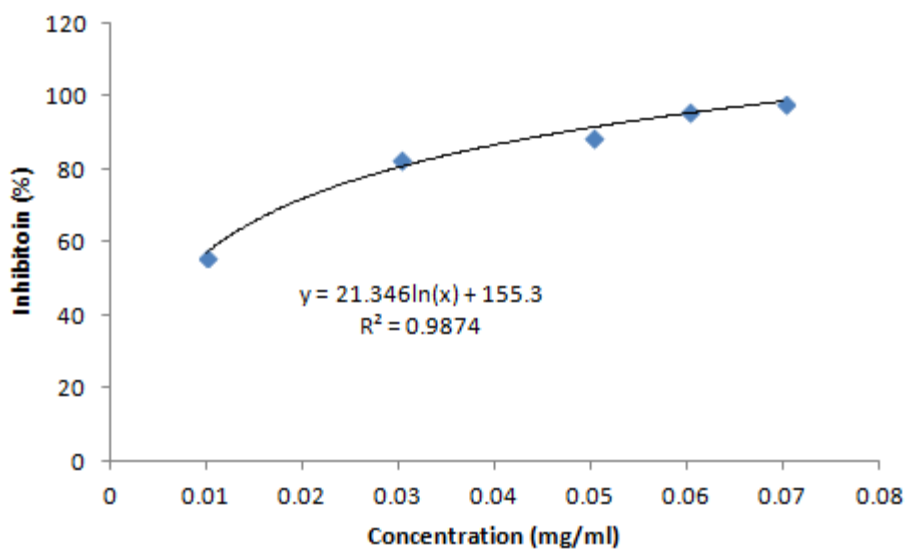
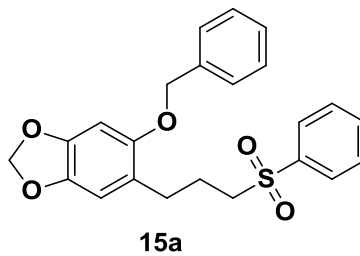


**Figure 6.** Percent inhibition of CYP 3A4 by dillapiol versus the log concentration (mg/ml). From this plot it was found that the  $IC_{50}$  of dillapiol was  $9.05\mu M$ .

An example of this calculation is shown below for:



To calculate the  $IC_{50}$  for , the concentration that provides 50% of the activity must be calculated.

$$y = 21.346 \ln(x) + 155.3$$

$$50 = 21.346 \ln(x) + 155.3$$

$$\ln(x) = -4.933$$

$$x = 0.007 \text{ mg/ml}$$

$$IC_{50} = 0.0852 \mu\text{M}$$

Considerable effort was made to ensure that the rather lipophilic molecules in are in solution for this aqueous assay. For example virtually all of the key molecules investigated had calculated (ChemDraw) log P >5 (**Figure 7**); dillapiol itself is the exception. Several examples are given below. In order to address this issue, the compounds the compounds were first dissolved in methanol and then diluted with water. This ended to 90% water and 10% water. These compounds in solution underwent sonification to ensure total dissolving.

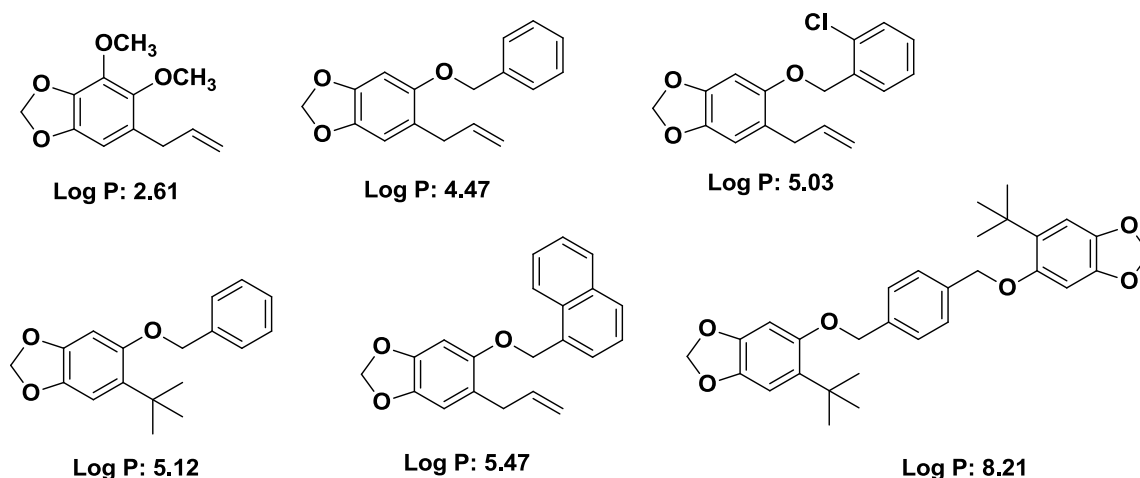


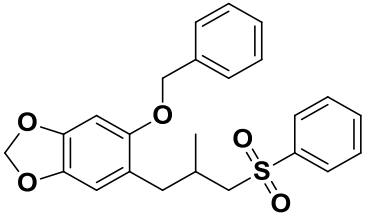
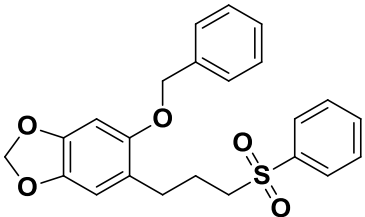
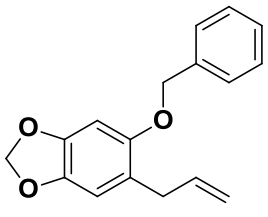
**Figure 7.** Structure of compounds synthesized with varying Log P values

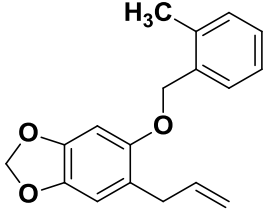
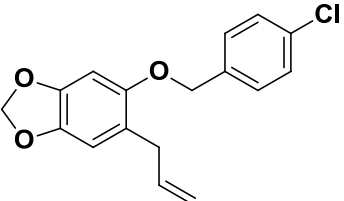
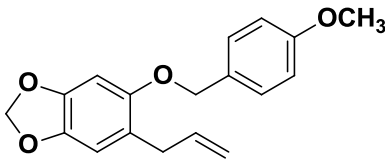
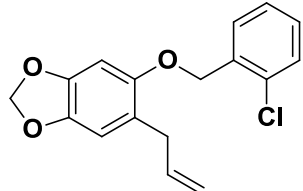
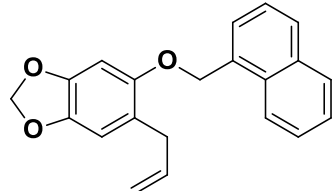
Another issue with this assay is that this assay has a light sensitive co-factor NADPH. NADPH was only opened and used in a dark room for all procedures; however, the plate reader was used under typical laboratory lighting. Thus as the plate was brought from the dark room to the plate reader, some of the NADPH was already quenched during the transportation process. Every effort was made to do this part of the assay in a consist manner The CYP3A4 enzyme from the company also results in statistical variation. The concentration of ions, properties of water organization very close to the active center of the enzyme are not always going to be one-hundred percent accurate in each batch of enzyme. Since enzyme activity is related to mass of

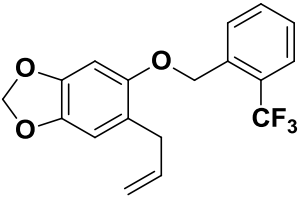
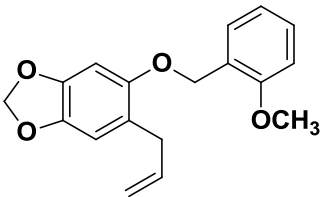
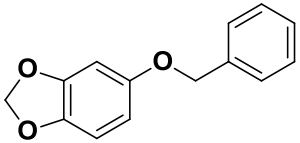
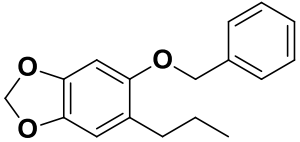
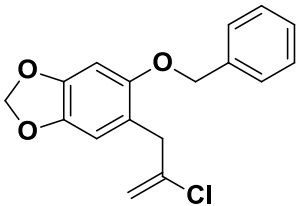
protein, it is difficult to accurately measure the mass of protein. Each of these, including the weighing of the samples introduces some uncertainty.

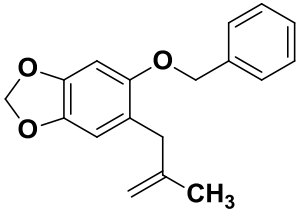
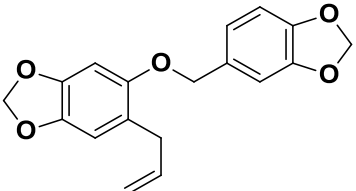
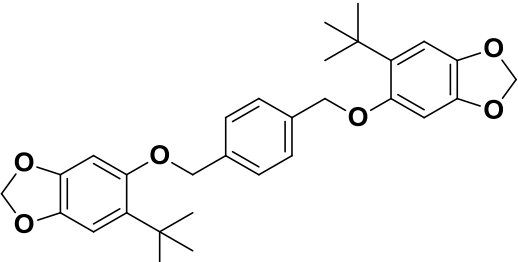
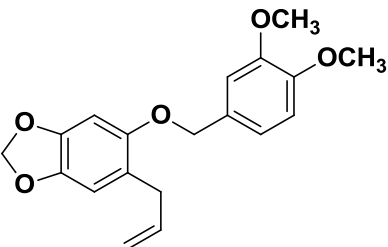
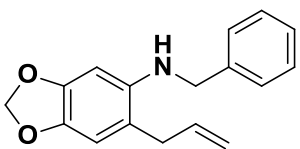
Compounds synthesized and found in the laboratory library were evaluated for CYP 3A4 inhibition activity by calculating  $IC_{50}$  value ( $\mu M$ ) and summarized in **Table 4**. For convenience purposes, the sub-groups of compounds (Ethers, Amines, Sulfones and miscellaneous) are discussed independently below.

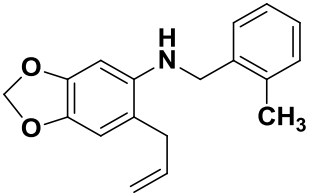
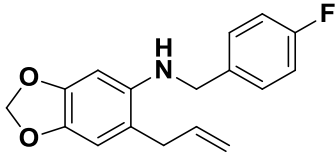
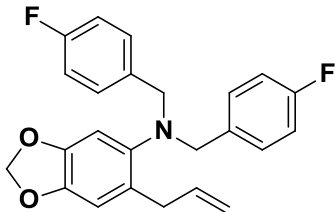
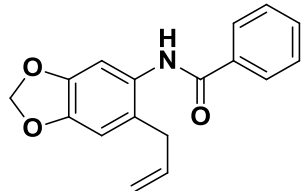
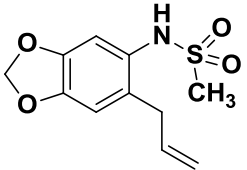
**Table 4.**  $IC_{50}$  values ( $\mu M$ ) of compounds tested for CYP3A4 inhibition. Activity relative to 21 and (=1) and activity relative to dillapiol (=1). Standard error is shown. C.I 95%, n= 3.

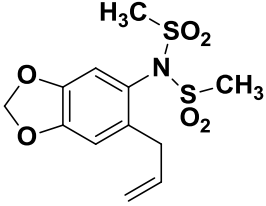
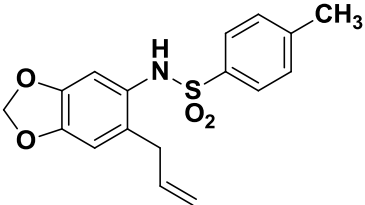
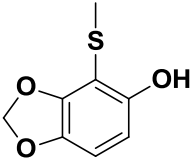
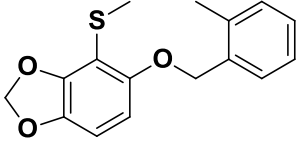
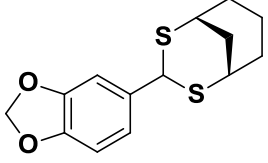
Compound Structure	$IC_{50}$ ( $\mu M$ )	Activity relative to 21 (=1)	Activity relative to Dillapiol (=1)
 <p style="text-align: center;"><b>15</b></p>	0.13±0.22	12.3X	70.0X
 <p style="text-align: center;"><b>15a</b></p>	0.085±0.05	18.8X	108.0X
 <p style="text-align: center;"><b>21</b></p>	1.8±0.38	1.0X	5.7X

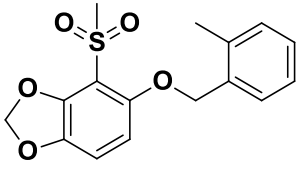
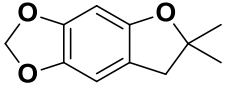
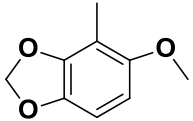
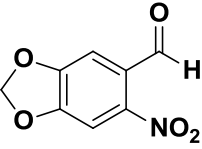
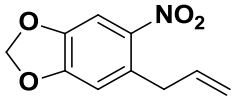
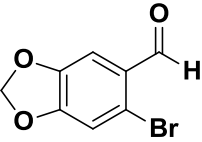
 <p style="text-align: center;"><b>22</b></p>	2.34±1.01	1.4X	8.0X
 <p style="text-align: center;"><b>23</b></p>	1.6±0.30	1.1X	6.8X
 <p style="text-align: center;"><b>25</b></p>	8.5±0.56	0.2X	1.0X
 <p style="text-align: center;"><b>48</b></p>	0.12±0.08	15.0X	86.3X
 <p style="text-align: center;"><b>49</b></p>	0.40±0.06	4.5X	25.9X

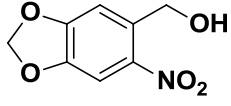
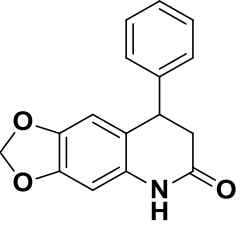
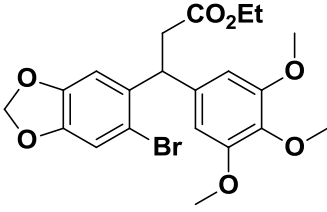
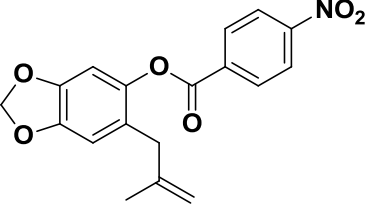
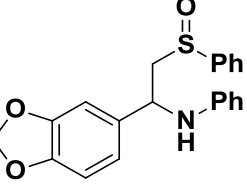
 <p style="text-align: center;"><b>50</b></p>	4.18±0.34	0.43X	2.4X
 <p style="text-align: center;"><b>51</b></p>	11.2±0.32	0.16X	0.92X
 <p style="text-align: center;"><b>52</b></p>	4.4±0.43	0.41X	2.35X
 <p style="text-align: center;"><b>53</b></p>	2.2±0.13	0.82X	4.71X
 <p style="text-align: center;"><b>54</b></p>	0.81±0.61	2.22X	12.7X

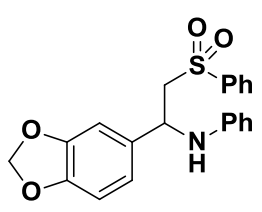
 <p style="text-align: center;"><b>55</b></p>	0.65±0.52	2.76X	15.8X
 <p style="text-align: center;"><b>56</b></p>	2.4±0.39	0.75X	4.31X
 <p style="text-align: center;"><b>57</b></p>	4.51±0.73	0.4X	2.3X
 <p style="text-align: center;"><b>58</b></p>	0.42±0.4	4.28X	24.6X
 <p style="text-align: center;"><b>61</b></p>	3.81±0.44	0.42X	2.41X

 <p style="text-align: center;"><b>62</b></p>	3.4±0.83	0.47X	2.7X
 <p style="text-align: center;"><b>63</b></p>	3.58±0.87	0.45X	2.58X
 <p style="text-align: center;"><b>64</b></p>	2.95±0.22	0.54X	3.1X
 <p style="text-align: center;"><b>65</b></p>	4.98±0.33	0.32X	1.84X
 <p style="text-align: center;"><b>66</b></p>	11.2±0.95	0.14X	0.8X

 <p style="text-align: center;">67</p>	4.96±0.37	0.32X	1.84X
 <p style="text-align: center;">68</p>	13.4±0.66	0.11X	0.63X
 <p style="text-align: center;">69</p>	10.5±0.15	0.15X	0.86X
 <p style="text-align: center;">70</p>	0.92±0.58	1.74X	10X
 <p style="text-align: center;">71</p>	5.16±0.045	0.31X	1.78X

 <p style="text-align: center;"><b>72</b></p>	4.95±0.36	0.32X	1.84X
 <p style="text-align: center;"><b>73</b></p>	12.62±1.02	0.14X	0.8X
 <p style="text-align: center;"><b>74</b></p>	8.46±1.4	0.21X	1.2X
 <p style="text-align: center;"><b>75</b></p>	14.18±0.25	0.11X	0.63X
 <p style="text-align: center;"><b>76</b></p>	10.21±0.24	0.18X	1.03X
 <p style="text-align: center;"><b>77</b></p>	14.67±0.68	0.12X	0.69X

 <p style="text-align: center;"><b>78</b></p>	13.7±1.69	0.13X	0.74X
 <p style="text-align: center;"><b>79</b></p>	7.27±0.31	0.25X	1.4X
 <p style="text-align: center;"><b>80</b></p>	4.45±0.21	0.4X	2.3X
 <p style="text-align: center;"><b>81</b></p>	13.5±1.77	0.13X	0.74X
 <p style="text-align: center;"><b>82</b></p>	9.31±0.55	0.17X	0.97X

 <p><b>83</b></p>	2.44±0.42	0.66X	3.79X
--	-----------	-------	-------

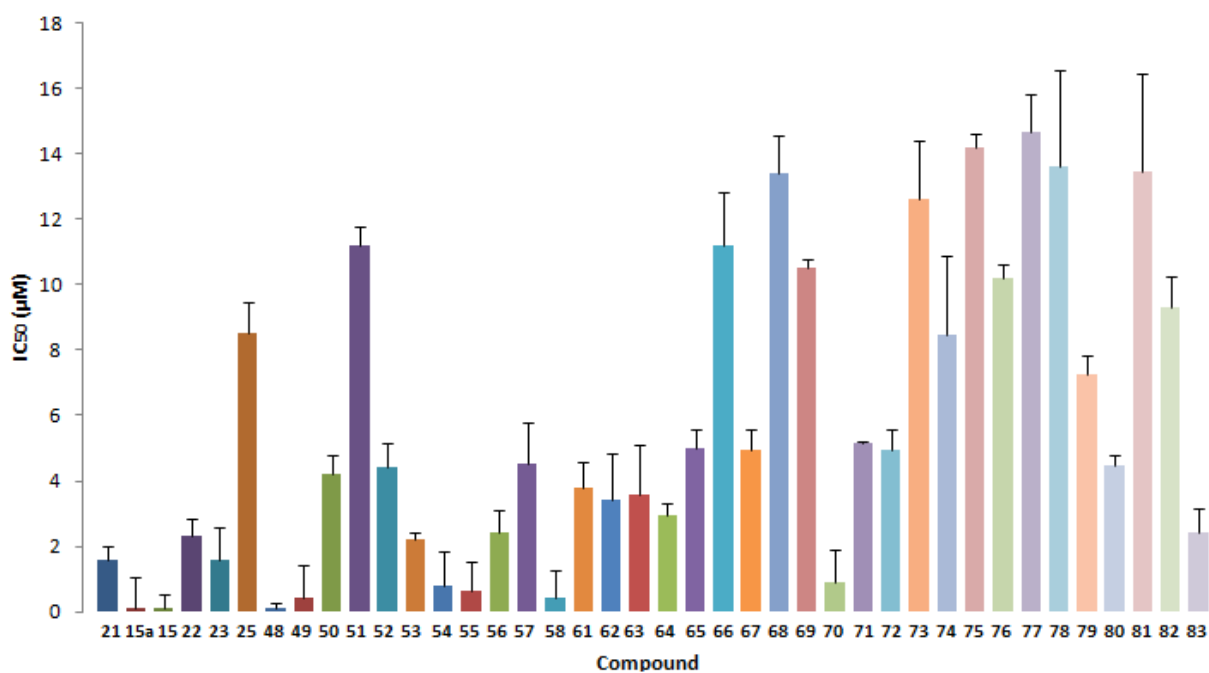


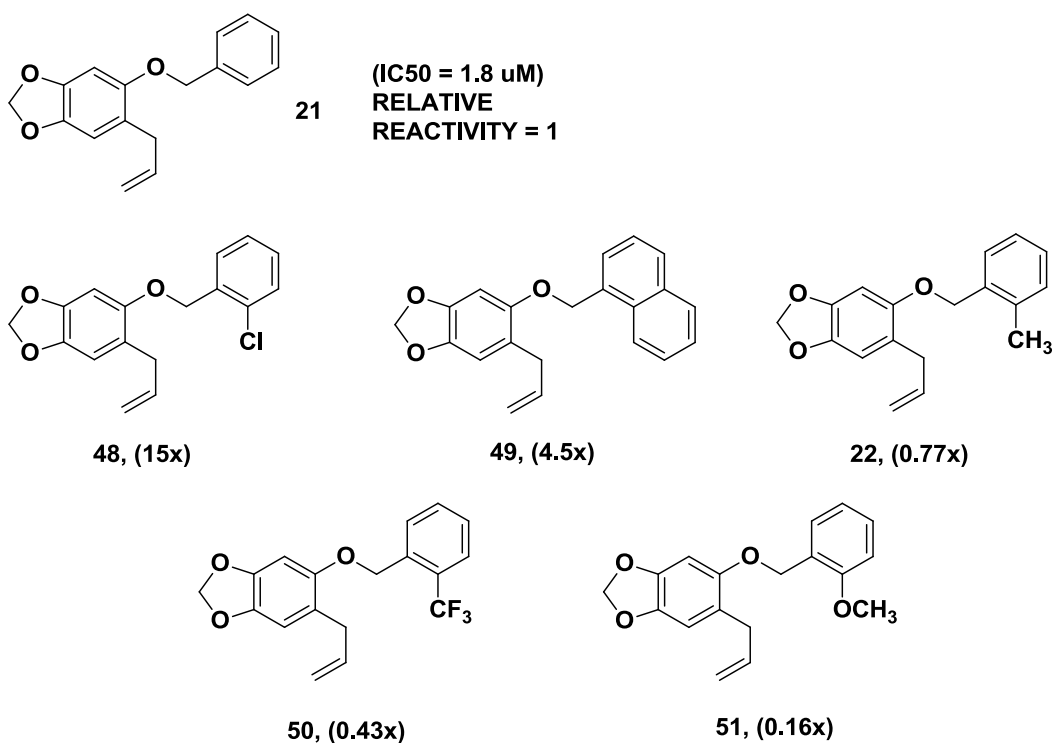
**Figure 8.** IC<sub>50</sub> values (µM) of compounds tested for CYP3A4 inhibition. A Millipore Cytofluor 4000 Fluorescence Measurement System set to 485nm excitation filter (20nm bandwidth) was used to analyze each plate after 20 minutes with endpoint reading. Standard error is shown. C.I 95%, n= 3.

### 3.6.2 Ethers

The benzylic ethers **21**, **22** and **23** were chosen in March 2018 from a larger group of fifteen compounds for field trials in Brazil. Because of the potential of these compounds and

since we had only a relatively small number of analogs it was decided to expand this group and prepare additional analogs with different substitution patterns on the aromatic ring with goal of gaining a better understanding of the influence of substituents on CYP3A4 inhibition. A potential by-product of these studies might be the discovery of one or more compounds with significantly higher CYP inhibition than the current lead structures.

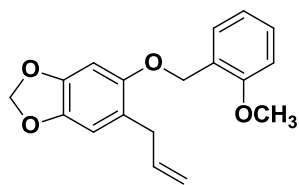
A major focus was placed on compounds which have *ortho*-substituents on the aromatic ring since **22** was 3.5 times more potent in the GST inhibition studies than **21** and roughly comparable to **21** (33% less) in their CYP3A4 inhibition. The CYP3A4 inhibition data is also included. In order to help assess the influence of *ortho*-substitution the relative activity of these compounds compared to the **21** = 1 is given together with the structures. The structures are arranged in order of decreasing potency.



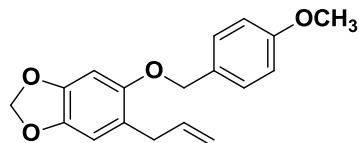
It is difficult to draw SAR conclusions based on these six compounds since we see no obvious patterns. Some compounds such as the *ortho*-chloro derivative **48** are much more potent than **21** while others, for example the *ortho*-methoxy compound **51**, is significantly less potent. The difference in potency between these two compounds is almost a factor of 100! It is hard to ascribe this to either a steric or electronic effect; the variations in logP do not explain the observed potency order.

Based on the results with the *ortho*-chloro compound we were disappointed that the *ortho*-CF<sub>3</sub> derivative **50** was much less potent. The high potency of the 1-naphthyl derivative **49** was largely unanticipated and difficult to explain in view of the data for the whole set.

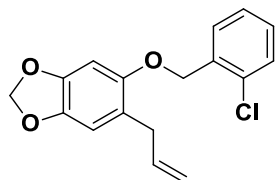
We have only two examples where we can compare the influence of a substituent in the *ortho*- vs *para*- position. In the case of the methoxy functionality, the *para*- methoxy compound **25** is slightly more active than the *ortho*-methoxy compound **51**. The *ortho*-chloro compound **48**, it is clearly much more active than the *para*-chloro **23**. At this point in time it is difficult to anticipate or explain whether a particular substituent in the *ortho*-position will inhibit CYP3A4 more than the *para*-position. A chlorine substituent, either *ortho*- or *para*-, is more effective than methoxy group in inhibiting CYP3A4.



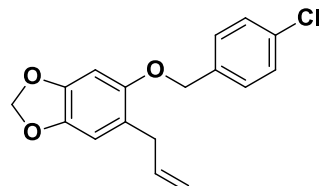
**51** 11.21  $\mu\text{M}$ , (0.16x)



**25** 9.83  $\mu\text{M}$ , (0.18x)



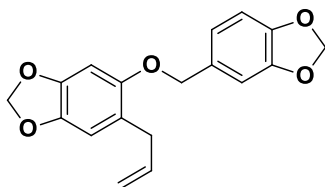
**48** 0.12  $\mu\text{M}$ , (15X)



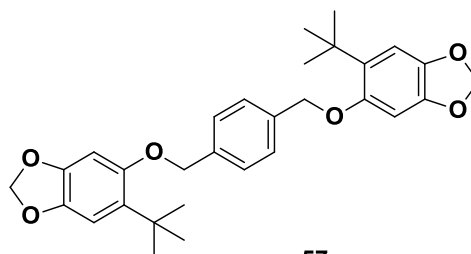
**23** 1.61  $\mu\text{M}$ , (1.18x)

The results for the remaining eight ethers are discussed below. In this group we probed the potential of having two methylenedioxyphenyl substituents in the molecule, the importance of the allyl group (**52**) at C6 and the double bond, that is allyl vs propyl (**53** vs **21**), the value of an additional substituent on the allyl group at C6 (**54** and **55** methyl).

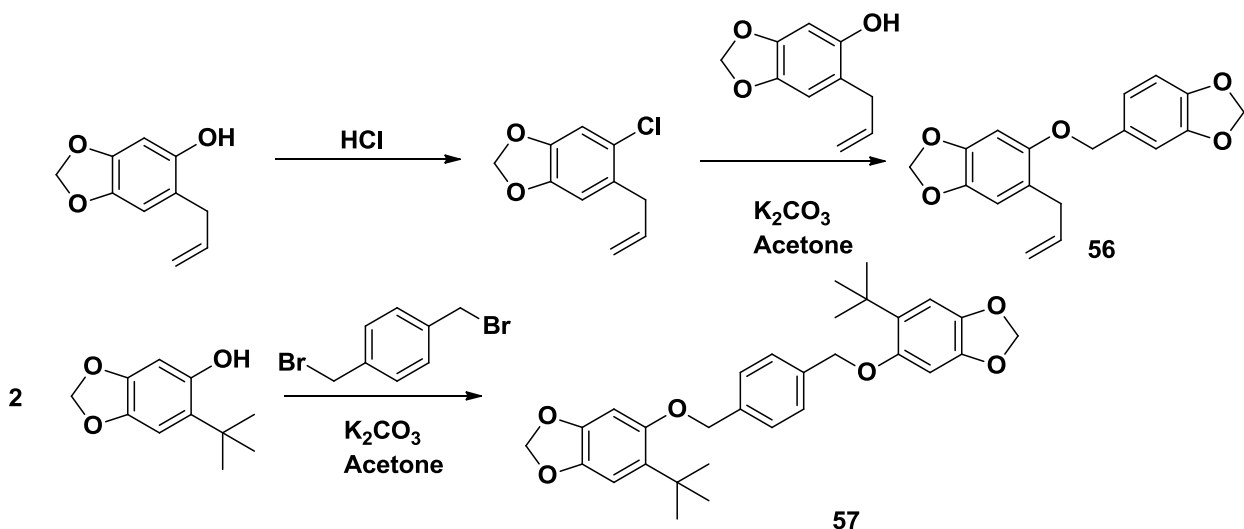
Compounds **56** and **57** each have two methylenedioxyphenyl units in the molecule. These have  $\text{IC}_{50\text{S}}$  of 2.4 and 4.5  $\mu\text{M}$ , respectively which makes them between two and four times as potent as dillapiol but less potent **21**. Thus the second MDP group does not enhance potency. The “dimer” **57** was prepared by reaction of two equiv. of *ortho*-*t*-butyl sesamol with 1 equiv. of 1,4-dichloromethylbenzene.



**56**  
2.4, 0.75X

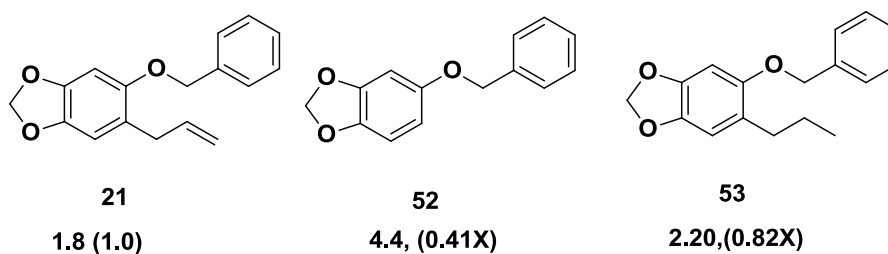


**57**  
4.51, 0.4X

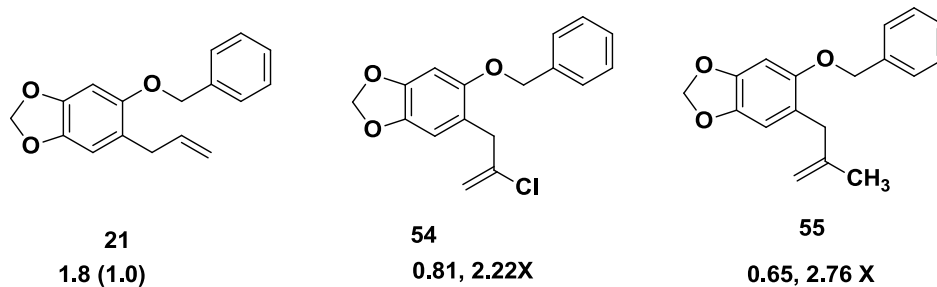


**Scheme 9.** Preparation of compounds **56** and **57**

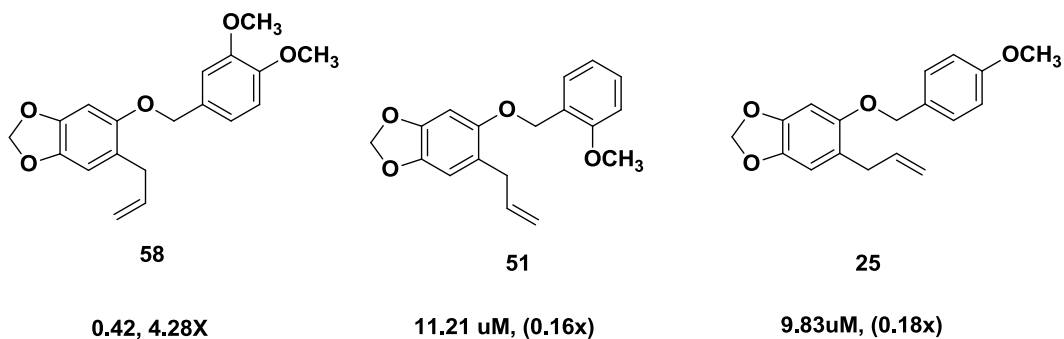
Comparison of **21** vs **53** indicates that unsaturation in the C6 side chain, allyl vs propyl, is helpful. We took it a step further back and compared importance of the allyl group or propyl group at C6. These compounds show relatively similar potency with the **52**, which lacks a substituent at C6 being the least and **21** which has the allyl group at C6 the most active.



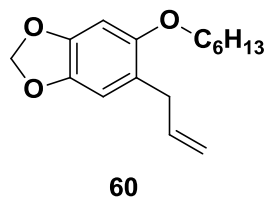
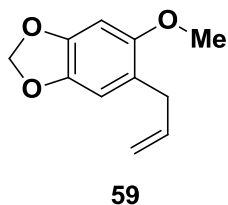
The  $IC_{50}$ 's for compounds **21**, **54** and **55** indicates that an additional substituents at C2' of the allyl side chain improve inhibition of CYP3A4. Although we have only two examples at this stage, one is tempted to conclude that the reason for the somewhat greater activity of the **55** is due to a greater steric requirement of the methyl group. Carballo<sup>30</sup> also concluded that an increase in the size of the substituents at C6 gave an increase in the potency of her compounds.



The rather high potency of the 3,4-dimethoxyphenyl derivative **58**, 4.3 times more potent than **21**, was very surprising considering that both the *ortho*- and the *para*- methoxy compounds, **51** and **25** were much less potent than **21**. Compound **58** is 27 and 20 times more potent than **51** and **25**, respectively. Taken at face value this suggests that the *meta*- methoxy substituent has a very positive effect on the inhibition, sufficient to more than overcome the negative effect of a methoxy group either *ortho*- or *para*-.

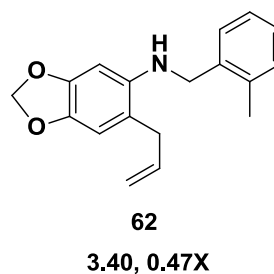
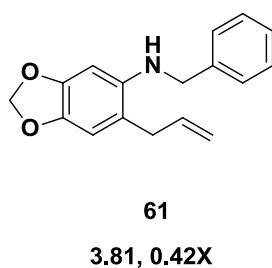
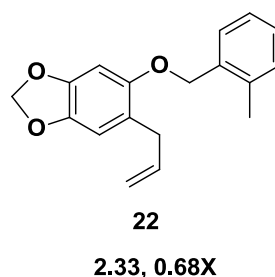
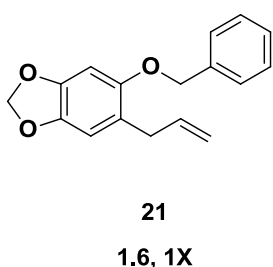


The discussion above focused on benzyl ethers. Carballo prepared a series of ether, **59** and **60** derived from sesamol and evaluated their ability to inhibit CYP3A4. These compounds where R is CH<sub>3</sub> and C<sub>6</sub>H<sub>13</sub> showed only modest potency in comparison to dillapiol with the methyl ether showing a 50% decrease, the hexyl ether a 6.4 and 4.8 fold increase, respectively, relative to dillapiol. Carballo also determined that IC<sub>50</sub> for **21** was 4.8 times that of dillapiol; this compares to 5 times obtain in this thesis.

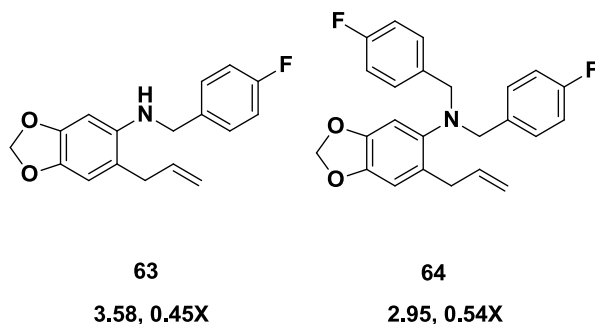


### 3.6.3 Amines and Amides

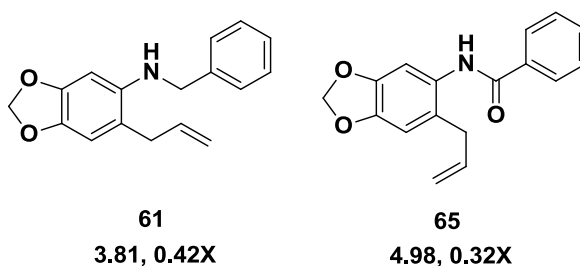
The CYP3A4 inhibition studies for this group of compounds are summarized below. All of the compounds are less potent than the ether **21**. These set of compounds can be categorized into amines, amides and sulfonamides. The amines, **61** and **62** all were moderately potent as CYP3A4 inhibitors as these compounds are all more potent than dillapiol but less potent compared to **21**. This could be a result of the -NH group or nitrogen atom. Compound **61** resembles **21**, and **62** resembles **22** the only difference is that an oxygen atom is replaced with a nitrogen atom. It is concluded that replacement of oxygen by nitrogen atom negatively inhibits CYP3A4 inhibition activity. The IC<sub>50</sub> of **61** is 3.81 which is 0.42 times of **21** and IC<sub>50</sub> of **62** is 3.40 which is 0.47 times of **22**.



The most potent amino compound is **64** with an  $IC_{50}$  of 2.95  $\mu$ M which was expected to be the most potent as this compound contains two bulky substituent and it is a tertiary amine. Compound **64**, was slightly more potent as a CYP3A4 inhibitor compared to **63**.

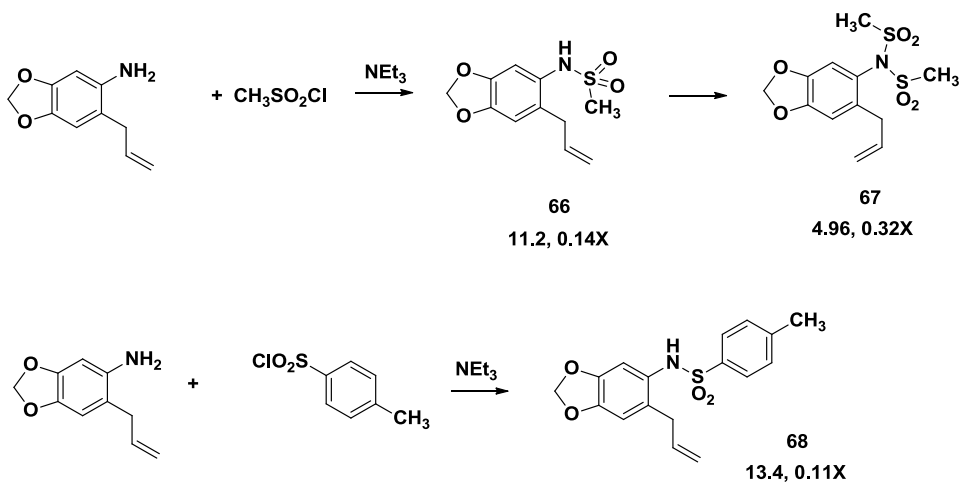


The amide **65** has an  $IC_{50}$  of 4.98  $\mu$ M, which is still better than dillapiol but not more potent than **21** or the amines mentioned above. Compound **65** contains an electron withdrawing group and electron density is withdrawn from the benzyl ring. The rationale was to determine whether electron withdrawing group would have any effect in CYP3A4 inhibition. Since only one compound was synthesized it is difficult to determine at this time if having an electron withdrawing group does indeed inhibit CYP3A4 more than an electron donating group; however, based on the result below, it only slightly decreased CYP3A4 inhibition.



The sulfonamides, shown below, were prepared by reacting the amino precursor with methanesulfonyl chloride and tosyl chloride in DCM in the presence of trimethylamine. In the first case both the mono and disulfonamide **66** and **67** were obtained. The sulfonamide group like

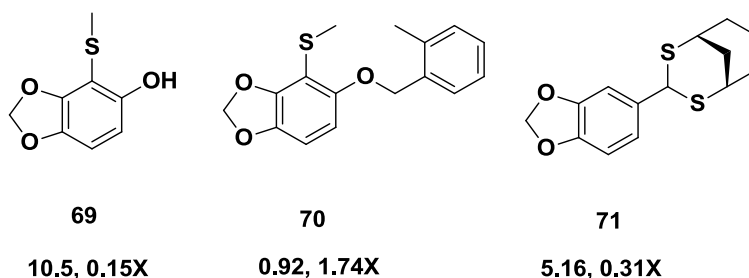
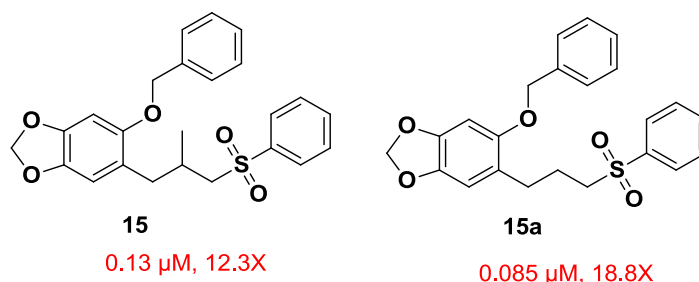
the benzoyl group exerts an electron withdrawing effect on the nitrogen. All of these compounds are somewhat less potent as CYP3A4 inhibitors but not significantly different than the basic amines such as **61**.



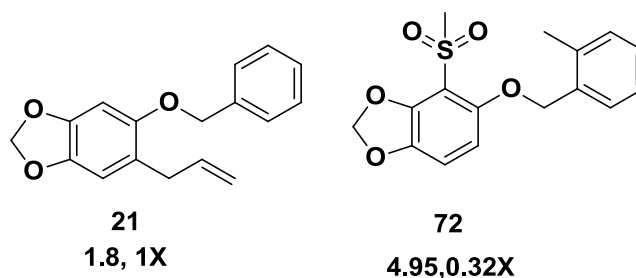
**Scheme 10.** Preparation of sulfonamides

### 3.6.4 Sulfides and Sulfones

The structures these groups of compounds are shown below. Several compounds are roughly comparable to **21**, but none are more potent. Sulfones groups when part of the substituents at C6 of the MDP structure such as **15** and **15a** and their analogs derived from dillapiole<sup>30</sup> are the most potent CYP3A4 inhibitors that our group has prepared during this project. Not surprisingly, sulfide **70** which has the same C5 substituent as **22** gave an IC<sub>50</sub> value of 0.92 μM which is 1.74 times as potent as **21**. Compounds **15** and **15a** are 12 times and approximately 19 times more potent as CYP3A4 inhibitors respectively, when compared to **21**.



Compound **72** was prepared by oxidizing compound **70**. In this case the conversion of sulfide to sulfone reduced CYP3A4 inhibition by a factor of about 6.



### 3.6.5 Miscellaneous methylenedioxyphenol compounds

These methylenedioxy compounds shown below were available from earlier projects in our lab except **82** and **83**. It was decided to test these for their CYP3A4 inhibition activity with the possibility of finding a new lead structure. Unfortunately, none stood out as CYP3A4 inhibitors. One can however conclude, that virtually all compounds containing the critical MD unit irrespective of other substituents will likely inhibit CYP3A4 with  $IC_{50}$  at about 10  $\mu$ M or

about the same as dillapiol which has an  $IC_{50}$  of  $(8.9 \pm 0.3)$  and is 0.2 times as potent as the ether

21.

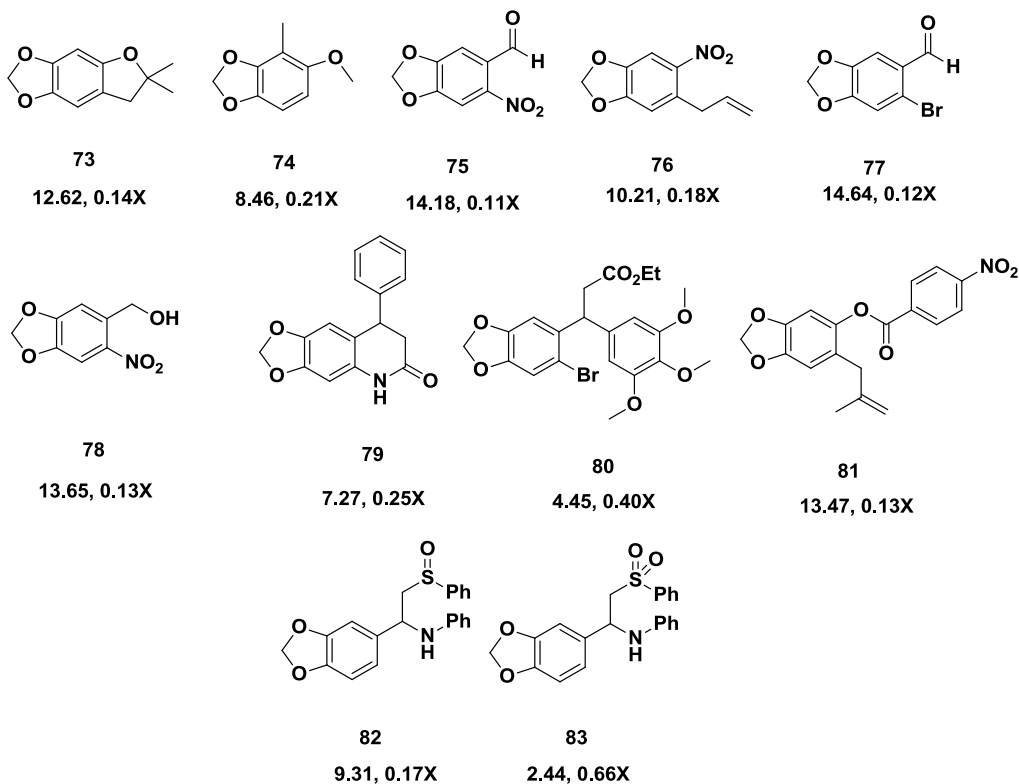
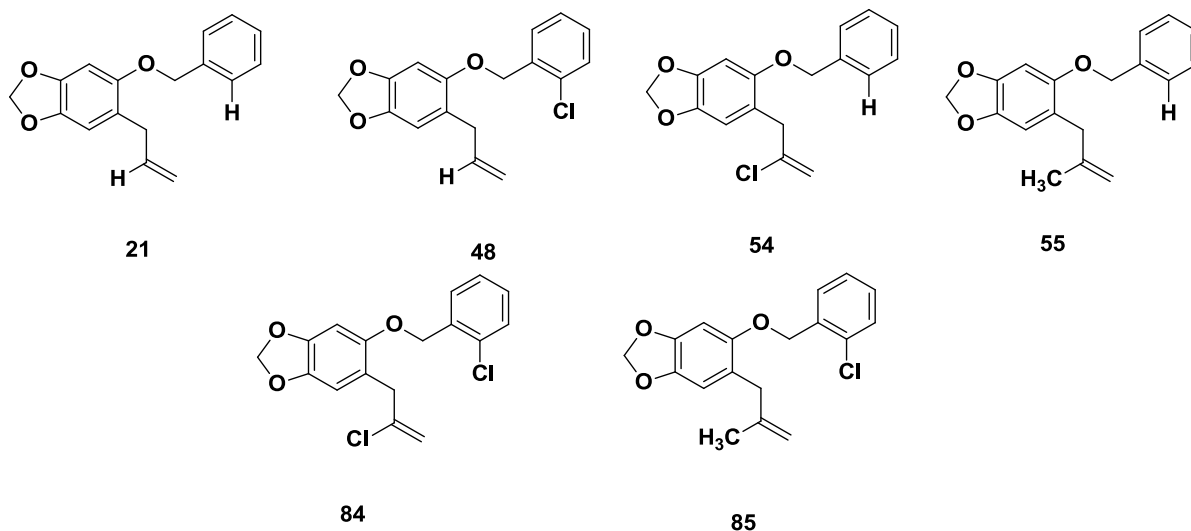


**Figure 9.** Miscellaneous MDP compounds and their relative CYP3A4 inhibition relative to **21** = 1.

#### 4.0 Conclusions and proposals for additional studies.

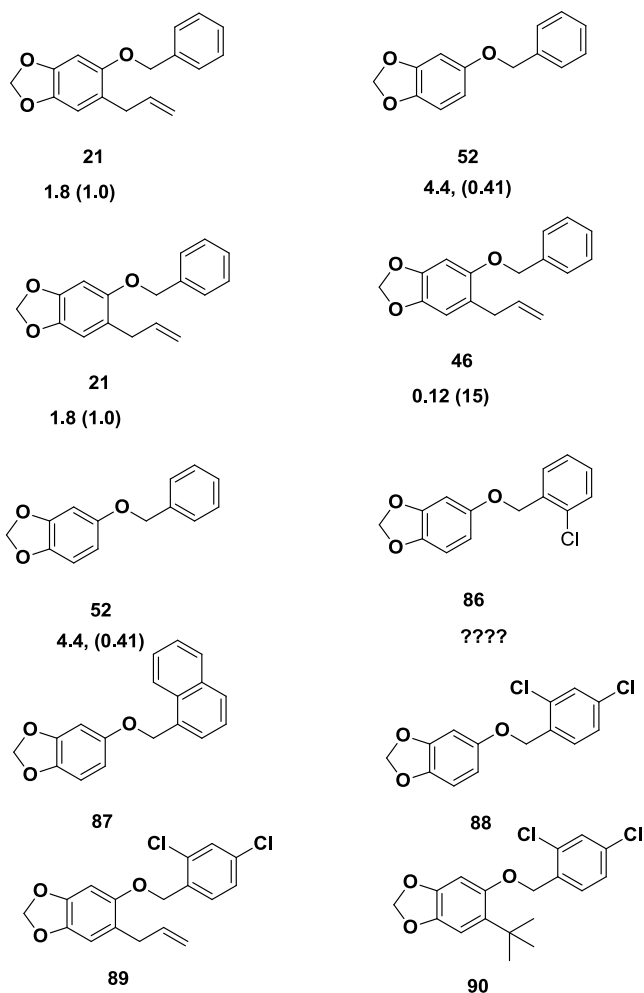
The ethers beginning with the lead compound **21** appear to have the most potential as insecticide synergists. They are significantly more potent inhibitors of CYP3A4 than dillapiol itself and have also been shown to inhibit insect GSTs much more strongly than the typical know electrophilic GST inhibitors.

During this study we have discovered that some *ortho*- substituents on the benzyl ether group at C5 increase potency relative to **21** with the the *ortho*-chloro derivative **48** being 15 times more potent than **21**. We have also observed that adding a substituent to the allyl group C6 of the MDP ring is also helpful with **54** and **55** being between 2 and 3 times more potent than **21**. It would seem plausible that a combination of these two structure feature as seen in **84** and **85** should yield even more potent compounds.



The *o*-chlorobenzyl derivative **54** is almost as potent an inhibitor CYP3A4 as are the sulfones **15** and **15a**. From a purely practical point of view, the ethers are much superior since they can be synthesized in a relatively simply three step sequence whereas the preparation of **15** and **15a** requires five steps, both starting from sesamol.

The ether **52** has almost 50% of the CYP3A4 activity of **21**. It should be kept in mind that this compound can be prepared in a single step from sesamol compared to the three steps required for the synthesis of **21**. It might be worthwhile to prepare a series of analogs of **52** including the *ortho*-chloro derivative **86** to see if the increase in the inhibition potency in going from **21** to **46** is translated to the pair **52** to **86**.



As mentioned in the Discussion, we were surprised that eighteen compounds derived from dillapiol and sesamol which were tested by Dr. Liu were potent inhibitors of insect GSTs. During the preparation of this thesis we had occasion to search “GST inhibitors” on the Internet. We discovered a large number of entries including reviews titled “The role of glutathione-S-

transferase in anti-cancer drug resistance<sup>31</sup> and Glutathione transferases: substrates, inhibitors and pro-drugs in cancer and neurodegenerative diseases.<sup>31</sup> We recognize that there are many versions of human GST and that these differ from insect GSTs. Nevertheless, since the compounds described in this thesis differ so drastically in structure and reactivity from the typical electrophilic inhibitors it would seem to us that it might be worth finding out if our compounds also inhibit human GSTs, ideally with some selectivity between the various forms. If so, would these compounds have potential applications in the human health field?

In recent findings it was proposed that GST inhibition plays an important part in xenobiotic detoxification, clearance of oxidative stress and modulation of cell proliferation and apoptosis signalling pathways.<sup>31</sup> These wide ranging functional properties may be used to modulate tumor cells drug resistance.<sup>31</sup> Over expression of GST in tumors was considered as a possible mechanism of tumor cell drug resistance and thus GST inhibitors remain a potential therapeutic tool in cancer cell resistance to drugs.<sup>31</sup> It was only during the time of writing this thesis that we managed to figure the wide functionalities of these compounds as cancer therapeutic agents. This represents yet another potential application for these compounds.

## 5.0 Reference

1. Ntalli, N. G. & Menkissoglu-spiroudi, U. Pesticides of botanical origin: A promising tool in plant protection. *Pesticides-Formulations, Effects, Fate* (2011).
2. Sifakis, S., Mparmpas, M., Soldin, O.P. & Tsatsakis, A. Pesticide Exposure and health related issues in male and femal reproductive system. *Pesticides-Formulations, Effects, Fate* (2011).
3. Ecobichon,D.J. Pesticide use in developing countires. *Toxicology* 160, 27-33 (2011)
4. European, C. Our food has become greener. (2009)
5. Lewis, W. M.J evolutionary interpretations of allelochemical interactions in phytoplankton algae. *The Americain Naturalist* 127, 184-194 (1986)
6. Isman, M.B. Botanical insecticides, deteerants, and repellents in modern agriculture and an increasingly regulated world. *Annual review of Entomology* 51, 45-66 (2006)
7. Dos Santos, P.R., De Limas Moreira, D., Guimares, E.F. &Kalpan, M. A essential oil analysis of 10 Piperaceae species from the brazillian Atlantic forest. *Phytochemistry* 58, 547-51 (2001)
8. C, Bernard, H.G. Krishnamurty, D. Chauret, I. & Durst, B.J.R. Philogene, j P. S.anchez-Vindas, C. Hasbun, L. Proveda, L. San Roman, and J.T. A. Insecticidad defenses of Piperaceae from the neotropics. *Journal of Chemical Ecolog*, 21, 803-814 (1995)
9. De Almeida, R.R.P., Souto, R.N.P., Bastos, C.N., Da silva, M.H.L. & Maia, J.G.S Chemical variation in Piper aduncan and biological properties of its dillapiol-rich essential oil. *Chemistry & biodiversity* 6, 1427-34 (2009)
10. Martinez, J., Rosa,P.T.V, Ming, L.C., Marques, M.O.M & Angela, M. Extraction of volatile oil from Piper aduncum L. With supercritical carbon dioxide. (2013)
11. Yu, S J, Terriere, L.C. Bimodal Effect of Methylenedioxyphenyl on Detoxifying Enzymes in the. *Pesticide Biochemistry and Physiology* 4, 160-169. (1973)
12. Casida, J.E. Mixed –function oxidases involvement in the biochemistry of insecticide synergists. *Journal of Agricultural and Food Chemistry* 18, 753-72 (1970)
13. Scott, J. G. & Wen, Z. Cytochromes P450 of insects: tip of the iceberg. *Pest Management Science* 57, 958-67 (2001)
14. Sun, Yun-Pei, Johnson, E.R. Synergistic and antagonistic actions of insecticide-synergist combinations and their mode of action. *Journal of Agricultural and Food Chemistry* 8, , 261-266 (1960)
15. Murray, M. Modulation of Cytochromes P450 by phytochemicals. *Cytochromes P450: role in the metabolism and toxicity of drugs and other xenobiotics*. RCS Publishing. First Ed. (2008).
16. Martin,J. Cytochrome P450 druginteractions: are they clinically relevant? *Australian Prescriber- An independent review*.24:10- 2(2001)

17. Ogu,C., & Maxa, J. Drug interactions due to cytochrome P450. Baylor University Medical Center Proceedings.;3(4):421–423. (2000)
18. Budzinski, JW., Foster BC., Vandenhoeck, S., & Arnason, JT. An *in vitro* evaluation of human cytochrome P450 3A4 inhibition by selected commercial herbal extract and tinctures. . *Journal of Phytomedicine*;7(4):273-82. (2000)
19. Liu, SQ., Scott, IM., Pelletier, Y., Kramp, K., Durst, T., Sims, SR., & Arnason, JT. Dillapiole: A pyrethrum synergist for control of the Colorado potato beetle.. *Journal of Economic Entomology*;107(2):797-805. (2014)
20. Belzile AS., Majerus SL., Podeszinski C., Guillet G., Durst T., & Arnason JT. Dillapiole derivatives as synergists: structure--- activity relationship analysis. *Pestic. Biochem. Phys.*; 66:33-40. (2000)
21. isman, M.B. Botanical insecticides: for richer, for poorer. *Pest Manag Sci* 11, 8-11. (2008)
22. Horton MK., Rundle A., Camann DE., Barr DB., Rauh VA., Whyatt RM. Impact of Prenatal Exposure to Piperonyl Butoxide and Permethrin on 36- Month Neurodevelopment. *American Academy of Pediatrics*; 127(3): 699-706.
23. Page SW. *Small Animal Clinical Pharmacology: Chapter 10- Antiparasitic Drugs*. Elsevier. 2<sup>nd</sup> edition 2008: 198-260. Print
24. Tomar, S.S., Maheshwari, M.L & Mukaerjee, S.K. Synthesis and Synergistic activity of dillapiol based pyrethrum synergists. *Journal of Agriculture and Food Chemistry* 27, 547-550 (1979).
- 25..Majerus, SL. A novel synthesis of dillapiol and its derivatives and their role as chemosensitizers and insecticide synergists. Master Thesis. Ottawa University. 133 (1997)
26. Onufrieva KS, Thorpe KW, Hickman AD, Leonard DS, Roberts EA, Tobin PC. Persistence of the Gypsy Moth pheromone, Disparlure, in the Environment in various Climates. *Insects*. 4(1): 104-116 (2013)
27. Ryall KL, Fidgen JG, Silk PJ, Scan TA. Efficacy of the pheromone (3Z)- lactone and the host kairomone (3Z)- hexenol at detecting early infestation of the emerald ash borer, *Agrilus planipennis*. *Entomologia Experimentalis et Applicata*. 147:126-131. (2013)

28. Francis AC, Liu Suqi, Pineda N, Raina V, Liu R, Jackiewicz V, Carranza D. Structure activity relationship of CYP inhibitors derived from dillapiol and sesamol. *Journal of agriculture and food chemistry*.(2018) submitted.
29. Kerr JA. Bond Dissociation Energies by Kinetic Methods. *Chem Rev.* 66(5), 465-500. (1966)
30. Carballo, AF. A novel synthesis of dillapiol and its derivatives and their role as chemosensitizers and insecticide synergists. Master Thesis. Ottawa University. 133 (1997)
31. Mathew N,; Kalyanasundaram M,; Balaraman K. Glutathione S-transferase (GST) inhibitors. *Expert Opin.Ther.Patents.* 16(4) (2006)
32. Townsend DM,; Tew KD. The role of glutathione-S-transferase in anti-cancer drug resistance. *Oncogene*, 47:7369-75 (2003)

## **PART B. Synthesis of analogs of Z02; compounds with potential to help regenerate partially severed spinal cords.**

### **6.0 Introduction**

#### **6.1 Spinal Cord Injury**

Every year, 250,000 to 300,000 people suffer from a spinal cord injury (SCI) worldwide<sup>1</sup>. The spinal cord is a highly organized set of nerve cells connecting sensory and motor reflexes from the point of sensation to the brain. The term spin-cord injury refers to damage to the spinal cord resulting in trauma or a form of disease or neurodegeneration. The majority of SCI is due to traumatic cases with the prevalence of non-traumatic cases increasing every year. Non-traumatic cases refer to diseases such as, tumor growth, inflammation or infection that arises in an individual.

Symptoms of SCI depend on the location of the injury on the spinal cord as well as the severity of the damage. These may include partial or complete loss of sensory function or loss of motor control in the upper, lower extremities and/or torso (body).<sup>1</sup> Some severe SCI affect vital systems that regulate breathing, heart-rate, blood pressure, bowel and bladder movements. Spinal cord injury can be associated with many secondary conditions that can be physically debilitating and even life-threatening which include deep-vein thrombosis, respiratory complications, urinary tract infections etc<sup>1</sup>. Acute health care and rehabilitation services are essential for prevention and management of these conditions<sup>1</sup>. SCI does not only affect the functionality of one's life but it also has a major impact on the socioeconomic and psychological aspects of living. For example,

impairment can cause mental strain, and the cost of medical treatment and mobility devices can become a major financial burden.

Although the majority of traumatic SCI cases are highly preventable, it is one of the most physiologically debilitating impairments due to the inability of the neurons to regenerate in the central nervous system (CNS). Individuals suffering from traumatic SCI cases are a result of injury induced neuroplasticity. Many studies are unraveling the rationale behind the deterrent physiological functionality and the possibility of therapeutic strategies is becoming more accessible. Spontaneous recovery after a spinal cord injury through neuronal rewiring is highly unlikely, however; theories behind neuroplasticity during growth have led to the possibility of inducing neurological recovery.

Dr. Arthur Brown is a scientist at the Robarts Research Institute at University of Western Ontario who is involved in unravelling the mystery behind genetic regeneration pathways of the spinal cord after injury<sup>1</sup>. His group has revealed how manipulating the regulation of regeneration-inhibiting enzymes can lead to partial functional recovery of damaged neurons in the CNS.

Currently, other than life support, there are no approved treatments for spinal cord injury, however; it has been demonstrated that after spinal cord injury, damaged axons of neurons can grow and re-wire damaged spinal circuits but are prevented from doing so due to the presence of axon repelling molecules<sup>2</sup>. The main inhibitory molecules are the chondroitin sulfate proteoglycans (CSPGs) produced by activated astrocytes responding to the SCI<sup>2</sup>.

## 6.2 Neuronal Regeneration Inhibition

In a normal healthy nervous system, astrocytes will secrete enzymes that facilitate the growth and generation of neurons and neuronal connections and other enzymes prevent the proper growth and neuronal connection formation<sup>20</sup>. The major class of enzymes involved in these processes are the chondroitin sulfate proteoglycans which are comprised of a protein core acting as a scaffold for many glycosaminoglycans (GAG) chains that branch off to act as axonal growth guides by creating barriers to this growth. Proteoglycan intervention fluctuates through the development of the CNS, as maturity is reached, plasticity will begin to decline which results in a decrease in enzymes that promote growth and an increase in enzymes that inhibit growth<sup>20</sup>. Fibronectin and laminin are two other important enzymes that promote growth and repair mechanisms, found in the developing neural networks<sup>20</sup>.

Since astrocytes have the ability to secrete generation promoting and generation inhibiting enzymes, generation is dependent on the amount of generating and inhibiting enzymes<sup>21</sup>. In SCI, astrocytes produce glial scar tissue at the damaged site which becomes involved in the upregulation of many extracellular matrix molecules, including CSPGs and the activity of newly abundant inhibitory enzymes dominates the generation enzymes.

In recent studies, chondroitinase, an enzyme that digests GAG chains of CSPGs into disaccharide units has been utilized for the development of SCI treatment. Although, this degradation enzyme has proven to promote growth of damaged spinal cords in animals by decreasing levels of CSPGs, it also does not fully eliminate inhibitory activity. This is the reason researchers have been more involved in focusing on targeting the regulation pathways of CSPG synthesis<sup>19</sup>.

### 6.3 Chondroitin sulfate proteoglycans and regulation pathway

Chondroitin sulfate proteoglycans are a class of extracellular matrix (ECM) macromolecules that consists of a common central core protein with a variety of chondroitin sulfate side chains<sup>3</sup>. Chondroitin sulfate side chain synthesis is activated by the addition of a xylose moiety to a serine amino acid of the core protein catalyzed by the enzyme xylosyltransferase-I and xylosyltransferase-II (XT-I and XT-II)<sup>4</sup>. These side chains are sulfated by the enzyme chondroitin 4-sulfotransferase (C4ST)<sup>5</sup>.

Chondroitin sulfate proteoglycans are the main components of the scars that forms at the lesion site after SCI and of perineural nets (PNNs), which are highly condensed matrices that surround cell bodies and dendrites of some classes of neurons<sup>6</sup>. Neurons and glia of some cells produce CSPGs and other components of PNNs<sup>7</sup>. One function of CSPGs in PNNs is to stabilize synapses by preventing axonal sprouting onto targets after the connections are made<sup>7</sup>. CSPGs are present in adult CNS and expression levels are greatly increased following SCI<sup>8</sup>.

Specific CSPGs have been shown to inhibit neurite outgrowth including: NG2, Versican, neurocan, brevican and phosphocan<sup>10-13</sup>. In a few studies, it has been shown that the digestion of chondroitin sulfate side chains by chondroitinase or by inhibiting XT-I increases axonal regeneration in mouse models after SCI<sup>14-19</sup>. From this, Dr Brown and his laboratory identified that SOX9, a transcription factor was responsible for the up-regulation of the expression of the enzymes XT-I, XT-II and C4ST in active astrocytes<sup>3</sup>.

## 6.4 SOX9 conditional knockouts improve neurological recovery

Loss of function experiments confirmed the idea that SOX9 transcription factor is directly involved in the up-regulation of generation inhibiting enzymes. To carry out this experiment, two mouse strains were used, the first that contains a floxed SOX9 alleles (exons 2 and 3 of SOX9 surrounded by loxP sites)<sup>31</sup>. Second, a tamoxifen-inducible Cre recombinase conditional SOX9 knock-out model, because traditional SOX9 knock-out mice were unable to survive without a proper CNS development. By breeding the (SOX9<sup>fllox/fllox</sup>; CAGGCre-ER) in which tamoxifen administration, followed by SCI allowed the Brown group to examine the molecular, cellular and neurological responses to SCI in the presence of reduced levels of SOX9<sup>31</sup>. The SOX9<sup>fllox/fllox</sup> mice that do not carry the CAGGCre-ER allele served as controls as they express normal levels of SOX9<sup>31</sup>. These mice models were exposed to a Thoracic -9 (T9) spinal segment injury using infinite Horizons Impactor and many experiments were run during a 14 day period.

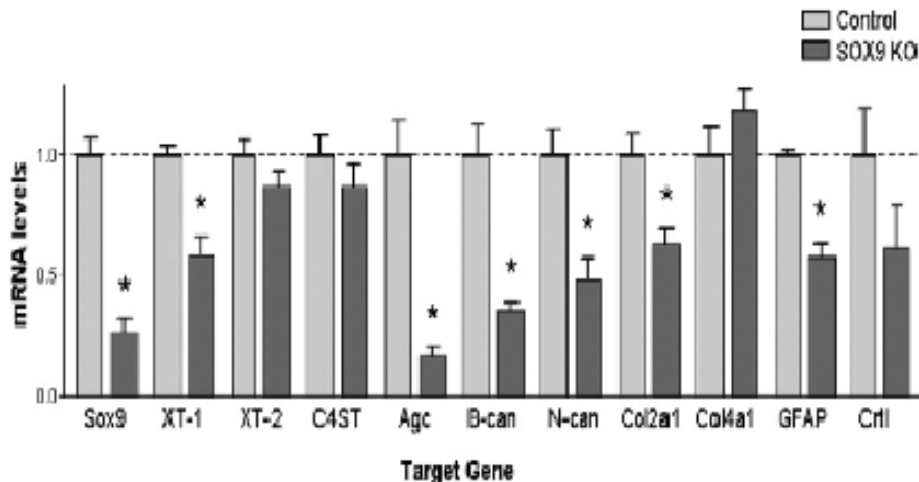


**Figure 10.** mRNA levels of specific inhibitory enzymes in SOX9 conditional knock-out and control mice with healthy spinal cords. Cell cultures were treated with 4-hydroxytamoxifen for one week and incubated for another week. The levels of mRNA were then measured for SOX9 and known inhibitory proteins<sup>23</sup>.

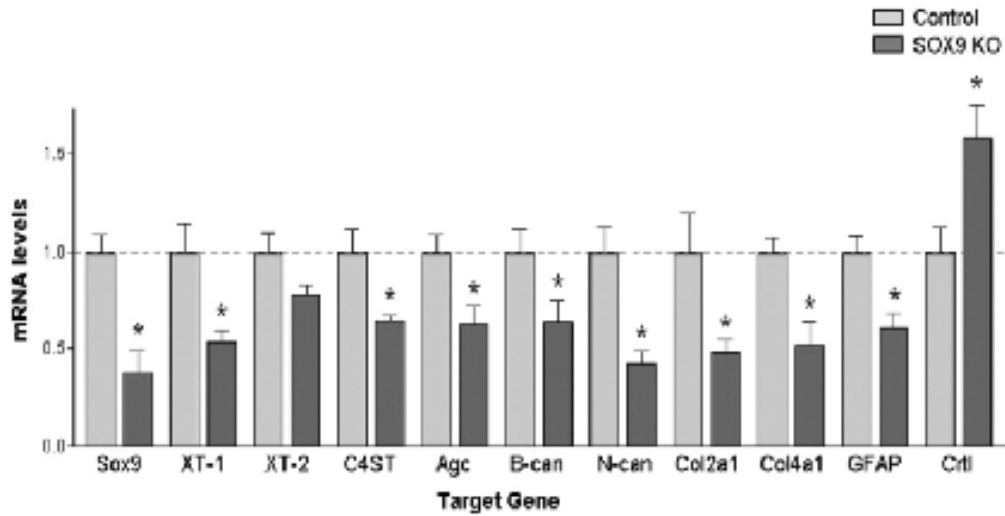


**Figure 11.** mRNA levels of specific inhibitory enzymes in SOX9 conditional knock-outs and control mice with T9 SCI. Cell cultures were derived from the SCI and treated with 4-hydroxytamoxifen. Seven days after SCI, the mRNA levels of SOX9 and various inhibitory enzymes were measured<sup>23</sup>.

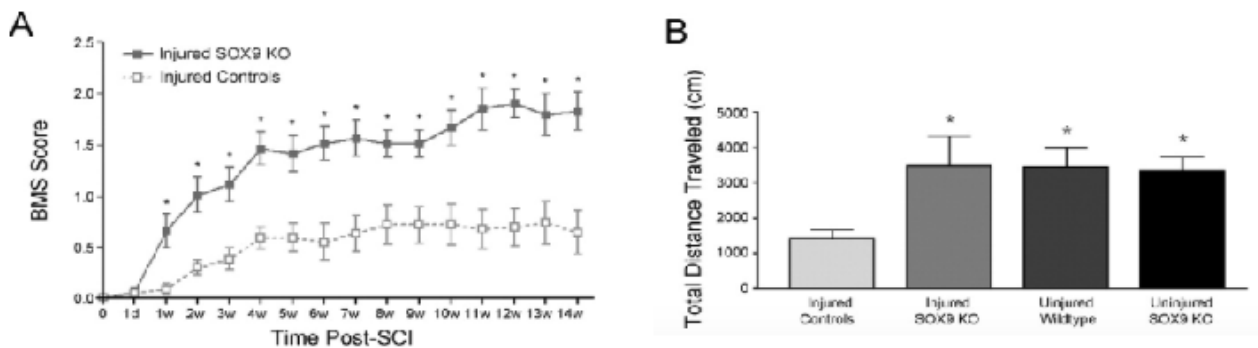


**Figure 12.** Assessment of locomotor functionality of SOX9 conditional knock-out and control mice after SCI. (A) The BBB score of locomotor ability of the mice were tested each week for 14 weeks after incubation of SCI. (B) The distance travelled by injured SOX9 conditional knock-out and control mice in a rodent activity box was tracked and compared to the distance travelled by uninflected mice<sup>23</sup>.

These studies demonstrated that SOX9 conditional knockouts had reduced CSPG levels compared to controls after SCI. Compared to spinal cord damaged controls, the RNA levels of the CSPG enzyme Xt-I and C4st-1 were decreased, as were the CSPG core proteins aggrecan, brevican and neurocan. It was concluded that knock-out mice showed a  $72 \pm 4\%$  reduction of SOX9 gene expression as well as other generation-inhibiting proteins as seen in **Figure 10**.

**Figure 11** shows a second test performed by evaluating astrocyte cultures taken from both gene models after mice were induced with T9- SCI. The data suggested that a reduction in expression was observed in SOX9 knock-out model. A  $62 \pm 11\%$  reduction in the expression of SOX9 was detected along with other generation inhibiting proteins. In addition, CSPG protein levels were decreased as a result of the reduction in RNA levels<sup>24</sup>.

Sox9 conditional knockouts improved locomotor recovery after SCI. Day 1 was associated with paralysis of the mice hind limbs with a score of zero on the Basso Mouse Scale (BMS)<sup>25</sup>. Control mice showed a plateau of  $0.63 \pm 0.21$  at 4 weeks post SCI. The BMS score of SOX9 conditional mice reached plateau around 11 weeks post SCI with a BMS score of  $1.81 \pm 0.19$ <sup>23</sup> as shown in **Figure 12**. This indicates that there was a significant increase in plantar placement of their hind limbs and an increase in mobility as indicated by the distance travelled in a two-hour time period measured in the rodent activity box<sup>23</sup>. Not only were the BMS scores of the knock-out mice much higher than those of the control mice, but the distance travelled in the rodent activity box by the knock-out mice was on par with those mice that were not inflicted with T9-SCI. This concludes that the ablation of SOX9 expression reduces the secretion of generation inhibition enzymes and allows the axons of neurons to grow and establish effective neural connections<sup>23</sup>.

The improved locomotor recovery in spinal cord-injured SOX9 conditional knock-out mice was due to reparative sprouting and dependent on the reduction of CSPG levels. The SOX9 conditional knockout mice displayed no increase in tissue sparing and no long-range regeneration after SCI compared to control mice. Reparative sprouting below the level of lesion was increased in SOX9 knockout mice after SCI which correlated to decreased PNN levels<sup>25</sup>. Brown group evaluated locomotor recovery in spinal cord-injured SOX9 conditional knock-out mice treated with matrix metalloproteinase (MMP) inhibitor doxycycline<sup>26</sup>. MMPs are the physiological mediators of matrix degradation<sup>27</sup>. After SCI doxycycline-treated SOX9 knock-out mice had higher CSPG levels and less locomotor recovery than the saline-treated SOX9 knockouts. In conclusion, SOX9 ablation after SCI leads to decreased CSPG levels and promotes reparative sprouting and improved mobility.

Using middle cerebral artery occlusion (MCAO) model of stroke, the Brown group showed that MCAO-injured SOX9 knockout mice had lower PNN levels in their brains and spinal cords than control. Reparative sprouting in MCAO-injured SOX9 knockout mice increased which showed corticorubral and corticospinal projections from the contralateral, uninjured cortex increased into the midbrain and spinal cord denervated by the injury demonstrated by anterograde tract tracing studies<sup>29</sup>. The decreased PNN levels and increased reparative sprouting after MCAO shown by the SOX9 knockout mice was correlated by improved neurological recovery<sup>29</sup>.

In conclusion, SOX9 knockout mice have improved recovery after SCI due to reduced CSPG levels in the PNN surrounding neurons that have been denervated by the injury and promote plasticity and increased recovery as seen in **Figure 13**.

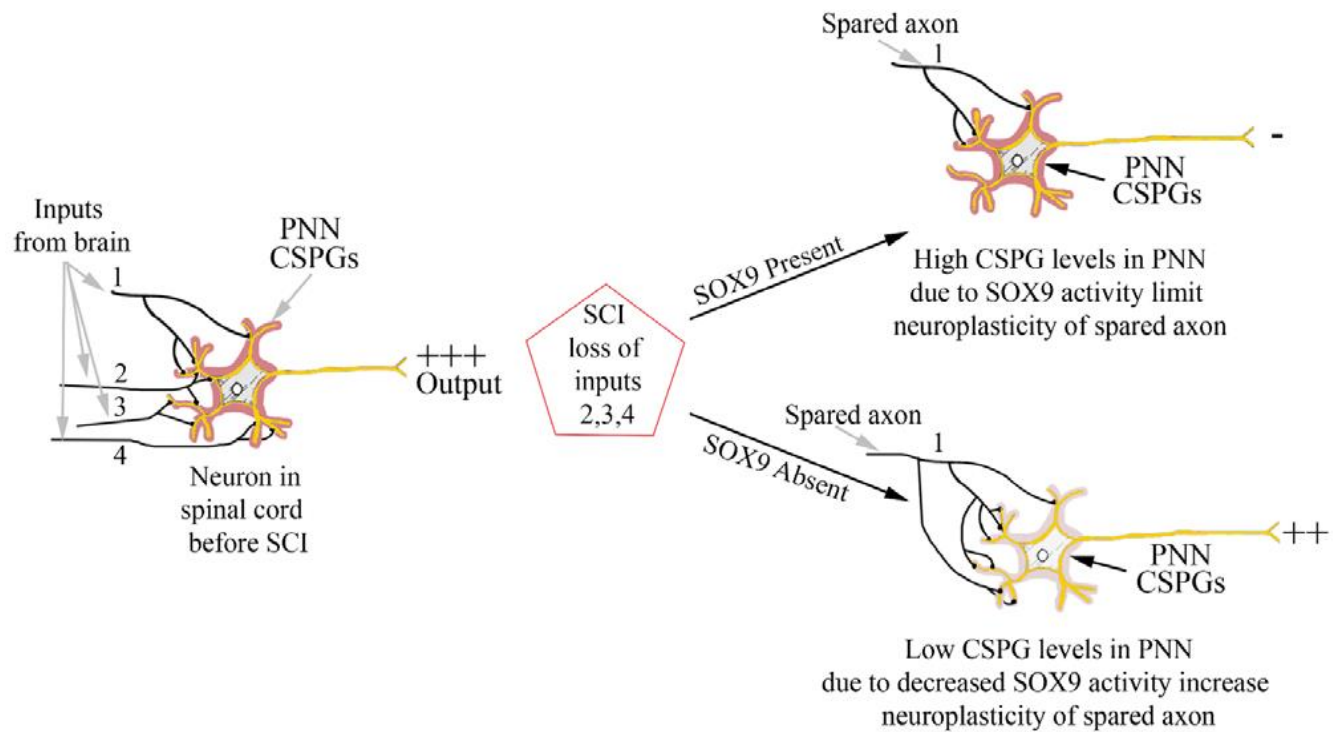


**Figure 13.** Model for how SOX9 ablation results in improved locomotor recovery after SCI. Synaptic connections between inputs (black) and dendrites of a neuron (yellow) are surrounded by a CSPG-rich PNN matrix (red) to restrict plasticity after developing connections have stabilized. After a SCI many synaptic inputs are lost. In the absence of SOX9, CSPG levels in the PNN decreased allowing for reactive sprouting by axons spared from the injury. This results in increased input onto the denervated neuron and better recovery than in controls, where SOX9 activity maintains the PNN and thus limits neuroplasticity<sup>29</sup>.

Therefore, an increase in recovery of locomotor function after SCI is possible through ablation of the SOX9 gene. The decrease in CSPG levels is not the only factor committing to this effect, but an increase in reactive sprouting also contributes to the advancement in rehabilitation. Since there are no current therapeutic treatments for SCI available, inhibition of SOX9 seems to be the optimal route of progression for its pharmacological medication; this applies to those with acute SCI but also those with long-term disability. Closer analytical computations of SOX9 have shown that for its expression to be carried out, its dimerization was necessary<sup>30-33</sup>. The logical

approach would be to use a dimerization motif contained molecules as an agent for the contraction of transportation targets. The SOX9 dimerization motif was fused with HIV-1 tat protein to ensure its accessibility into cells, creating a peptide that produced a SOX9 inhibition response within the astrocyte<sup>30-33</sup>. This SOX-DIMER peptide displayed promising results as it was successful in inhibiting SOX9 expression. The data presented in **Figure 14** shows that there is a reduction in SOX9 and some ECM molecules, including Xt-II, hapln1, col2a1, Acan and Bcan, when exposed to SOX-DIMER.

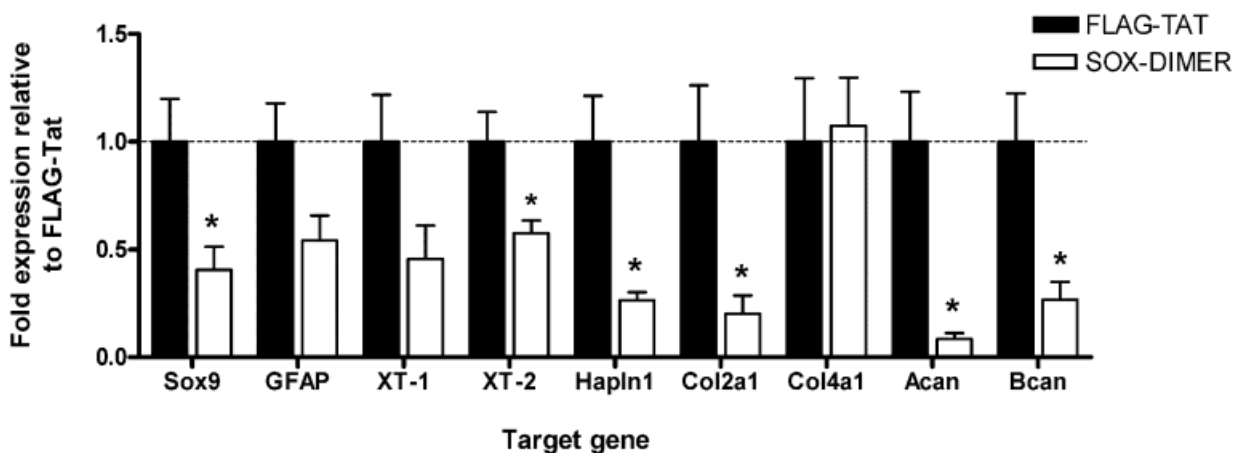


**Figure 14.** The expression of SOX9 and various regeneration-inhibiting enzymes after exposure to the dimerization-inhibiting molecules SOX-DIMER. Primary mouse astrocytes were treated with 10 $\mu$ M SOX-DIMER or with the control compound FLAG-TAT for 48 hours and levels of expression of each target gene were then measured. \* indicates statistical significance P<0.05, two-tailed Student's t-test, n=4. (Figure was taken from report generated by the Brown group)

### 6.5 Z02, a small molecule inhibitor of SOX9

In order to develop therapeutic agents for this purpose, a small molecule that served the same function as the SOX-DIMER was required. These deductions through collaboration with Critical Outcomes Technologies Inc. (COTI), led to the search for a small molecule that would

inhibit SOX9 transcription factors<sup>33</sup>. Over 12 million compounds were screened in silico to find one that showed good results in rat astrocyte culture, which was named **Z02**, compound **1**; its structure is shown in **Figure 15**. **Z02** decreased SOX9 target gene expression in primary mouse and rat astrocytes cultures.

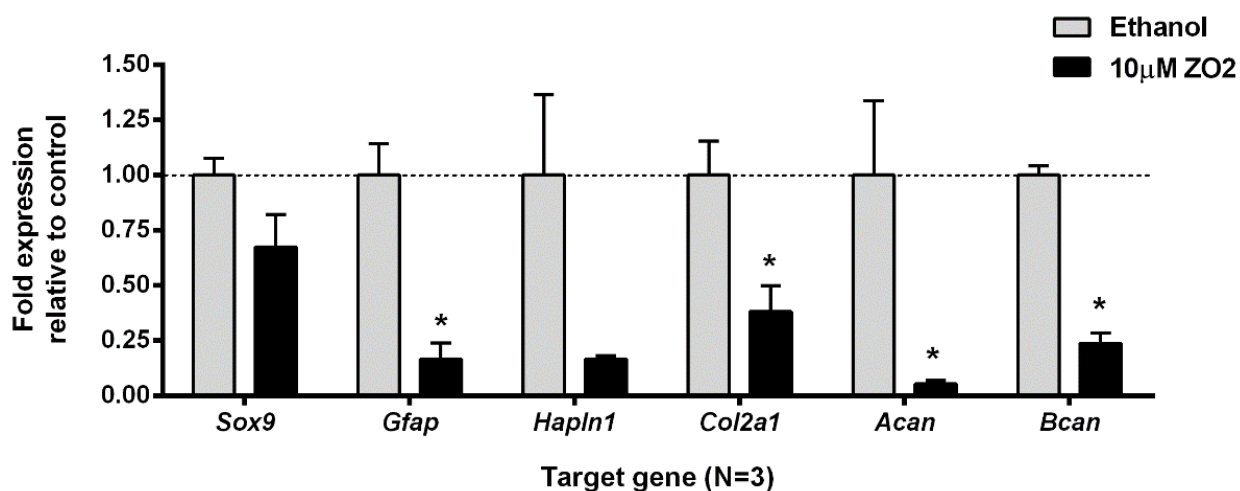


**Figure 15.** The expression of SOX9 and various regeneration-inhibiting enzymes after exposure to the dimerization-inhibiting molecule Z02. Rat astrocyte culture were treated with ethanol vehicle or with 10µM Z02 for 48 hours. The level of gene expression in the labeled target genes was then measured. \*indicates statistical significance  $P < 0.05$ , two-tailed Student's t-test,  $n=3$ . (Figure was taken from a report generated by the brown group.)

Although **Z02** (**Figure 18**) is a promising small molecule It is unlikely that **Z02** is the most potent form of this family of molecules. The next logical step is to optimize its potency through Structure Activity Relationship (SAR) studies. SAR studies are expected to produce modifications which are expected to improve both the efficacy and potency compared to **Z02**.

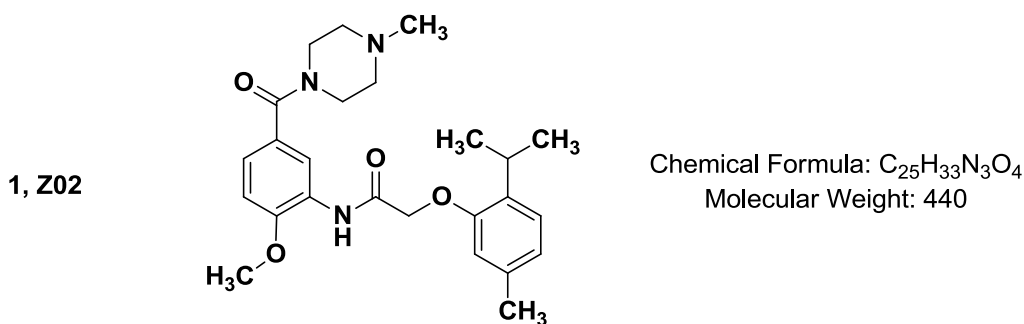


**Figure 16.** Dimerization-inhibiting small molecule lead compound Z02

### 6.6 Synthesis of Z02

The synthesis of the lead compound **Z02** was accomplished in a four step process. N-methylpiperazine, unit A, was reacted with the acid chloride derived from the 4-methoxy-3-nitrobenzoic acid, unit B as seen in **Figure 17**. This high yielding reaction resulted after reduction of the nitro group to an amino group upon refluxing with iron and aqueous NH<sub>4</sub>Cl solution in the AB unit. This AB unit is coupled to the CD unit. The CD moiety was prepared by reacting thymol with (unit D) with chloroacetic acid (unit C) in the presence of excess sodium carbonate. The phenoxyacetic acid was converted to its acid chloride with thionyl chloride-DMF and then coupled with the AB unit.

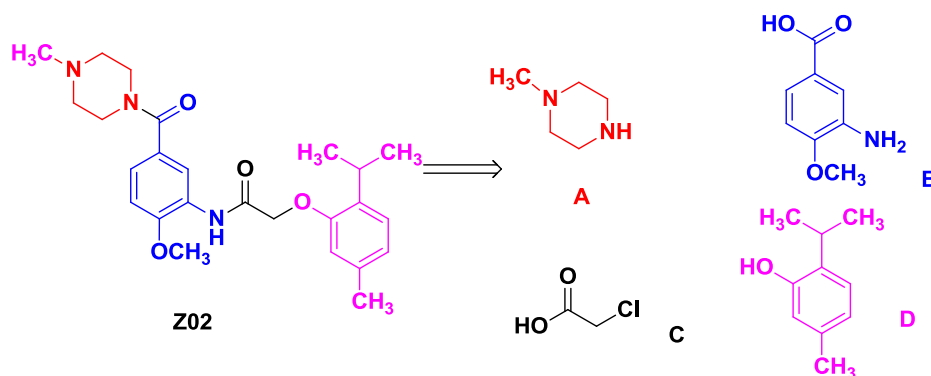


**Figure 17.** Structure of Z02. Retrosynthesis to four distinct units (A,B,C,D)

## 7.0 Objective

The goal of this project was to prepare a small number of analogs of **Z02** by focusing on changes in the A and D parts of the ZO2 molecule. These compounds would be sent to the Brown group for evaluation in their luciferase bioassay as a measure of the inhibition of the SOX9 transscription factor. It was hoped that the results would allow subsequent students to be able to design more potent SOX9 inhibitors.

## 8.0 Results and Discussion

### 8.1 Retrosynthetic analysis and potential analogs of Z02.

As pointed out in Section 2.6 the lead compound **Z02** can be divided into the four units, A, B, C and D. One can imagine a number of sequences to combine these units as seen in **Figure 18**. One of the simplest is to consider B as an amino acid which can be connected to A to form A-B and then combined with a CD unit both via an amide bond forming reaction.

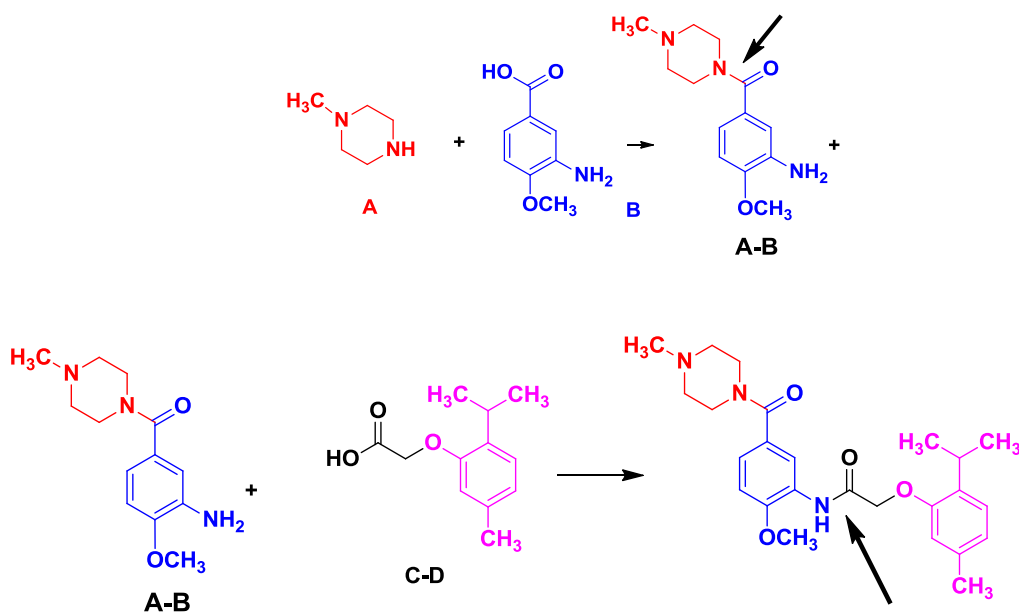


**Figure 18.** Synthesis of Z02 analogs by combining AB units and CD units through amide bonds.

The first approach was to consider modifying the units A and D while keeping B and C constant. Potential replacements of the N-methylpiperazine as A were piperidine, morpholine and pyrrolidine as seen in **Figure 19**. It was anticipated that these changes would show whether the basic nature of the N-CH<sub>3</sub> group in piperazine was crucial to good activity

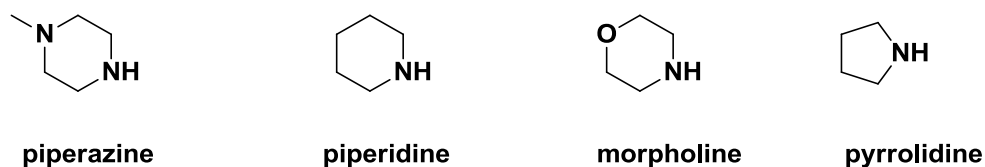


**Figure 19.** Potential cyclic A units

Changes in the D unit could easily be imagined by using phenols other than thymol as the part of the CD moiety. The following phenols were considered (**Figure 20**). These would allow us to test for the importance of the *ortho*-substituents in the ring D or a strongly electron donating substituent in the *para*- position

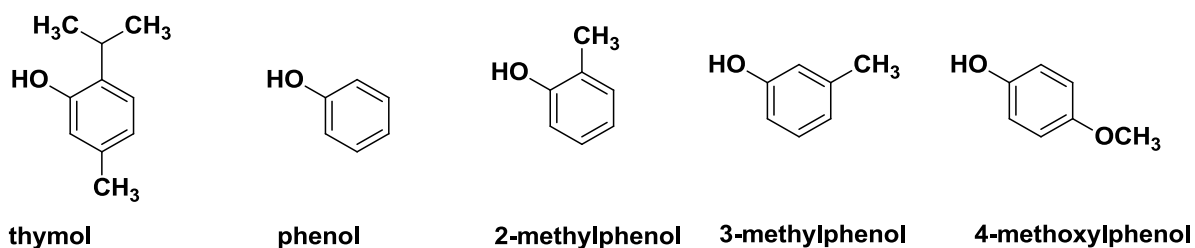


**Figure 20.** Potential phenols as replacements for the D unit.

It is hypothesized that the relatively large *ortho*-isopropyl group may have considerable importance relative to no *ortho*- substituent since it this is likely to change the shape of this part of the molecule and force the aryl D ring out of the plane (**Figure 21**).

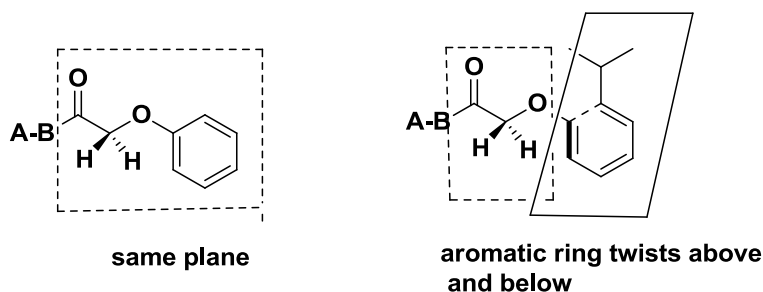


**Figure 21.** Shape of the molecule changes with the no ortho substituent in the D unit to the isopropyl group from being in the same plane to a twist shape.

We also considered changes in the key ring B. The first change considered was the importance of the 4 methoxy group and what effect its removal or its replacement by a methyl group might have. The second major change we considered was whether the *meta*- relationship between the amino and carbonyl substituent was a key requirement. Would compounds in which this relationship was *ortho*- or *para*- have similar activity or better activity than **Z02** or more likely is inactive?

It is easy to imagine that any of the proposed changes in B should significantly affect the potency of these compounds since these changes should change the overall shape of these molecules and therefore affect their ability to bind to a receptor.

For example, in **Z02** one might expect that hydrogen bonding between the 4-methoxy substituent should stabilize the conformation I in which ring B and its substituents are all more or less in the same plane. In contrast ring B should twist out of the plane of the CD unit due to steric interactions between the 4-methyl group and the amide substituent (structure II). The shape of the 4-unsubstituted derivative III should be similar to that that of I.

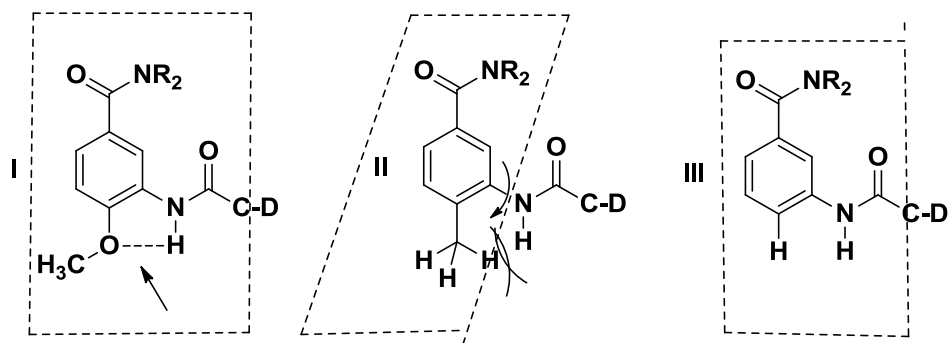


**Figure 22.** I. Hydrogen bonding between the 4-methoxy substituent and the amide nitrogen. II. Ring B twist out of the plane of the CD unit due to the steric interactions. III. The shape of the 4-unsubstituted derivative.

The overall shape of compounds with the *ortho*-, *meta*- and *para*- arrangement in ring B will be substantially different as illustrated in **Figure 23** below. For example, one would expect hydrogen bonding between the NH and the amide carbonyl group in the compound having the *ortho*- arrangement as shown, but not for the *meta*- and *para*- analogs. In the *meta*- isomer, the dipoles created by the two carbonyl groups should favor the conformation shown below. For the *para*- isomer, the difference in energy between the various amide rotamers is likely quite small.

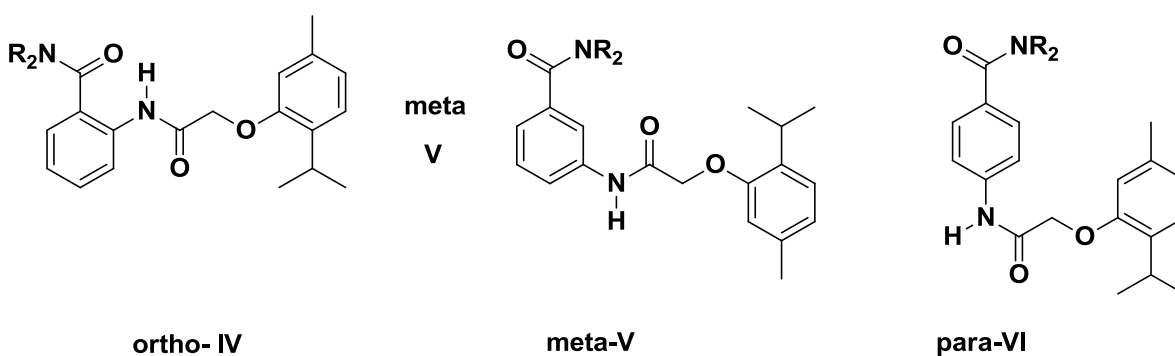


**Figure 23.** *Ortho*-, *meta*- and *para*- contributes to the shape of compounds in ring B.

The difference between the overall shape of the *ortho*- and *para*- vs the *meta*- isomers is shown in the coloured overlays shown below (**Figure 24**).

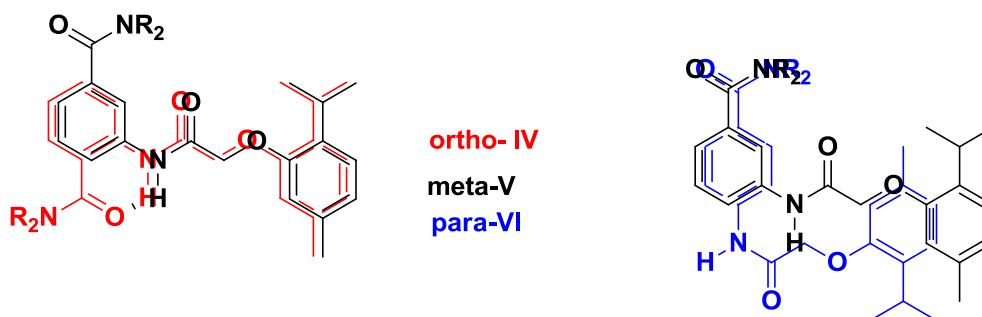
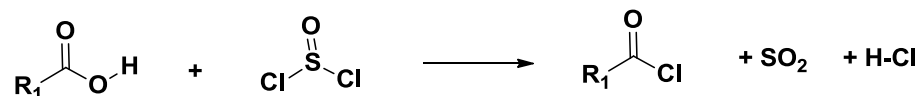


**Figure 24.** Difference in the overall shape of *ortho*-, *para*- vs the *meta* isomers.

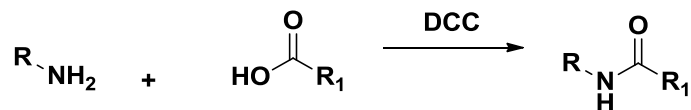
Since we have no knowledge of any binding interaction between these molecules and the protein receptor we hoped that the results from the above preliminary compounds would be informative and provide guidance for the preparation of second generation analogs.

Due to the importance of peptides both natural and synthetic many methods have been developed for the preparation of amide bonds. The general approach is the same in all cases. The acid OH group is converted into a very good leaving group either in situ or in a separate step and the “activated acid” acid is then reacted with the amine. In the simplest cases the acid is converted into the acid chloride generally either by heating with thionyl chloride or  $P(O)Cl_3$  or by reaction with oxalyl chloride, usually in the presence of DMF. Evaporation of the solvent and the volatile by-products furnishes the acid chloride which may be used as such or for the purified by distillation if reasonable volatile. For example:



**Scheme 11.** Thionyl chloride reaction

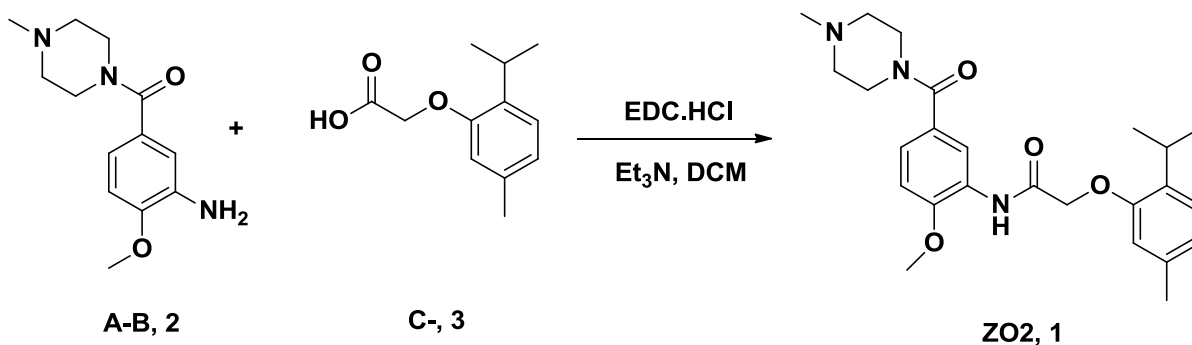
In more complex cases the acid is activated in situ. A variety of in situ activating agents have been developed. These include DCC, DIC, EDCI, DEPBT, CDI etc. For example:



**Scheme 12.** Amide bond coupling with DCC

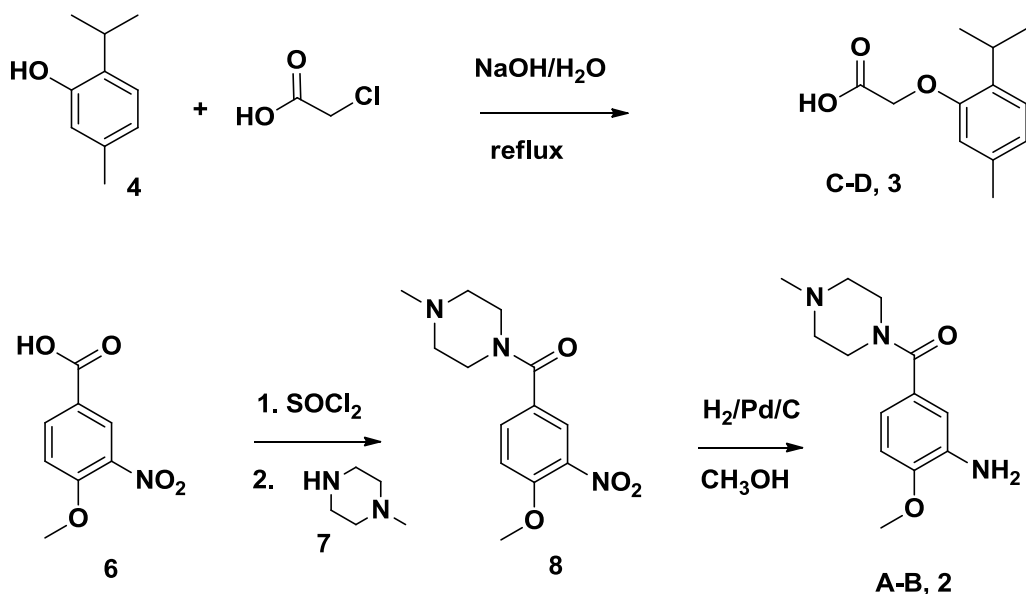
## 8.2 Synthesis of Z02

A search of the literature for synthetic routes in the production of **Z02** revealed that the synthesis of **Z02** was not described despite the fact that **Z02** was available for purchase. The initial preparation of **Z02** was carried out by coupling of the AB, **2**, unit with CD, **3**, using EDC.HCl and DCC as coupling reagents as shown in **Scheme 13**.



**Scheme 13.** Synthesis of Z02 analogs using EDCI.HCl as a coupling agent

The CD unit **3** was obtained by heating thymol, **4**, with chloroacetic acid in the presence of NaOH. The preparation of the AB unit **2** required two steps: i) coupling of 3-nitro-4-methoxybenzoic acid, **5**, with N-methylpiperidine, **6**, via its acid chloride generated with thionyl chloride; ii) reduction of the nitro group using H<sub>2</sub>, Pd/C.

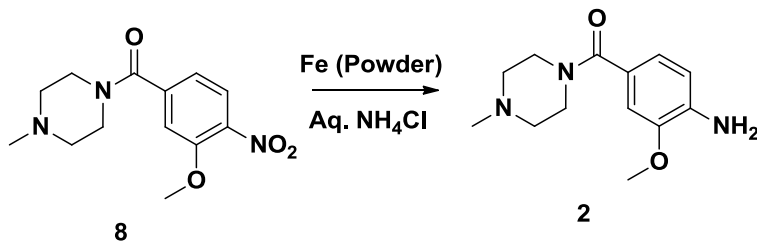


**Scheme 14.** Synthesis of the A-B and C-D units required for the preparation of **Z02**, **1**.

Unfortunately, we obtained **Z02** in only 8.7% yield which is not enough to scale into mass production of a pharmaceutical company and barely enough for characterization and use as standard in future bioassays. After multiple attempts and using a variety of reaction conditions it was theorized that the basic moiety present on the A subunit may be more reactive towards the activated CD acid than the weakly nucleophilic aromatic amine of ring B. The use of DCC as coupling reagent was also unsuccessful due to the poor solubility of DCC in DCM. The use of other various solvents also failed to yield significant amounts of **Z02** as seen by thin-layer chromatography (TLC).

Rowan Swan, a COOP student who worked jointly and concurrently with the author on this project succeeded developing a superior somewhat more successful route to the lead structure **1** using essentially the same concept outlined above with a different set of reagents. The nitro group in the intermediate **8** was reduced the amine **2** much more conveniently by refluxing **8** in an ethanol–water mixture with iron filings in the presence of  $\text{NH}_4\text{Cl}$ . This

reduction method occurred in essentially quantitative yield has served well for the preparation of many other A-B units.



**Scheme 15.** Reduction of AB nitro unit to an amino group using iron fillings and ammonium chloride.

The coupling of **2** to **3** was accomplished in good yield by first converting thymol acetic acid, **3**, to its acid chloride **9** using oxalyl chloride in DCM with DMF catalysis, evaporating the solvent and the biproducts on a Rotovap, re-dissolving the crude acid chloride in DCM and then adding a mixture of **2** and trimethylamine. The final coupling yield, still not very good, was 25%. The NMR spectrum of the synthetic **1**, **Figure 25** was compared with that of that of the commercial material.

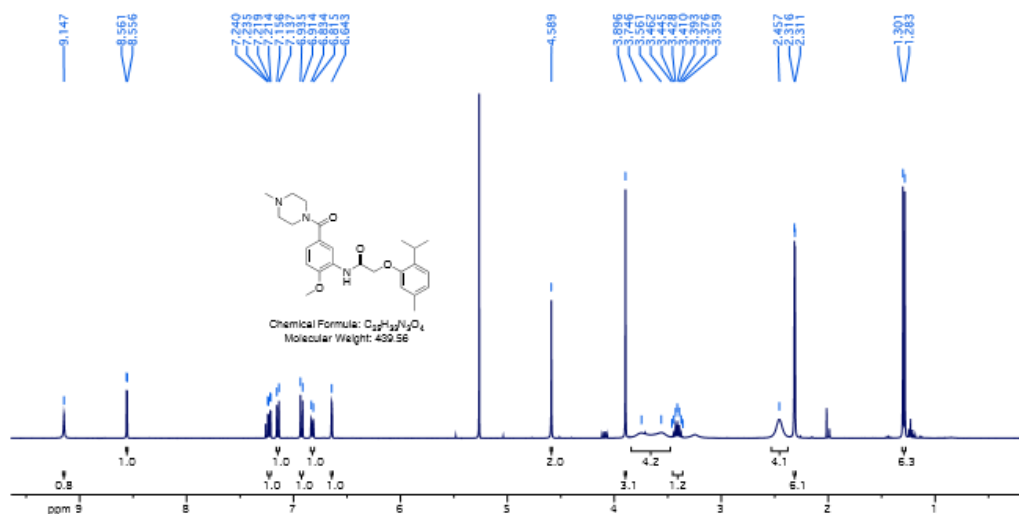
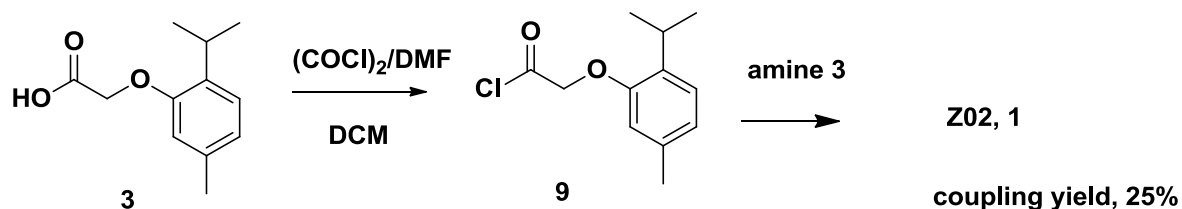


**Figure 25.** <sup>1</sup>H NMR of **Z02** (synthetic **1**).

All of the required peaks of I were present in both samples. Interestingly, the commercial sample showed an impurity as evidenced by additional peaks in the aromatic H region.



**Scheme 16.** Halogenation of carboxylic acid into an acid chloride using oxalyl chloride then coupling with AB amino group to yield Z02.

We first focused on the replacement of the N-methyl piperazine of **Z02** in order to determine if the basicity of this unit was a required feature. Over a period of time compounds in which the A units was replaced by morpholine, piperidine, pyrrolidine, propylamine dimethylamine, diethylamine, dipropylamine and diisopropylamine were prepared. The replacement of the amide by a methyl ester, by methyl ketone and phenyl ketone has been investigated. Many of these compounds were prepared jointly with Rowan Swan during the summer of 2017, the others subsequently by Ashleigh Lew as part of her Honours Research Project in 2017-2018. Credit is given these two collaborators. Only the compounds prepared by the author or ones where the author was closely involved in are reported in the Experimental Section.

The current state of the project is described at the end of this chapter and includes bio-assay data from all of the collaborators.

We have also prepared analogs in which the relationship between the carbonyl and the amine was *ortho*- and *para*- compared to *meta*-. In addition, we removed the methoxy group and replaced it with a methyl group in unit B. Finally, in the D ring, we investigated replacement of

the isopropyl group *ortho*- to the oxygen by methyl or hydrogen and also placing a methyl group *meta*- to the oxygen linker.

As was pointed out earlier we could only speculate which features of the structure of the lead compounds were important for observed biological activity. Initially many of the synthetic targets were selected keeping in mind the hypotheses expressed above tempered with availability of the four building blocks in our laboratory and in the Department of Chemistry and ease of synthesis. We hoped rapid feedback from the bioassays would eventually allow us to become more rational in our choice of targets. Indeed this has happened, but only after more than fifty compounds has been prepared and bio-assayed.

The first group of analogs featured ring B derived from 3-aminobenzoic acid that was available in our group. The four compounds are shown below (**Figure 26**). All four have the same ABC units and thus focused on the substitution pattern in ring D. The N-methyl piperazine A unit in **1** and the methoxy group have been replaced by the six membered piperidine and a hydrogen atom, respectively. The A units no longer has a basic site.

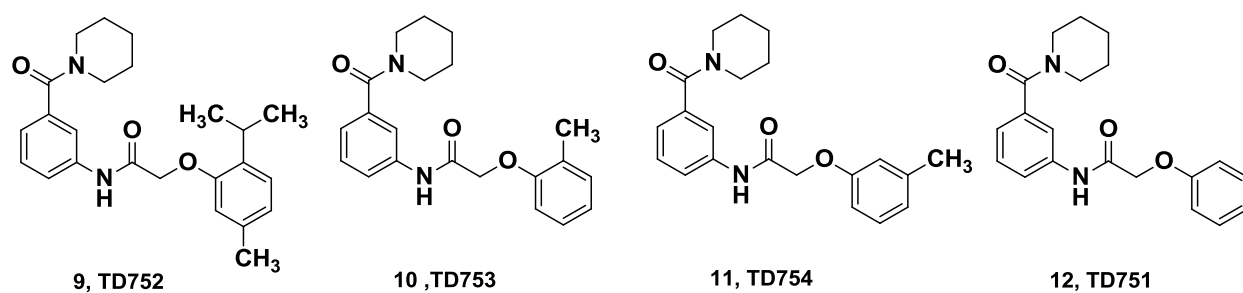


**Figure 26.** The first group of compounds featuring ring B derived from 3-amino benzoic acid.

The preparation of these compounds followed the schemes outlined above. Details can be found in the Experimental Section. The  $^1\text{H}$  NMR of compound **9** is shown in **Figure 27**.

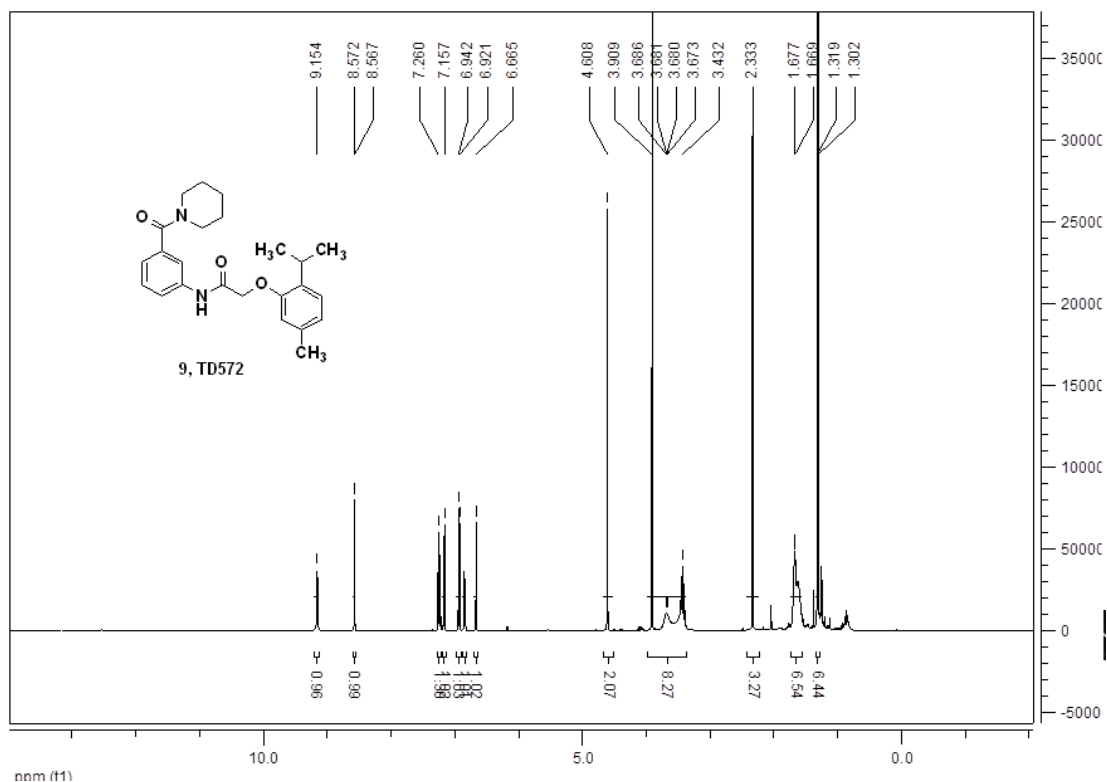


**Figure 27.** <sup>1</sup>H NMR of compound **9**.

As seen by the NMR of compound **9**, there is a characteristic isopropyl peak at 1.31 denoted by 6H. The methyl peak on the D unit has a chemical shift of 2.30 and denoted with an integration of 3H. There is barrier to rotation of the amide bond in unit A causing the various CH<sub>2</sub> groups to be broad and in different environments. There are 7H in the aromatic region of the spectrum (Chemical Shift 6.65-7.20). The amide hydrogen has an integration of 1H and has a chemical shift of 9.15.

The yields of the overall reactions were very low at 8.7%, 6.7%, 10.0% and 10.0% for compounds **TD751**, **TD752**, **TD75 3**, and **TD754**, respectively, sufficient amounts of material was available to allow us to completely characterize these compounds and send them to the Brown group for the bioassay.

Although the compounds tested did show some activity in the assay, none were comparable to the activity portrayed by **Z02** as seen in **Figure 28**. We had expected that compound **9 (TD572)** would show the most inhibition of SOX9 since it has most of the features of the lead structure **Z02** with the main difference being the replacement of the basic piperazine amide unit by the neutral piperidine amide. Compounds **10 (TD753)** and **11 (TD754)** are the most active in this series shown comparable activity. This allowed us to make the tentative conclusion that the *ortho*- isopropyl group in the D ring of **Z02** may not be as crucial as we had initially imagined.

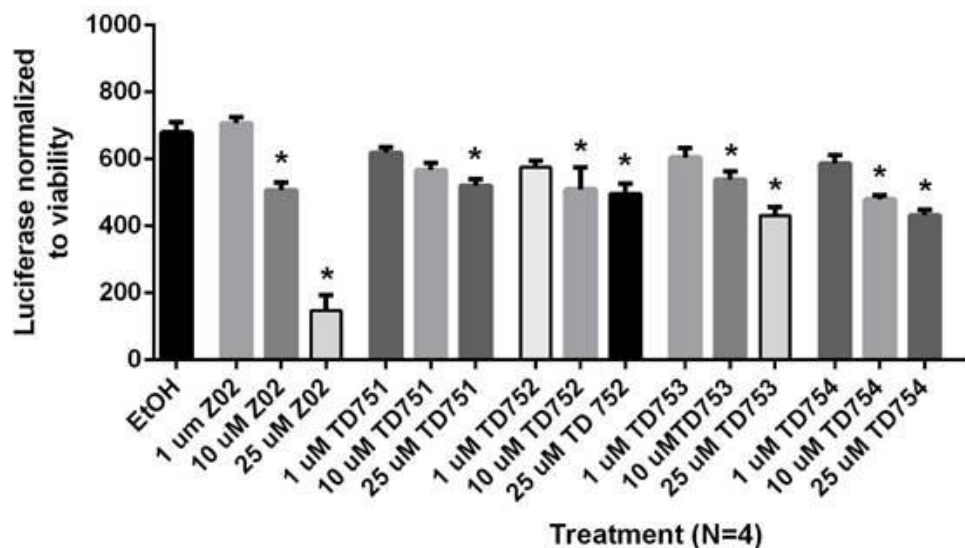
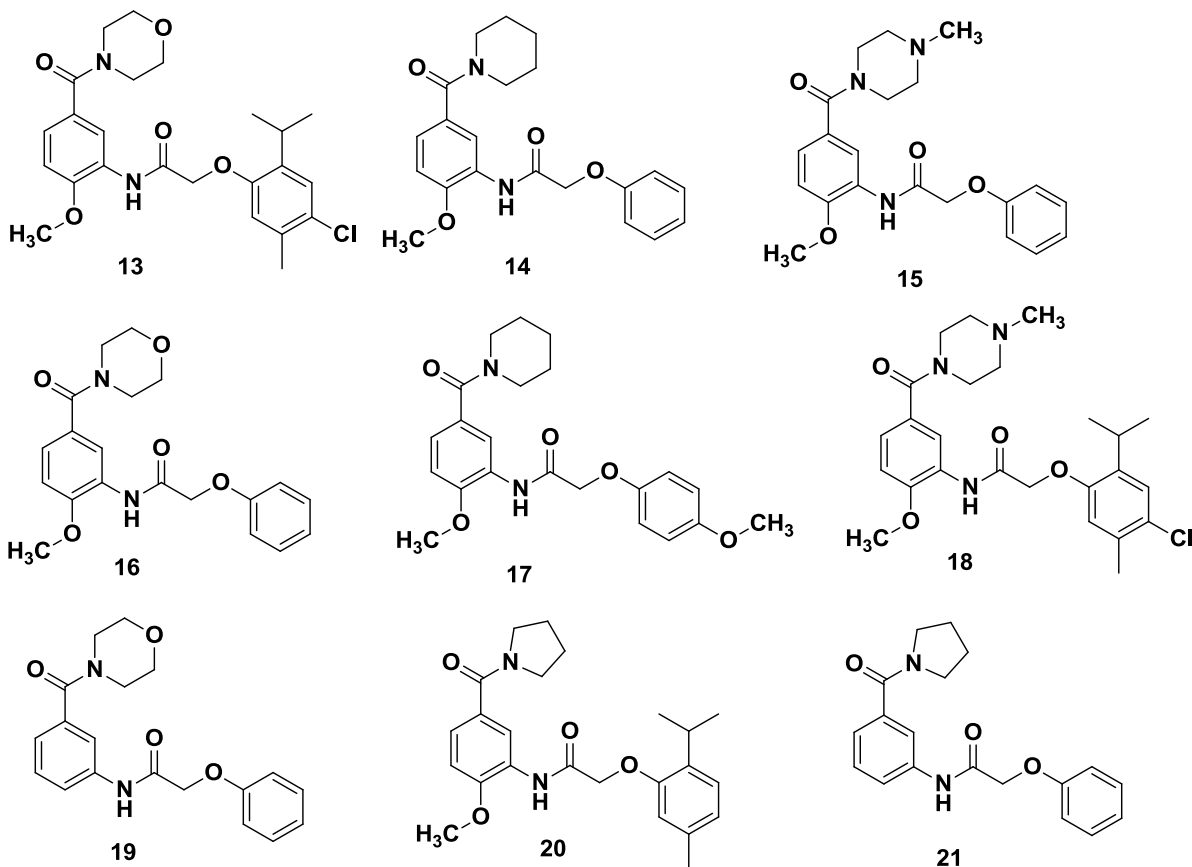


**Figure 28.** Bioassay for the first four synthesized derivatives using ATDC5 cells that have been stably transfected with PGL4.11 SOX9 4x48bp. Compounds **12(TD751)**, **9 (TD752)**, **10 (TD753)** and **11(TD754)** are compared to **Z02**.

A series of compounds, **13-21** was constructed in which the B ring was identical to that found in **Z02**. The preparation of these compounds followed the schemes outlined above. We initially used the palladium on carbon and H<sub>2</sub> to reduce the nitro group. This typically required several days to even one week with the catalyst available in the lab in order to achieve a

reasonable yield. It was later discovered that this reduction could be carried out much more efficiently within one to two hours of time by refluxing the nitro derivative with iron filings and  $\text{NH}_4\text{Cl}$  in a 2:1 mixture of ethanol and water. Details can be found in the Experimental Section.



Bioassay data comparing for the compounds **9-21** showing the effect on luciferase activity relative to control is shown in **Table 5**.

**Table 5.** Bioassay data comparing compounds **9-21**

Compound	luciferase activity (10uM)	Compound	luciferase activity (10uM)
Control =1		Control =1	
9	0.71	10	0.75
11	0.79	12	0.83
13	0.51	14	0.86
15	0.68	16	0.56
17	0.74	18	0.40
19	0.74	20	0.29
21	0.76		

The notion was to compare the bioassay results by pairing compounds of this group with those from the series **9-12** and also compound **1 (Z02)**

For example

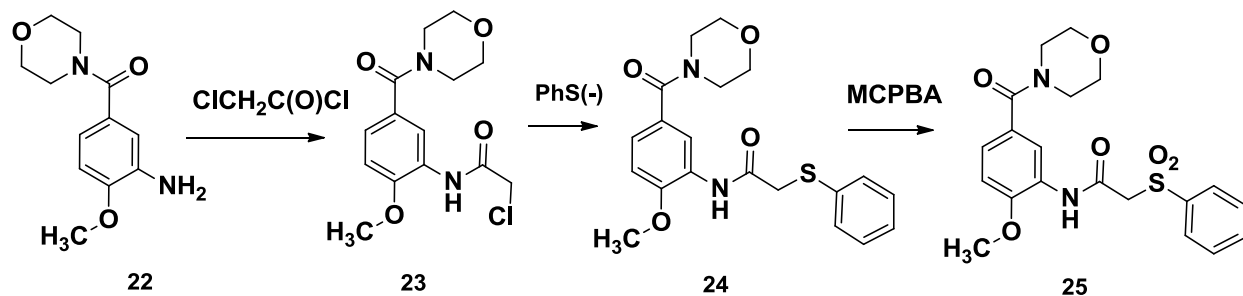
- i) The comparison of **13 vs 16 15 vs 18** and **20 vs 21** should establish the importance of the *ortho*- isopropyl group in ring D; we are assuming that the second methyl group

- and the chlorine on ring D are relatively unimportant. In each set the partner carrying the ortho-isopropyl group showed greater activity.
- ii) Compounds **14** and **12** differ only by the presence of the methoxy group in ring B. How important is this group? The activity of both these compounds is essentially identical suggesting that the methoxy group may ortho to the amide nitrogen may not be important.
- iii) The results for **14** vs **16** should indicate whether the morpholino amide which contains the H-bond accepting group in ring D is superior to the piperidino amide moiety in **14**. The available data from this pair indicates the morpholine amid is superior to the piperidine amide.
- iv) Comparison of **17** to **14** might show if an additional strongly electron donating group in ring D exerts a desirable effect. The difference in activity is small; if anything the data hints that an electron donating group on ring D might have a positive effect.
- v) Compound **20** is significantly more active in the luciferase assay than either **13** or **18**. This indicates that a hydrogen bonding site in unit A might not be crucial after all and opposite to iii) above.

We recognize that the conclusions drawn above are rather tentative and based on limited data. Probably the most important one is that a sterically large substituent *ortho*- to the oxygen in ring D is preferred. This is most readily supplied by using thymol acetic acid as the CD unit.

The replacement of the D ring phenol by thiophenyl and or a phenylsulfony group was also investigated. These compounds were prepared in the following manner. The AB amine **22**

was reacted with chloroacetyl chloride to give **23**. Subsequent reaction afforded the thiophenyl analog **24** which was oxidized with MCPBA to the sulfone **25**.



### Scheme 17. Synthesis of analog 25

The effect of **24** and **25** on luciferase activity indicates that replacement of phenoxy acetic acid (**16**) by thiophenoxy acetic acid (**24**) as the CD unit results in reduced activity. In contrast the phenylsulfonyl acetic acid as the CD unit in **25** results in much greater activity. The sulfone **25** was the most active compound in the series beginning with compound **9** showing a reduction of luciferase activity to 0.23 of control. It suggested the possibility that a phenylsulfonyl acetic acid CG moiety might be superior to thymol acetic acid. It was proposed that several additional examples of compounds with this group as the CD unit should be

### 8.3 *Ortho* and *Para* Substituted Analogs

A number of analogs which have the *ortho*- and *para*- substitution pattern in ring B were prepared. It was recognized that there was a low probability that these compounds would show significant activity since they have distinctly different shapes compared to the ring B *meta*-substitution arrangement. This is readily apparent from the overall analysis of the *ortho*- vs *meta*- and *para*- vs *meta*- structures reproduced in **Figure 29**. Nevertheless we felt it important to confirm this hypothesis.

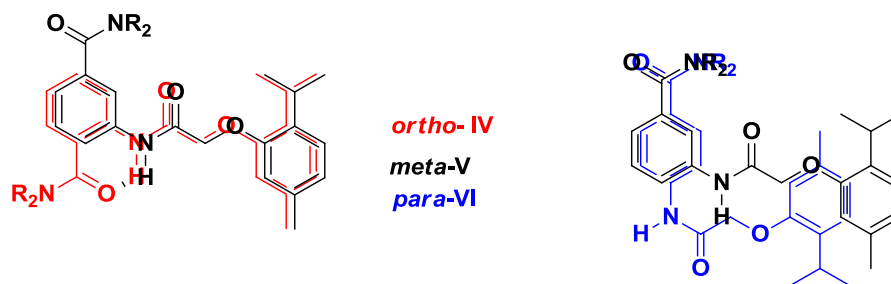
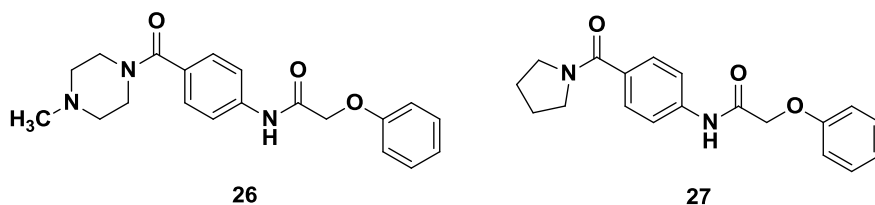
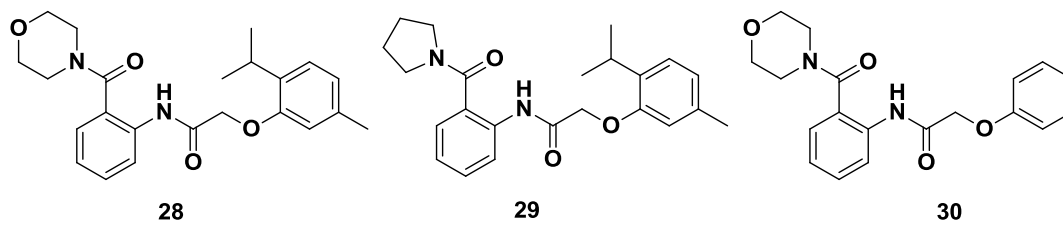


**Figure 29.** This is readily apparent from the overalys of the *ortho*- vs *meta*- and *para*- vs *meta*-structures reproduced below

The syntheses of these compounds followed the same sequence used to prepare the analogs having the *meta*- arrangement. Since we were still unsure of the optimum nature of both the A and D units we settled on the combinations shown below: N-methylpiperazine and pyrrolidine for the A and phenol for the D unit I the *para*- arrangement, compounds **22** and **23**, respectively.

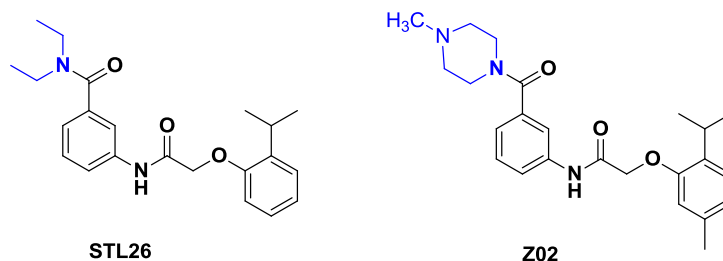


For the *ortho*- isomers the A and D units chosen were: morpholine and pyrrolidine as unit A and thymol, the D unit in **Z02**, and phenol for building block D as illustrated in compounds **28** to **30**. The latter three compounds were prepared by Rowan Swan as part of her 2016-2017 Honours project.



As anticipated neither these five compounds showed significant activity relative to control thereby confirming the expectations.

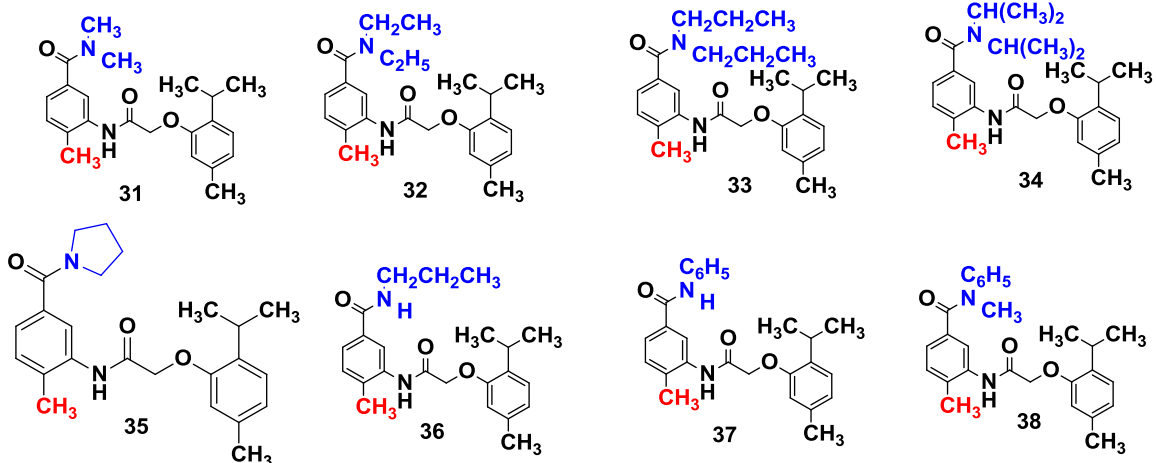
Shortly after completion of my part of this project Dr. Arthur Brown reported that another commercially available compound named **STL26** was much more effective in SCI recovery than **Z02**. **STL26** was found to inhibit 60% of SOX9 activity at 1 $\mu$ M concentration, a level of inhibition that requires 10mM of **Z02**. The key difference between **Z02** and **STL26** is in the A unit where N-methylpiperazine amide has been replaced by an N,N-diethylamide. Future target analogs would take this new information into account.



#### 8.4 Open chain vs. cyclic A unit

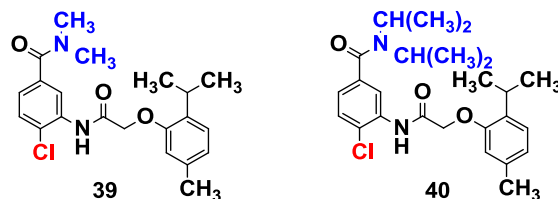
This section is included so that the reader is brought up date regarding the status of this project at the time of the writing of this thesis.

Based on the structure information provided by **STL26** our group for the past year has focused heavily on determining whether the N,N-diethylamide group could be improved upon. Thus a series of compounds was prepared in which the CD ring was derived from thymol acetic acid and ring B had the *meta*- arrangement common to both **Z02** and **STL 26**. Key compounds that were prepared are shown below.

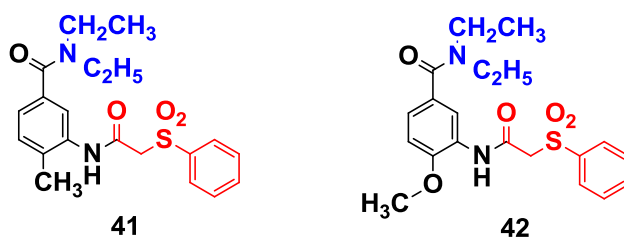


Briefly, the bioassay results indicated that the N,N-diethylamide **32** was equally active as **STL26**. Surprisingly, neither reducing the size of the substituents on nitrogen nor increasing it resulted in more active compounds. For example the N, N-dimethylamide **31** and the pyrrolidine amide **35** which differs from **STL26** by only 2H but is sterically somewhat smaller were less active. Increasing the size of the two amide substituents as in **33** (N,N-dipropyl), and in **34** (N,N-diisopropyl) also caused a reduction of activity although less than for the compounds with the smaller substituents. The secondary amides **36** and **37** were much less active than **32**. Compound **38** which is N-methyl and N-phenyl substituent was comparable to control.

The importance of the N,N-diethyl amide as the A unit was confirmed by the observation that **39** which has a chlorine substituent on ring B in place of a methyl was equally active as **32**. Interestingly the N,N-diisopropyl compound **40** like **34** was somewhat less active.



We had speculated that thymol acetic acid might be replaceable by phenylsuofonyl acetic acid as the CD unit precursor. Unfortunately this has turned out not to be true. Neither of the two compounds **41** and **42** each of which has the N,N-dimethylamide A unit displayed activity comparable to **STL26** and compounds **32** and **39**.



The level of activity, about 60 % inhibition of SOX9 by **STL26**, **32** and **38** at 1uM seems to us quite low. Ideally, one would like to have compounds with 10 or even 100 times higher inhibition of the peptide. We are however encouraged by the observation that these compounds have been shown to cross into the spinal cord and the very early observation that **Z02** when administered to mice whose had spinal cord had been partially severed enabled these animals to recover their mobility to a greater extent than those in the control group. Thus compounds such as the above three may have potential in the treatment of spinal cord injuries.

## 8.5 NMR studies

The NMR spectra of amides are complicated because resonance results in a partial double bond between the nitrogen and the carbonyl carbon. The strength of this partial  $\pi$  bond is 16-20 kcal /mole. Bond rotation is slow (restricted) on the NMR time scale and both rotamers can be observed in the proton NMR at room temperature at higher ends. For example, the NMR of N,N-dimethylformamide (**Figure 30**) shows two distinct methyl signals each integrating for 3H at room temperature.

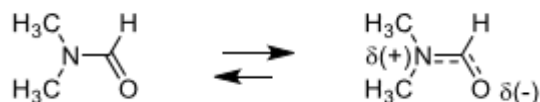


**Figure 30.** N,N-dimethylformamide barrier to rotation

When the sample is heated, the rate of rotation increases and the two methyl signals coalesce into a broad band. An increase in the temperature causes rotation about the C-N bond to be rapid and the two methyl groups are observed as a singlet integrating for 6H relative to the formyl hydrogen. The 400 MHz  $^1\text{H}$  and  $^{13}\text{C}$  NMR of compound 2 (**Figure 33** and **34**), especially the proton spectrum, are both quite unusual. The proton spectrum shows a very narrow spaced three-line pattern at 3.20 ppm (2H), and two broad peaks centered at 3.60 ppm (2H) and 3.78 ppm (4H). The aromatic region is as expected for four Hs on an *ortho*-substituted phenyl ring. The carbon spectrum shows all four carbons of the morpholine ring at different chemical shifts. When taken at higher field (600 MHz) the eight hydrogens of the morpholine ring absorb at seven different positions (**Figure 35**):  $\delta = 2.55$  ppm (1H), 2.65 (1H) 3.06 (1H), 3.27 (1H), 3.32, (1H), 3.59 (2H) and 3.71 ppm (1H). The HETCOR spectrum (**Figure 36**) showed that the peaks at 2.55 ppm and 2.65 ppm were both attached to the carbon resonating at 47.2 ppm; this carbon is one of the two adjacent to the nitrogen of the morpholine ring. The H at 3.79 and one of the two at 3.59 are attached to the other carbon ( $\delta = 42.2$  ppm) bearing nitrogen. The two carbons adjacent to oxygen absorb at  $\delta = 66.2$  ppm and 66.4 ppm. These carry the Hs which are found at 3.06 and 3.59 and 3.32 and 3.59 ppm, respectively. Thus, at 600 MHz and room temperature, all four carbons of the morpholine and all eight hydrogens are found observed at different chemical shifts. This can be explained by assuming two restricted rotations. One of these is the typical

amide restricted, rotation a), and the other is restricted rotation in the aromatic to carbonyl carbon-carbon double bond, restricted rotation b).

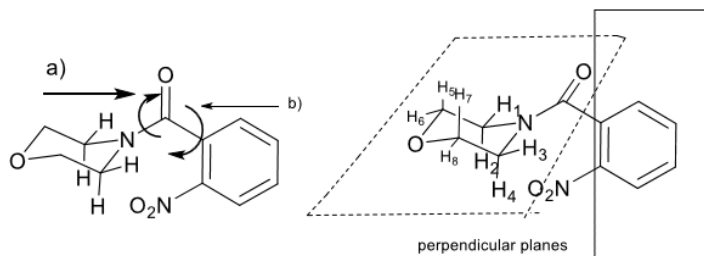


**Figure 31.** Amide restricted rotation a). Restricted rotation in the aromatic to carbonyl carbon-carbon double bond b)

The most probable arrangement of the groups in this molecule would be one where the aromatic ring is perpendicular to the average plane of the morpholine ring. In this situation H3 and H4 are much closer to the nitro group and should be deshielded relative to H1 and H3. Variable temperature NMR in DMSO-d<sub>6</sub> (400 MHz) showed considerable fine structure for the various peaks at -40 °C coalescence at about 15 °C some sharpening at 60 °C and another coalescence at 80-100 °C. It is hypothesized that the first coalescence is due to the C-C bond rotation b) and the second is due to the C-N bond restricted rotation; bond a). Reduction of the nitro group to the amine greatly simplified both spectra (**Figure 37** and **38**) since only the amide bond restricted rotation remained. It is assumed that intramolecular hydrogen bonding fixes the amide carbonyl group and the *ortho*-amino group in the same plane as the aromatic ring. The two carbons alpha to nitrogen is still different assuming restricted rotation. These appear to be coalesced at about 53 ppm. The two carbons attached to oxygen of the morpholine ring appears as a single sharp resonance at 64.4 ppm. In the proton spectrum both the hydrogens alpha to nitrogen and alpha to oxygen appear as broad peaks, one at  $\delta = 3.46$  ppm

and the other at 3.52 ppm; the broad peaks are consistent with the axial and equatorial hydrogens in each case undergoing slow exchange of position.

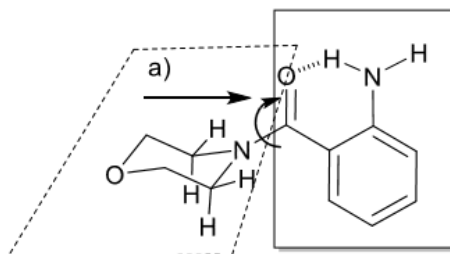


**Figure 32.** Axial and equatorial hydrogens in each case undergoing slow exchange of position.

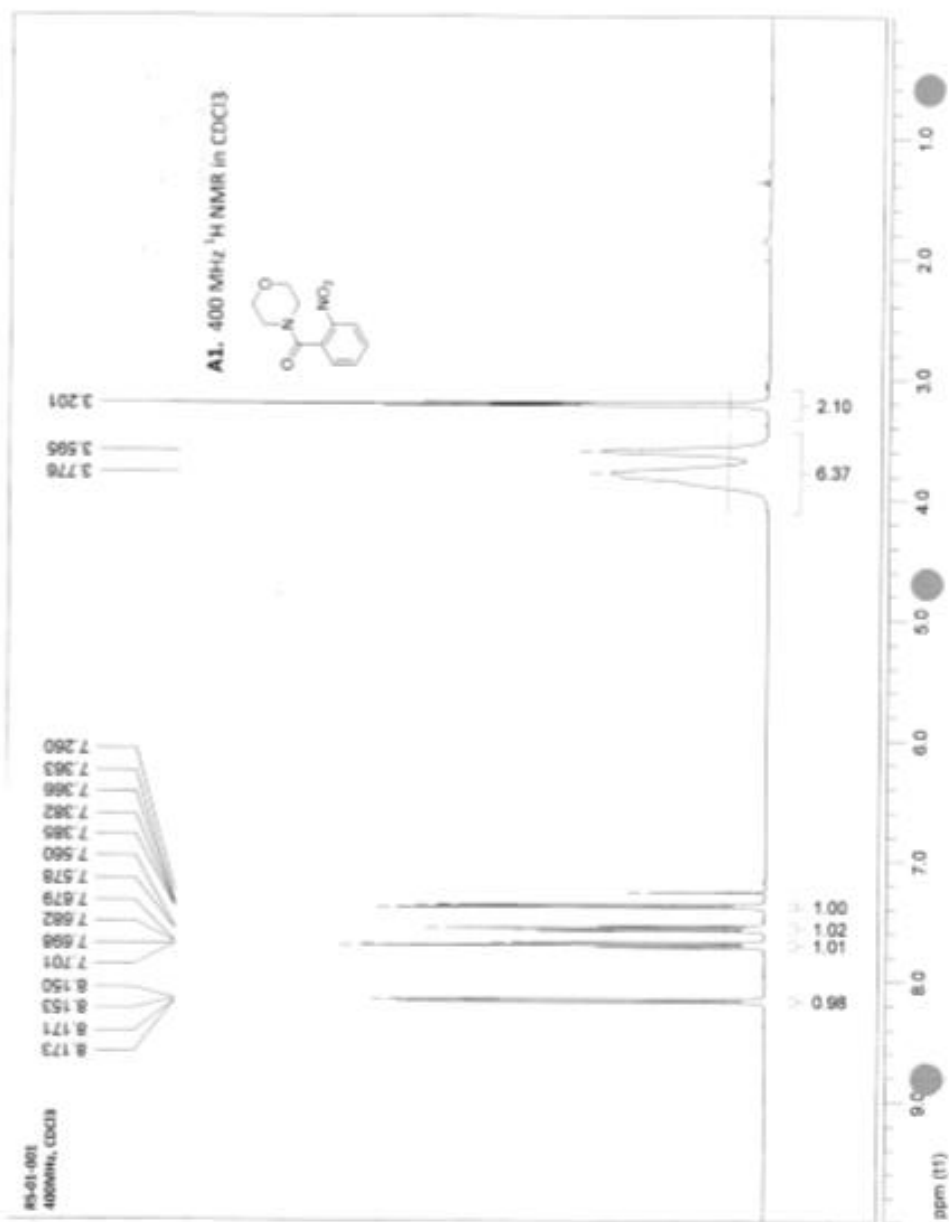
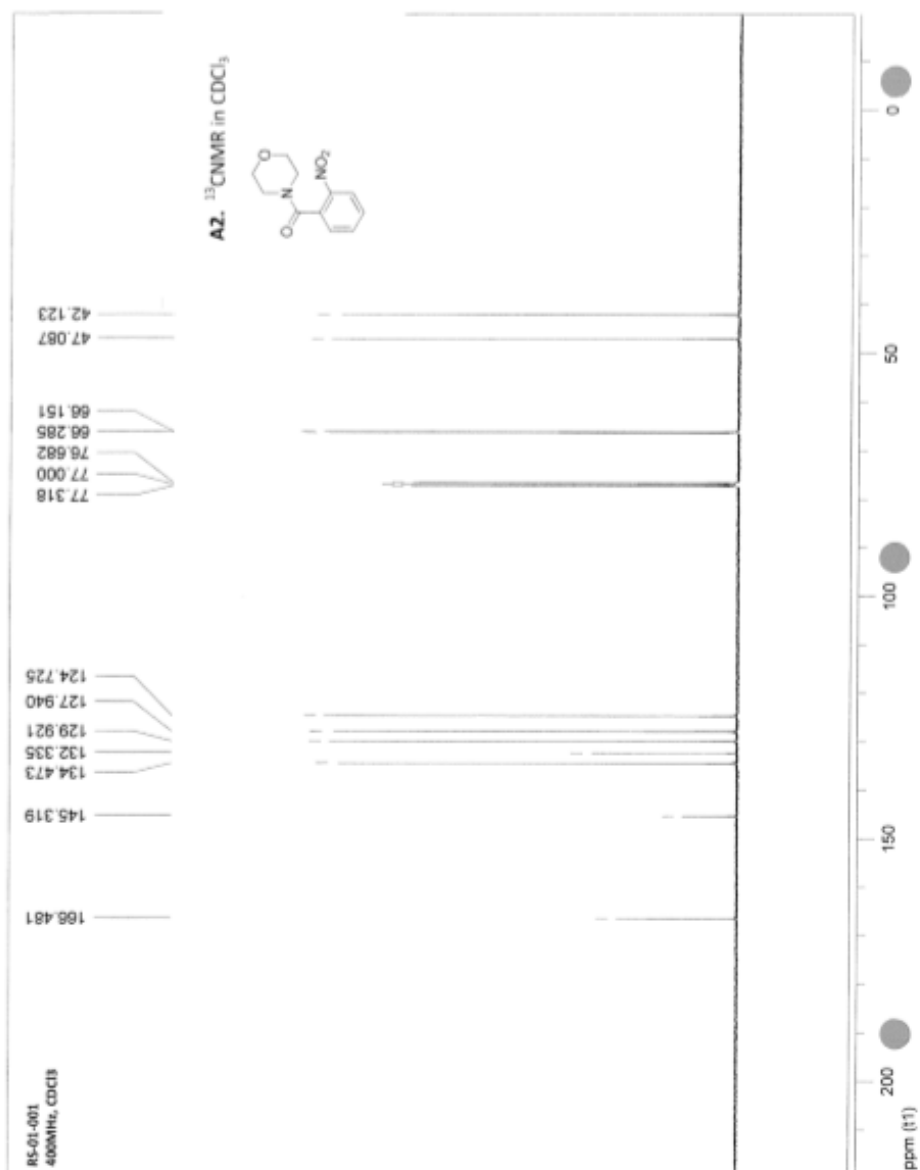


Figure 33. 400 MHz <sup>1</sup>H NMR Spectrum in CDCl<sub>3</sub>



**Figure 34.** 100 MHz <sup>13</sup>C NMR spectrum in CDCl<sub>3</sub>.

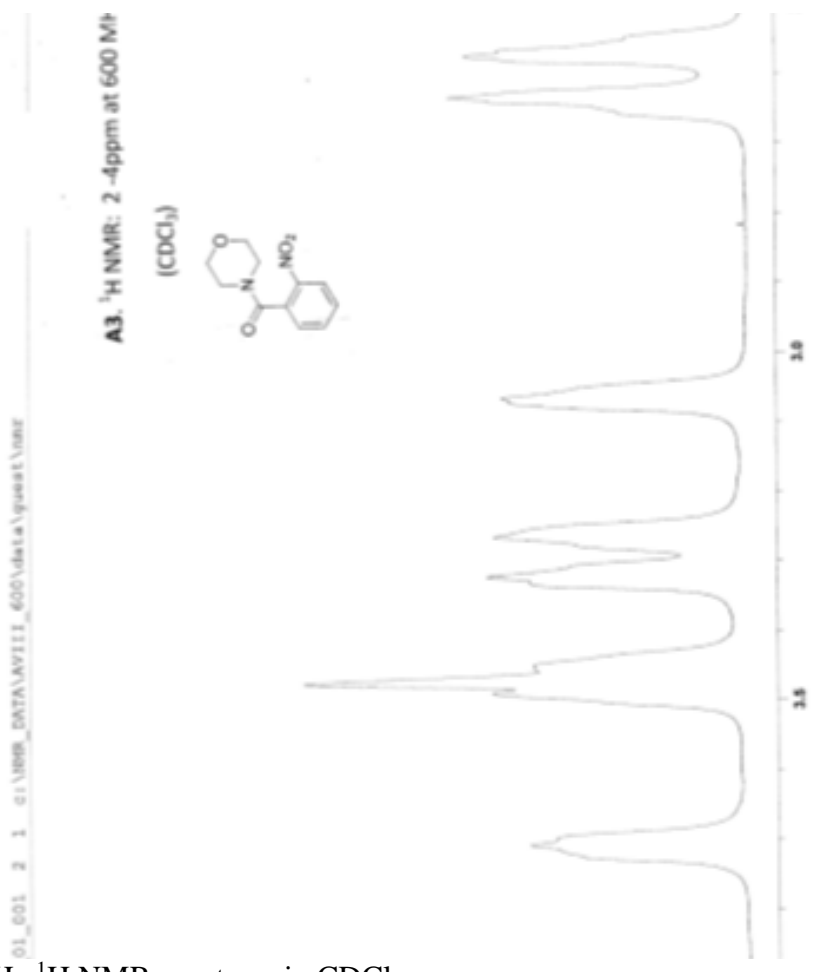


Figure 35. 600 MHz <sup>1</sup>H NMR spectrum in CDCl<sub>3</sub>.



**Figure 36.** 600 MHz HETCOR spectrum in CDCl<sub>3</sub>

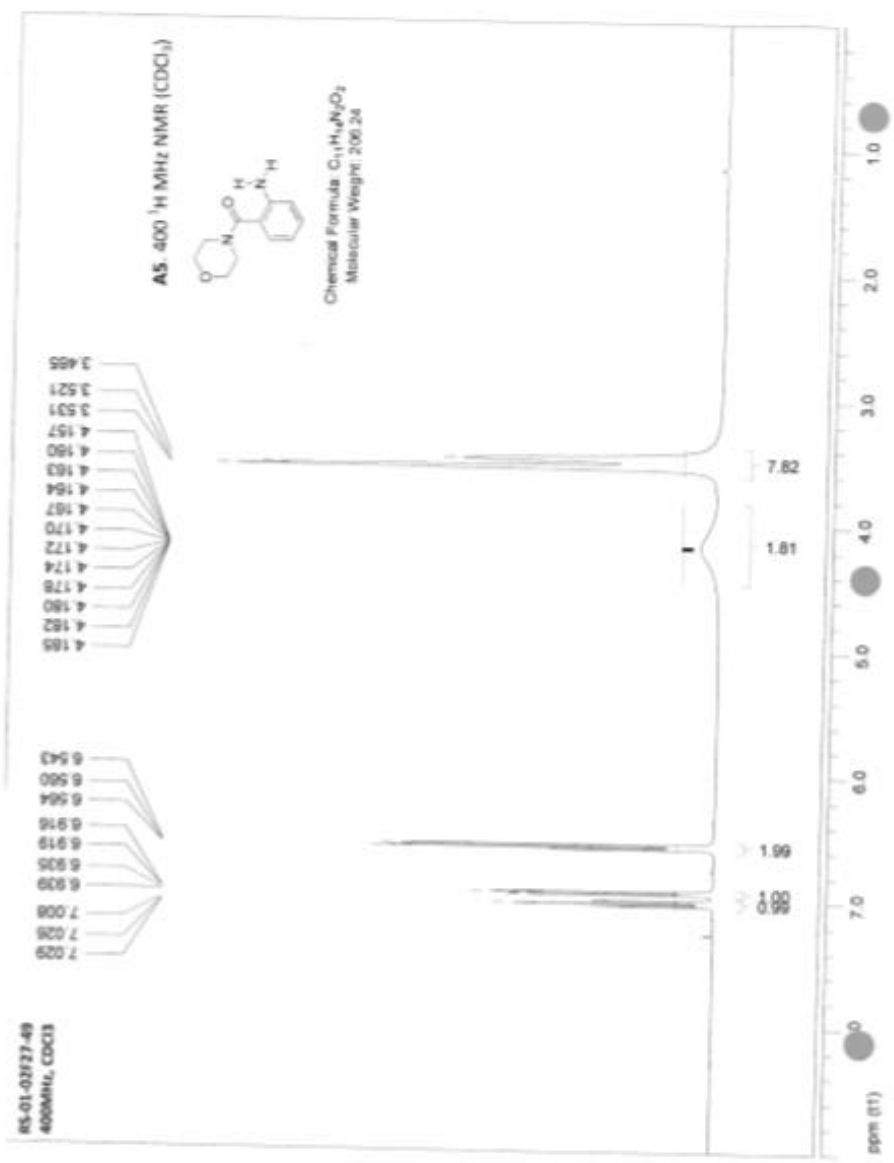


Figure 37. 400 MHz <sup>1</sup>H NMR Spectrum in CDCl<sub>3</sub>.

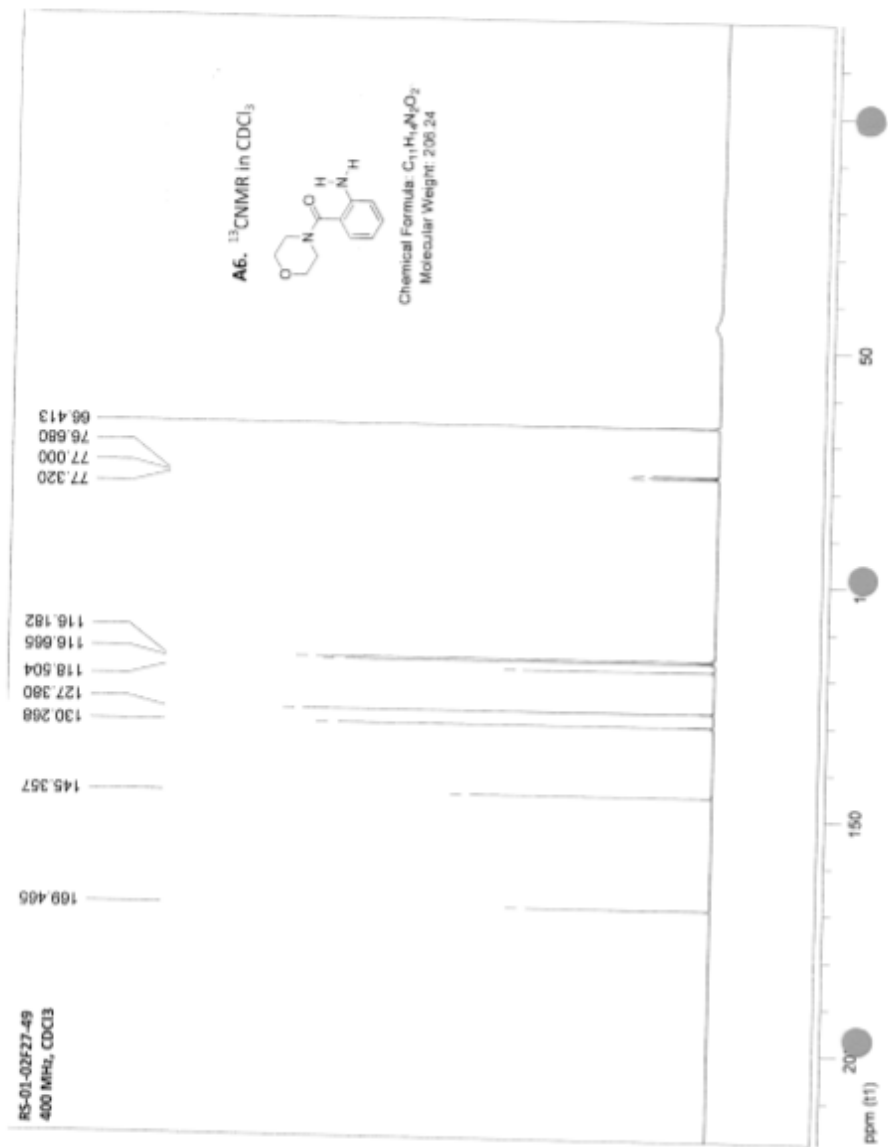


Figure 38. 100 MHz <sup>13</sup>C NMR spectrum in CDCl<sub>3</sub>.

## 9.0 Future Directions and conclusions

To date, not all of the results for the compounds have been prepared or made available, some conclusions have been made. It can be said that the *ortho*-substituted analogs do not show an improved activity relative to **Z02** or to the analogs in which the amide and carbonyl group in the B unit have *meta*- orientation. Therefore, *ortho*- substituent analogs are not going to be explored more readily compared to other orientations. It is planned to make more meta-oriented composition and further test the effects of structural changes. It is important to further determine the relevance of a small A unit on the *meta*-oriented analogs and to assess whether an amide is necessary or not. On the other hand a methoxy group *ortho*- to the amine in the B unit has been demonstrated, however, it will be interesting to develop more analogs with a small group at the A unit position. Currently, diethylamine, dimethyl amine and methyl amine derivatives are currently sent to the Brown group to assess for bioassay results. The possibilities for these structural changes are endless and therefore, in order to progress with this research, it is essential to correctly interpret results and make more conclusions for future predictions.

## 10.0 References

1. Schmalfeldt M, Bandtlow CE, Dours-Zimmermann MT, Winterhalter KH, Zimmermann DR. Brain derived versican V2 is a potent inhibitor of axonal growth. *J Cell Sci.* **2000**; *113*: 807–16.
2. Thuret, S., Moon, L.D. & Gage, F.H. Therapeutic interventions after spinal cord injury. *Nat Rev Neurosci* **7**, 628-643 (2006).
3. Gris, P., Tighe, A., Levin, D., Sharma, R. & Brown, A. Transcriptional regulation of scar gene expression in primary astrocytes. *Glia* **55**, 1145-1155 (2007).
4. Gotting, C., Kuhn, J., Zahn, R., Brinkmann, T. & Kleesiek, K. Molecular cloning and expression of human UDP-d-Xylose:proteoglycan core protein beta-d-xylosyltransferase and its first isoform XT-II. *J. Mol. Biol.* **304**, 517-528 (2000).
5. Yamauchi, S., *et al.* Molecular cloning and expression of chondroitin 4-sulfotransferase. *J. Biol. Chem.* **275**, 8975-8981 (2000).
6. Celio, M.R. & Blumcke, I. Perineuronal nets--a specialized form of extracellular matrix in the adult nervous system. *Brain Res. Brain Res. Rev.* **19**, 128-145 (1994).
7. Galtrey, C.M. & Fawcett, J.W. The role of chondroitin sulfate proteoglycans in regeneration and plasticity in the central nervous system. *Brain Res Rev* **54**, 1-18 (2007).
8. Lemons, M.L., Howland, D.R. & Anderson, D.K. Chondroitin sulfate proteoglycan immunoreactivity increases following spinal cord injury and transplantation. *Exp. Neurol.* **160**, 51-65. (1999).
9. Dou, C.L. & Levine, J.M. Inhibition of neurite growth by the NG2 chondroitin sulfate proteoglycan. *J. Neurosci.* **14**, 7616-7628 (1994).
10. Schmalfeldt, M., Bandtlow, C.E., Dours-Zimmermann, M.T., Winterhalter, K.H. & Zimmermann, D.R. Brain derived versican V2 is a potent inhibitor of axonal growth. *J. Cell Sci.* **113** ( Pt 5), 807-816 (2000).
11. Friedlander, D.R., *et al.* The neuronal chondroitin sulfate proteoglycan neurocan binds to the neural cell adhesion molecules Ng-CAM/L1/NILE and N-CAM, and inhibits neuronal adhesion and neurite outgrowth. *J. Cell Biol.* **125**, 669-680 (1994).
12. Yamada, H., *et al.* The brain chondroitin sulfate proteoglycan brevican associates with astrocytes ensheathing cerebellar glomeruli and inhibits neurite outgrowth from granule neurons. *J. Neurosci.* **17**, 7784-7795 (1997).

13. Milev, P., *et al.* Interactions of the chondroitin sulfate proteoglycan phosphacan, the extracellular domain of a receptor-type protein tyrosine phosphatase, with neurons, glia, and neural cell adhesion molecules. *J. Cell Biol.* **127**, 1703-1715 (1994).
14. Bradbury, E.J., *et al.* Chondroitinase ABC promotes functional recovery after spinal cord injury. *Nature* **416**, 636-640. (2002).
15. Caggiano, A.O., Zimmer, M.P., Ganguly, A., Blight, A.R. & Gruskin, E.A. Chondroitinase ABCI improves locomotion and bladder function following contusion injury of the rat spinal cord. *J. Neurotrauma* **22**, 226-239 (2005).
16. Corvetti, L. & Rossi, F. Degradation of chondroitin sulfate proteoglycans induces sprouting of intact purkinje axons in the cerebellum of the adult rat. *J. Neurosci.* **25**, 7150-7158 (2005).
17. Garcia-Alias, G., Barkhuysen, S., Buckle, M. & Fawcett, J.W. Chondroitinase ABC treatment opens a window of opportunity for task-specific rehabilitation. *Nat. Neurosci.* **12**, 1145-1151 (2009).
18. Huang, W.C., *et al.* Chondroitinase ABC promotes axonal re-growth and behavior recovery in spinal cord injury. *Biochem. Biophys. Res. Commun.* **349**, 963-968 (2006).
19. Grimpe, B. & Silver, J. A novel DNA enzyme reduces glycosaminoglycan chains in the glial scar and allows microtransplanted dorsal root ganglia axons to regenerate beyond lesions in the spinal cord. *J. Neurosci.* **24**, 1393-1397 (2004).
20. Laabs, T.; Carulli, D.; Geller, H.; Fawcett, J.; Chondroitin sulfate proteoglycans in neural development and regeneration. *Curr. Opin. Neurobiol.* **15**(2), 116-120 (2005).
21. Gris, P.; Tighe, A.; Levin, D.; Sharma, R.; Brown, A.; Transcriptional regulation of scar gene expression in primary astrocytes. *Glia* **55**(11), 1145-1155 (2007).
22. Hayashi, S. & McMahon, A.P. Efficient recombination in diverse tissues by a tamoxifeninducible form of Cre: a tool for temporally regulated gene activation/inactivation in the mouse. *Dev. Biol.* **244**, 305-318 (2002).
23. McKillop, W.; Dragan, M.; Schedl, A.; Brown, A.; Conditional SOX9 ablation reduces chondroitin sulfate proteoglycan levels and improved motor function following spinal cord injury. *Glia* **61**(2), 164-177 2012.
24. McKillop, W.M., Dragan, M., Schedl, A. & Brown, A. Conditional Sox9 ablation reduces chondroitin sulfate proteoglycan levels and improves motor function following spinal cord injury. *Glia* **61**, 164-177 (2013).
25. Basso, D.M., *et al.* Basso Mouse Scale for locomotion detects differences in recovery after spinal cord injury in five common mouse strains. *J. Neurotrauma* **23**, 635-659 (2006).

26. McKillop, W.M., *et al.* Conditional Sox9 ablation improves locomotor recovery after spinal cord injury by increasing reactive sprouting. *Exp. Neurol.* **283**, 1-15 (2016).
27. Peterson, J.T. Matrix metalloproteinase inhibitor development and the remodeling of drug discovery. *Heart failure reviews* **9**, 63-79 (2004).
28. Pizzi, M.A. & Crowe, M.J. Matrix metalloproteinases and proteoglycans in axonal regeneration. *Exp. Neurol.* **204**, 496-511 (2007).
29. Xu, X., *et al.* Sox9 knockout mice have improved recovery and increased reparative sprouting following stroke. *J. Cereb. Blood Flow Metab.* **in revision**(2017).
30. Bernard, P., *et al.* Dimerization of SOX9 is required for chondrogenesis, but not for sex determination. *Hum. Mol. Genet.* **12**, 1755-1765 (2003).
31. Sock, E., *et al.* Loss of DNA-dependent dimerization of the transcription factor SOX9 as a cause for campomelic dysplasia. *Hum. Mol. Genet.* **12**, 1439-1447 (2003).
32. Coustry, F., *et al.* The dimerization domain of SOX9 is required for transcription activation of a chondrocyte-specific chromatin DNA template. *Nucleic Acids Res* **38**, 6018-6028 (2010).
33. Schwarze, S.R., Ho, A., Vocero-Akbani, A. & Dowdy, S.F. In vivo protein transduction: delivery of a biologically active protein into the mouse. *Science* **285**, 1569-1572 (1999).

## APPENDIX A. Copies of NMR spectra of synergists.

### Experimental Section

#### *Reactions*

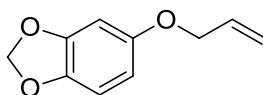
All reactions were monitored by TLC using aluminum backed TLC plates (EMD Chemicals, TLC Silica Gel 60 F<sub>254</sub>), which were visualized by UV lamp (254 nm – fixed wavelength). Plates were then permanently stained with Hannessian's stain. All moisture sensitive reactions were carried out under nitrogen or argon atmosphere. Anhydrous THF was prepared by distillation from sodium and benzophenone and DCM from calcium hydride.

#### *Purification*

Purification by column chromatography was performed using SiliCycle SiliFlash® F60 silica gel of 230-400 mesh and glass columns fitted with a cotton piece and sand or fritted glass filter. Elutions were carried out with mixtures of hexanes and ethyl acetate.

#### *NMR*

<sup>1</sup>H NMR and <sup>13</sup>C NMR were recorded on Bruker Avance 400 spectrometer. Samples were dissolved in deuterated chloroform, methanol or acetone as indicated. All chemical shifts are reported in parts per million (ppm) and are referenced accordingly to the deuterated solvent used. Integrations are listed in parentheses along with coupling constants which are reported in Hz, where applicable.



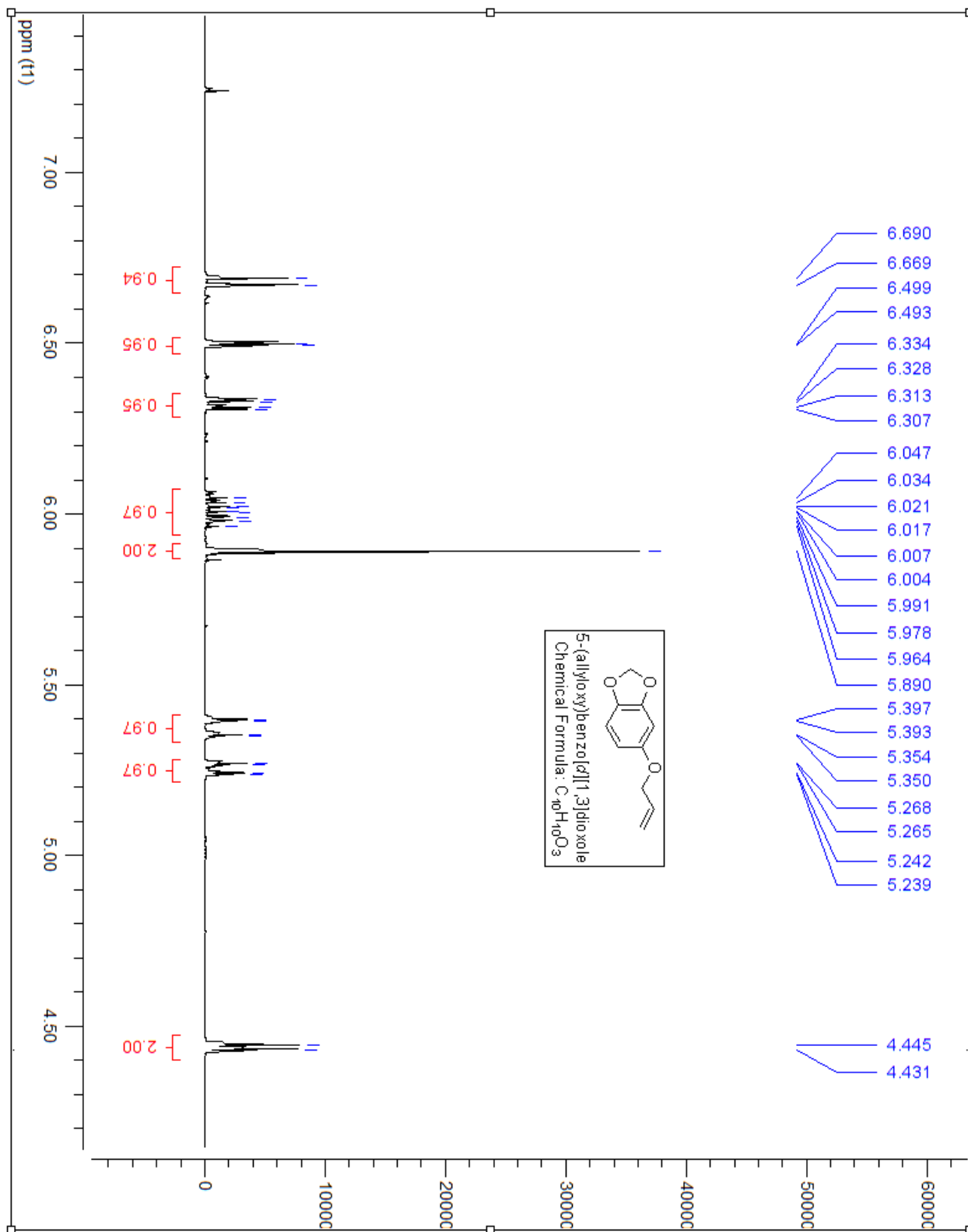
Chemical Formula: C<sub>10</sub>H<sub>10</sub>O<sub>3</sub>  
Molecular Weight: 178.18

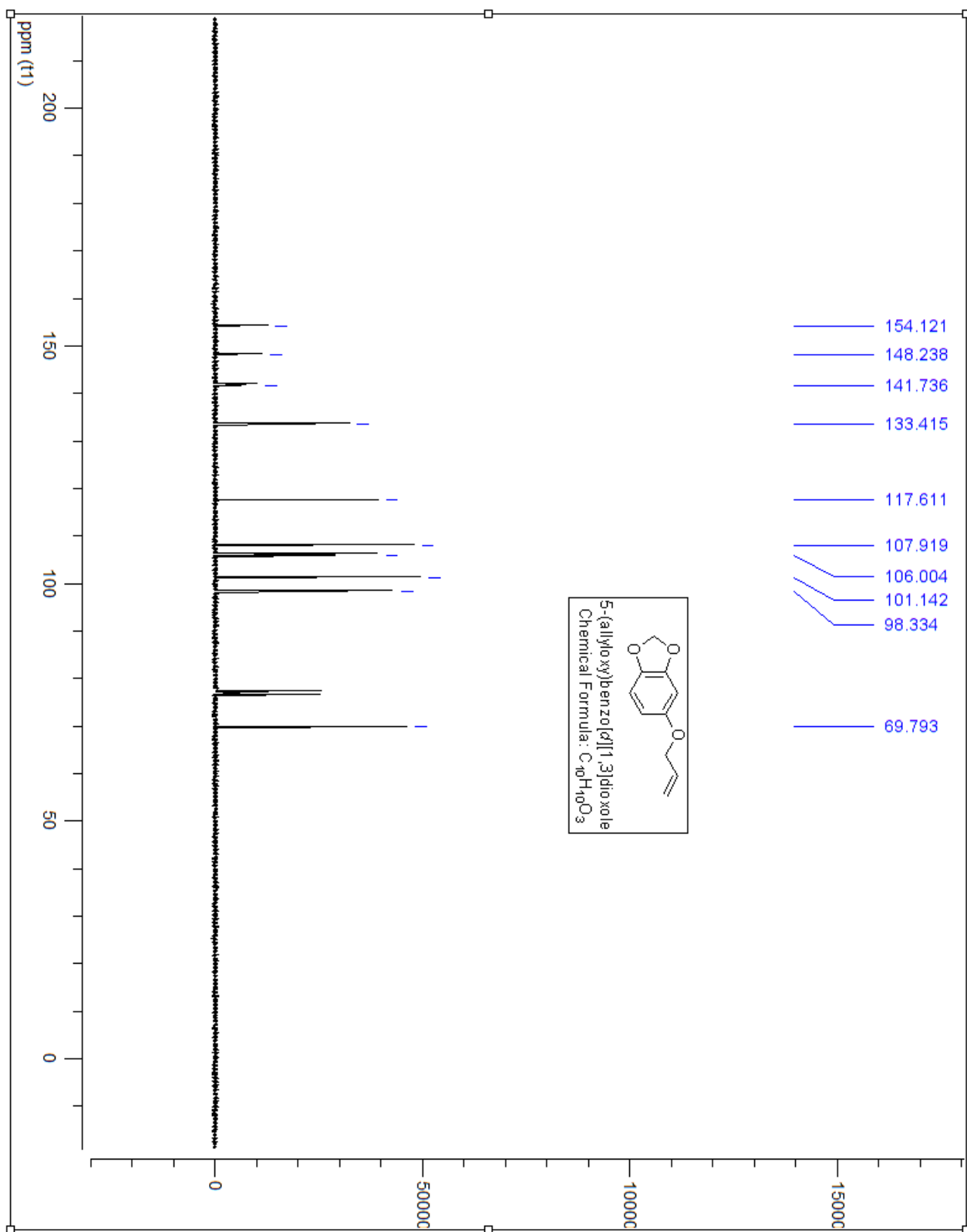
### 21a

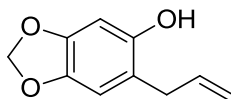
This compound was prepared using **sesamol** (11g, 79.6 mmol), in 40 ml of Acetone, potassium carbonate (25g, 180.1 mmol) was added and stirred for 10 minutes before the addition of allyl bromide (6.73ml, 79.4mmol) and refluxed for 6 hours. The reaction mixture was extracted with EtOAc and water. The phenol was washed with 10% NaOH. The crude product (8.92 g) was purified via gradient column chromatography (2.5% EtOAc in hexanes) resulting as a clear oil (8.1g, Rf= 0.3 in 2:8 EtOAc:Hexanes).

<sup>1</sup>H NMR (400 MHz, CDCl<sub>3</sub>) δ ppm 6.69-6.67 (d, *J* = 9.33 Hz, 1H), 6.50-6.49 (d, *J* = 8.47 Hz, 1H), 6.33-6.30 (d, *J* = 8.47 Hz, 1H), 6.04-5.96 (m, 1H), 5.88 (s, 2H), 5.39-5.35 (dd, *J* = 17.26, 17.26 Hz, 1H), 5.27-5.24 (dd, *J* = 10.5, 10.5 Hz, 1H), 4.44-4.42 (dt, (*J* = 5.32, 5.32, 5.32 Hz, 2H)

<sup>13</sup>C NMR (100 MHz, CDCl<sub>3</sub>) δ ppm 154.12, 148.23, 141.73, 133.41, 117.61, 107.91, 106.00, 101.14, 98.33, 69.79







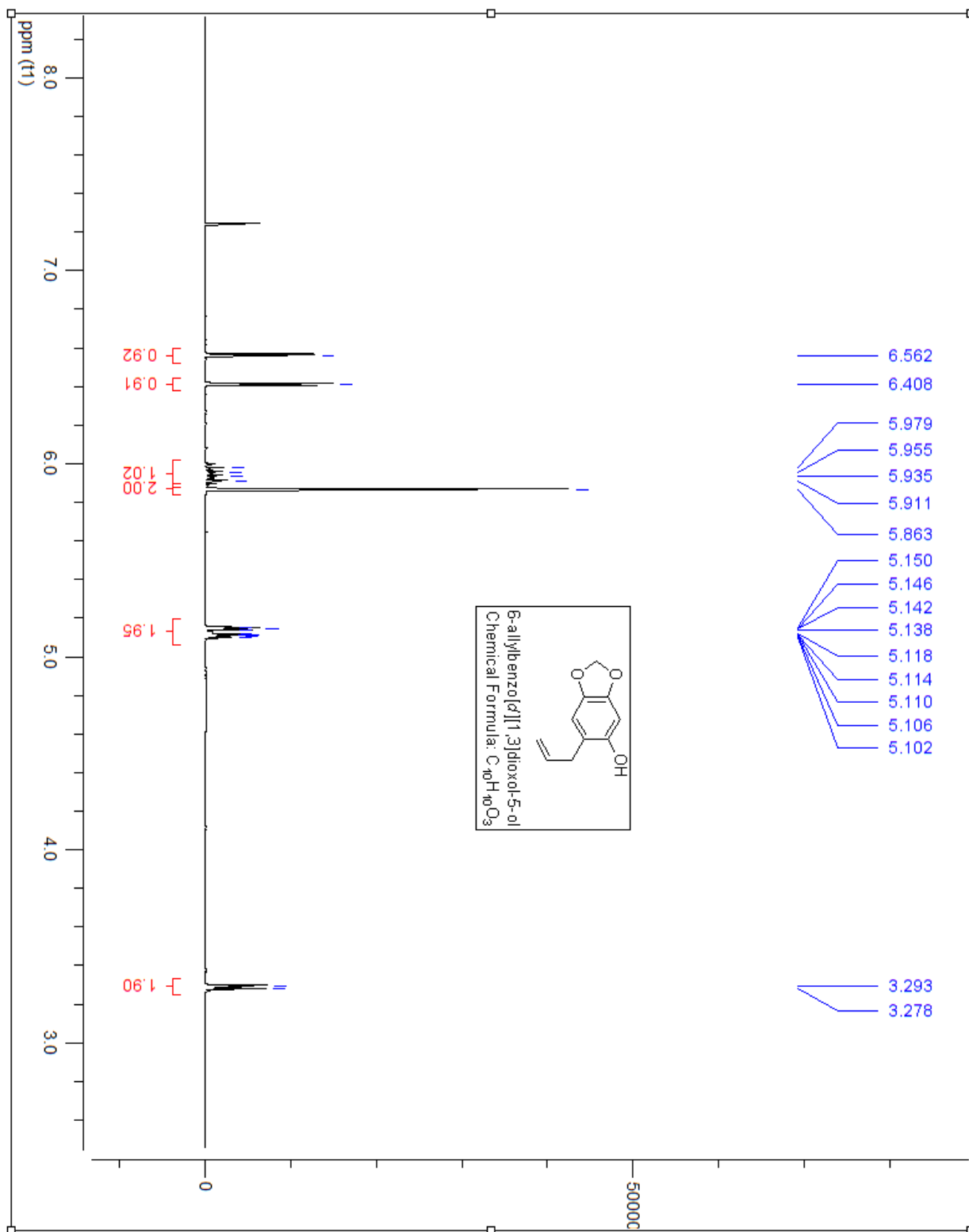
Chemical Formula: C<sub>10</sub>H<sub>10</sub>O<sub>3</sub>  
Molecular Weight: 178.18

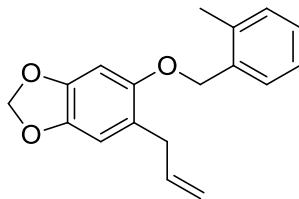
### 21b

This compound was prepared using **21a** (6g, 33.6 mmol), in 40 ml of decalin and stirred for 8 hours at 180-200°C. The reaction mixture was cooled to room temperature. The reaction mixture was extracted with EtOAc and 1N NaOH solution (3x 50ml). Alkaline extract was acidified with conc. HCl and aqueous phase was extracted with ethyl acetate (3x 40ml). Combined organic extracts were dried with MgSO<sub>4</sub>, filtered and concentrated *in vacuo* to yield a black solid (4.6g, R<sub>f</sub> = 0.15 in 2:8 EtOAc:Hexanes).

<sup>1</sup>H NMR (400 MHz, CDCl<sub>3</sub>) δ ppm 6.56 (s, 1H), 6.41 (s, 1H), 5.99-5.88 (m, 1H), 5.86 (s, 2H), 5.15-5.13 (dd, J = 3.39, 3.39 Hz, 1H), 5.11-5.10 (m, 1H), 3.29-3.27 (dt, J = 6.23, 6.23, 6.23 Hz, 2H)

<sup>13</sup>C NMR (100 MHz, CDCl<sub>3</sub>) δ ppm 148.62, 146.74, 141.51, 136.42, 116.80, 116.42, 109.53, 101.00, 98.68, 35.05





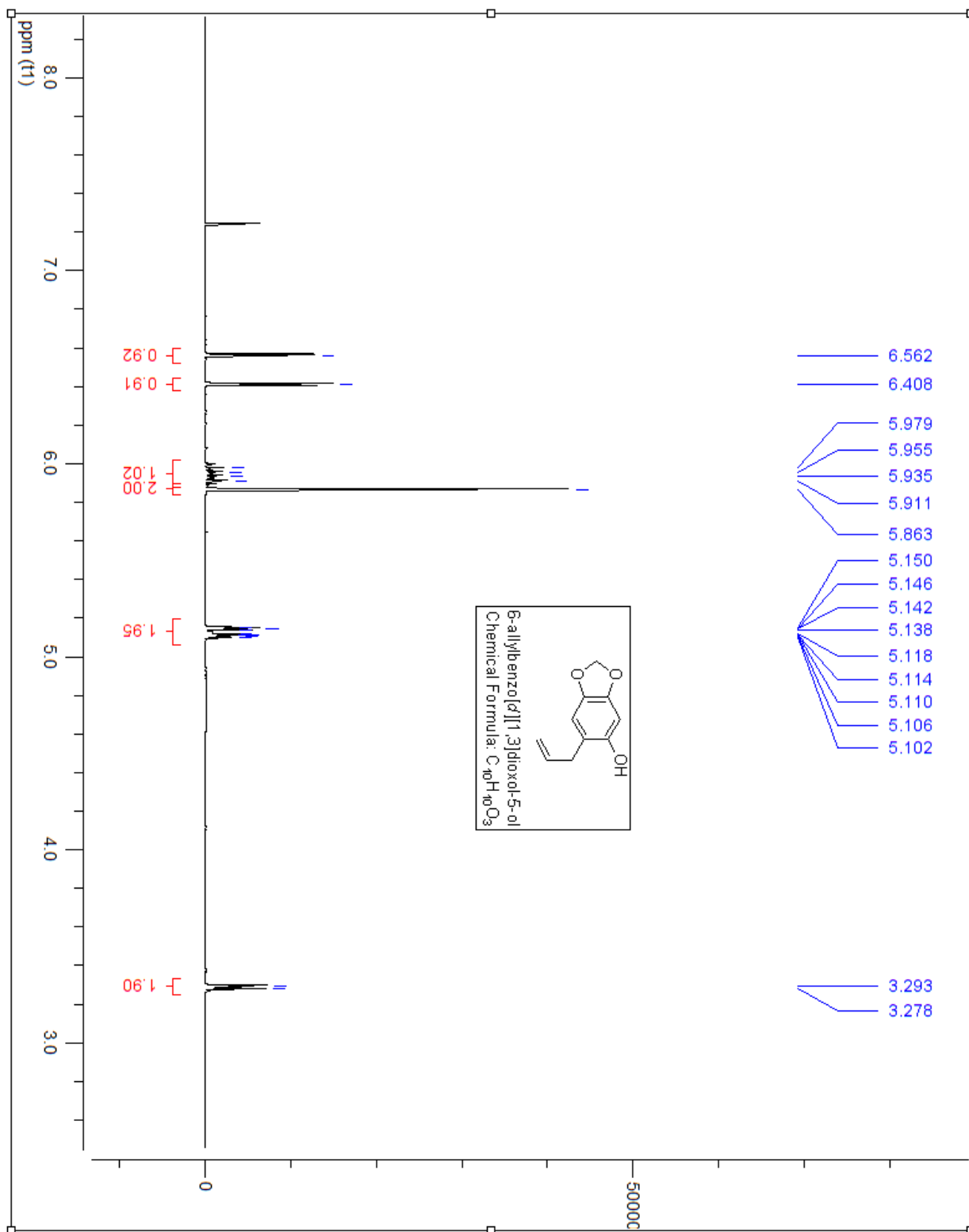
Chemical Formula: C<sub>18</sub>H<sub>18</sub>O<sub>3</sub>  
Molecular Weight: 282.33

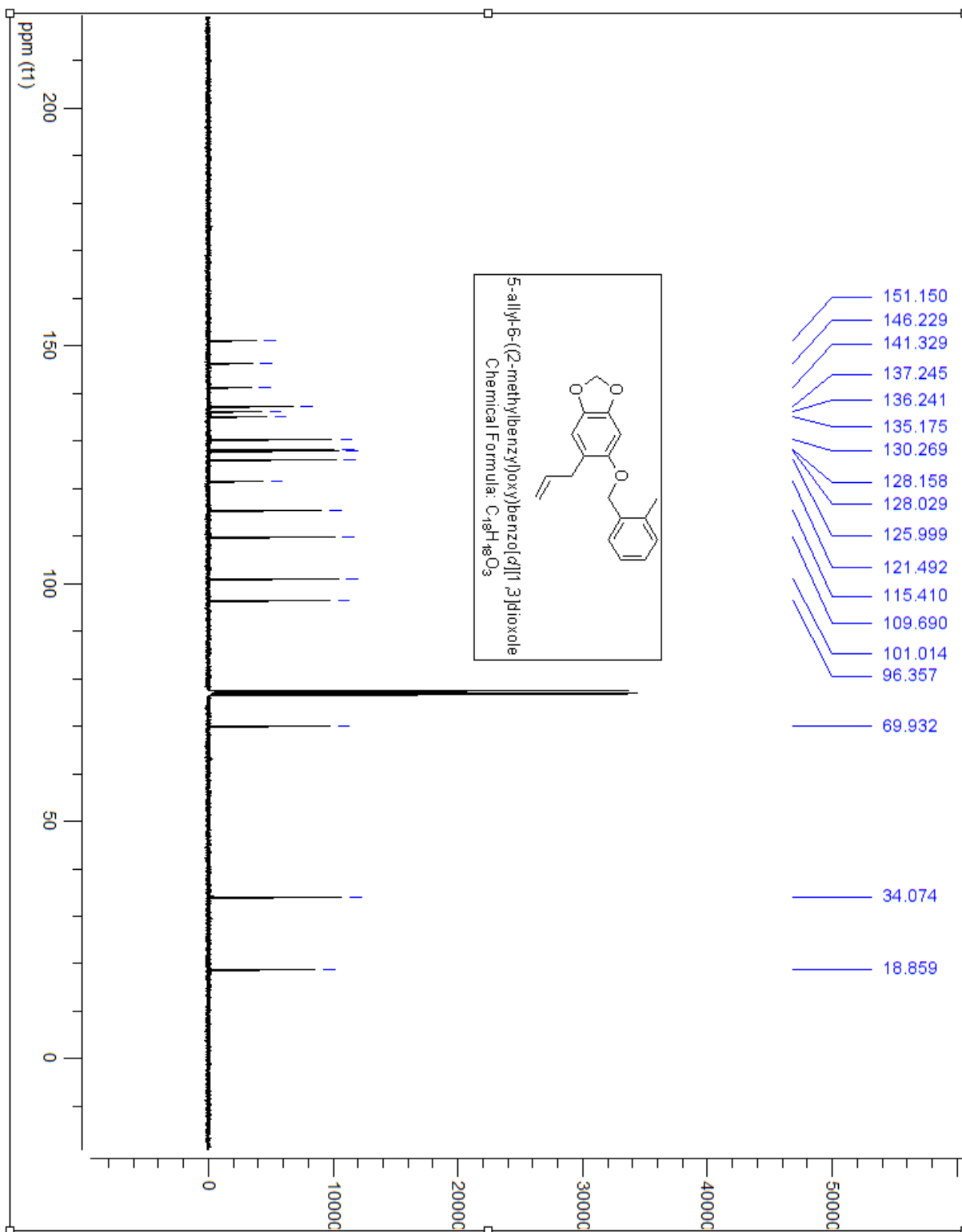
## 22

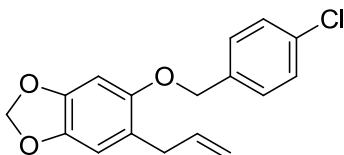
This compound was prepared using **21b** (1.67 g, 9.37 mmol), in 20 ml of Acetone, potassium carbonate (4.56 g, 3.3 mmol) was added and stirred for 10 minutes before the addition of 2-methylbenzyl bromide (1.51ml, 1.11mmol) and refluxed for 6 hours. The reaction mixture was extracted with EtOAc and water. The phenol was washed with 10% NaOH. The crude product (3.07g) was purified via gradient column chromatography (2.5% EtOAc in hexanes) resulting as a white solid (0.156 g, Rf= 0.85 in 2:8 EtOAc:Hexanes).

<sup>1</sup>H NMR (400 MHz, CDCl<sub>3</sub>) δ ppm 7.41-7.39(d, J= 7.25Hz, 1H), 7.24-7.18(m, 3H), 6.66(s, 1H), 6.59(s, 1H), 5.94-5.87(m, 3H), 5.03-4.98(m, 2H), 4.94(s, 2H), 3.32(d, J=6.61Hz, 2H), 2.35(s, 3H)

<sup>13</sup>C NMR (100MHz, CDCl<sub>3</sub>) δ ppm 151.15, 146.22, 141.32, 137.24, 136.24, 135.17, 130.26, 128.15, 128.02, 125.99, 121.49, 115.41, 109.69, 101.01, 96.35, 69.93, 34.07, 18.85







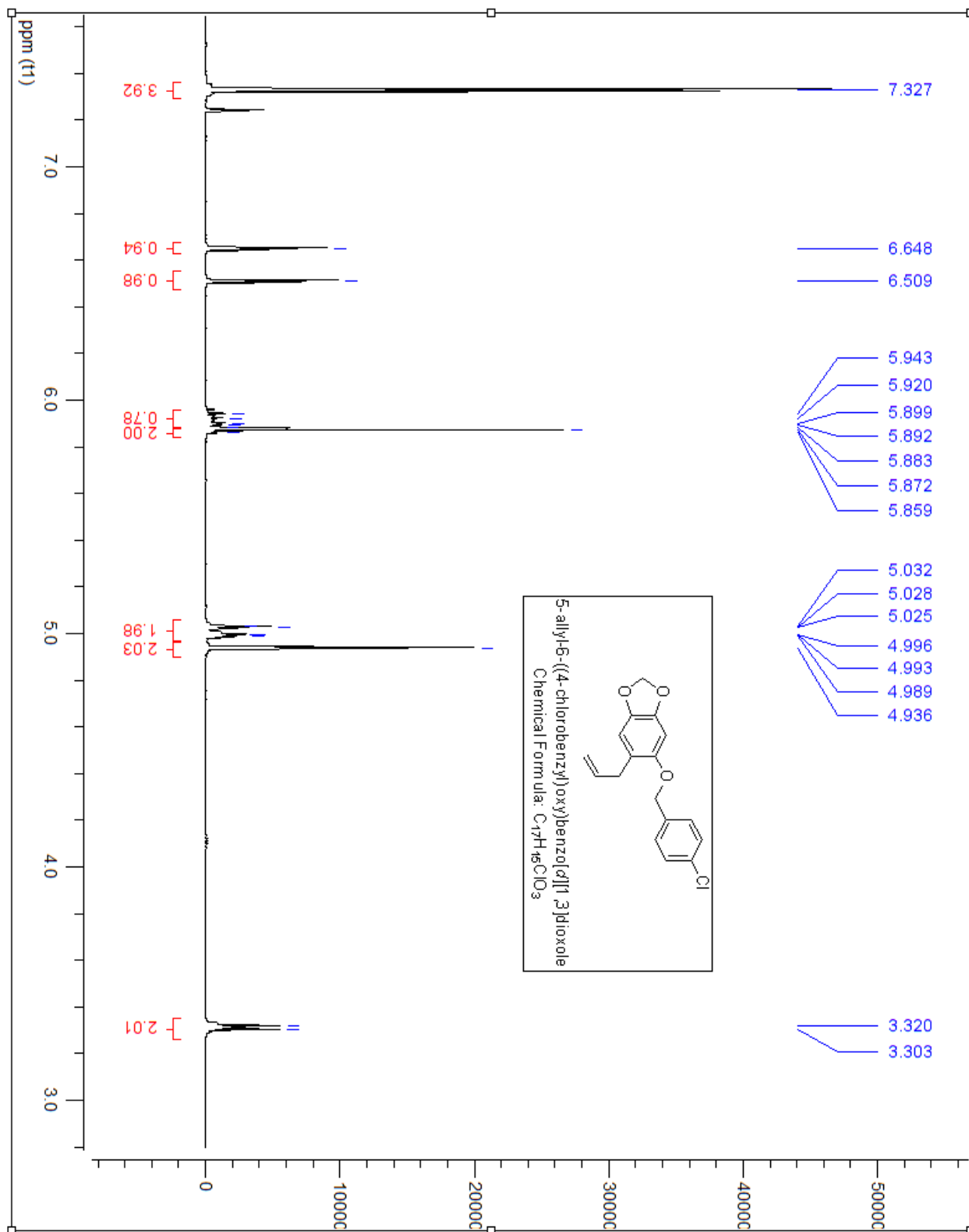
Chemical Formula: C<sub>17</sub>H<sub>15</sub>ClO<sub>3</sub>  
Molecular Weight: 302.75

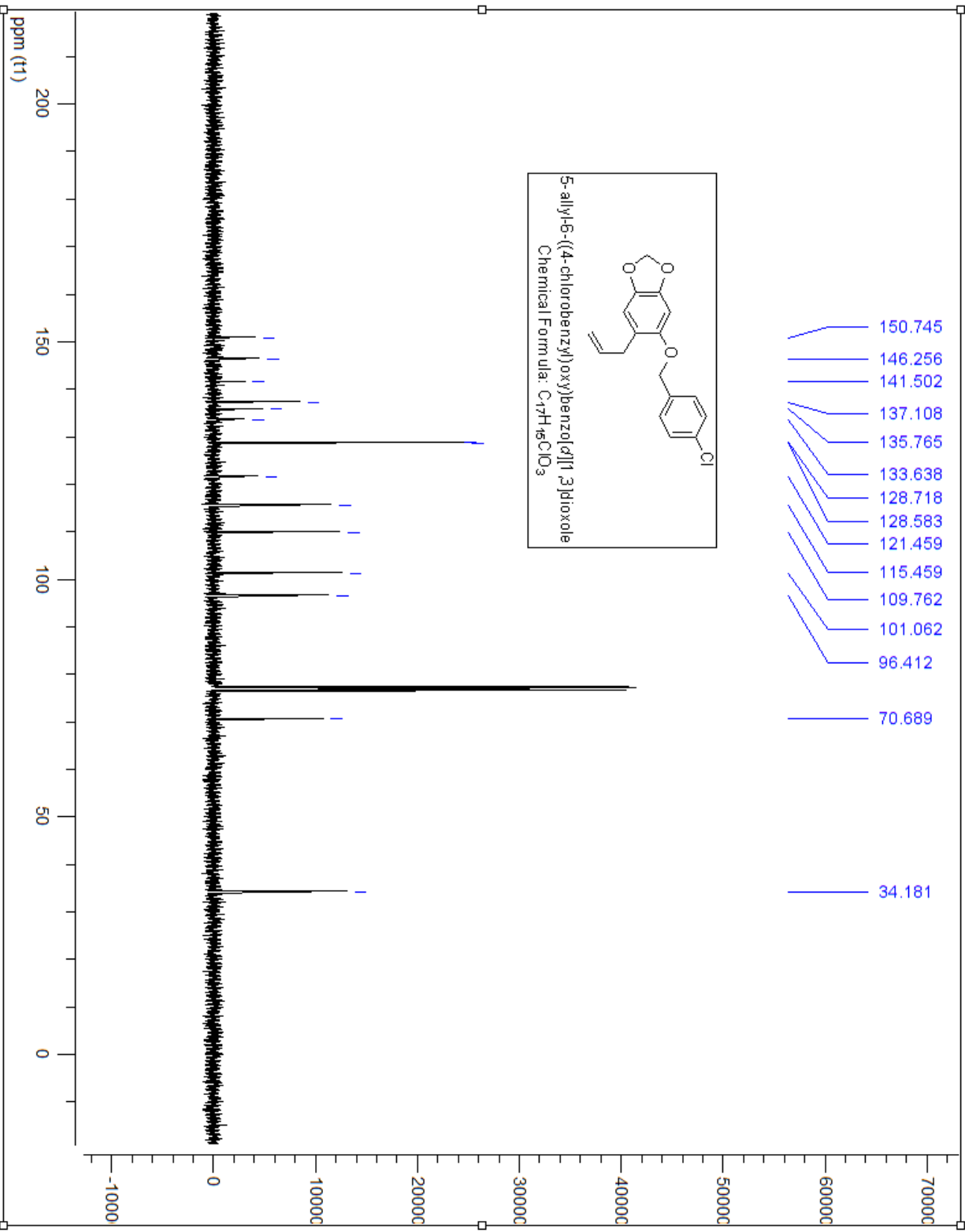
### 23

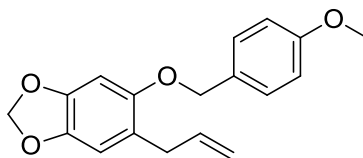
This compound was prepared using **21b** (0.2 g, 1.12 mmol), in 15 ml of Acetone, potassium carbonate (0.465 g, 3.37 mmol) was added and stirred for 10 minutes before the addition of para-chloro benzyl chloride (0.181 g, 1.12mmol) and refluxed for 6 hours. The reaction mixture was extracted with EtOAc and water. The phenol was washed with 10% NaOH. The crude product was purified via gradient column chromatography (2.5% EtOAc in hexanes) resulting as a white solid (0.12 g, Rf= 0.25 in 2:8 EtOAc:Hexanes).

<sup>1</sup>H NMR (400 MHz, CDCl<sub>3</sub>) δ ppm 7.32(s, 4H), 6.64(s, 1H), 6.51(s, 1H), 5.94-5.87(m, 1H), 5.85(s, 2H), 5.03-4.99(m, 2H), 4.93(s, 2H), 3.32-3.30(d, J= 6.69 Hz, 2H)

<sup>13</sup>C NMR (100MHz, CDCl<sub>3</sub>) δ ppm 159.15, 150.78, 146.28, 141.59, 137.17, 129.60, 129.52, 129.49, 124.52, 124.38, 124.23, 124.19, 121.67, 115.41, 115.18, 109.65, 101.05, 96.63, 65.40, 65.36, 34.14







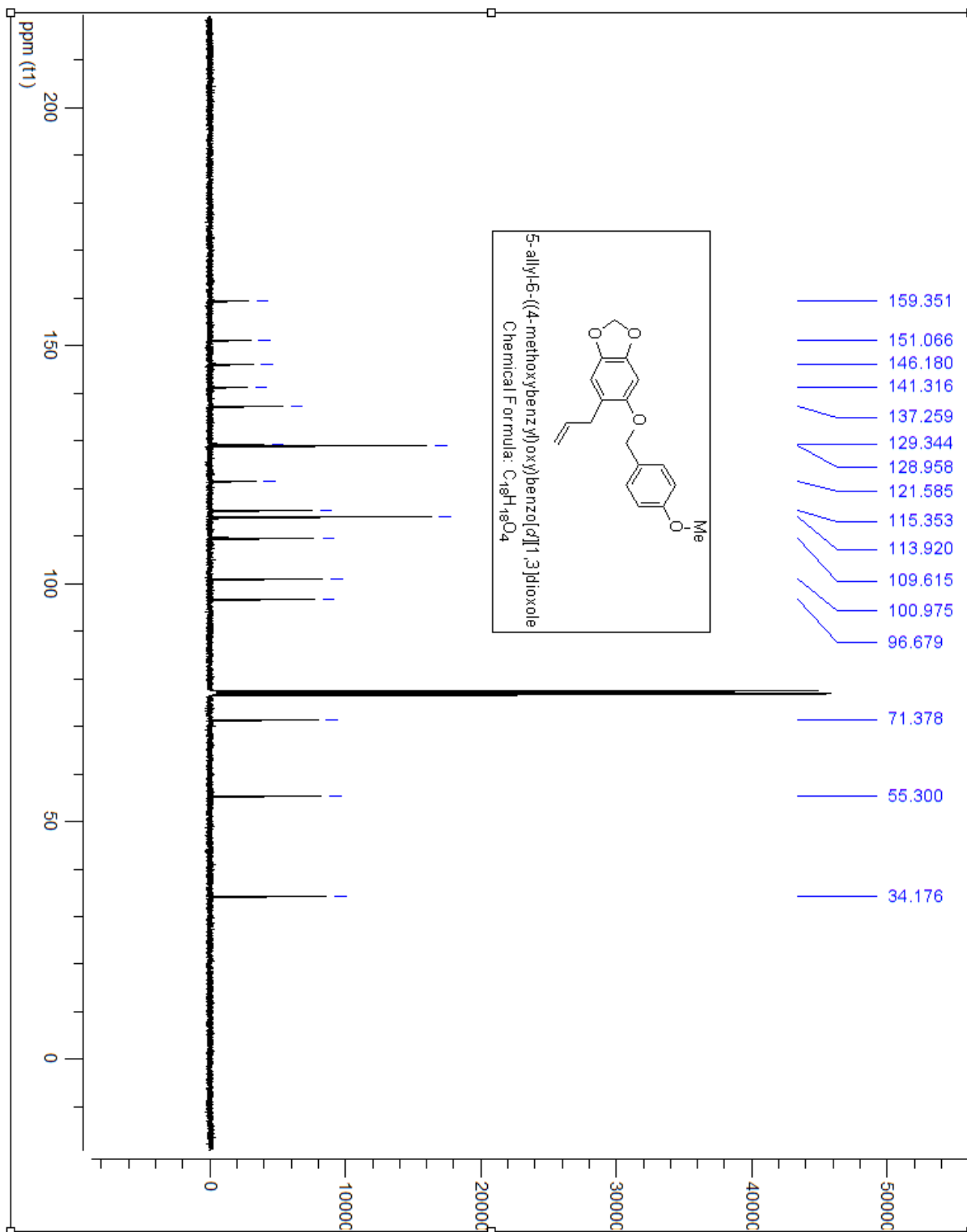
Chemical Formula: C<sub>18</sub>H<sub>18</sub>O<sub>4</sub>  
Molecular Weight: 298.33

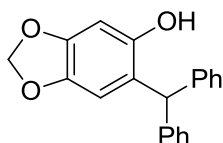
## 25

This compound was prepared using **21b** (2.91 g, 16.33 mmol), in 30 ml of Acetone, potassium carbonate (6.77 g, 48.9 mmol) was added and stirred for 10 minutes before the addition of 4 methoxy benzyl bromide (2.2ml, 16.16mmol) and refluxed for 6 hours. The reaction mixture was extracted with EtOAc and water. The phenol was washed with 10% NaOH. The crude product was purified via gradient column chromatography (2.5% EtOAc in hexanes) resulting as a white powder (2.6g, R<sub>f</sub>= 0.7 in 2:8 EtOAc:Hexanes).

<sup>1</sup>H NMR (400 MHz, CDCl<sub>3</sub>) δ ppm 7.32-7.30 (d, J= 8.69Hz, 2H), 6.89-6.87 (d, J= 8.68Hz, 2H), 6.63 (s, 1H), 6.55(s, 1H), 5.98-5.78 (m, 1H), 5.86(s, 2H), 5.03-4.98(m, 2H), 4.90(s, 2H), 3.80(s, 3H), 3.31-3.29(d, J= 6.61Hz, 2H)

<sup>13</sup>C NMR (100 MHz, CDCl<sub>3</sub>) δ ppm 159.35, 151.06, 146.18, 141.31, 137.25, 129.34, 128.95, 121.58, 115.35, 113.92, 109.61, 100.97, 96.67, 71.37, 55.30, 34.17





Chemical Formula: C<sub>20</sub>H<sub>16</sub>O<sub>3</sub>

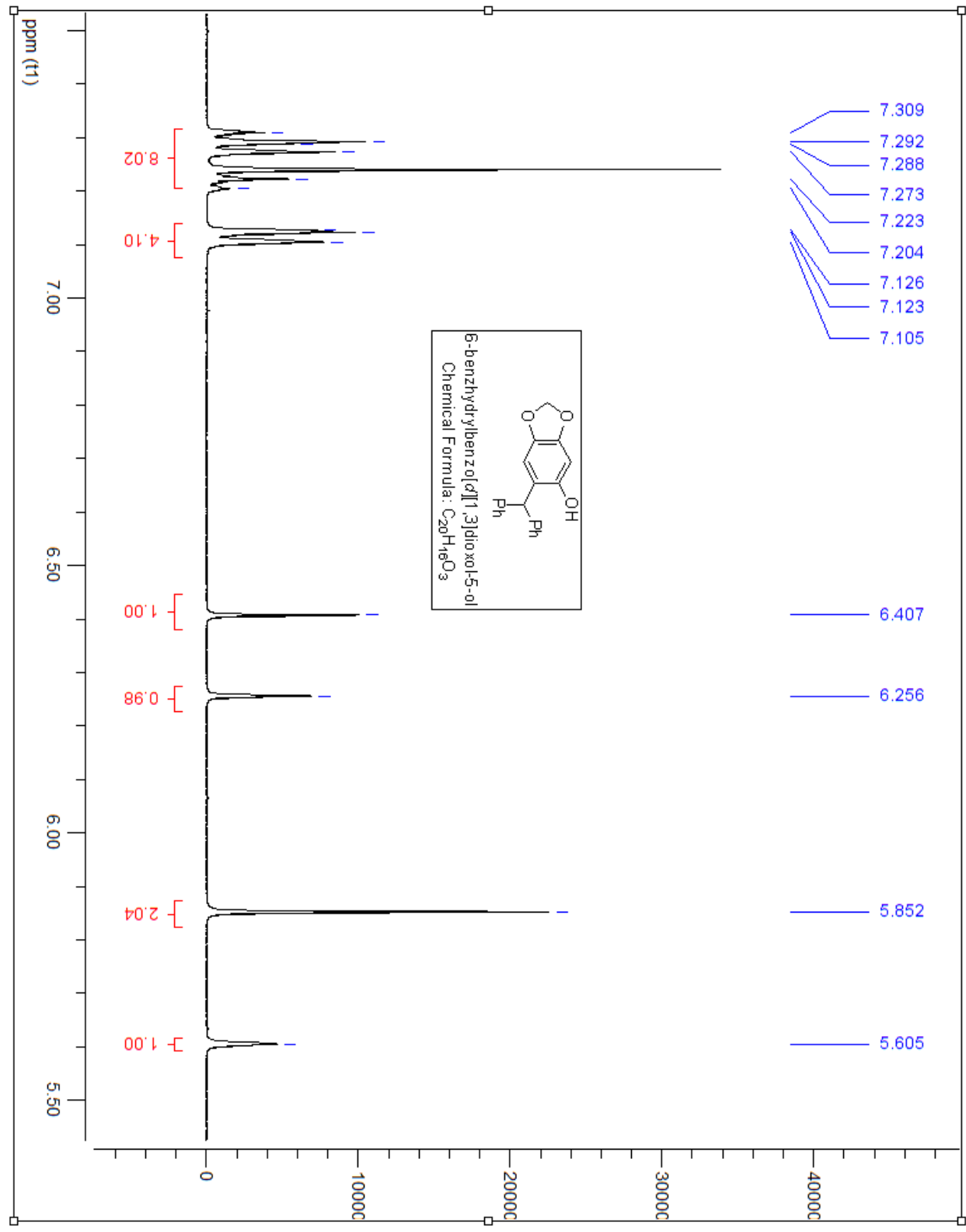
Molecular Weight: 304.34

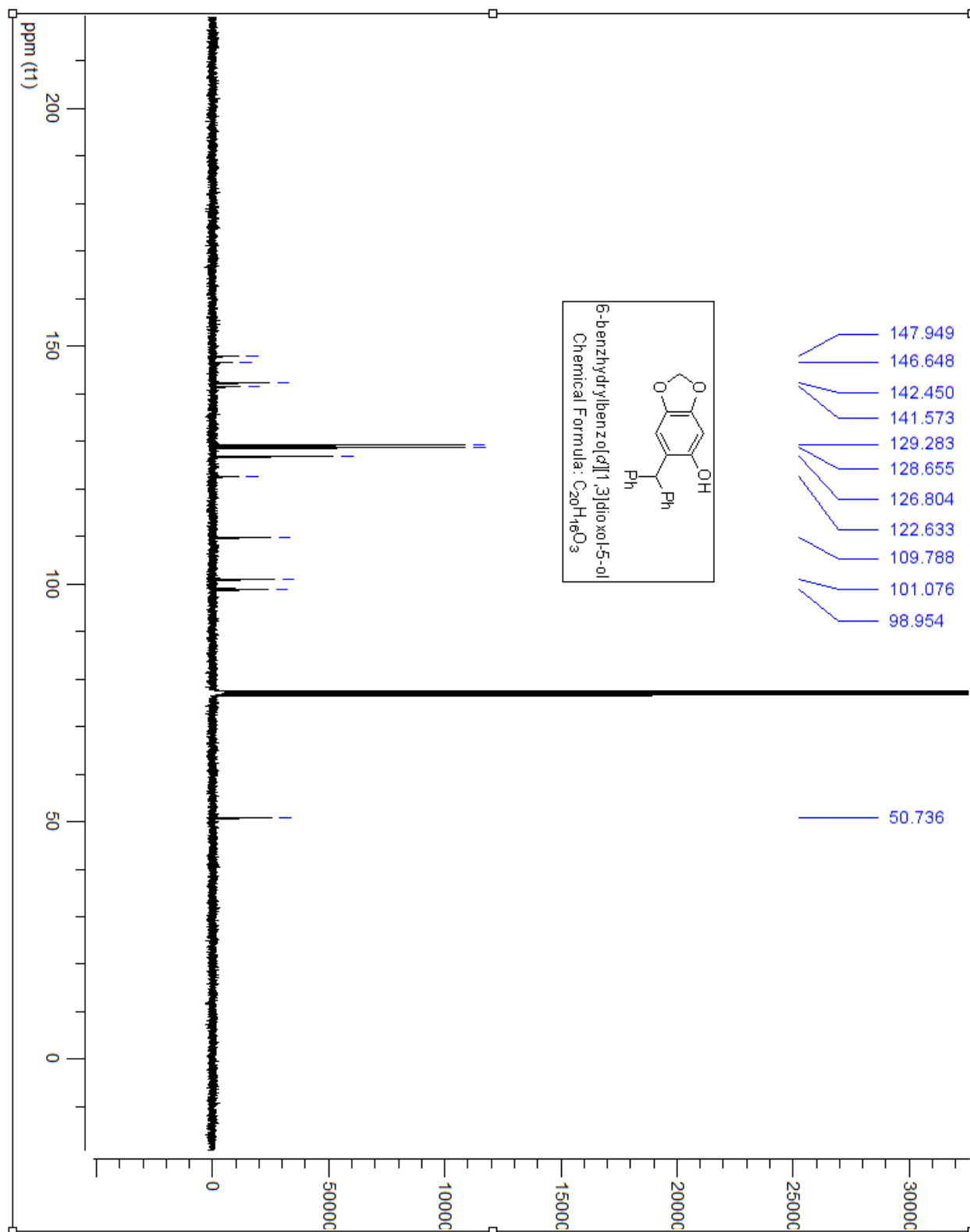
**29**

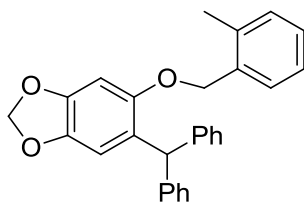
This compound was prepared using **sesamol** (2 g, 14.4 mmol), in 20 ml of dry DCM and benzhydrol (2.66g, 14.4mmol). The reaction mixture was stirred for 10 minutes before the addition of boron trifluoride diethyletherate (3.57ml, 28.9 mmol) was added over a period of an hour. After 2 hours, the reaction mixture was quenched with saturated NaHCO<sub>3</sub>, and organic layers were separated. Organic layers washed with water and brine (3x40ml) and dried with MgSO<sub>4</sub>, filtered and concentrated *in vacuo*. The crude product was purified via gradient column chromatography (2.5% EtOAc in hexanes) resulting as a brown solid (1.79g, R<sub>f</sub>= 0.20 in 2:8 EtOAc:Hexanes).

<sup>1</sup>H NMR (400 MHz, CDCl<sub>3</sub>) δ ppm 7.31-7.22 (m, 6H), 7.12-7.10 (m, 4H), 6.40 (s, 1H), 6.25 (s, 1H), 5.85 (s, 2H), 5.60 (s, 1H), 4.31 (b, 1H)

<sup>13</sup>C NMR (100 MHz, CDCl<sub>3</sub>) δ ppm 147.94, 146.64, 142.45, 141.57, 129.28, 128.65, 126.80, 122.63, 109.78, 101.07, 98.95, 50.73







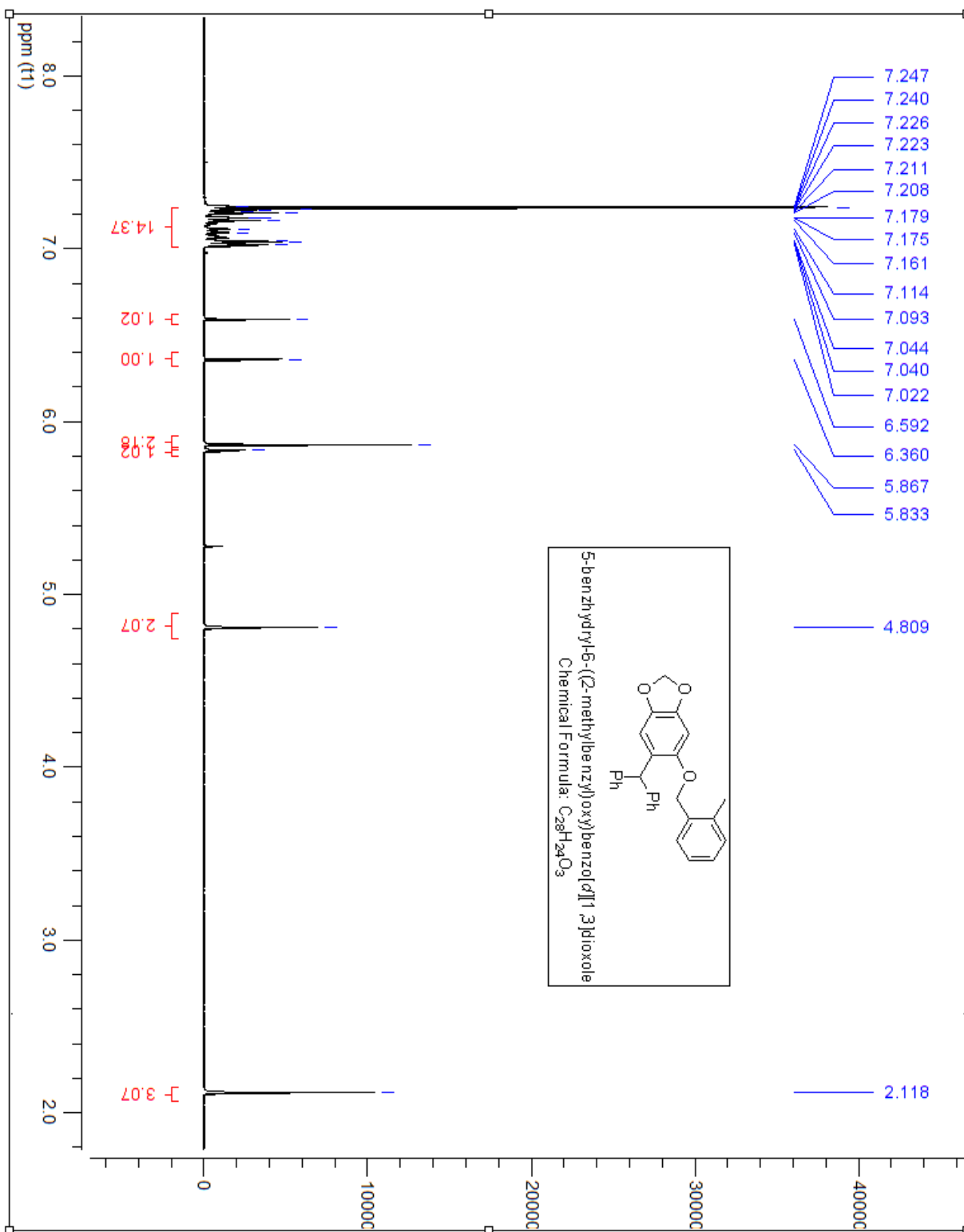
Chemical Formula:  $C_{28}H_{24}O_3$   
Molecular Weight: 408.49

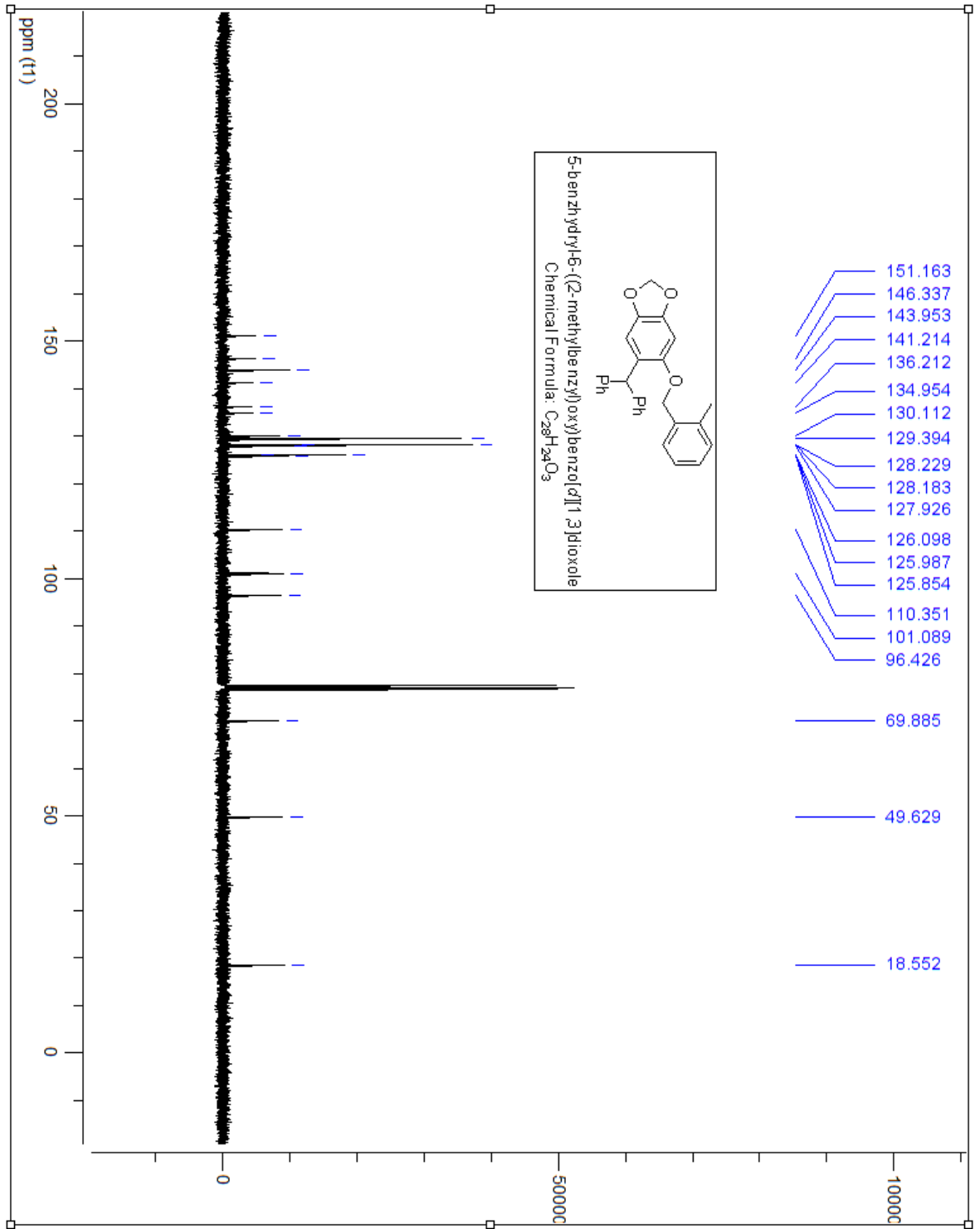
### 32

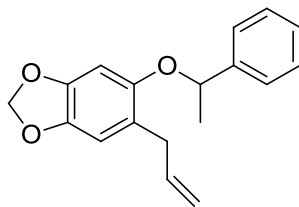
This compound was prepared using **29** (1.6 g, 5.27 mmol), in 20 ml of Acetone, potassium carbonate (2.9 g, 21.1 mmol) was added and stirred for 10 minutes before the addition of 2-methyl benzyl bromide (0.63ml, 4.74mmol) and refluxed for 6 hours. The reaction mixture was extracted with EtOAc and water. The phenol was washed with 10% NaOH. The crude product was purified via gradient column chromatography (2.5% EtOAc in hexanes) resulting as a white powder (1.5g, Rf= 0.7 in 2:8 EtOAc:Hexanes).

$^1\text{H}$  NMR (400 MHz,  $CDCl_3$ )  $\delta$  ppm 7.22-7.02 (m, 13H), 6.59 (s, 1H), 6.36 (s, 1H), 5.86 (s, 2H), 5.83 (s, 1H), 4.81 (s, 2H), 2.11 (s, 3H)

$^{13}\text{C}$  NMR (100 MHz,  $CDCl_3$ )  $\delta$  ppm 151.16, 146.33, 143.95, 141.21, 136.21, 134.95, 130.11, 129.39, 128.22, 128.18, 127.92, 126.09, 125.98, 125.85, 110.35, 101.08, 96.42, 69.88, 49.62, 18.55







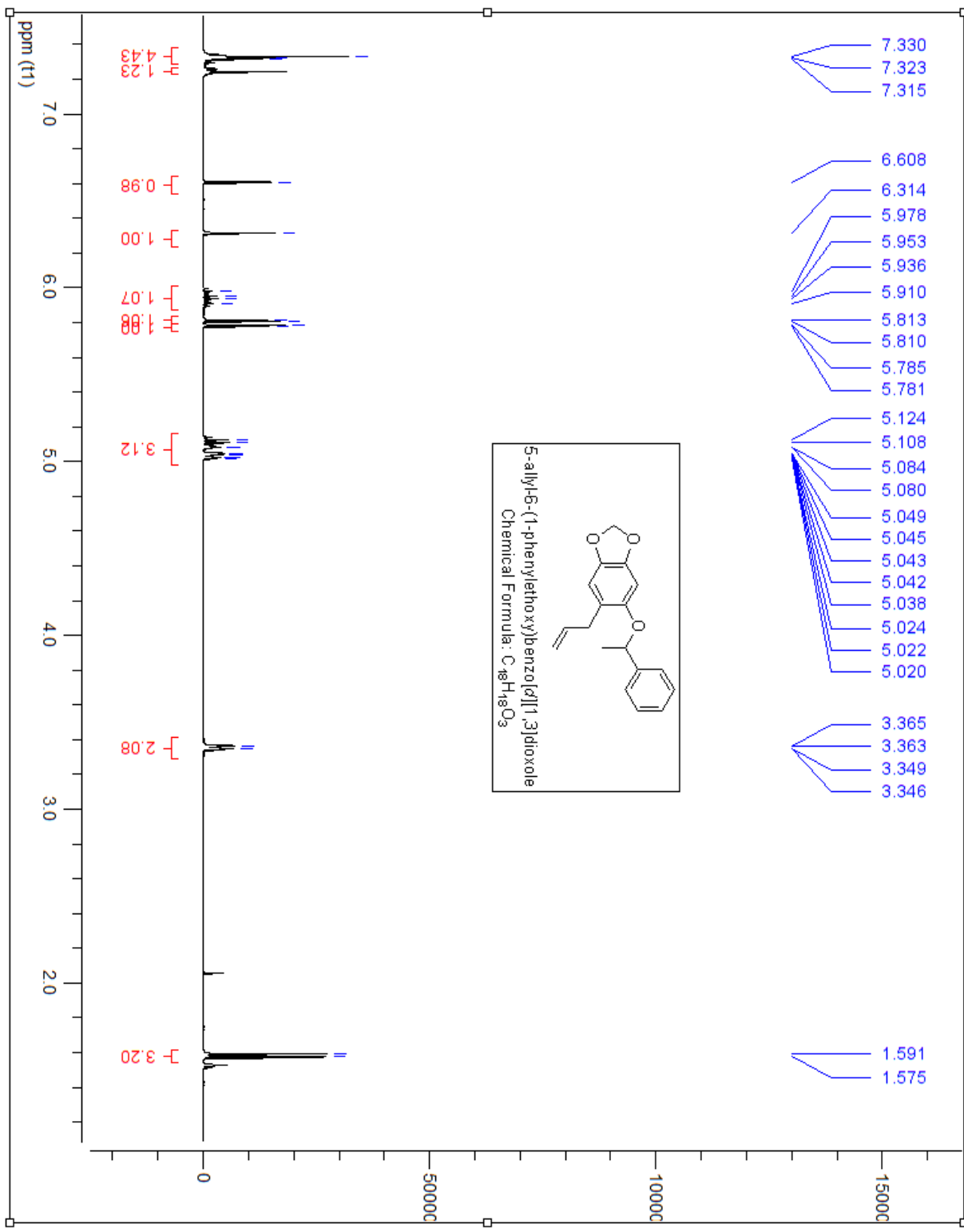
Chemical Formula: C<sub>18</sub>H<sub>18</sub>O<sub>3</sub>  
Molecular Weight: 282.33

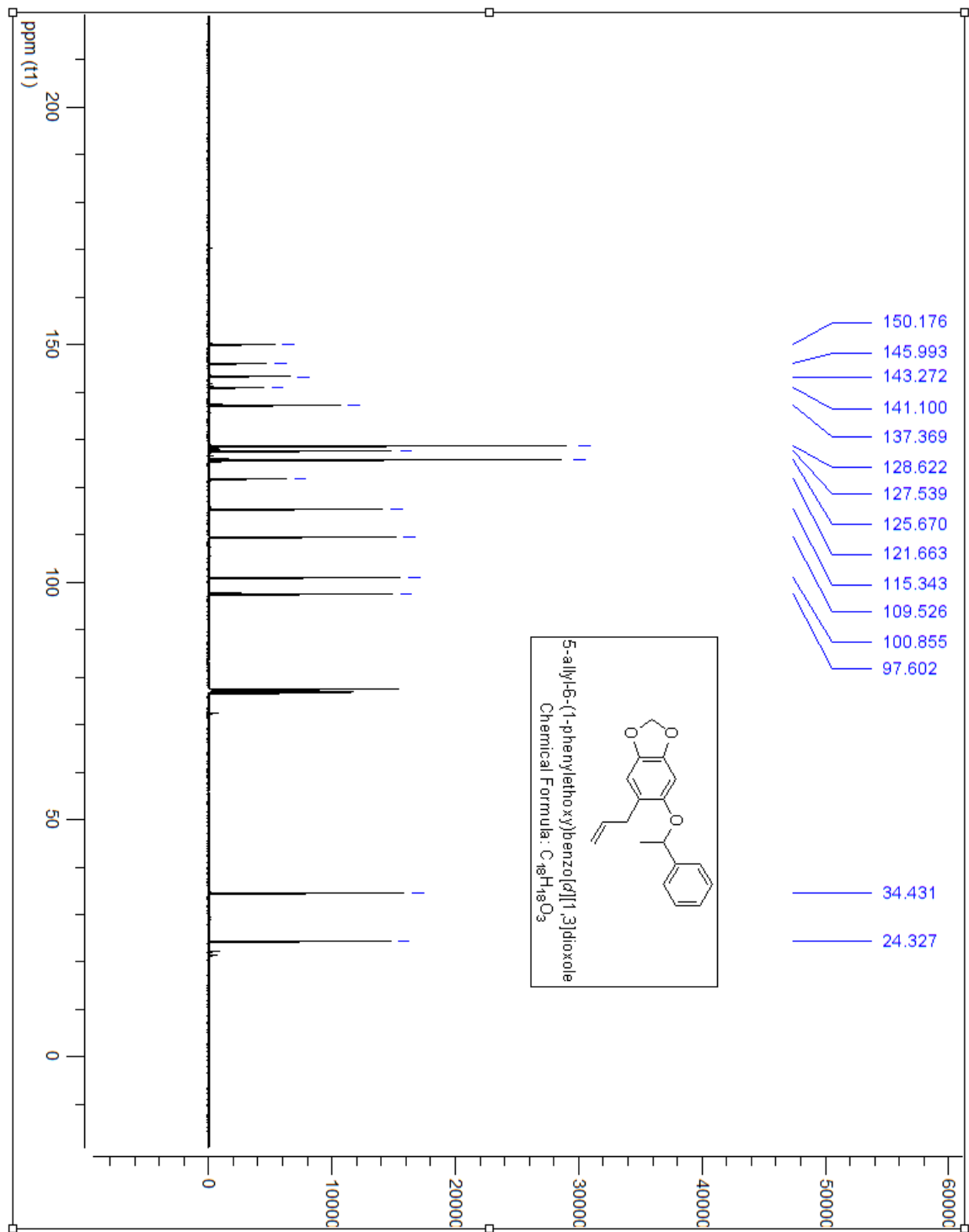
### 37

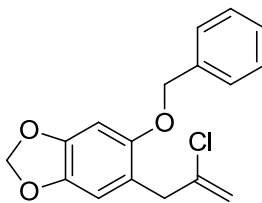
This compound was prepared using **21b** (2 g, 11.2 mmol), in 20 ml of Acetone, potassium carbonate (4.65 g, 33.7mmol) was added and stirred for 10 minutes before the addition of 1-bromoethylbenzene (1.0ml, 11.2 mmol) and refluxed for 6 hours. The reaction mixture was extracted with EtOAc and water. The phenol was washed with 10% NaOH. The crude product (3.14 g) was purified via gradient column chromatography (2.5% EtOAc in hexanes) resulting as a brown solid (2.5g, Rf= 0.8 in 2:8 EtOAc:Hexanes).

<sup>1</sup>H NMR (400 MHz, CDCl<sub>3</sub>) δ ppm 7.33-7.31(m, 6H), 6.60(s, 1H), 6.31(s, 1H), 5.97-5.81(m, 1H), 5.78 (m, 2H), 5.12-5.02(m, 3H), 3.36-3.34(dd, J= 6.51, 6.51Hz, 2H), 1.59-1.57(d, J= 6.42Hz, 3H)

<sup>13</sup>C NMR (100 MHz, CDCl<sub>3</sub>) δ ppm 150.17, 145.99, 143.27, 141.10, 137.36, 128.62, 127.53, 125.67, 121.66, 115.34, 109.52, 100.85, 97.60, 77.40, 34.43, 24.32







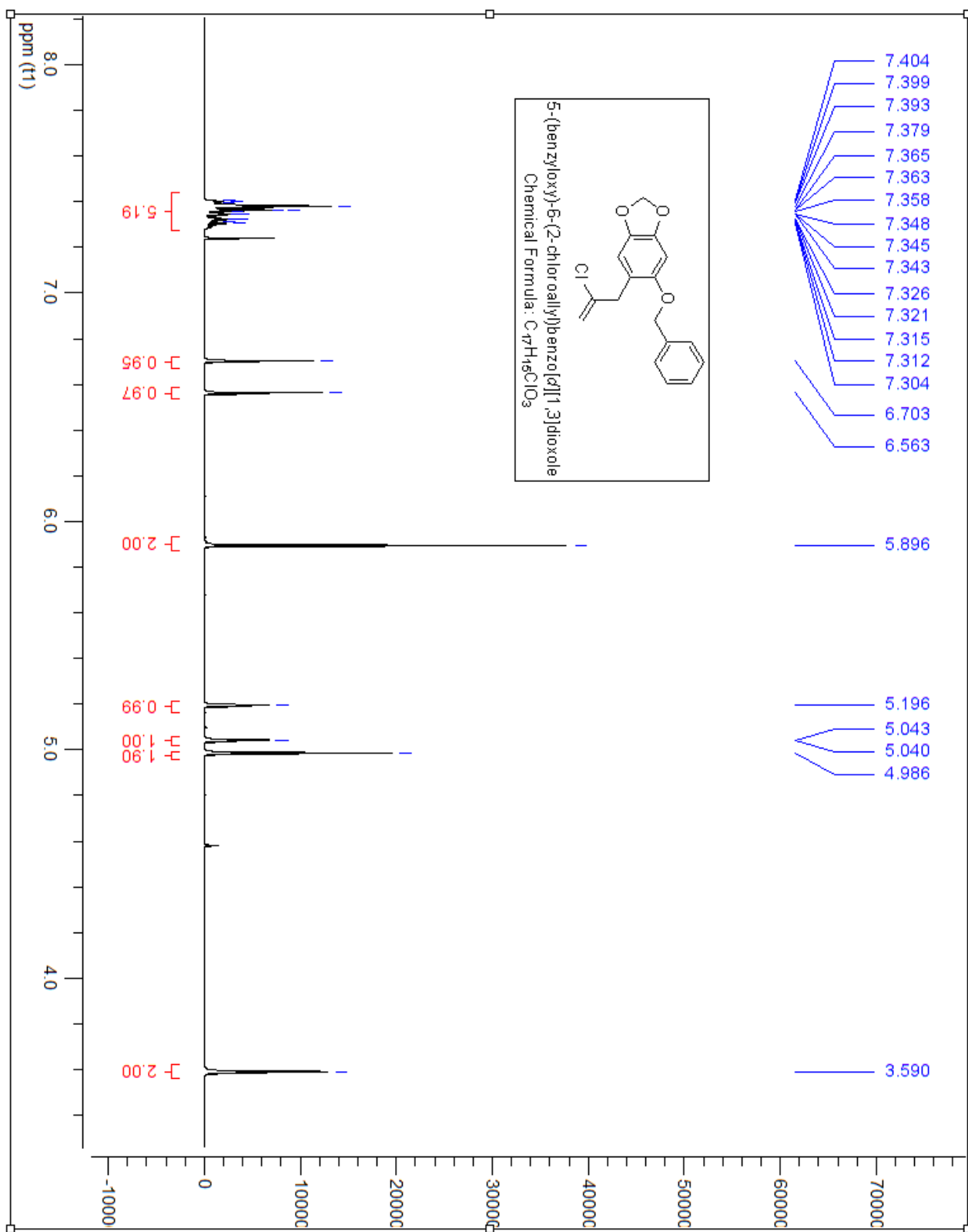
Chemical Formula:  $C_{17}H_{15}ClO_3$   
Molecular Weight: 302.75

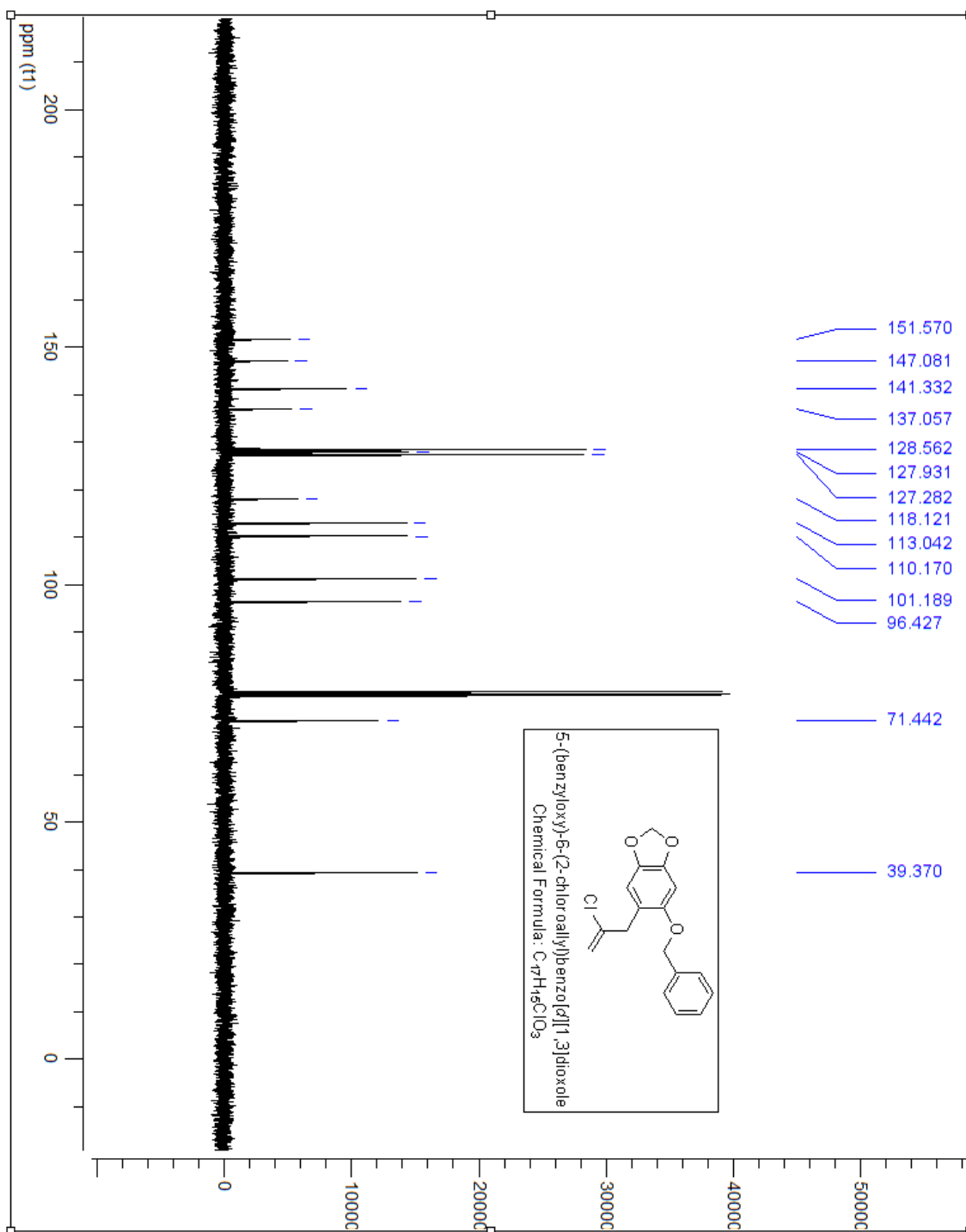
### 39

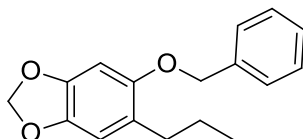
This compound was prepared using **chloroallylated sesamol** (2g, 9.38 mmol), in 20 ml of Acetone, potassium carbonate (4 g, 28.16 mmol) was added and stirred for 10 minutes before the addition of benzyl bromide (1.1 ml, 9.39mmol)) and refluxed for 8 hours. The reaction mixture was extracted with EtOAc and water. The reaction mixture was extracted with EtOAc and water. The phenol was washed with 10% NaOH. The crude product (3.14 g) was purified via gradient column chromatography (2.5% EtOAc in hexanes) resulting as a white solid (1.3g, Rf= 0.75 in 2:8 EtOAc:Hexanes).

$^1H$  NMR (400 MHz,  $CDCl_3$ )  $\delta$  ppm 7.39-7.30(m, 5H), 6.70(s, 1H), 6.56(s, 1H), 5.89(s, 2H), 5.19(s, 1H), 5.04 (s, 1H), 4.98(s, 2H), 3.59(s, 2H)

$^{13}C$  NMR (100 MHz,  $CDCl_3$ )  $\delta$  ppm 151.57, 147.08, 141.33, 137.05, 128.56, 127.93, 127.28, 118.12, 113.04, 110.17, 101.18, 96.42, 71.44, 39.37







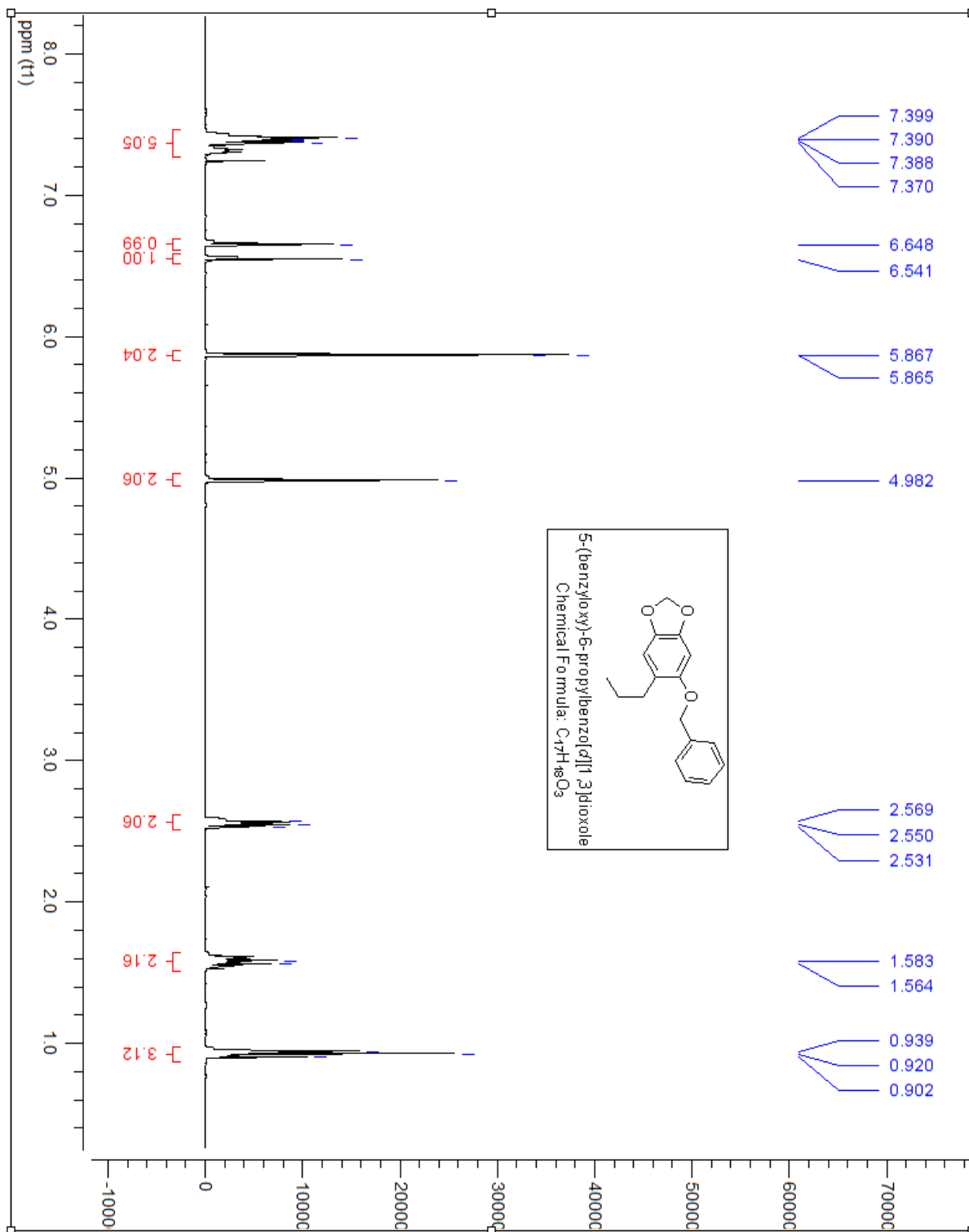
Chemical Formula: C<sub>17</sub>H<sub>18</sub>O<sub>3</sub>  
Molecular Weight: 270.32

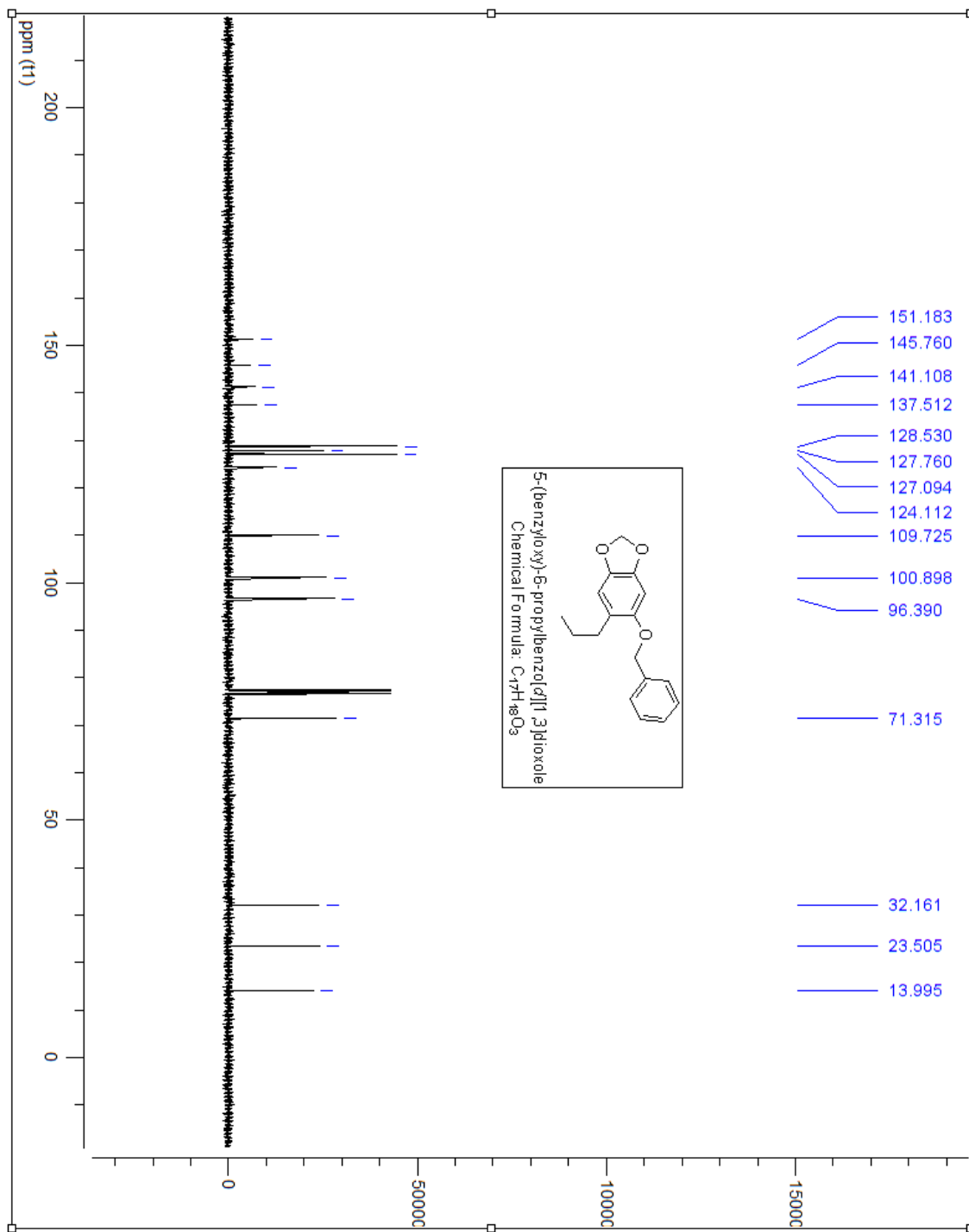
#### 41

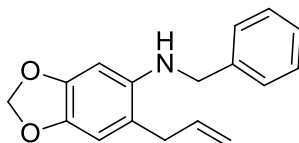
This compound was prepared using reduced **21b** (2.0 g, 11.12 mmol), in 15 ml of Acetone, potassium carbonate (6.13 g, 44.39 mmol) was added and stirred for 10 minutes before the addition of benzyl chloride (1.31 ml, 11.122 mmol) and refluxed for 6 hours. The reaction mixture was extracted with EtOAc and water. The phenol was washed with 10% NaOH. The crude product was purified via gradient column chromatography (2.5% EtOAc in hexanes) resulting as a white solid (1.9 g, R<sub>f</sub> = 0.78 in 2:8 EtOAc:Hexanes).

<sup>1</sup>H NMR (400 MHz, CDCl<sub>3</sub>) δ ppm 7.39-7.37(m, 5H), 6.64(s, 1H), 6.54(s, 1H), 5.86(s, 2H), 4.98(s, 2H), 2.56(dd, J = 7.45, 7.45 Hz, 2H), 1.58-1.56(dd, J = 15.03 Hz, 2H), 0.93-0.92(dd, J = 13.71 Hz, 3H)

<sup>13</sup>C NMR (100 MHz, CDCl<sub>3</sub>) δ ppm 151.18, 145.76, 141.10, 137.51, 128.53, 127.76, 127.09, 124.11, 109.72, 100.89, 96.39, 71.31, 32.16, 23.51, 13.99







Chemical Formula: C<sub>17</sub>H<sub>17</sub>NO<sub>2</sub>

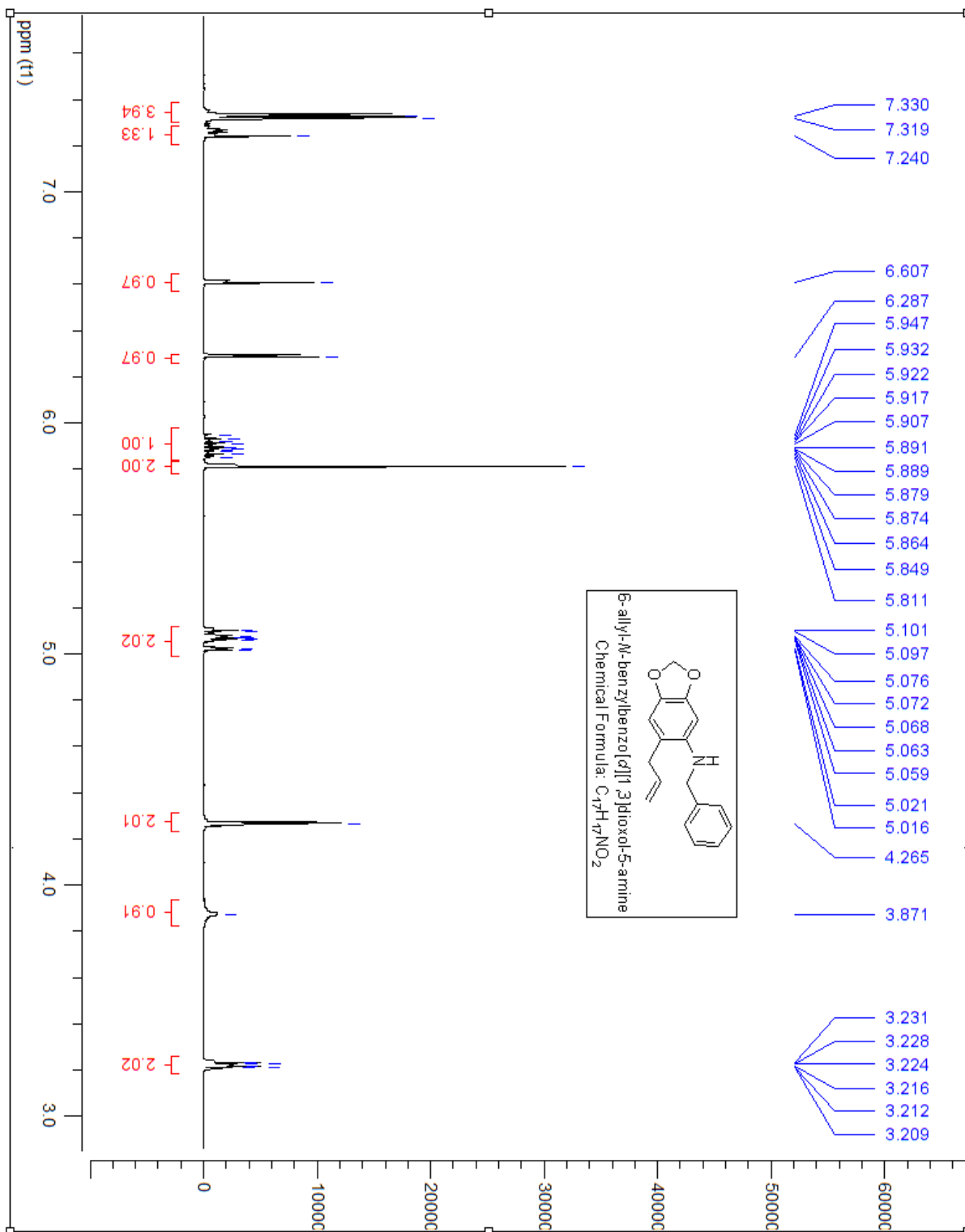
Molecular Weight: 267.32

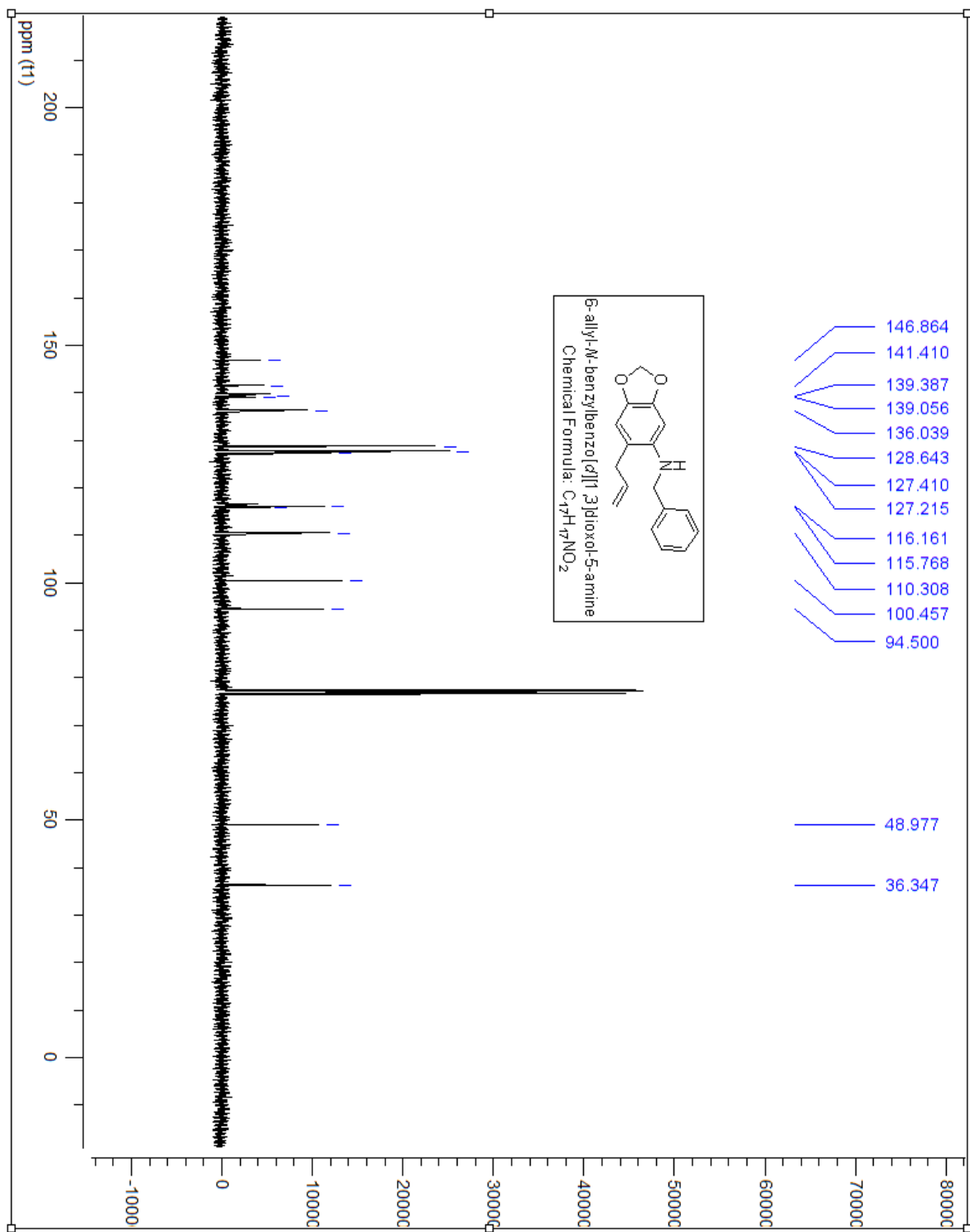
## 42

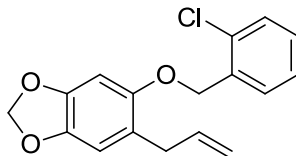
This compound was prepared using **45** (2.5 g, 14.1mmol), in 10 ml of THF, triethylamine (3.9ml, 5.07mmol) was added and stirred for 10 minutes before the addition of benzyl chloride (1.62ml, 14.1 mmol) and let stir for 2 hours. The reaction mixture was extracted with EtOAc and water. The crude product was purified via gradient column chromatography (2.5% EtOAc in hexanes) resulting as a white powder (400mg, R<sub>f</sub>= 0.74 in 2:8 EtOAc:Hexanes).

<sup>1</sup>H NMR (400 MHz, CDCl<sub>3</sub>) δ ppm 7.33-7.31(m, 4H), 7.24(m, 1H), 6.60(s, 1H), 6.28(s, 1H), 5.94-5.84(m, 1H), 5.81(s, 2H), 5.10-5.01(m, 2H), 4.26(s, 2H), 3.87(b, 1H), 3.23-3.21(dt, J=6.06, Hz, 2H)

<sup>13</sup>C NMR (100MHz, CDCl<sub>3</sub>) δ ppm 146.86, 141.41, 139.38, 139.05, 136.03, 128.64, 127.41, 127.21, 116.16, 115.76, 110.31, 100.45, 94.50, 48.97, 36.34







Chemical Formula:  $C_{17}H_{15}ClO_3$

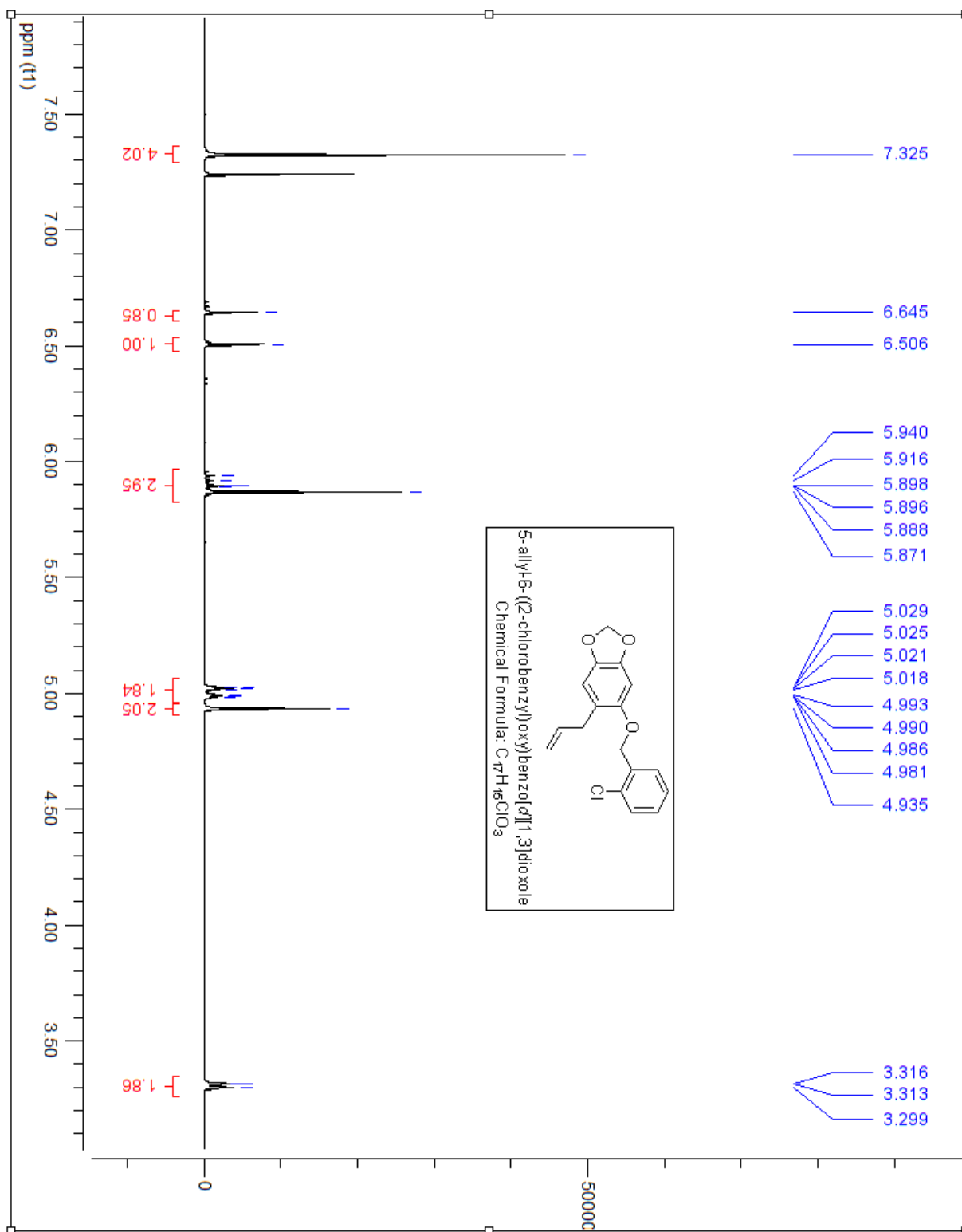
Molecular Weight: 302.75

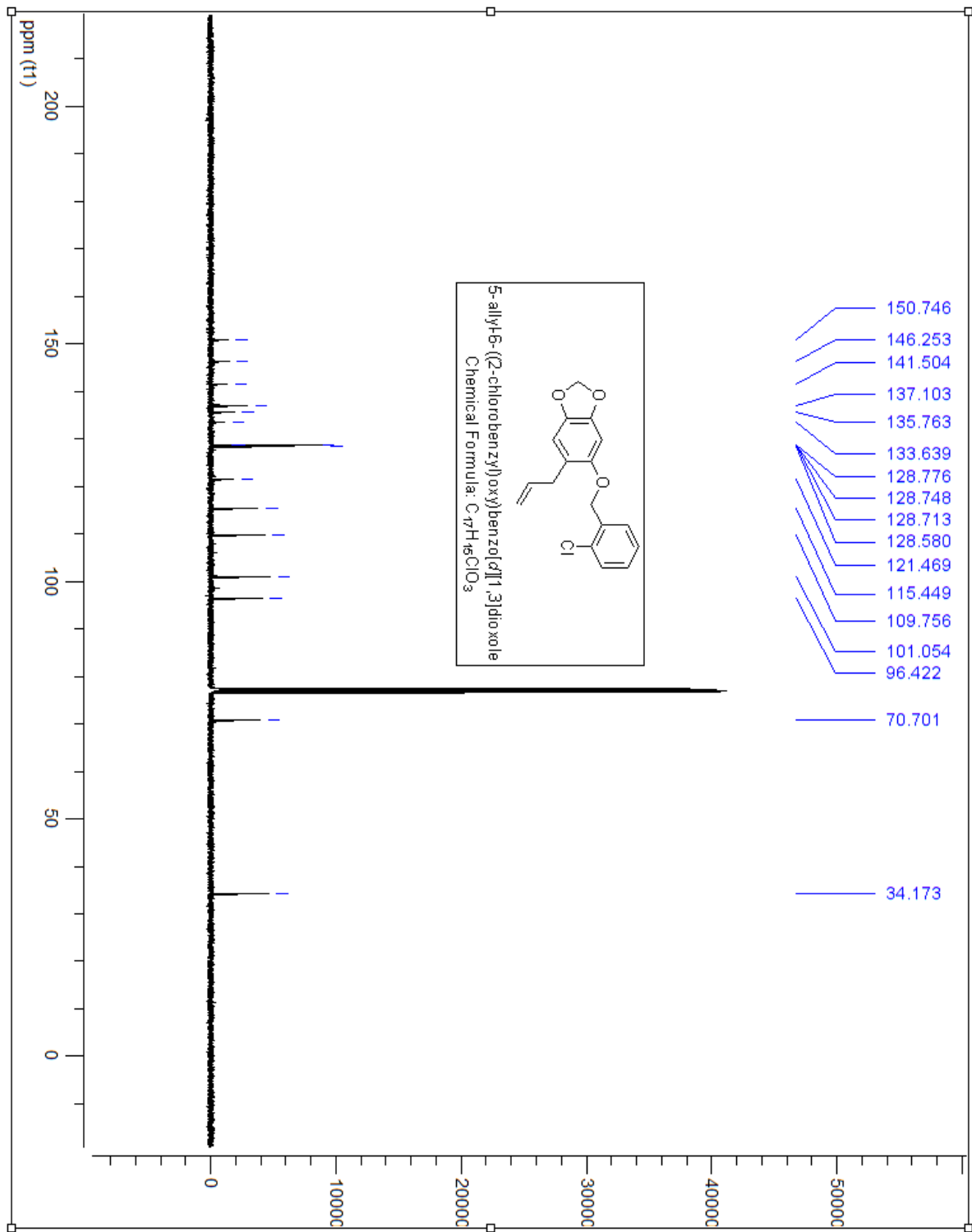
## 48

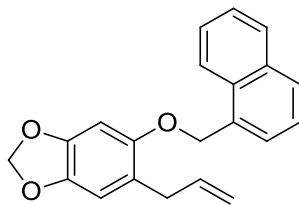
This compound was prepared using **21b** (0.5 g, 2.81 mmol), in 20 ml of Acetone, potassium carbonate (1.16 g, 8.41 mmol) was added and stirred for 10 minutes before the addition of 4-chlorobenzyl bromide (0.43ml, 2.81mmol) and refluxed for 6 hours. The reaction mixture was extracted with EtOAc and water. The phenol was washed with 10% NaOH. The crude product was purified via gradient column chromatography (2.5% EtOAc in hexanes) resulting as a white solid (0.43 g, Rf= 0.70 in 2:8 EtOAc:Hexanes).

$^1\text{H}$  NMR (400 MHz,  $CDCl_3$ )  $\delta$  ppm 7.58-7.57(d, J= Hz, 1H), 7.40-7.38(m, 4H), 6.69(s, 1H), 6.59(s, 1H), 6.02-5.95(m, 1H), 5.88(s, 2H), 5.08(s, 4H), 3.41(d, J=6.55Hz, 2H)

$^{13}\text{C}$  NMR (100MHz,  $CDCl_3$ )  $\delta$  ppm 150.77, 146.36, 141.59, 137.21, 135.08, 132.43, 129.34, 128.89, 128.58, 126.98, 121.45, 115.52, 109.74, 101.11, 96.43, 68.58, 34.27







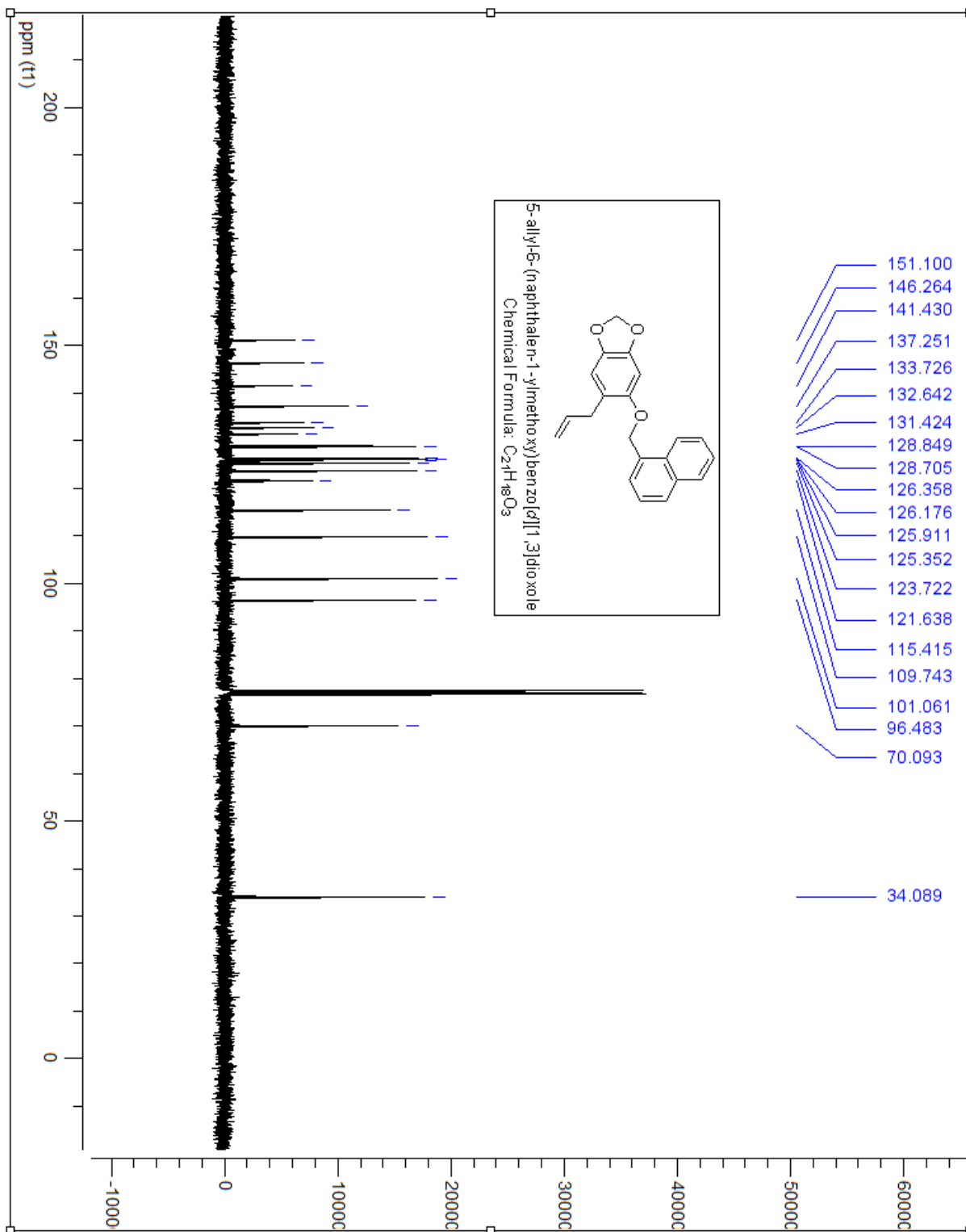
Chemical Formula: C<sub>21</sub>H<sub>18</sub>O<sub>3</sub>  
Molecular Weight: 318.37

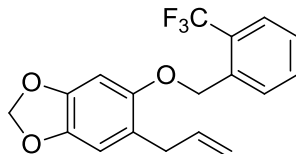
## 49

This compound was prepared using **21b** (0.5 g, 2.81 mmol), in 20 ml of Acetone, potassium carbonate (1.16 g, 8.41 mmol) was added and stirred for 10 minutes before the addition of 2-bromoethyl naphthalene (0.42ml, 2.81mmol) and refluxed for 6 hours. The reaction mixture was extracted with EtOAc and water. The phenol was washed with 10% NaOH. The crude product was purified via gradient column chromatography (2.5% EtOAc in hexanes) resulting as a white solid (0.43 g, R<sub>f</sub>= 0.80 in 2:8 EtOAc:Hexanes).

<sup>1</sup>H NMR (400 MHz, CDCl<sub>3</sub>) δ ppm 8.03-7.90(m, 1H), 7.88-7.83(m, 2H), 7.58-7.43(m, 4H), 6.69-6.67(d, J=3.08 Hz, 2H), 5.89 (m, 3H), 5.41(s, 2H), 4.99-4.95(m, 2H), 3.29-3.28(d, J=6.59 Hz, 2H)

<sup>13</sup>C NMR (100MHz, CDCl<sub>3</sub>) δ ppm 151.10, 146.26, 141.43, 137.25, 133.72, 132.64, 131.42, 128.84, 128.70, 126.35, 126.17, 125.91, 125.35, 123.72, 121.63, 115.41, 109.74, 101.06, 96.48, 70.09, 34.08





Chemical Formula: C<sub>18</sub>H<sub>15</sub>F<sub>3</sub>O<sub>3</sub>

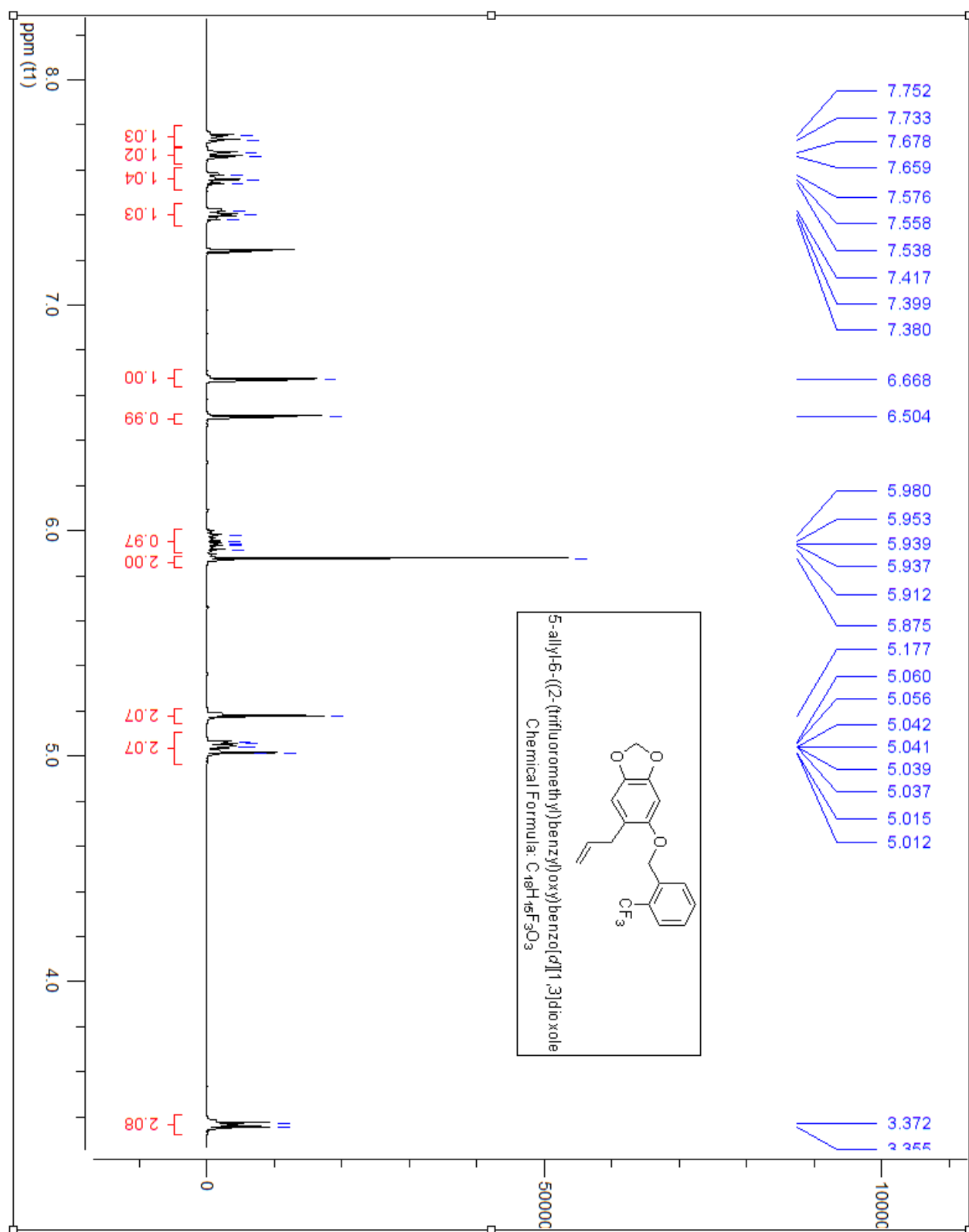
Molecular Weight: 336.31

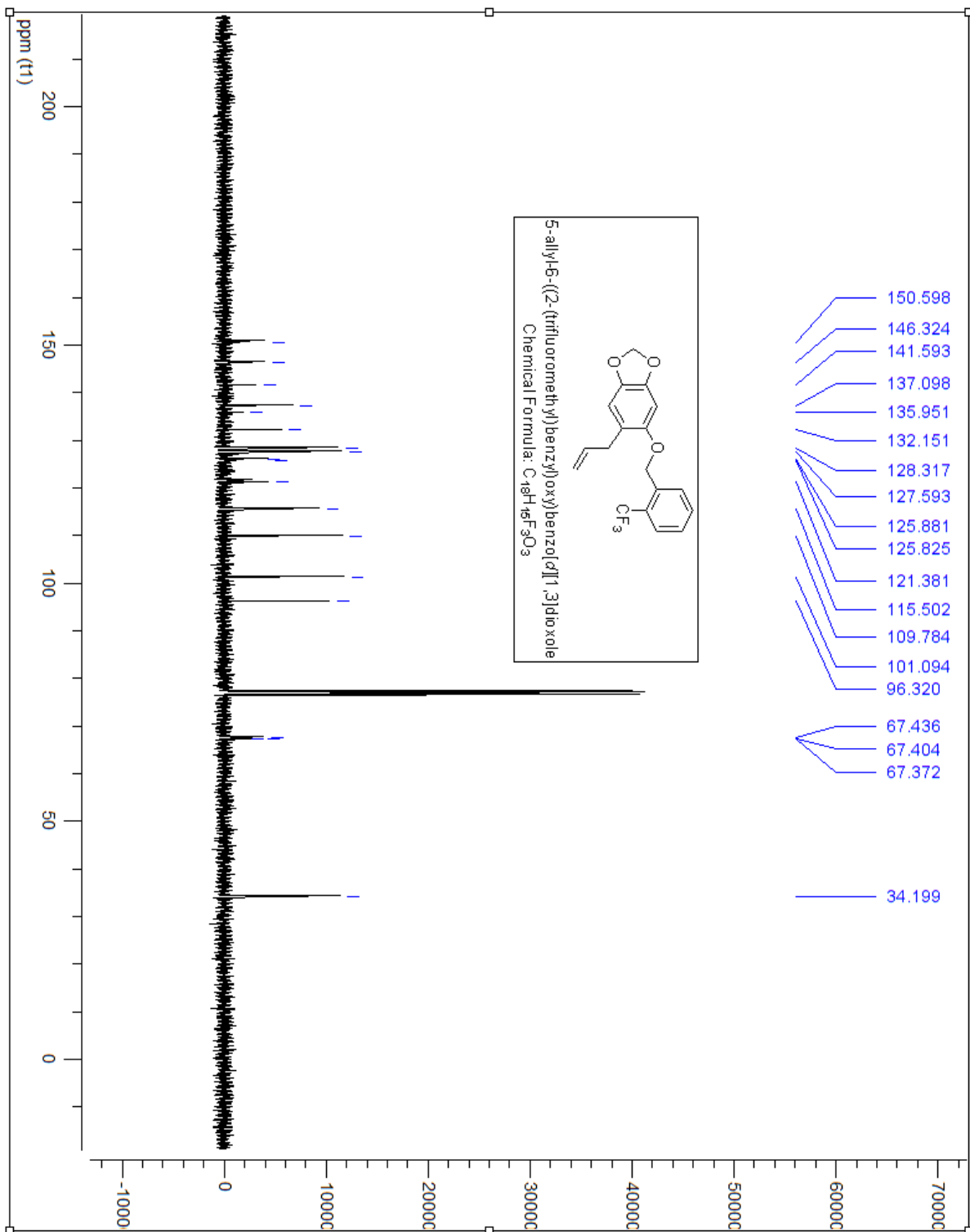
## 50

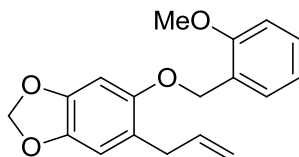
This compound was prepared using **21b** (0.5 g, 2.81 mmol), in 20 ml of Acetone, potassium carbonate (1.16 g, 8.41 mmol) was added and stirred for 10 minutes before the addition of 2-trifluorobenzyl bromide (0.43ml, 2.81mmol) and refluxed for 6 hours. The reaction mixture was extracted with EtOAc and water. The phenol was washed with 10% NaOH. The crude product was purified via gradient column chromatography (2.5% EtOAc in hexanes) resulting as a white solid (0.41 g, R<sub>f</sub>= 0.75 in 2:8 EtOAc:Hexanes).

<sup>1</sup>H NMR (400 MHz, CDCl<sub>3</sub>) δ ppm 7.75-7.73(d, J=7.79Hz, 1H), 7.67-7.65(d, J=7.79Hz, 1H), 7.57-7.53(t, J=7.48Hz, 1H), 7.41-7.38(t, J=7.54Hz, 1H), 6.66(s, 1H), 6.50(s, 1H), 5.98-5.91(m, 1H), 5.87(s, 2H), 5.17(s, 2H), 5.06-5.01(m, 2H), 3.37-3.35(d J=6.55Hz, 2H)

<sup>13</sup>C NMR (100MHz, CDCl<sub>3</sub>) δ ppm 150.59, 146.32, 141.59, 137.09, 132.15, 128.31, 127.59, 125.88, 125.82, 121.38, 115.50, 109.78, 101.09, 96.32, 67.43, 67.40, 34.19







Chemical Formula: C<sub>18</sub>H<sub>18</sub>O<sub>4</sub>

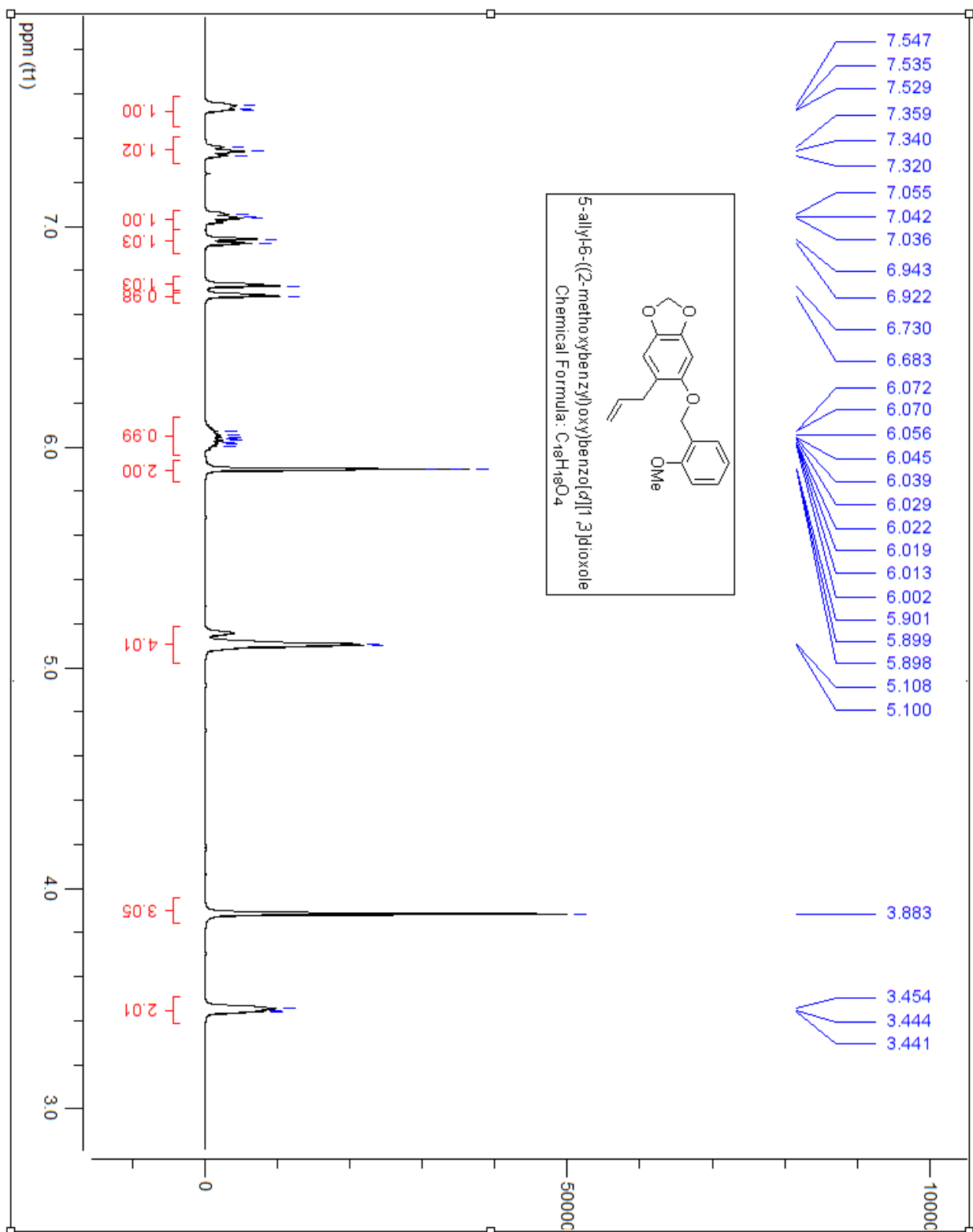
Molecular Weight: 298.33

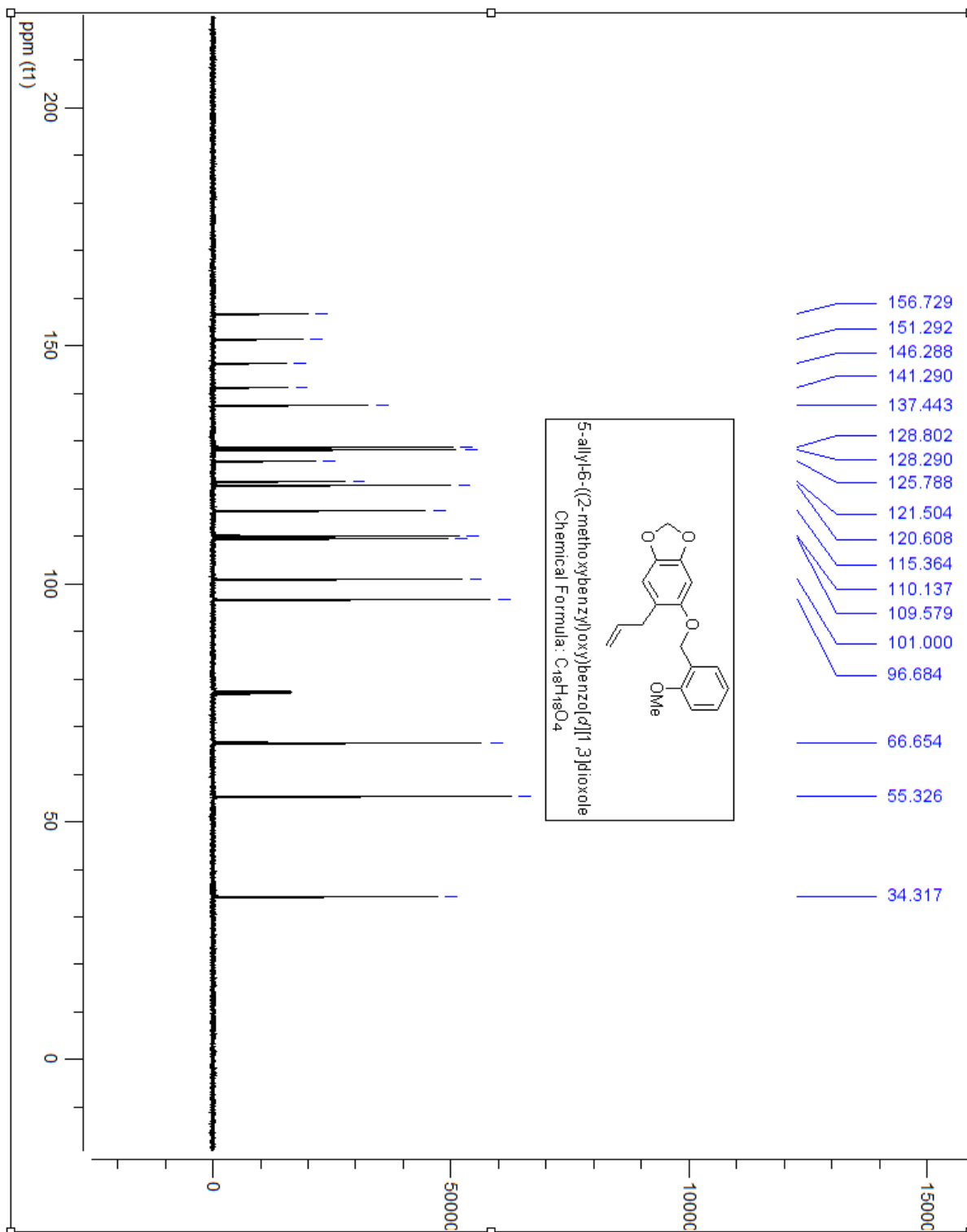
## 51

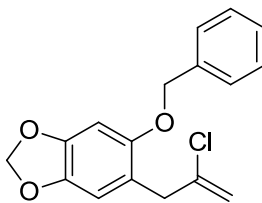
This compound was prepared using **21b** (0.5 g, 2.81 mmol), in 20 ml of Acetone, potassium carbonate (1.16 g, 8.41 mmol) was added and stirred for 10 minutes before the addition of 4-methoxy benzyl bromide (0.43ml, 2.81mmol) and refluxed for 6 hours. The reaction mixture was extracted with EtOAc and water. The phenol was washed with 10% NaOH. The crude product was purified via gradient column chromatography (2.5% EtOAc in hexanes) resulting as a white solid (0.45 g, Rf= 0.80 in 2:8 EtOAc:Hexanes).

<sup>1</sup>H NMR (400 MHz, CDCl<sub>3</sub>) δ ppm 7.51-7.49(d, J=7.14Hz, 1H), 7.33-7.29(m, 1H), 7.03-7.01(m, 1H), 6.99-6.90(d, J=3.08 Hz, 1H), 6.70-6.65(m, 2H), 6.03-5.89(m, 1H), 5.88(s, 2H), 5.07(m, 4H), 3.87(s, 3H), 3.29-3.28(d, J= 5.48Hz, 2H)

<sup>13</sup>C NMR (100MHz, CDCl<sub>3</sub>) δ ppm 156.72, 151.29, 146.28, 141.29, 137.44, 128.80, 128.29, 125.78, 121.50, 120.60, 115.36, 110.13, 109.57, 101.00, 96.68, 66.65, 55.32, 34.31







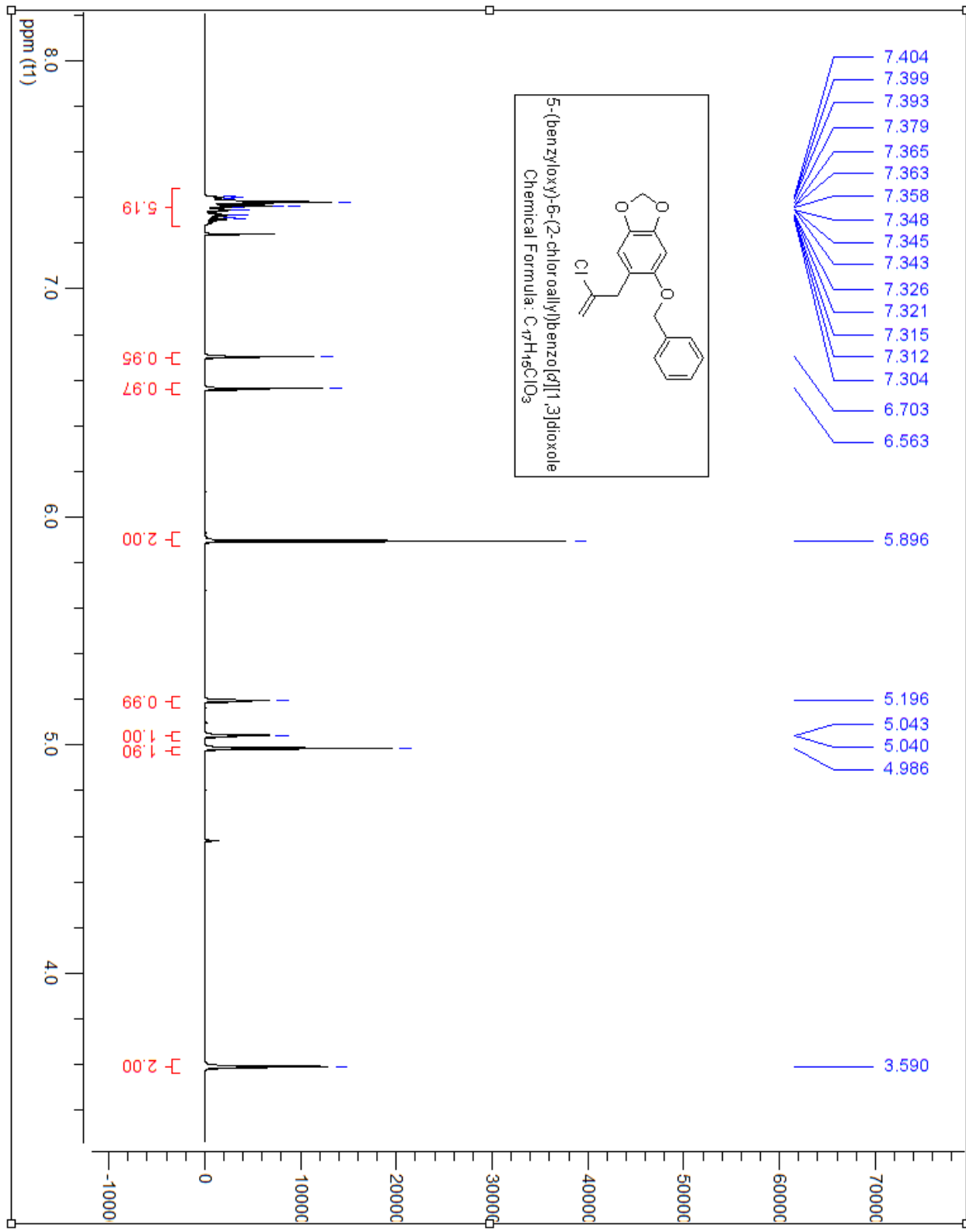
Chemical Formula:  $C_{17}H_{15}ClO_3$   
Molecular Weight: 302.75

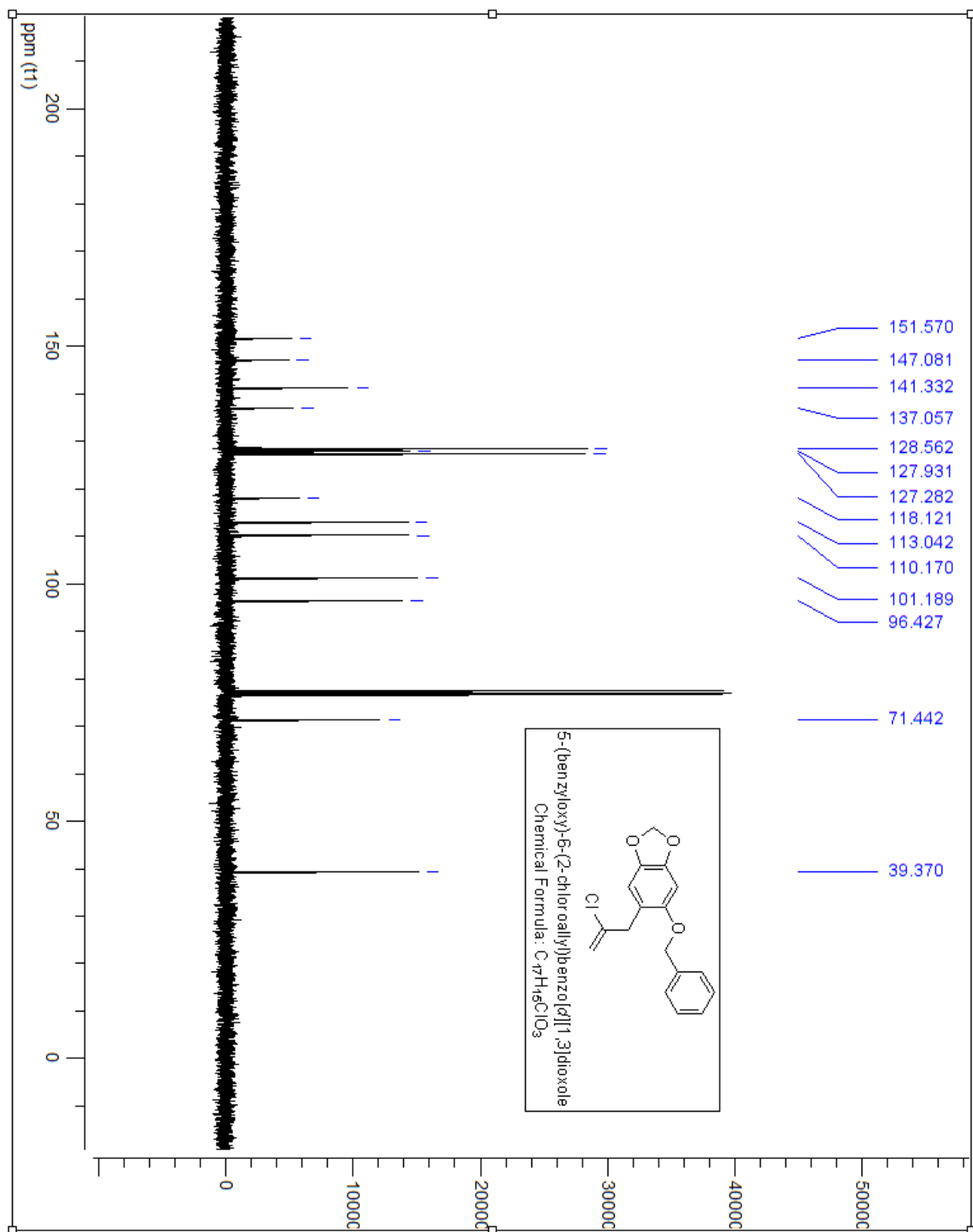
54

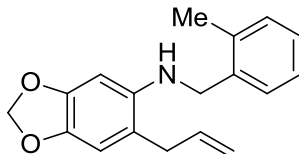
This compound was prepared using **chloroallylated sesamol** (2g, 9.38 mmol), in 20 ml of Acetone, potassium carbonate (4 g, 28.16 mmol) was added and stirred for 10 minutes before the addition of benzyl bromide (1.1 ml, 9.39mmol)) and refluxed for 8 hours. The reaction mixture was extracted with EtOAc and water. The reaction mixture was extracted with EtOAc and water. The phenol was washed with 10% NaOH. The crude product (3.14 g) was purified via gradient column chromatography (2.5% EtOAc in hexanes) resulting as a white solid (1.3g, Rf= 0.75 in 2:8 EtOAc:Hexanes).

$^1\text{H}$  NMR (400 MHz,  $CDCl_3$ )  $\delta$  ppm 7.39-7.30(m, 5H), 6.70(s, 1H), 6.56(s, 1H), 5.89(s, 2H), 5.19(s, 1H), 5.04 (s, 1H), 4.98(s, 2H), 3.59(s, 2H)

$^{13}\text{C}$  NMR (100 MHz,  $CDCl_3$ )  $\delta$  ppm 151.57, 147.08, 141.33, 137.05, 128.56, 127.93, 127.28, 118.12, 113.04, 110.17, 101.18, 96.42, 71.44, 39.37







Chemical Formula: C<sub>18</sub>H<sub>19</sub>NO<sub>2</sub>

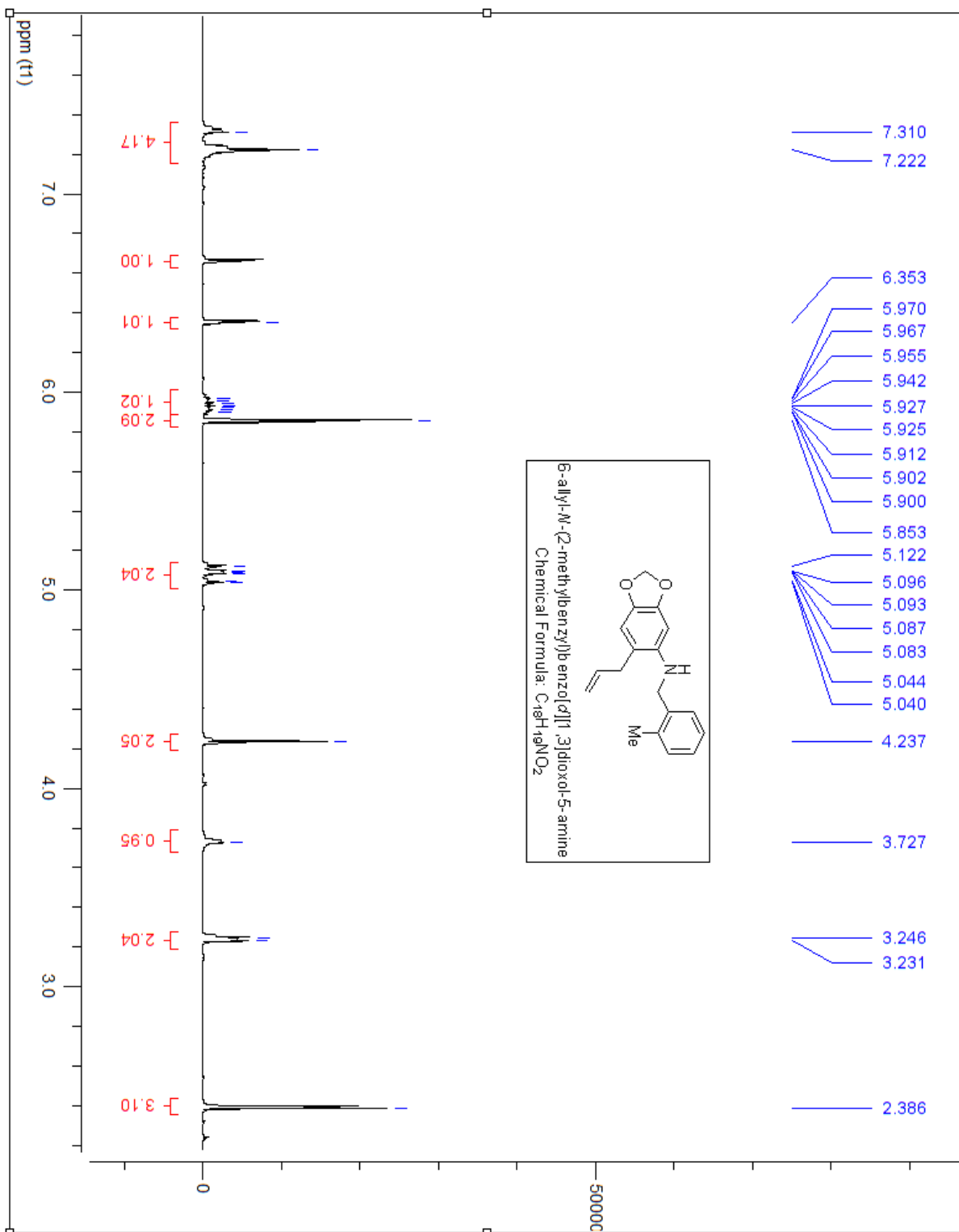
Molecular Weight: 281.35

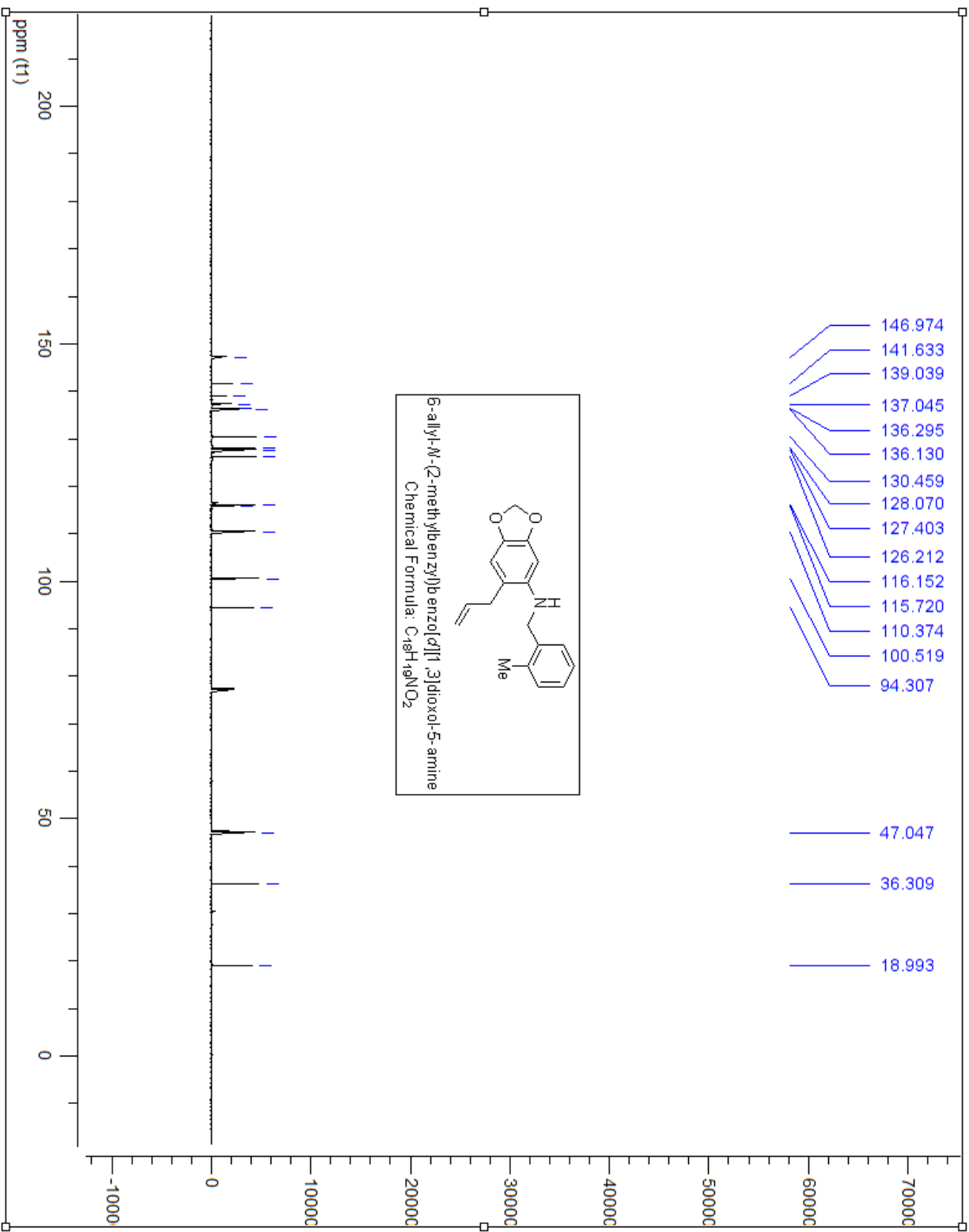
## 62

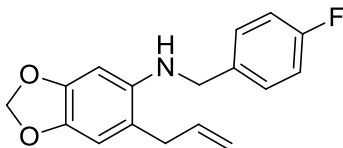
This compound was prepared using **45** (0.3 g, 1.69mmol), in 10 ml of THF, triethylamine (0.71ml, 5.07mmol) was added and stirred for 10 minutes before the addition of 2-methylbenzylchloride (0.23ml, 1.67mmol) and let stir for 2 hours. The reaction mixture was extracted with EtOAc and water. The crude product (0.28g) was purified via gradient column chromatography (2.5% EtOAc in hexanes) resulting as a white crystal (69mg, R<sub>f</sub>= 0.9 in 2:8 EtOAc:Hexanes).

<sup>1</sup>H NMR (400 MHz, CDCl<sub>3</sub>) δ ppm 7.32-7.22(m, 4H), 6.66(s, 1H), 6.35(s, 1H), 5.96-5.90(m, 1H), 5.85(s, 2H), 5.12-5.04(m, 2H), 4.23(s, 2H), 3.72(b, 1H), 3.24-3.23(d, J=5.96 Hz, 2H), 2.38(s, 3H)

<sup>13</sup>C NMR (100MHz, CDCl<sub>3</sub>) δ ppm 146.97, 141.63, 139.03, 137.04, 136.29, 136.13, 130.45, 128.07, 127.40, 126.21, 116.21, 115.72, 110.37, 100.51, 94.30, 47.04, 36.30, 18.99







Chemical Formula: C<sub>17</sub>H<sub>16</sub>FNO<sub>2</sub>

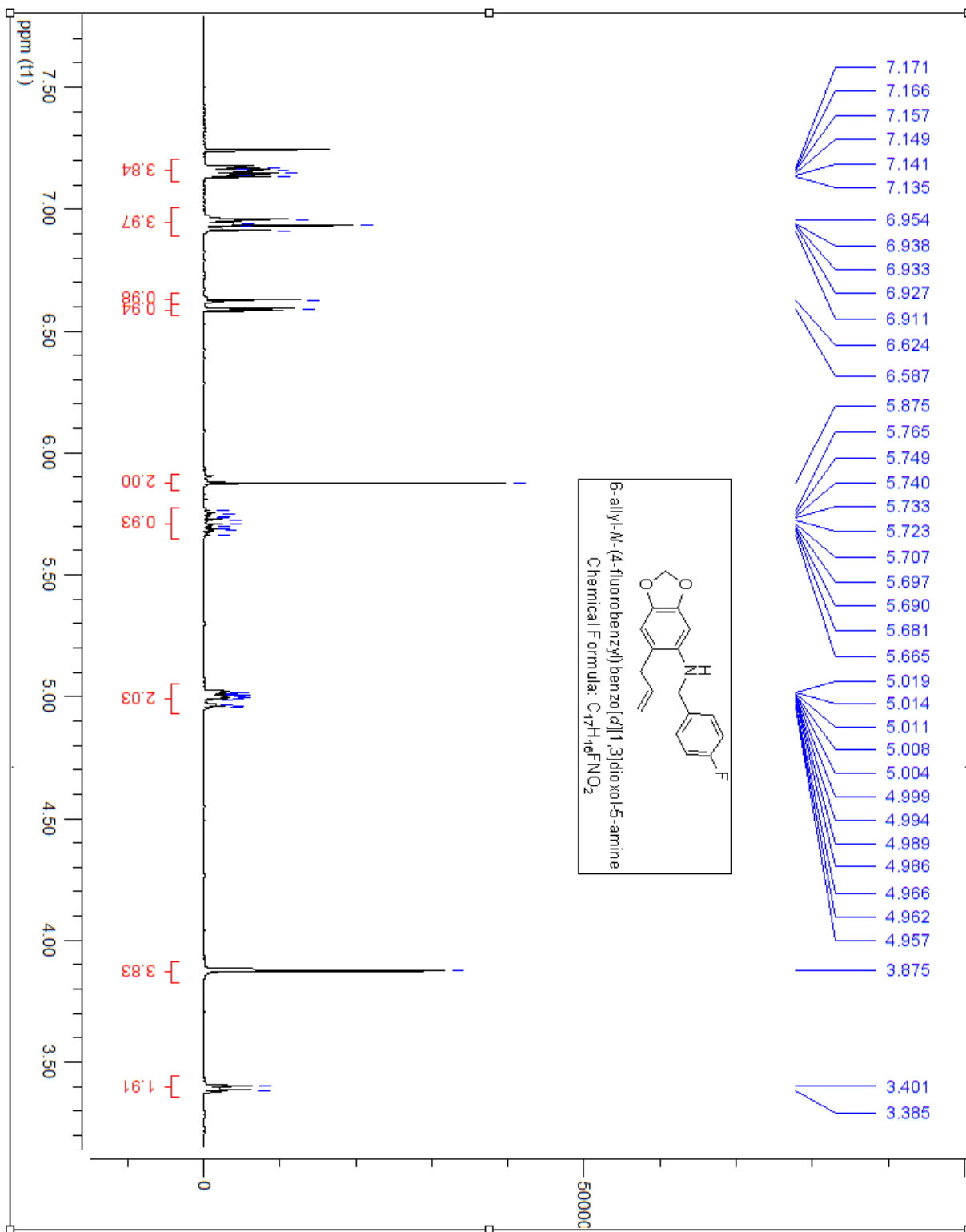
Molecular Weight: 285.31

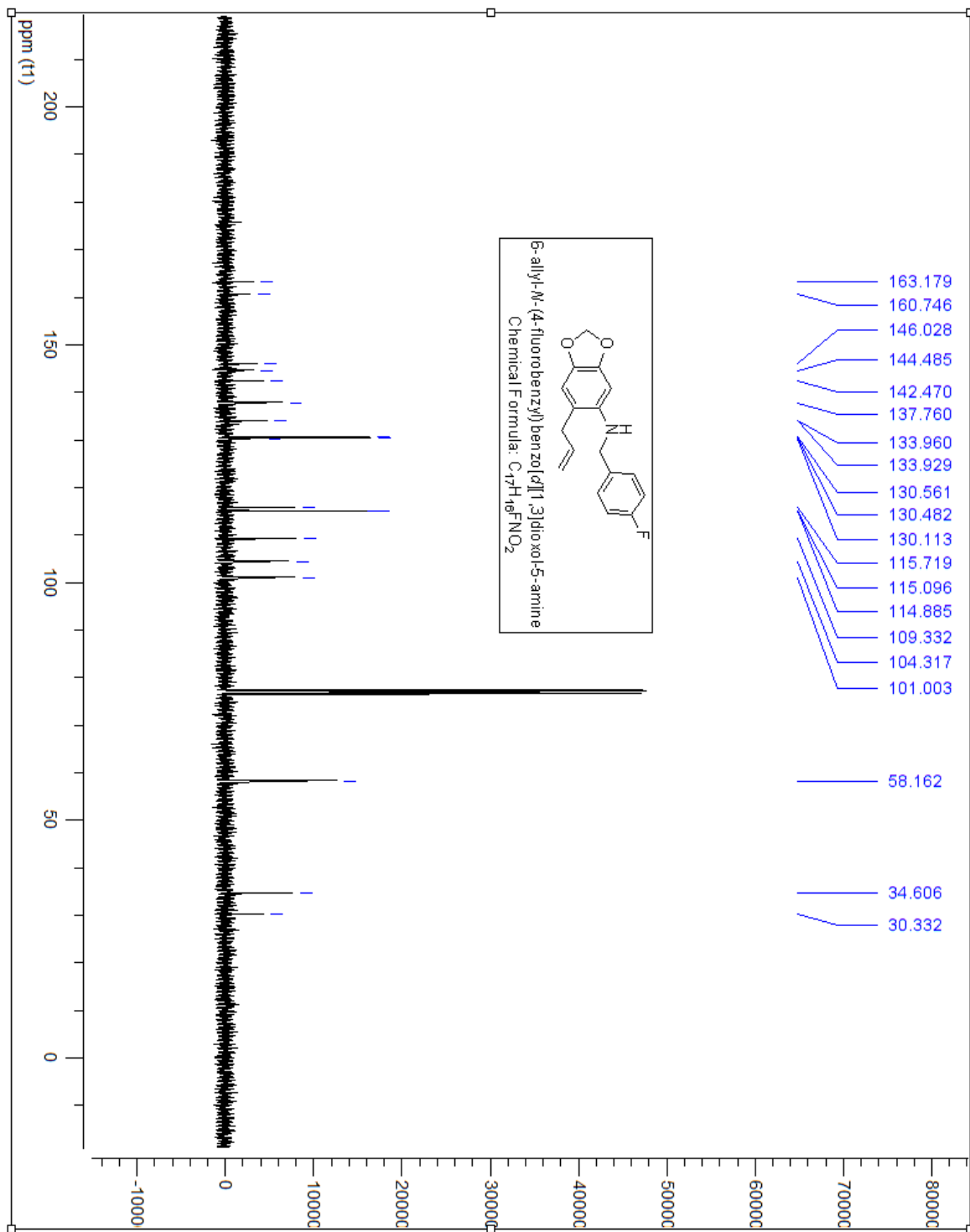
### 63

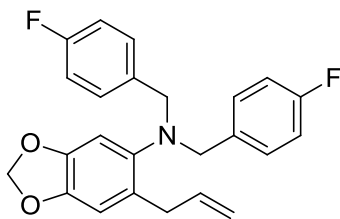
This compound was prepared using **45** (0.3 g, 1.69mmol), in 10 ml of THF, triethylamine (0.71ml, 5.07mmol) was added and stirred for 10 minutes before the addition of 4-fluorobenzylchloride (0.20ml, 1.67mmol) and let stir for 2 hours. The reaction mixture was extracted with EtOAc and water. The crude product (0.10g) was purified via gradient column chromatography (2.5% EtOAc in hexanes) resulting as a white powder (57mg, Rf= 0.9 in 2:8 EtOAc:Hexanes).

<sup>1</sup>H NMR (400 MHz, CDCl<sub>3</sub>) δ ppm 7.17-7.13(m, 4H), 6.95-6.91(m, 4H), 6.62(s, 1H), 6.58(s, 1H), 5.87(s, 2H), 5.76-5.66(m, 1H), 5.01-4.95(m, 2H), 3.87(s, 4H), 3.40-3.38(d, J=6.49, 2H)

<sup>13</sup>C NMR (100MHz, CDCl<sub>3</sub>) δ ppm 163.17, 160.74, 146.02, 144.48, 142.47, 137.76, 133.96, 133.92, 130.56, 130.48, 130.11, 115.71, 115.09, 114.88, 109.33, 104.31, 101.00, 58.16, 34.61, 30.33







Chemical Formula:  $C_{24}H_{21}F_2NO_2$

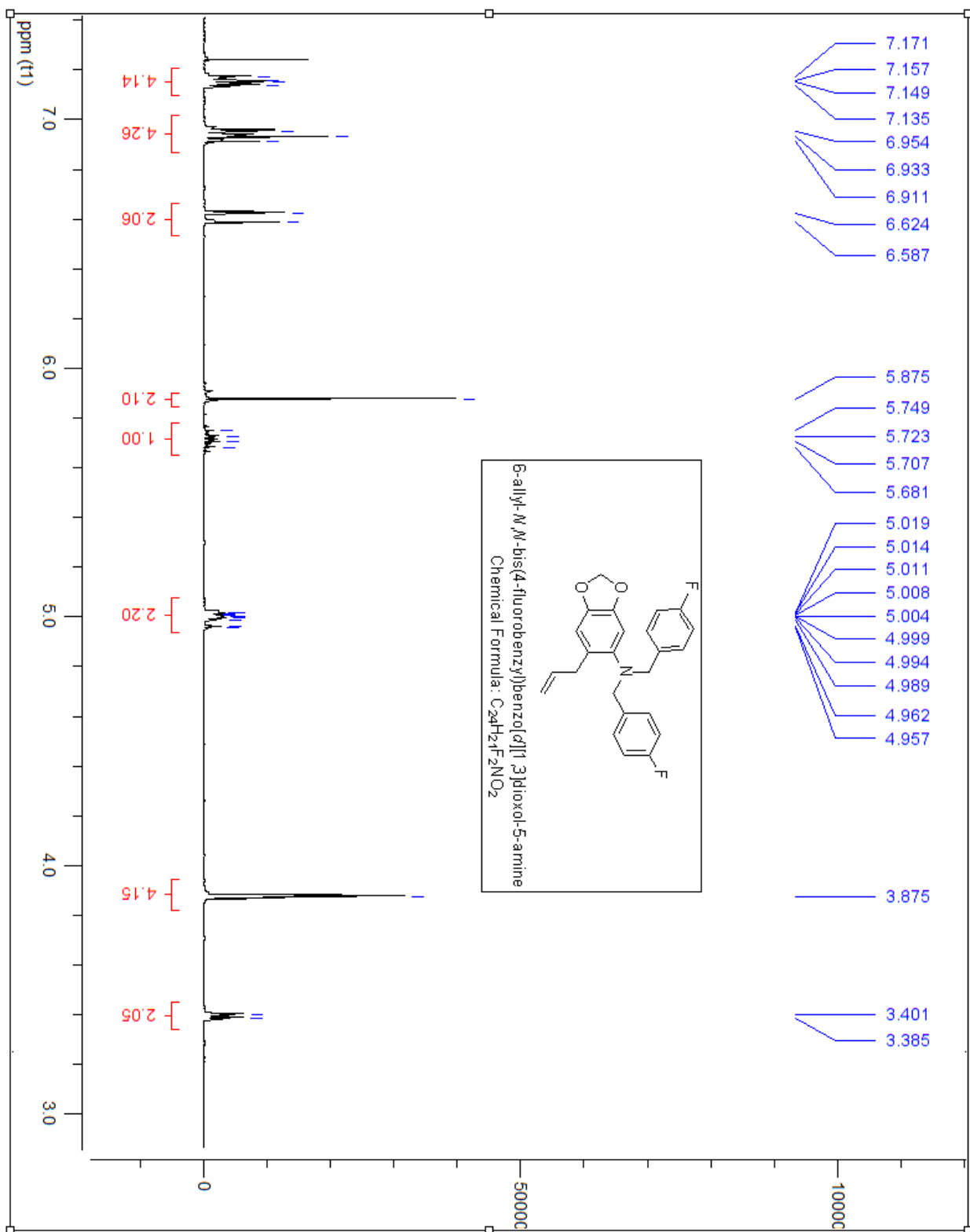
Molecular Weight: 393.43

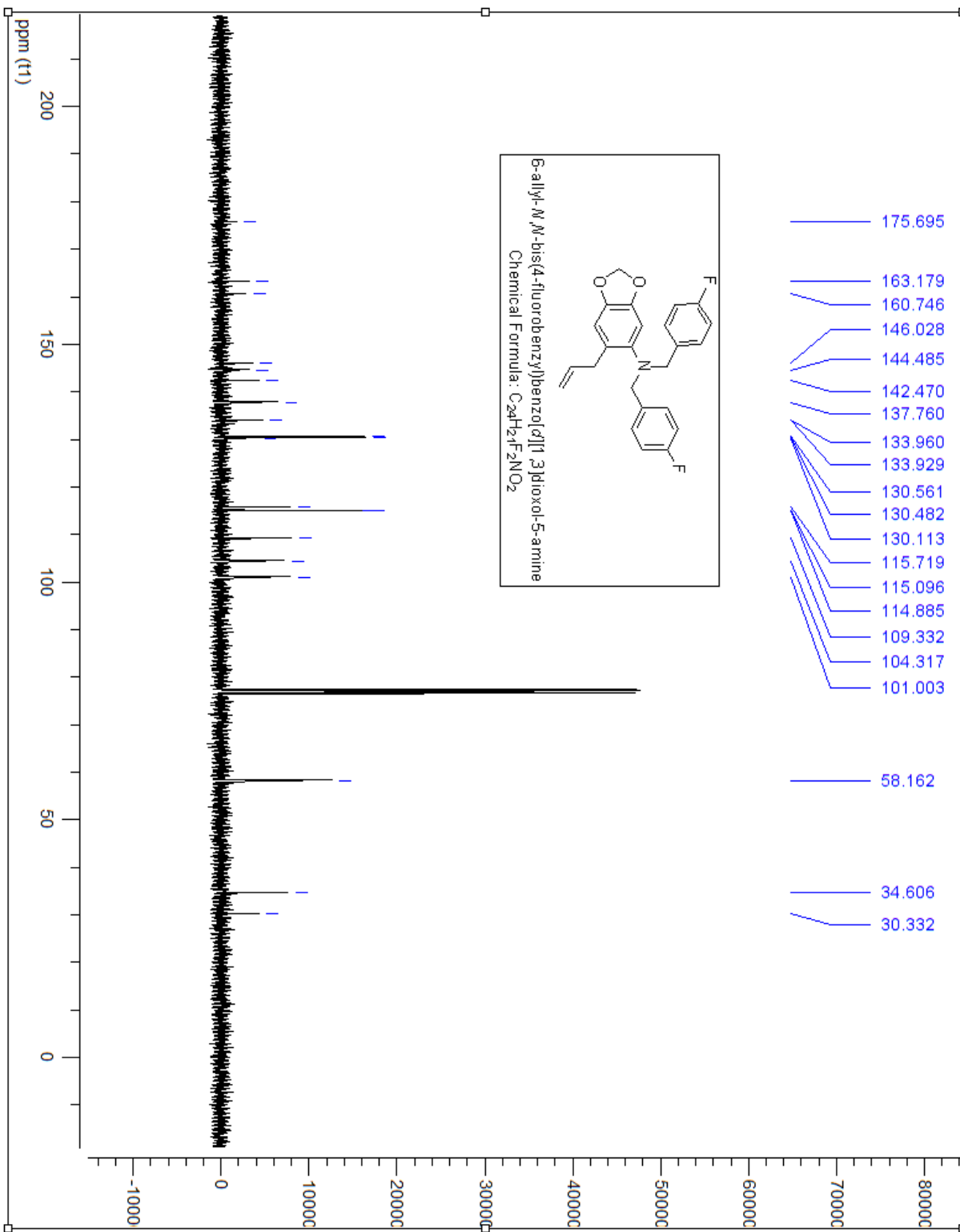
## 64

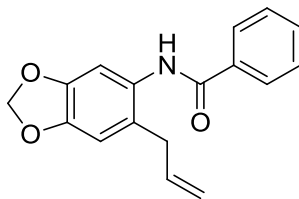
This compound was prepared using **45** (0.3 g, 1.69mmol), in 10 ml of THF, triethylamine (0.71ml, 5.07mmol) was added and stirred for 10 minutes before the addition of 4-fluorobenzylchloride (0.20ml, 1.67mmol) and let stir for 2 hours. The reaction mixture was extracted with EtOAc and water. The crude product (0.19g) was purified via gradient column chromatography (2.5% EtOAc in hexanes) resulting as a white powder (57mg, Rf= 0.3 in 2:8 EtOAc:Hexanes).

$^1H$  NMR (400 MHz,  $CDCl_3$ )  $\delta$  ppm 7.17-7.13(m, 4H), 6.95-6.91(m, 4H), 6.62(s, 1H), 6.58(s, 1H), 5.87(s, 2H), 5.76-5.66(m, 1H), 5.01-4.95(m, 2H), 3.87(s, 4H), 3.40-3.38(d, J=6.48 Hz, 2H)

$^{13}C$  NMR (100MHz,  $CDCl_3$ )  $\delta$  ppm 175.69, 163.17, 160.74, 146.02, 144.48, 142.47, 137.76, 133.96, 133.92, 130.56, 130.48, 130.11, 115.71, 115.09, 114.88, 109.33, 104.31, 101.00, 58.16, 34.60, 30.33







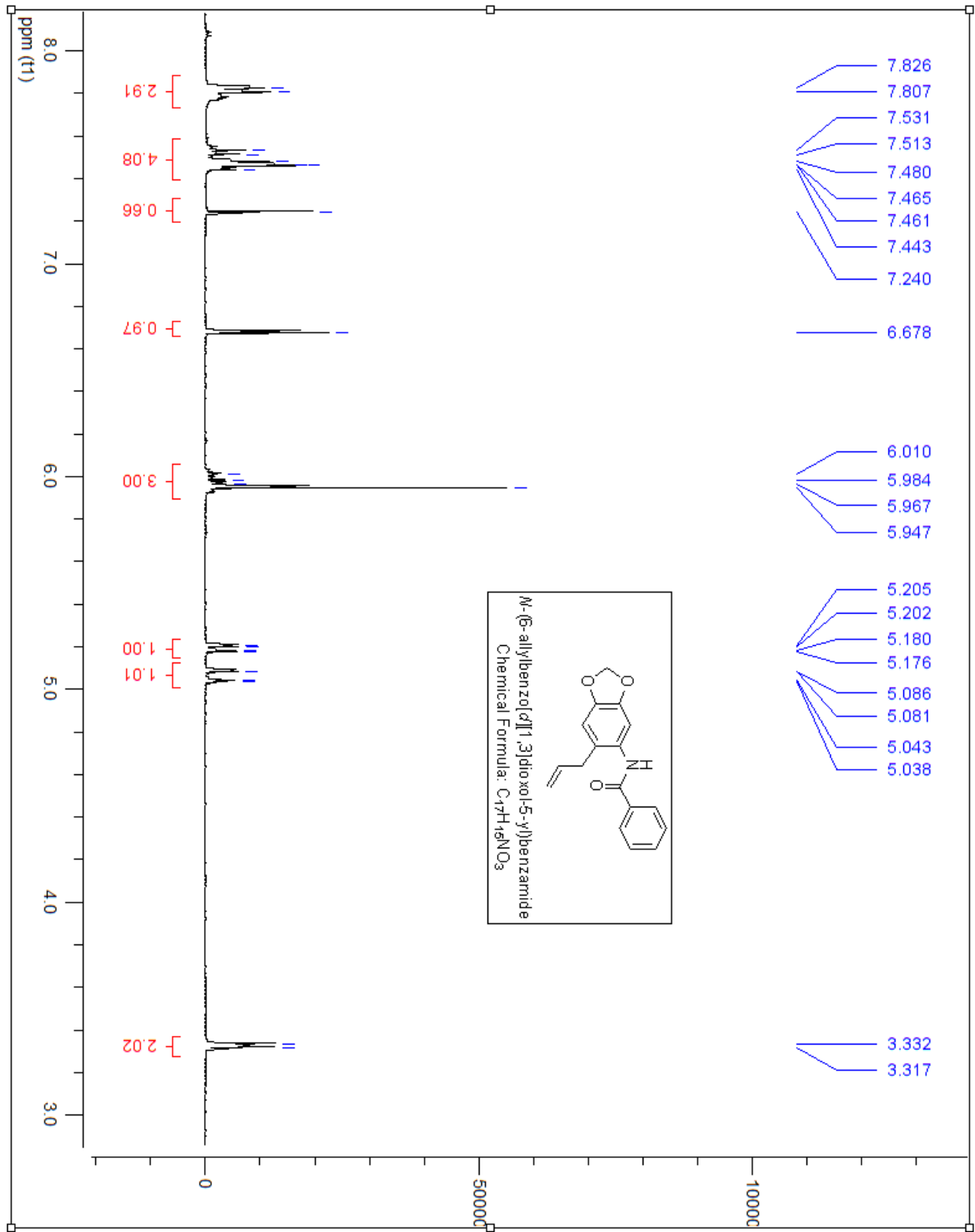
Chemical Formula: C<sub>17</sub>H<sub>15</sub>NO<sub>3</sub>  
Molecular Weight: 281.31

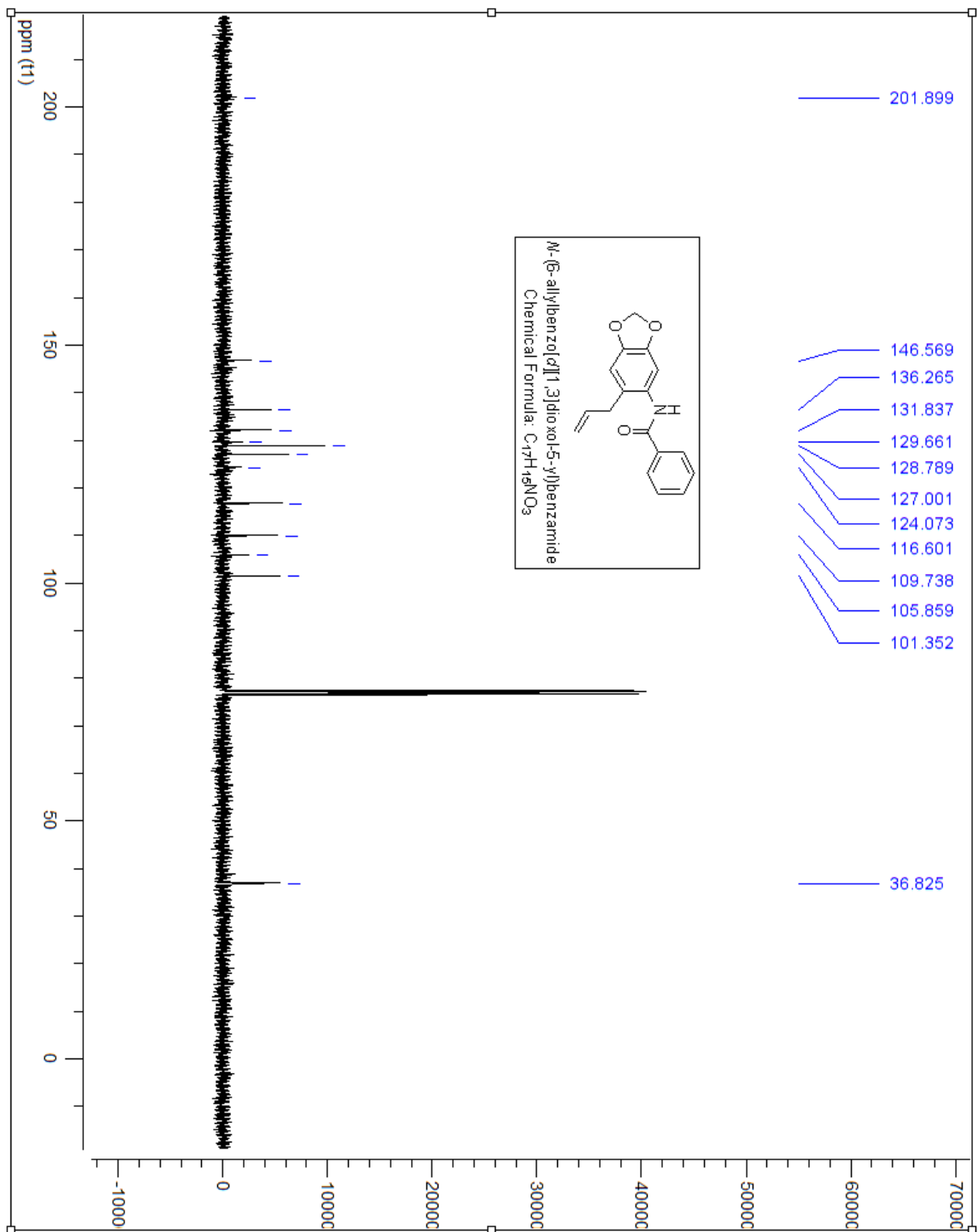
## 65

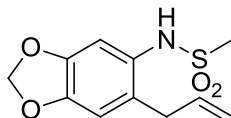
This compound was prepared using **45** (0.2 g, 1.12mmol), in 10 ml of THF, triethylamine (0.16ml, 1.12 mmol) was added and stirred for 10 minutes before the addition of benzoyl chloride (0.13ml, 1.12mmol) and let stir for 2 hours. The reaction mixture was extracted with EtOAc and water. The crude product (0.21g) was purified via gradient column chromatography (2.5% EtOAc in hexanes) resulting as a white crystal (190mg, R<sub>f</sub>= 0.73 in 2:8 EtOAc:Hexanes).

<sup>1</sup>H NMR (400 MHz, CDCl<sub>3</sub>) δ ppm 7.82-7.77(m, 3H), 7.53-7.44(m, 4H), 6.67(s, 1H), 6.01-5.92(m, 3H), 5.20-5.17(dd, J=10.12, 10.12Hz, 1H), 5.08-5.03(dd, J= 17.19, 17.19Hz, 1H), 3.33-3.31(d, J= 5.87Hz, 2H)

<sup>13</sup>C NMR (100MHz, CDCl<sub>3</sub>) δ ppm 201.89, 161.02, 146.56, 145.20, 136.26, 131.83, 131.75, 129.66, 128.78, 127.00, 124.07, 116.60, 109.73, 105.85, 101.35, 36.82







Chemical Formula: C<sub>11</sub>H<sub>13</sub>NO<sub>4</sub>S

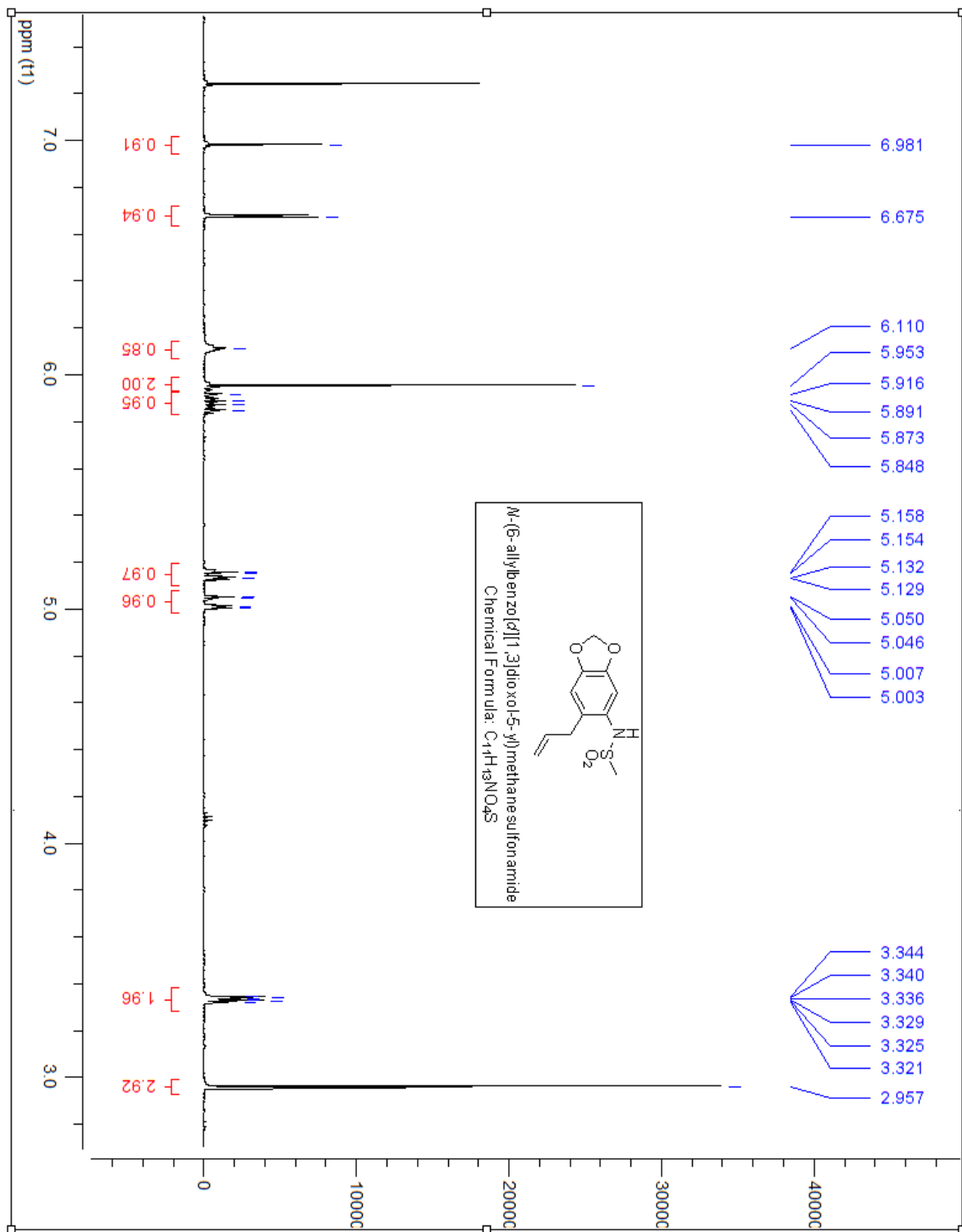
Molecular Weight: 255.29

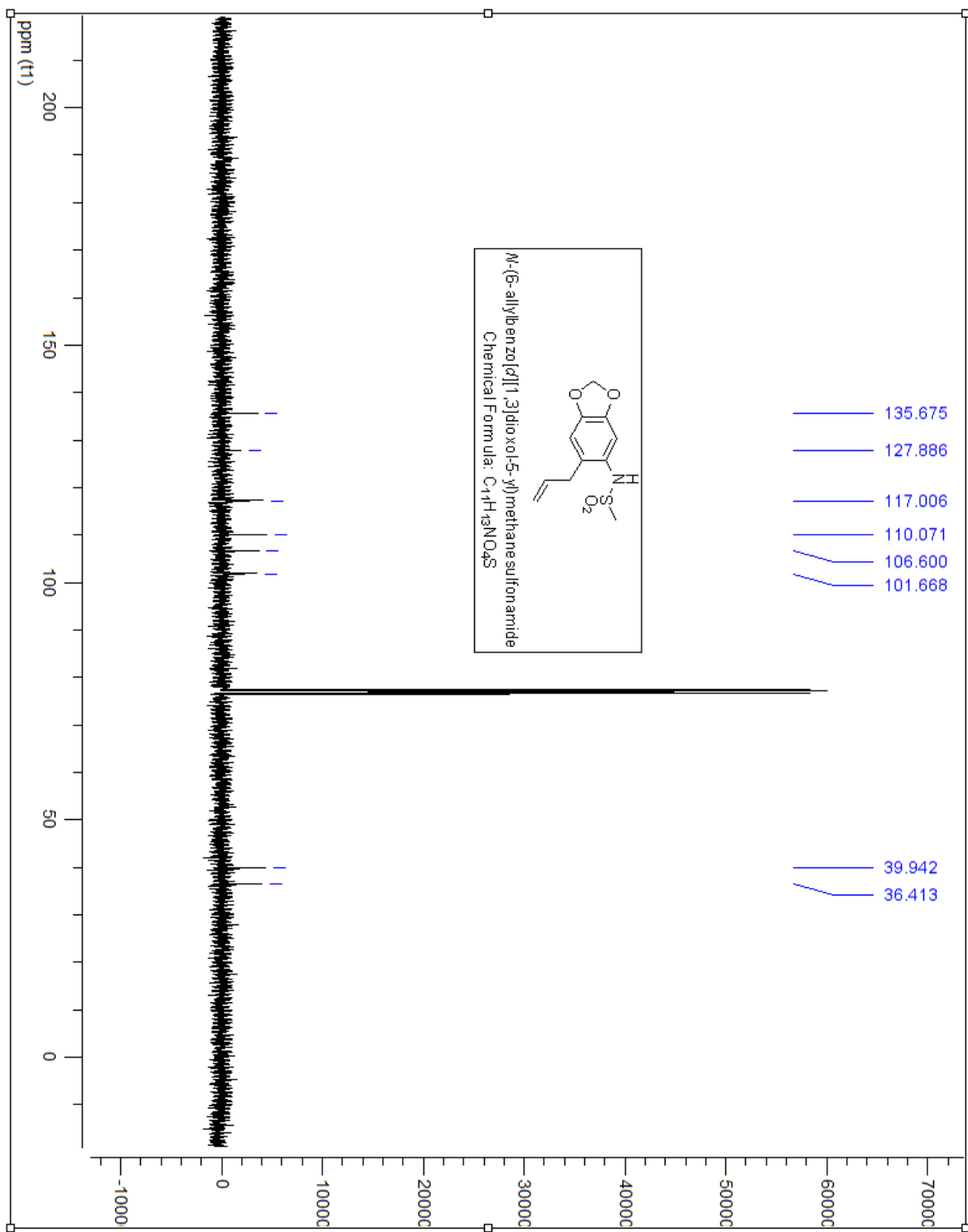
## 66

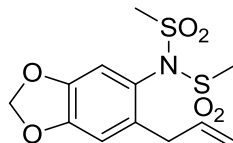
This compound was prepared using **45** (0.3 g, 1.69mmol), in 10 ml of DCM, triethylamine (0.35ml, 2.54mmol) was added and stirred for 10 minutes before the addition of methanesulfonyl chloride (0.157ml, 2.03mmol) and let stir for 2 hours. The reaction mixture was extracted with EtOAc and water. The crude product (0.26g) was purified via gradient column chromatography (2.5% EtOAc in hexanes) resulting as a white crystal (126mg, Rf= 0.3 in 2:8 EtOAc:Hexanes).

<sup>1</sup>H NMR (400 MHz, CDCl<sub>3</sub>) δ ppm 6.98(s, 1H), 6.67(s, 1H), 6.1(b, 1H), 5.95(s, 2H), 5.91-5.84(m, 1H), 5.15-5.12(dd, J=10.12, 10.12Hz, 1H), 5.05-5.00(dd, J=17.16, 17.16 Hz, 1H), 3.34-3.32(dt, J=5.97, 5.97, 5.97Hz, 2H), 2.95(s, 3H)

<sup>13</sup>C NMR (100MHz, CDCl<sub>3</sub>) δ ppm 148.75, 146.99, 135.67, 127.88, 117.00, 110.07, 106.60, 101.66, 39.94, 36.41







Chemical Formula: C<sub>12</sub>H<sub>15</sub>NO<sub>6</sub>S<sub>2</sub>

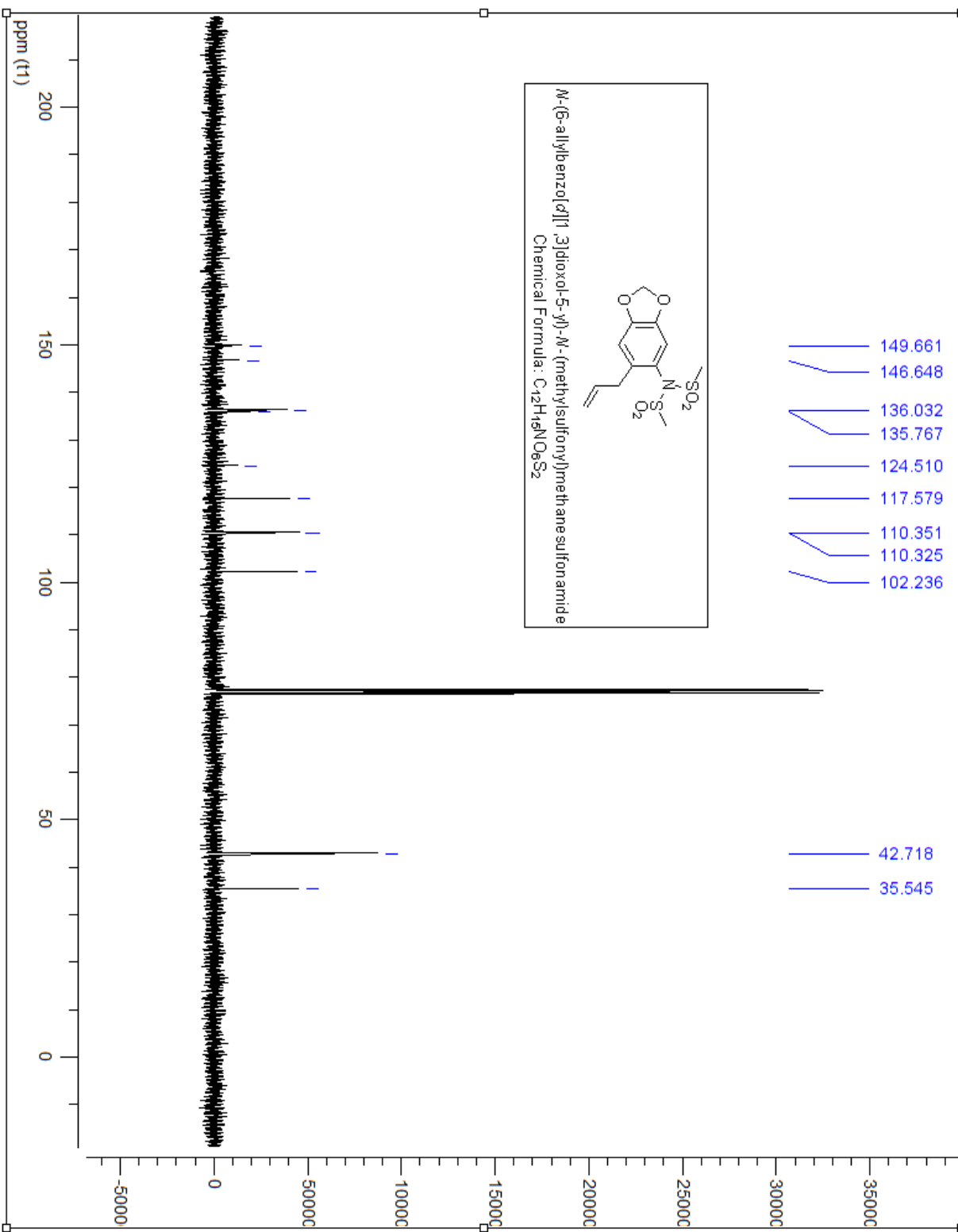
Molecular Weight: 333.38

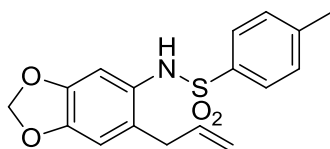
## 67

This compound was prepared using **45** (0.3 g, 1.69mmol), in 10 ml of DCM, triethylamine (0.35ml, 2.54mmol) was added and stirred for 10 minutes before the addition of methylsulfonyl chloride (0.157ml, 2.03mmol) and let stir for 2 hours. The reaction mixture was extracted with EtOAc and water. The crude product (0.26g) was purified via gradient column chromatography (2.5% EtOAc in hexanes) resulting as a white crystal (26mg, Rf= 0.5 in 2:8 EtOAc:Hexanes).

<sup>1</sup>H NMR (400 MHz, CDCl<sub>3</sub>) δ ppm 6.77(s, 1H), 6.70(s, 1H), 6.00(s, 2H), 5.93-5.86(m, 1H), 5.15-5.13(dd, J=17.11, 17.11Hz, 1H), 5.08-5.03(dd, J=9.71, 9.71Hz, 1H), 3.42-3.39(m, 8H)

<sup>13</sup>C NMR (100MHz, CDCl<sub>3</sub>) δ ppm 149.66, 146.64, 136.03, 135.76, 124.51, 117.57, 110.35, 110.32, 102.23, 42.71, 35.54





Chemical Formula: C<sub>17</sub>H<sub>17</sub>NO<sub>4</sub>S

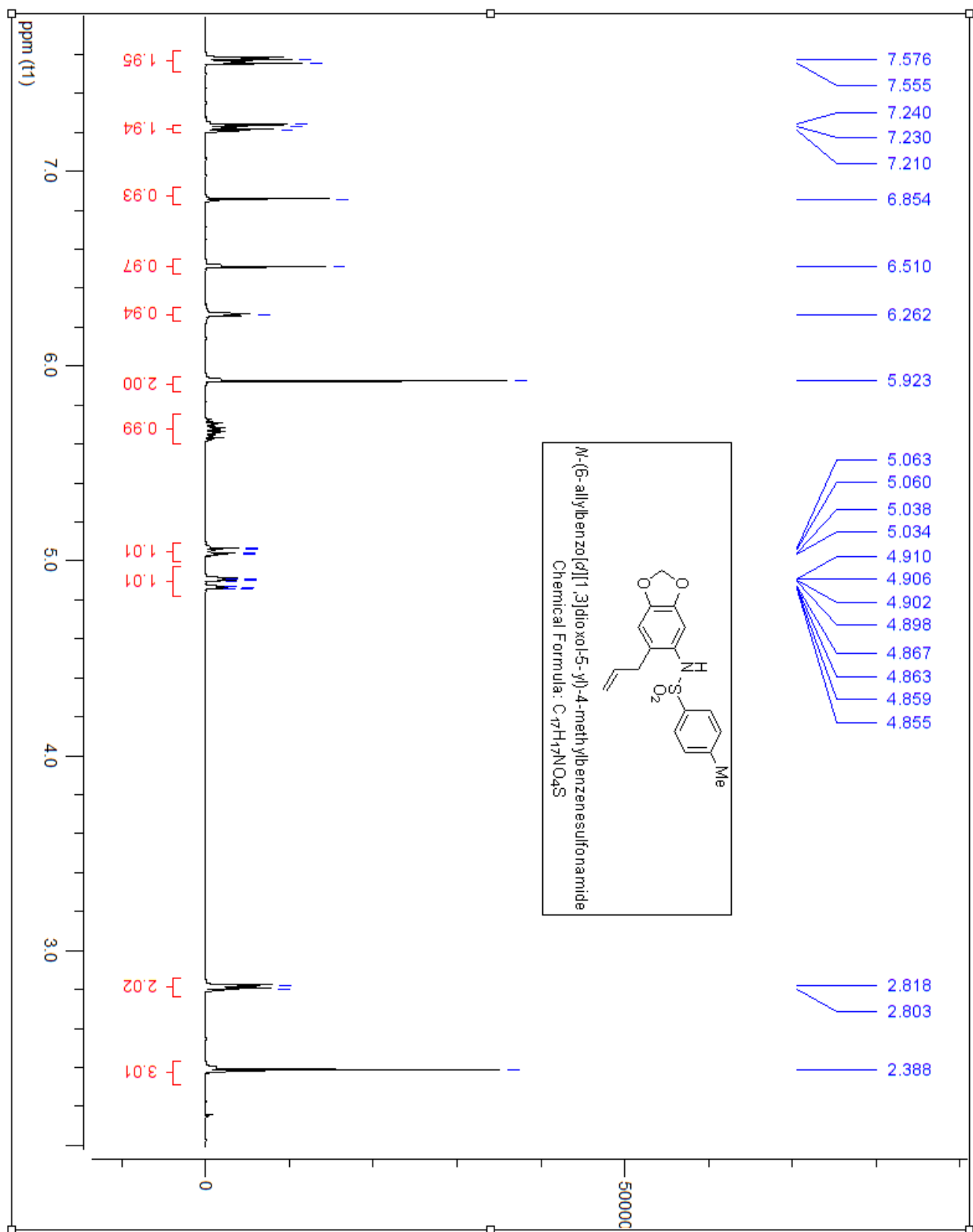
Molecular Weight: 331.39

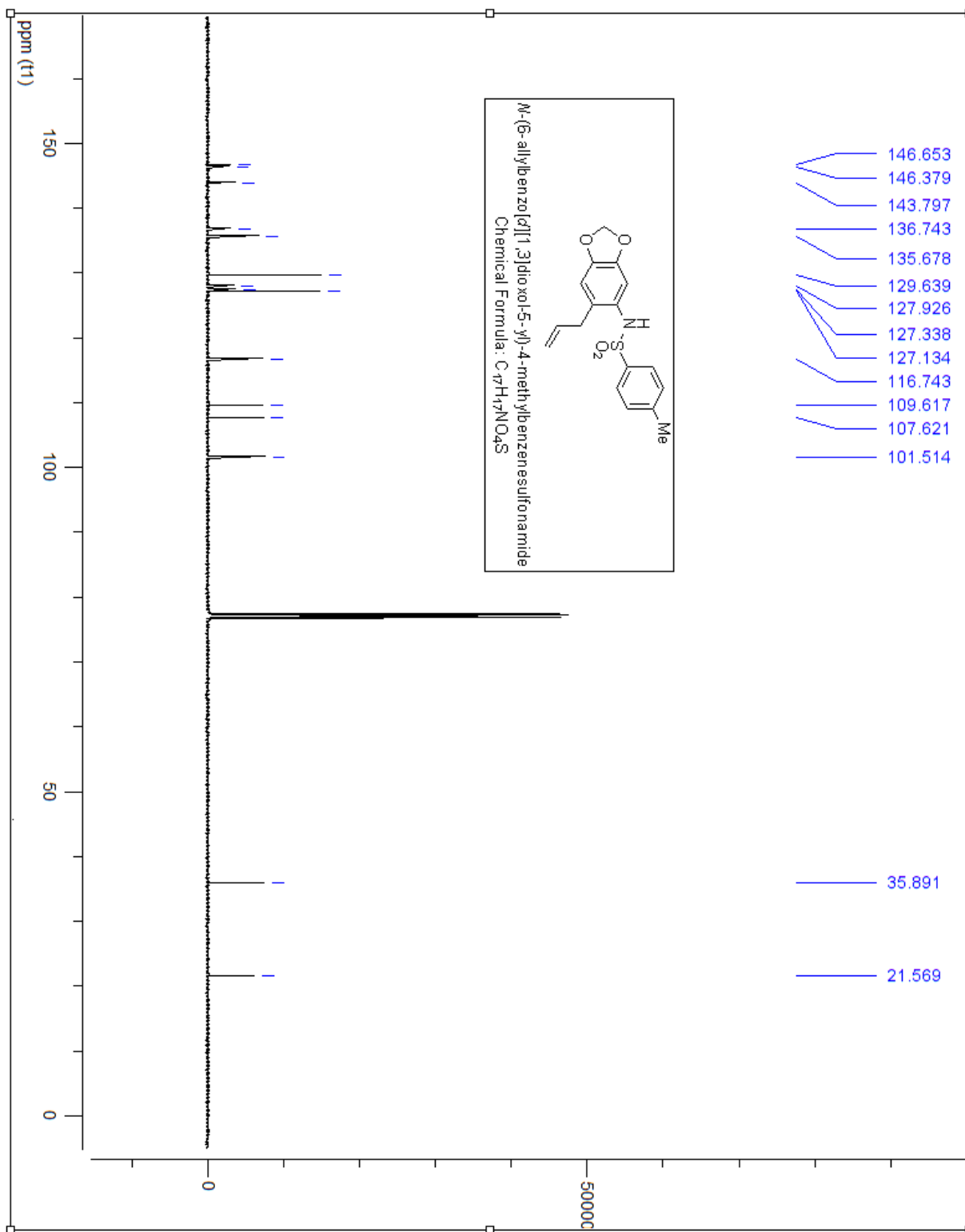
## 68

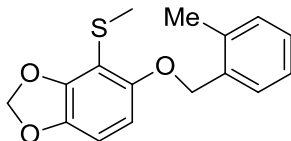
This compound was prepared using **45** (0.2 g, 1.12mmol), in 10 ml of THF, triethylamine (0.16ml, 1.12 mmol) was added and stirred for 10 minutes before the addition of p-toluenesulfonyl chloride (0.215g, 1.12mmol) and let stir for 2 hours. The reaction mixture was extracted with EtOAc and water. The crude product (0.36g) was purified via gradient column chromatography (2.5% EtOAc in hexanes) resulting as a white crystal (290mg, Rf= 0.73 in 2:8 EtOAc:Hexanes).

<sup>1</sup>H NMR (400 MHz, CDCl<sub>3</sub>) δ ppm 7.57-7.55(d, J=Hz, 2H), 7.23-7.21(m, 2H), 6.85(s, 1H), 6.51(s, 1H), 6.26(s, 1H), 5.92(s, 2H), 5.71-5.61(m, 1H), 5.06-5.03(dd, J=10.0, 10.0Hz, 1H), 4.90-4.85(dq, J= 17.14, 17.14, 17.14, 17.14Hz, 1H), 2.81-2.80(d, J=6.04 Hz, 2H), 2.38(s, 3H)

<sup>13</sup>C NMR (100MHz, CDCl<sub>3</sub>) δ ppm 146.65, 146.37, 143.79, 136.74, 135.67, 129.63, 127.92, 127.33, 127.13, 116.74, 109.61, 107.62, 101.51, 35.89, 21.56







Chemical Formula: C<sub>16</sub>H<sub>16</sub>O<sub>3</sub>S

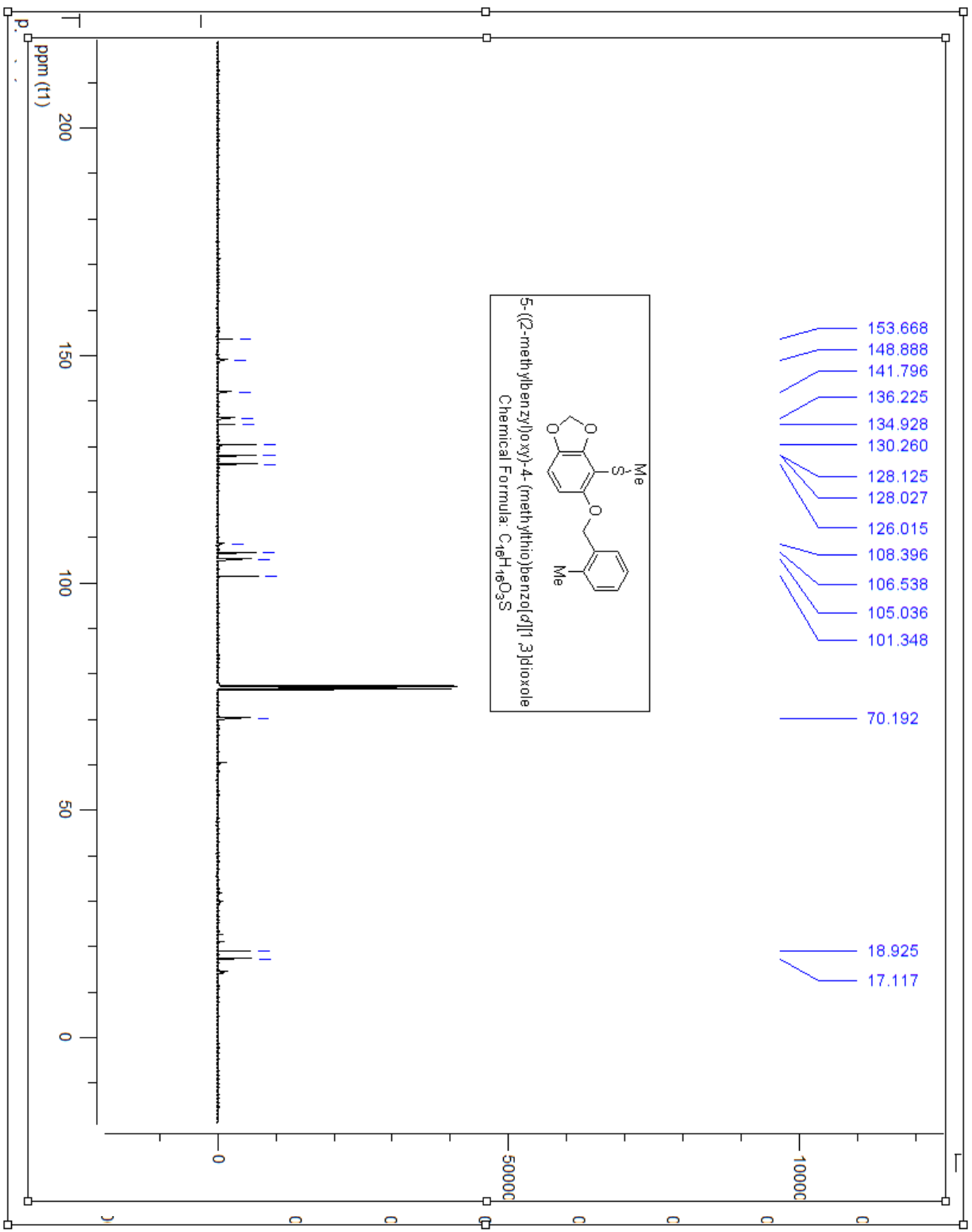
Molecular Weight: 288.36

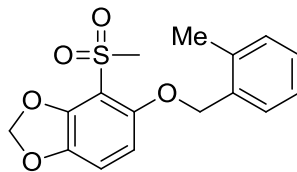
## 70

This compound was prepared using **69** (0.2 g, 1.08 mmol), in 20 ml of Acetone, potassium carbonate (4.65 g, 3.25 mmol) was added and stirred for 10 minutes before the addition of 2 methylbenzyl bromide (0.145ml, 1.08mmol) and refluxed for 6 hours. The reaction mixture was extracted with EtOAc and water. The phenol was washed with 10% NaOH. The crude product (251mg) was purified via gradient column chromatography (2.5% EtOAc in hexanes) resulting as a white solid (0.18 g, Rf= 0.20 in 2:8 EtOAc:Hexanes).

<sup>1</sup>H NMR (400 MHz, CDCl<sub>3</sub>) δ ppm 7.47-7.45(m, 1H), 7.21-7.16(m, 3H), 6.63-6.61(d, J=8.5 Hz, 1H), 6.37-6.35(d, J= 8.5 Hz, 1H), 5.96(s, 2H), 5.01(s, 2H), 2.41(s, 3H), 2.37(s, 3H)

<sup>13</sup>C NMR (100MHz, CDCl<sub>3</sub>) δ ppm 153.66, 148.88, 141.79, 136.22, 134.92, 130.26, 128.12, 128.02, 126.01, 106.53, 105.03, 101.34, 70.19, 18.92, 17.11





Chemical Formula: C<sub>16</sub>H<sub>16</sub>O<sub>5</sub>S

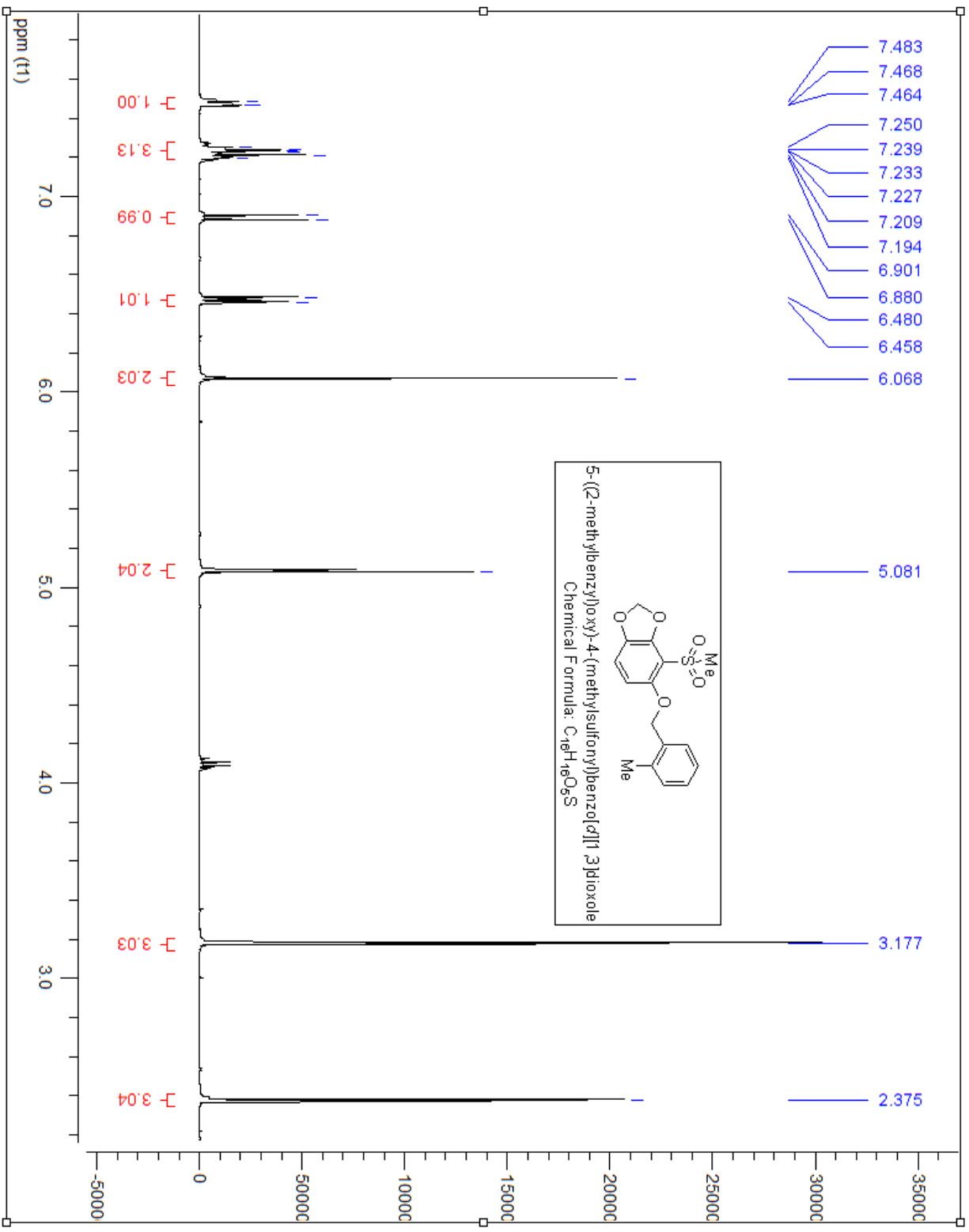
Molecular Weight: 320.36

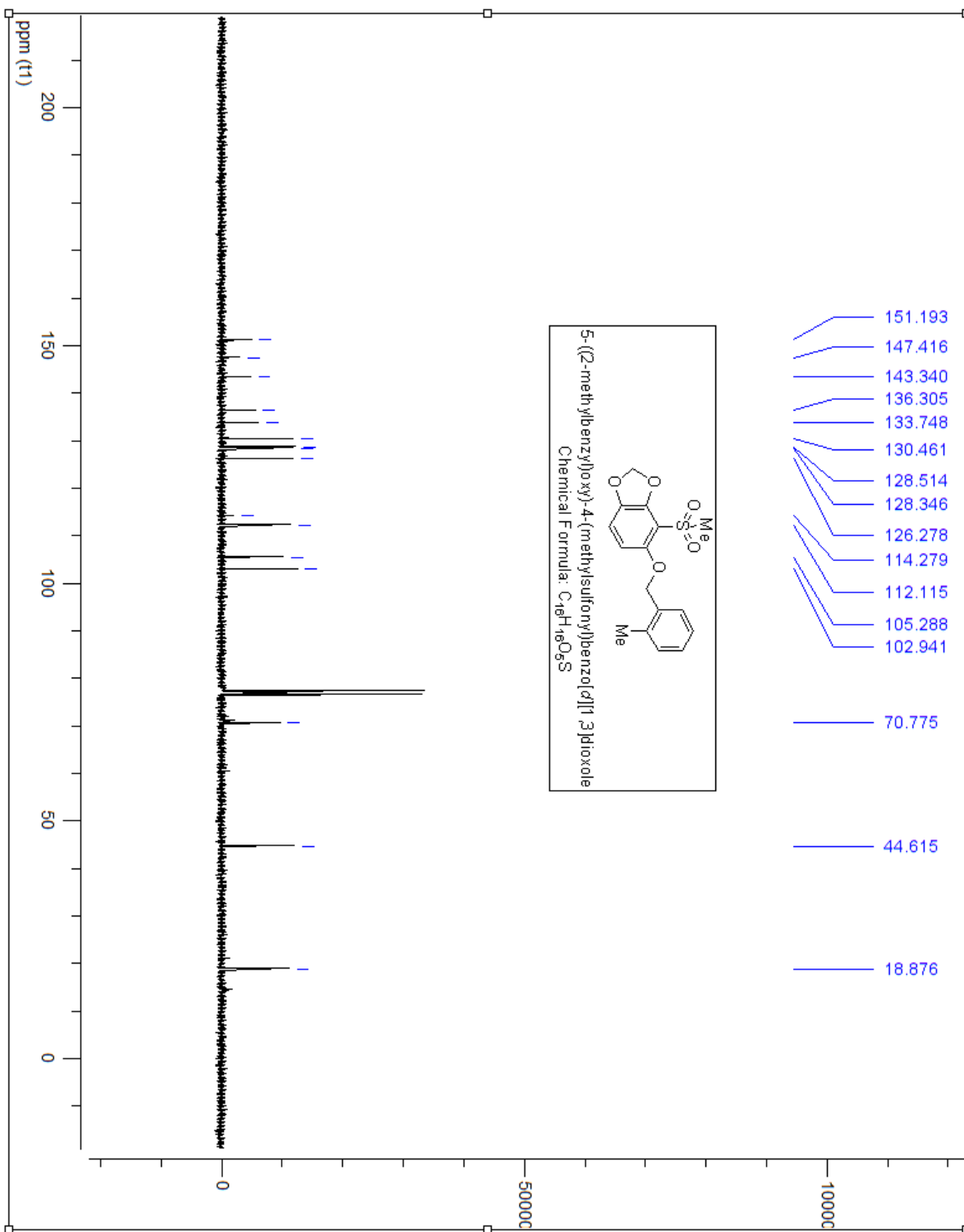
## 72

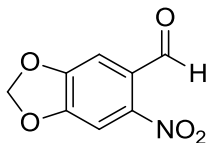
This compound was prepared using **70** (0.14 g, 0.48 mmol), in 10 ml of DCM, mCPBA (83mg, 0.48mmol) was added and stirred for 1 hour under 0°C. The reaction mixture was diluted with DCM and NaHCO<sub>3</sub>. The mixture was extracted with DCM (3X20ml). The phenol was washed with 10% NaOH. The crude product (123mg) was purified via gradient column chromatography (2.5% EtOAc in hexanes) resulting as a white crystal (0.100 g, Rf= 0.35 in 2:8 EtOAc:Hexanes).

<sup>1</sup>H NMR (400 MHz, CDCl<sub>3</sub>) δ ppm 7.48-7.46(m, 1H), 7.25-7.20(m, 3H), 6.90-6.88(d, J=8.56 Hz, 1H), 6.48-6.45(d, J= 8.59 Hz, 1H), 6.06(s, 2H), 5.08(s, 2H), 3.17(s, 3H), 2.37(3H)

<sup>13</sup>C NMR (100MHz, CDCl<sub>3</sub>) δ ppm 151.19, 147.41, 143.34, 136.30, 133.74, 130.46, 128.51, 128.34, 126.27, 1114.27, 112.11, 105.28, 102.94, 70.77, 44.61, 18.87







Chemical Formula: C<sub>8</sub>H<sub>5</sub>NO<sub>5</sub>

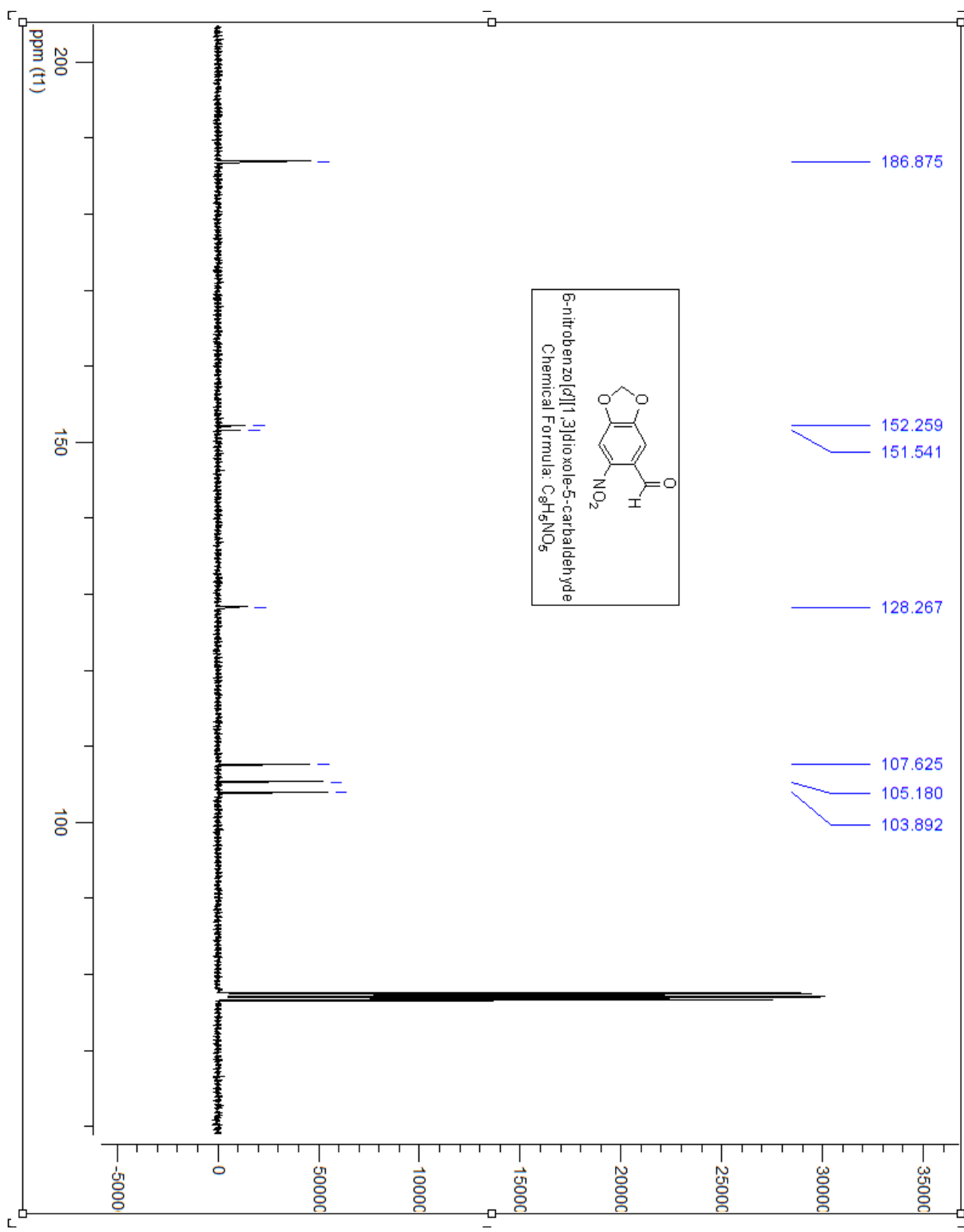
Molecular Weight: 195.13

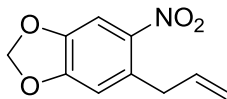
## 75

This compound was prepared using **pipernal** (1 g, 6.66mmol), in 0.38ml l of acetic acid under 5°C, and conc. HNO<sub>3</sub> in 1.5ml of acetic acid was slowly added and stirred for 1 hour. The mixture was taken up in 100ml of water and extracted with EtOAc (3x50ml). Organic solutions was washed with water, filtered, dried with MgSO<sub>4</sub> and concentrated *in vacuo*. The crude product (1.2g) was purified via gradient column chromatography (2.5% EtOAc in hexanes) resulting as a orange crystals (800mg, Rf= 0.25 in 2:8 EtOAc:Hexanes).

<sup>1</sup>H NMR (400 MHz, CDCl<sub>3</sub>) δ ppm 10.28(s, 1H), 7.51(s, 1H), 7.32(s, 1H), 6.20(s, 2H)

<sup>13</sup>C NMR (100MHz, CDCl<sub>3</sub>) δ ppm 186.87, 152.25, 151.54, 128.26, 107.62, 105.18, 103.89





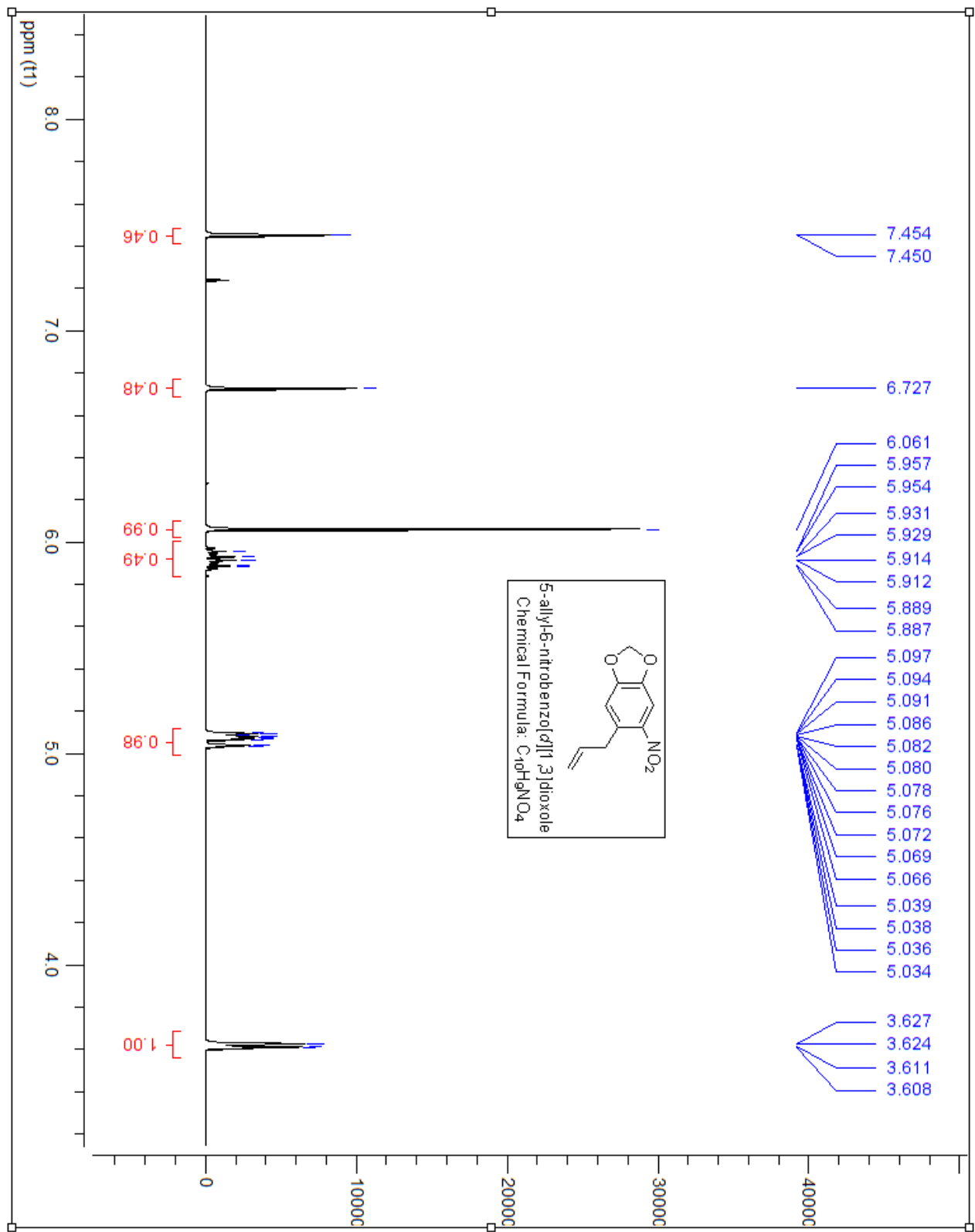
Chemical Formula: C<sub>10</sub>H<sub>9</sub>NO<sub>4</sub>  
Molecular Weight: 207.18

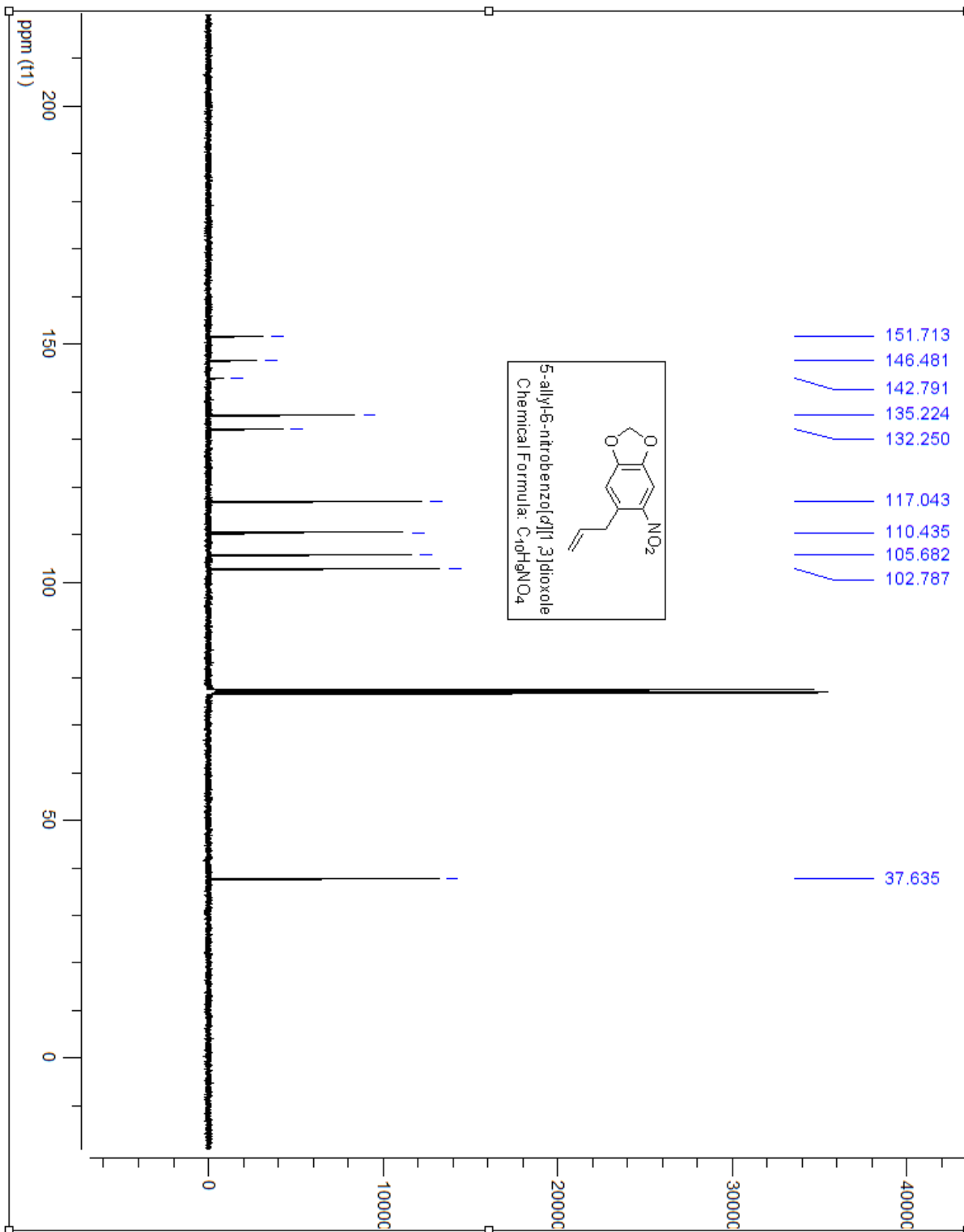
## 76

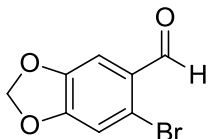
This compound was prepared using **safrole** (10 g, 61.65 mmol), in 3.53 ml of acetic acid under 5°C and conc. HNO<sub>3</sub> in 1.5ml of acetic acid was slowly added. After 2 hours the mixture was taken up in 100ml of water and extracted with 50ml of EtOAc. Organic was washed with water, filtered and dried with MgSO<sub>4</sub>, filtered and concentrated *in vacuo*. The crude product (8.6 g) was purified via gradient column chromatography (2.5% EtOAc in hexanes) resulting as a black oil (3.3g, Rf= 0.5 in 2:8 EtOAc:Hexanes).

<sup>1</sup>H NMR (400 MHz, CDCl<sub>3</sub>) δ ppm 7.47(s, 1H), 6.73(s, 1H), 6.06(s, 2H), 5.96-5.88(m, 1H), 5.10-5.04(m, 2H), 3.64-3.62(dd, J= 6.46Hz, 6.46Hz, 2H)

<sup>13</sup>C NMR (100 MHz, CDCl<sub>3</sub>) δ ppm 151.71, 146.48, 142.79, 135.22, 132.25, 117.04, 110.04, 105.43, 102.78, 37.63







Chemical Formula:  $C_8H_5BrO_3$

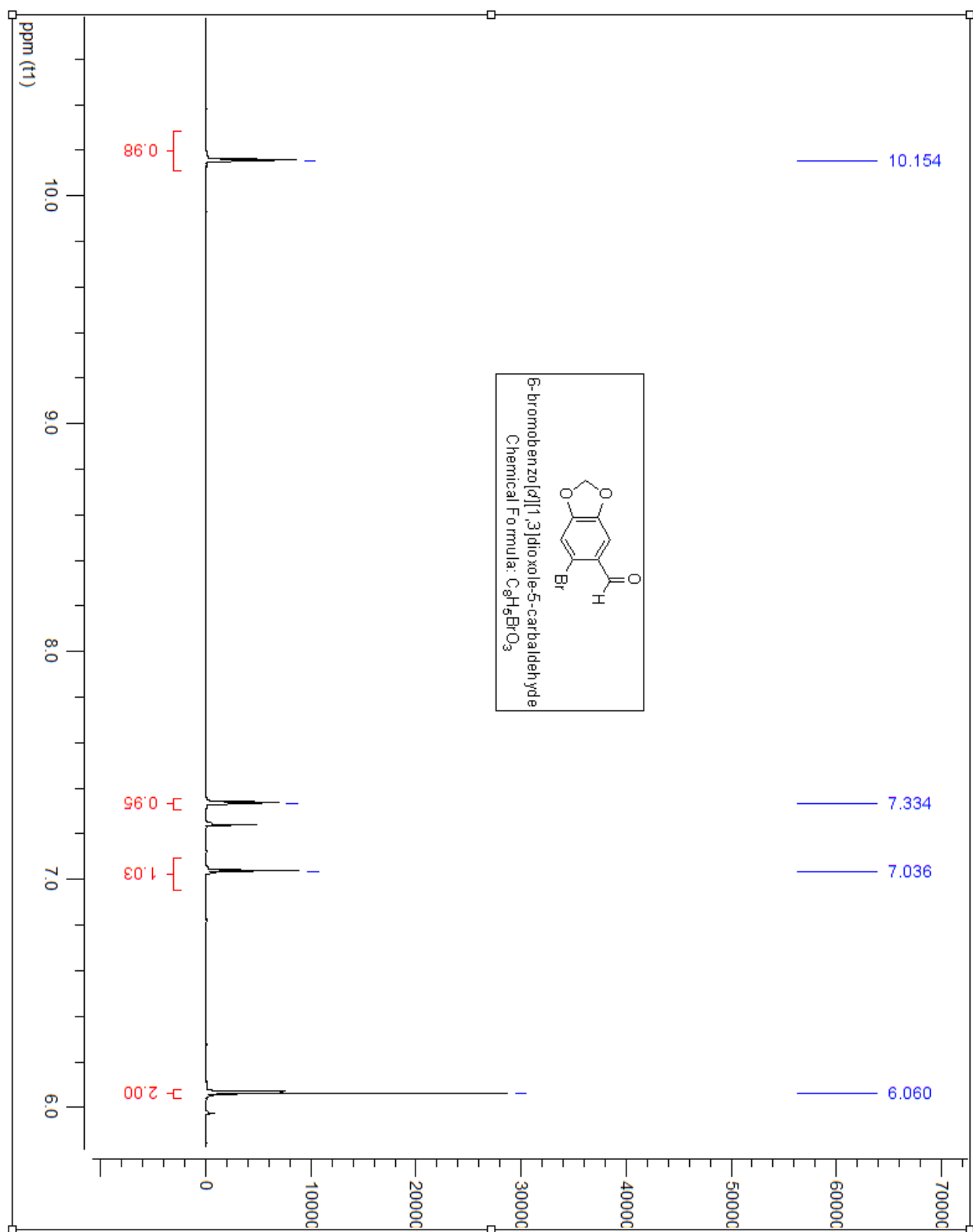
Molecular Weight: 229.03

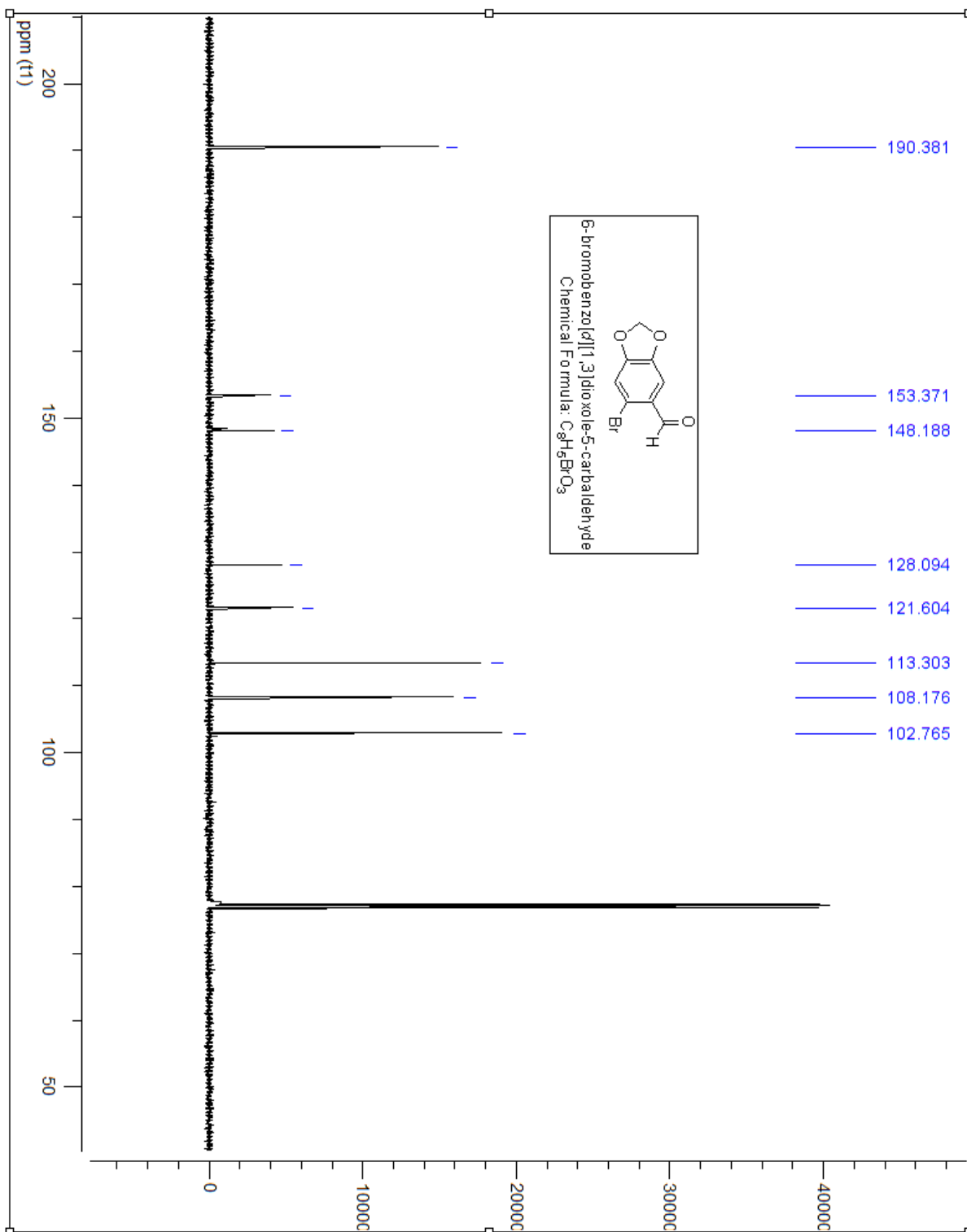
## 77

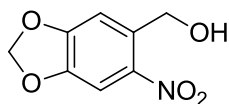
This compound was prepared using **pipernal** (15g, 0.1 mol), into 100ml of glacial acetic acid and bromine (6ml, 0.12mol) for 18 hours. Water (100ml) was added to precipitate the product. Solid was collected on a Buchner funnel and recrystallized (ethanol) as colourless needles to give product (8.79g, Rf= 0.40 in 2:8 EtOAc:Hexanes).

$^1H$  NMR (400 MHz,  $CDCl_3$ )  $\delta$  ppm 10.16 (s, 1H), 7.34-7.33(s, 1H), 7.04-7.03(s, 1H), 6.06(s, 2H)

$^{13}C$  NMR (100MHz,  $CDCl_3$ )  $\delta$  ppm 190.38, 153.37, 148.18, 128.09, 121.60, 113.30, 108.17, 102.76







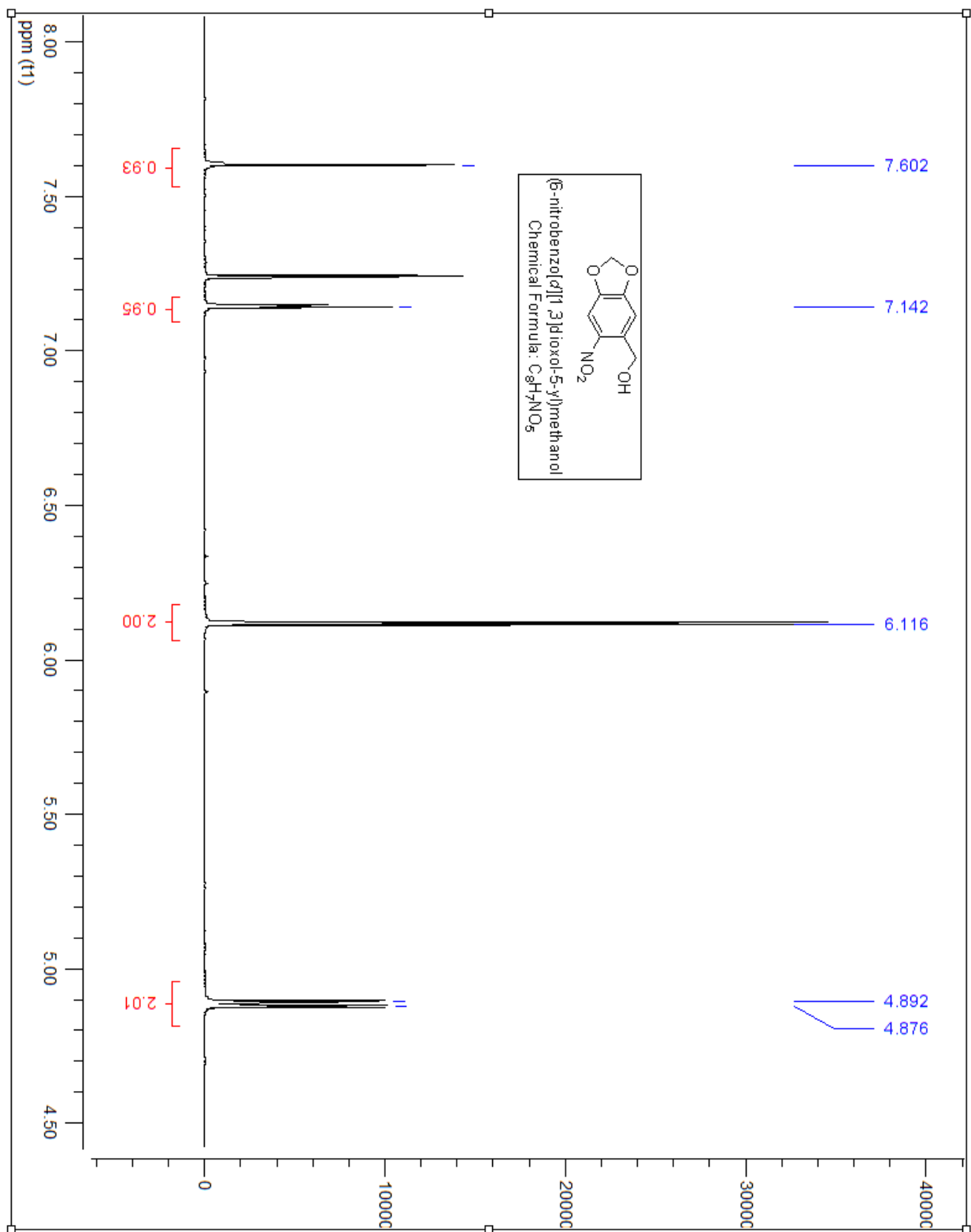
Chemical Formula: C<sub>8</sub>H<sub>7</sub>NO<sub>5</sub>  
Molecular Weight: 197.14

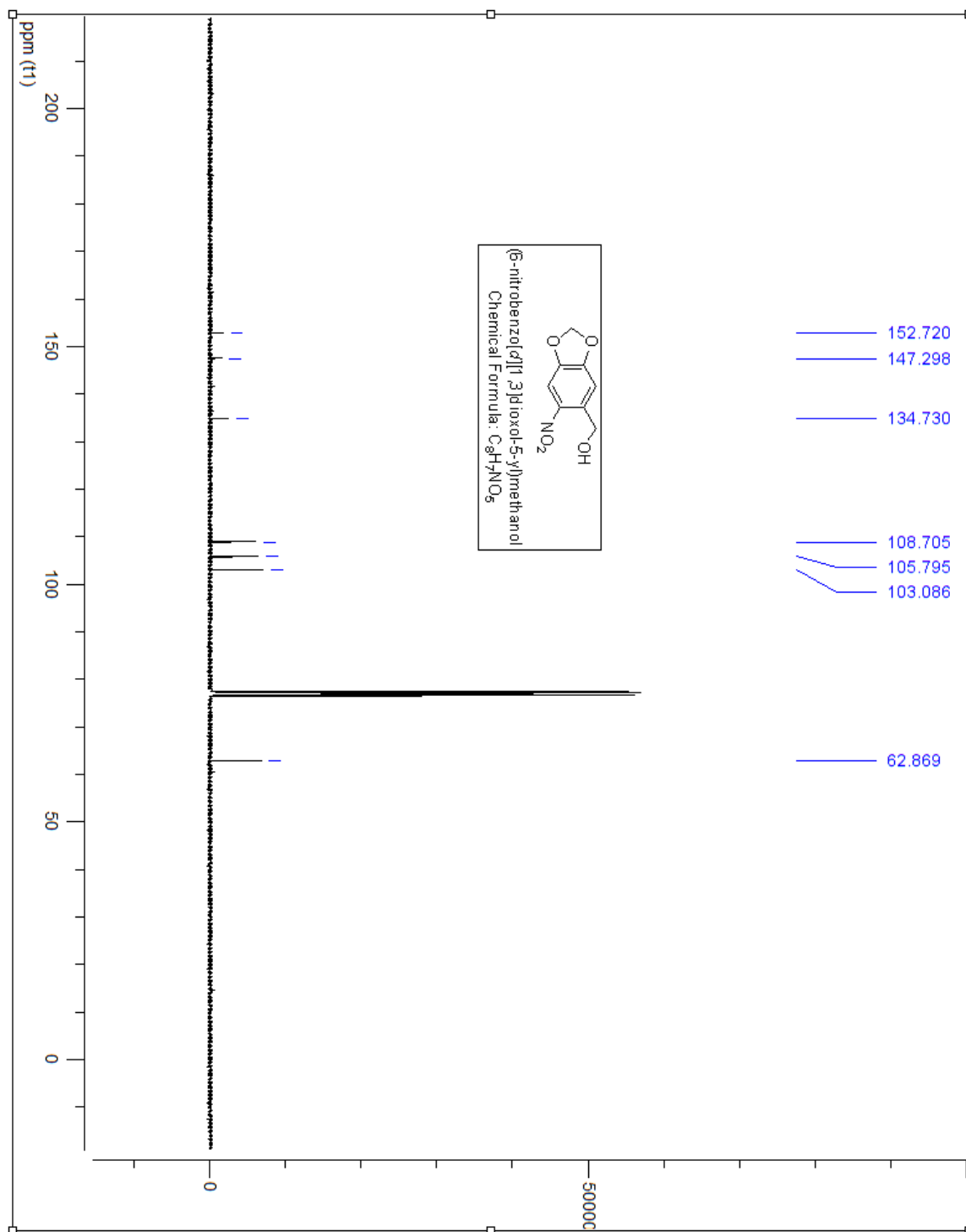
## 78

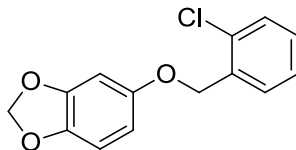
This compound was prepared using **75** (700mg, 4.09mmol), into methanol and add NaBH<sub>4</sub> (465mg, 12.29mmol) and let stir until bubbling ceases. Ammonium chloride was added to quench the reaction followed by extraction of DCM. All the organic fractions were collected dried with MgSO<sub>4</sub>, filtered and concentrated *in vacuo*. The crude product (820mg) was purified via gradient column chromatography (2.5% EtOAc in hexanes) resulting as a yellow powder (631mg, Rf= 0.10 in 2:8 EtOAc:Hexanes).

<sup>1</sup>H NMR (400 MHz, CDCl<sub>3</sub>) δ ppm 7.60(s, 1H), 7.14(s, 1H), 6.11(s, 2H), 4.89-4.87(d, J= 6.54 Hz, 2H)

<sup>13</sup>C NMR (100MHz, CDCl<sub>3</sub>) δ ppm 152.72, 147.29, 134.73, 108.70, 105.79, 103.08, 62.86







Chemical Formula:  $C_{14}H_{11}ClO_3$

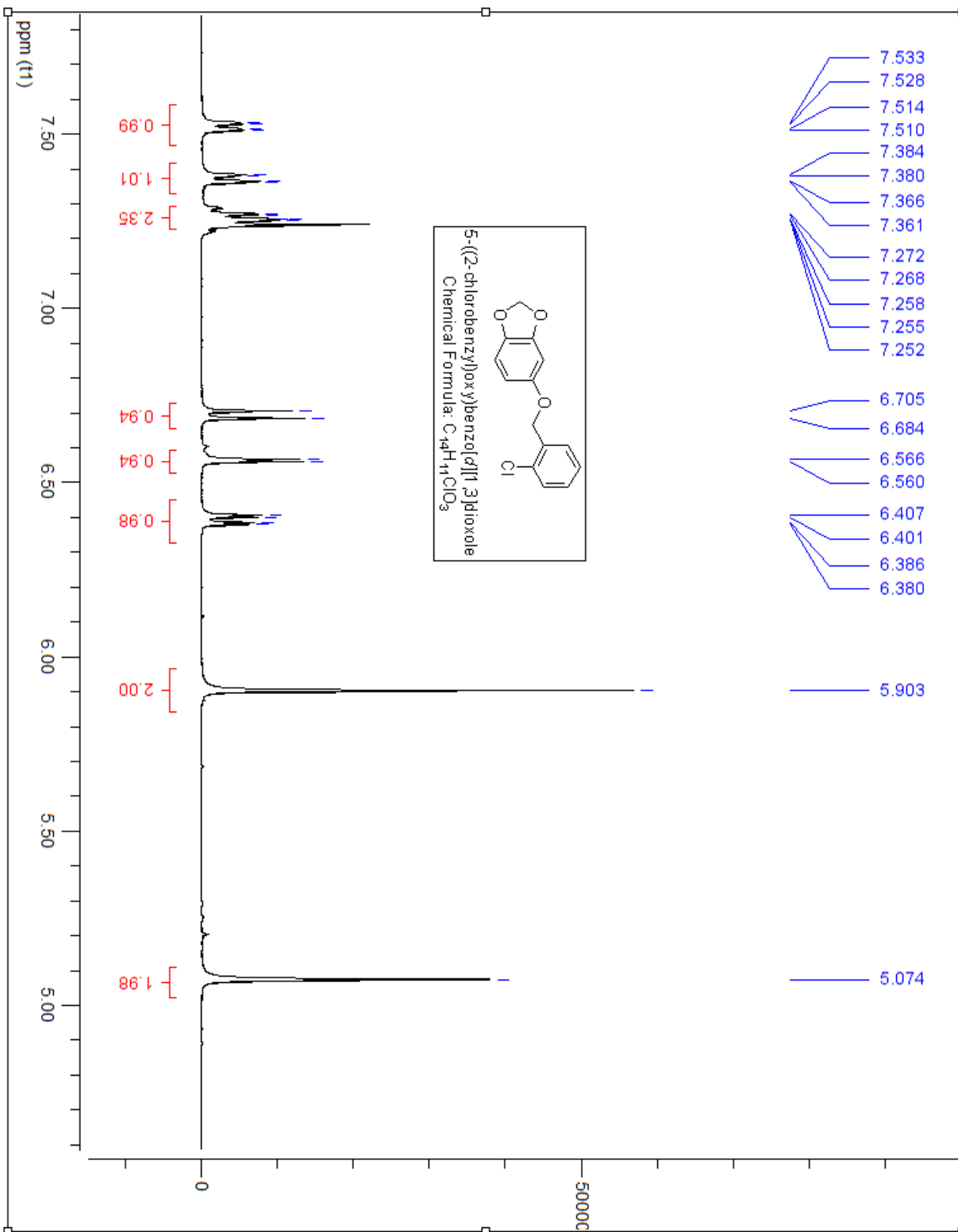
Molecular Weight: 262.69

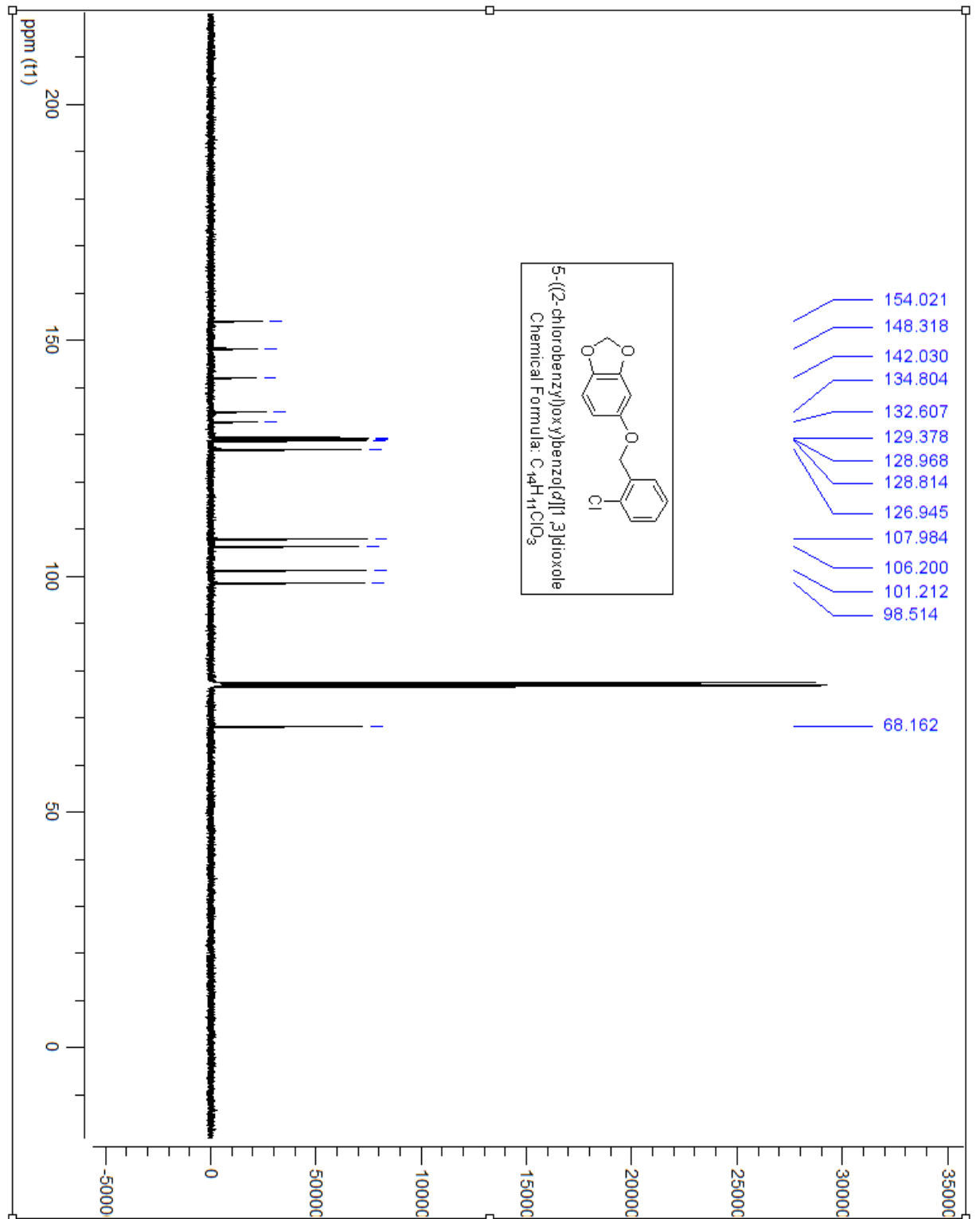
## 86

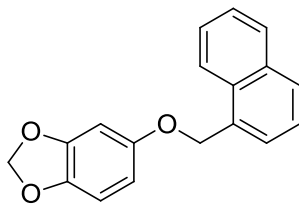
This compound was prepared using **sesamol** (0.2 g, 1.44 mmol), in 20 ml of Acetone, potassium carbonate (0.60 g, 4.34mmol) was added and stirred for 10 minutes before the addition of 2-chlorobenzyl chloride (0.18ml, 1.4 mmol) and refluxed for 6 hours. The reaction mixture was extracted with EtOAc and water. The phenol was washed with 10% NaOH. The crude product was purified via gradientcolumn chromatography (2.5% EtOAc in hexanes) resulting as a white powder (168mg, Rf= 0.85 in 2:8 EtOAc:Hexanes).

$^1H$  NMR (400 MHz,  $CDCl_3$ )  $\delta$  ppm 7.53-7.51(dd,  $J=7.47,7.47Hz$ , 1H), 7.38-7.36(dd,  $J=7.24,7.24Hz$ , 1H), 7.28-7.23(m, 2H), 6.71-6.68(d,  $J=8.47Hz$ , 1H), 6.56 (d,  $J=2.48Hz$ , 1H), 6.41-6.38(dd,  $J=8.47,8.47Hz$ , 1H), 5.90(s, 2H), 5.07(s, 2H)

$^{13}C$  NMR (100 MHz,  $CDCl_3$ )  $\delta$  ppm 154.02, 148.31, 142.03, 134.80, 132.61, 129.38, 128.96, 128.81, 126.94, 107.98, 106.20, 101.21, 98.51, 68.16







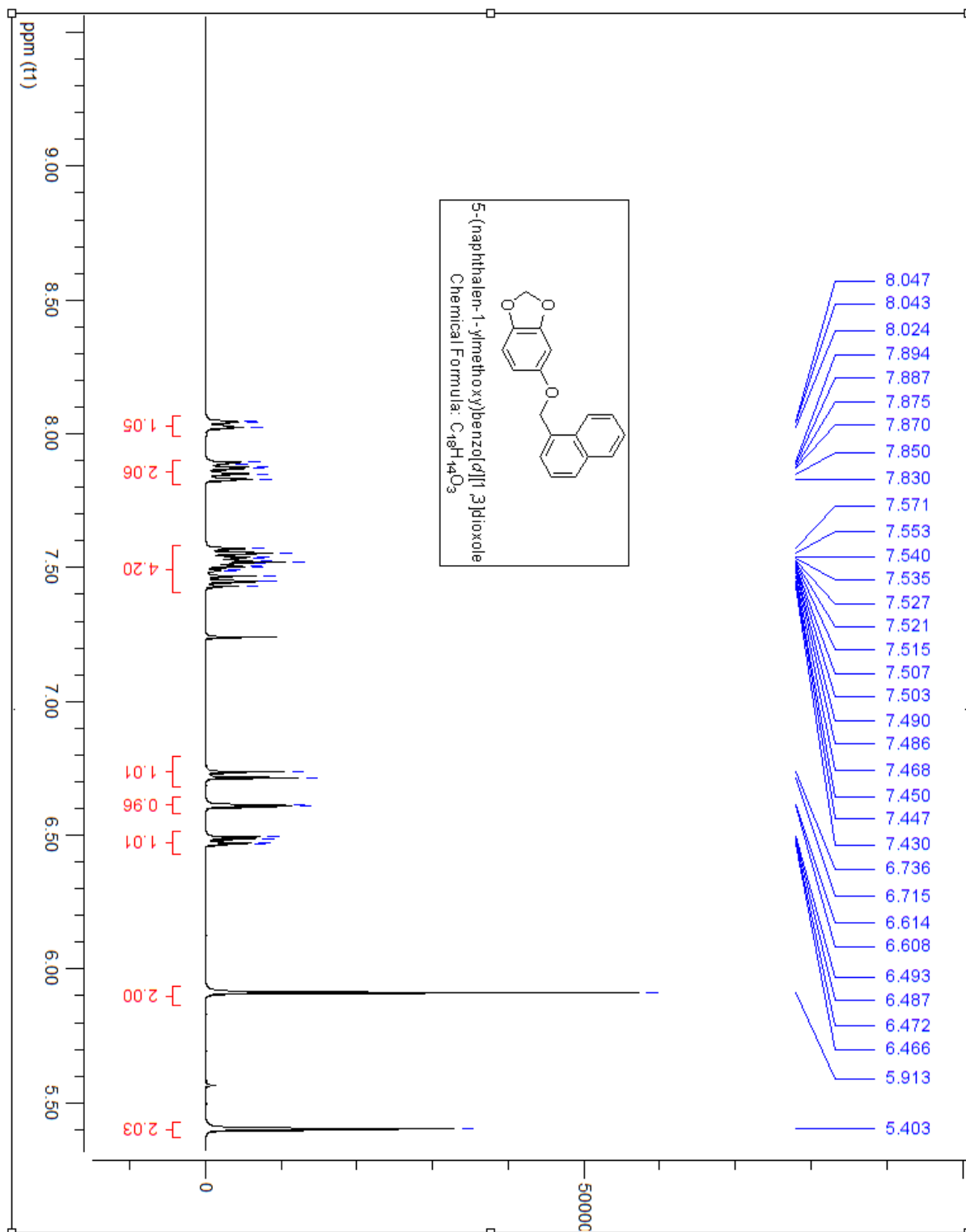
Chemical Formula: C<sub>18</sub>H<sub>14</sub>O<sub>3</sub>  
Molecular Weight: 278.30

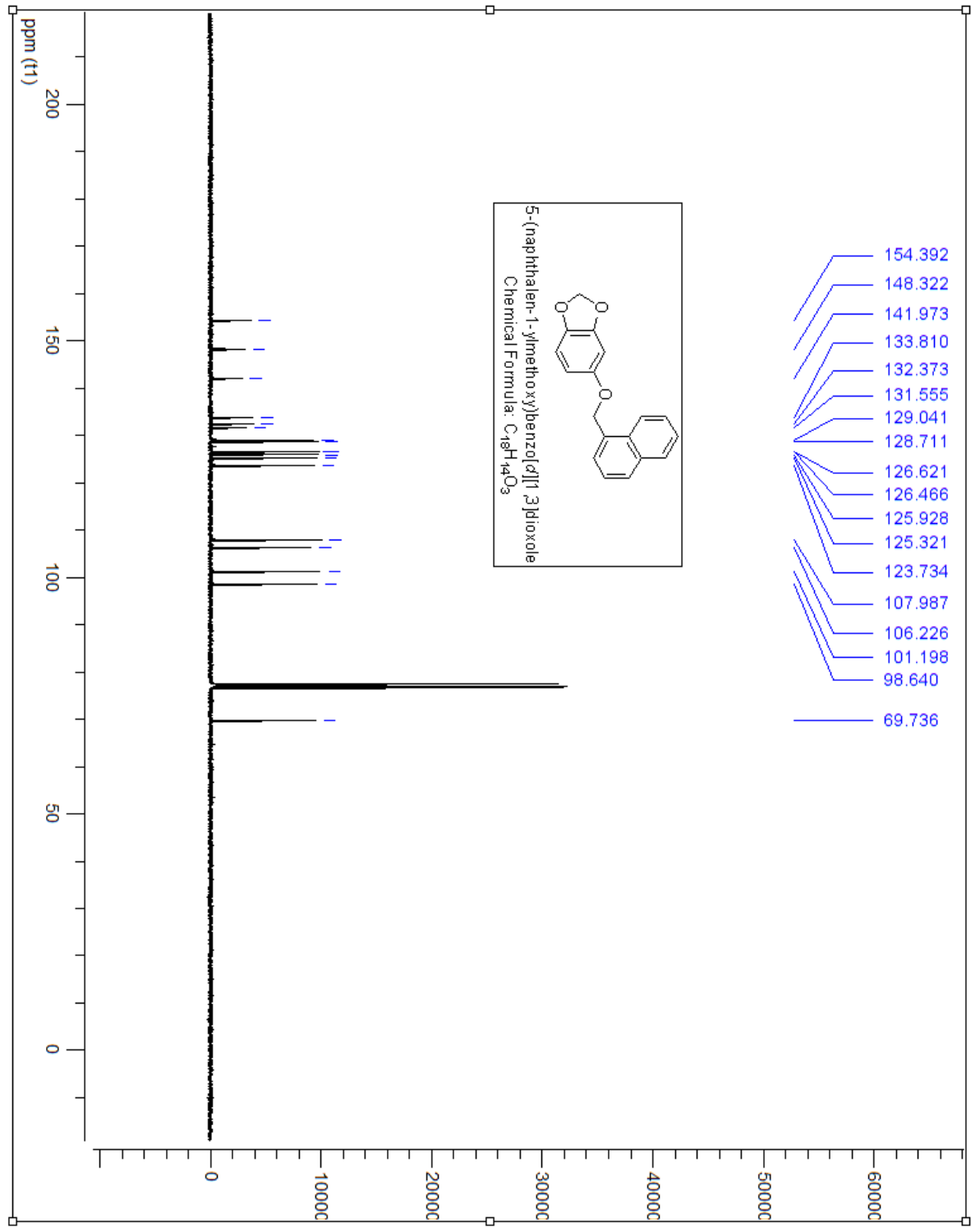
### 87

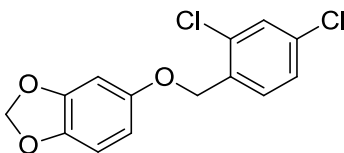
This compound was prepared using **sesamol** (0.2 g, 1.44 mmol), in 20 ml of Acetone, potassium carbonate (0.60 g, 4.34mmol) was added and stirred for 10 minutes before the addition of 2-(1-methyl)chloronaphelene chloride (0.21ml, 1.4 mmol) and refluxed for 6 hours. The reaction mixture was extracted with EtOAc and water. The phenol was washed with 10% NaOH. The crude product was purified via gradientcolumn chromatography (2.5% EtOAc in hexanes) resulting as a white powder (210mg, Rf= 0.80 in 2:8 EtOAc:Hexanes).

<sup>1</sup>H NMR (400 MHz, CDCl<sub>3</sub>) δ ppm 8.01-8.02(m, 1H), 7.89-7.83(m, 2H), 7.51-7.43(m, 4H), 6.73(d, J=8.45Hz, 1H), 6.61(d, J=2.47Hz, 1H), 6.49(dd, J=8.46, 8.46Hz, 1H), 5.91(s, 2H), 5.40(s, 2H)

<sup>13</sup>C NMR (100 MHz, CDCl<sub>3</sub>) δ ppm 154.39, 148.32, 141.97, 133.81, 132.37, 131.55, 129.04, 128.71, 126.62, 126.46, 125.92, 125.32, 123.73, 107.98, 106.22, 101.19, 98.64, 69.73







Chemical Formula:  $C_{14}H_{10}Cl_2O_3$

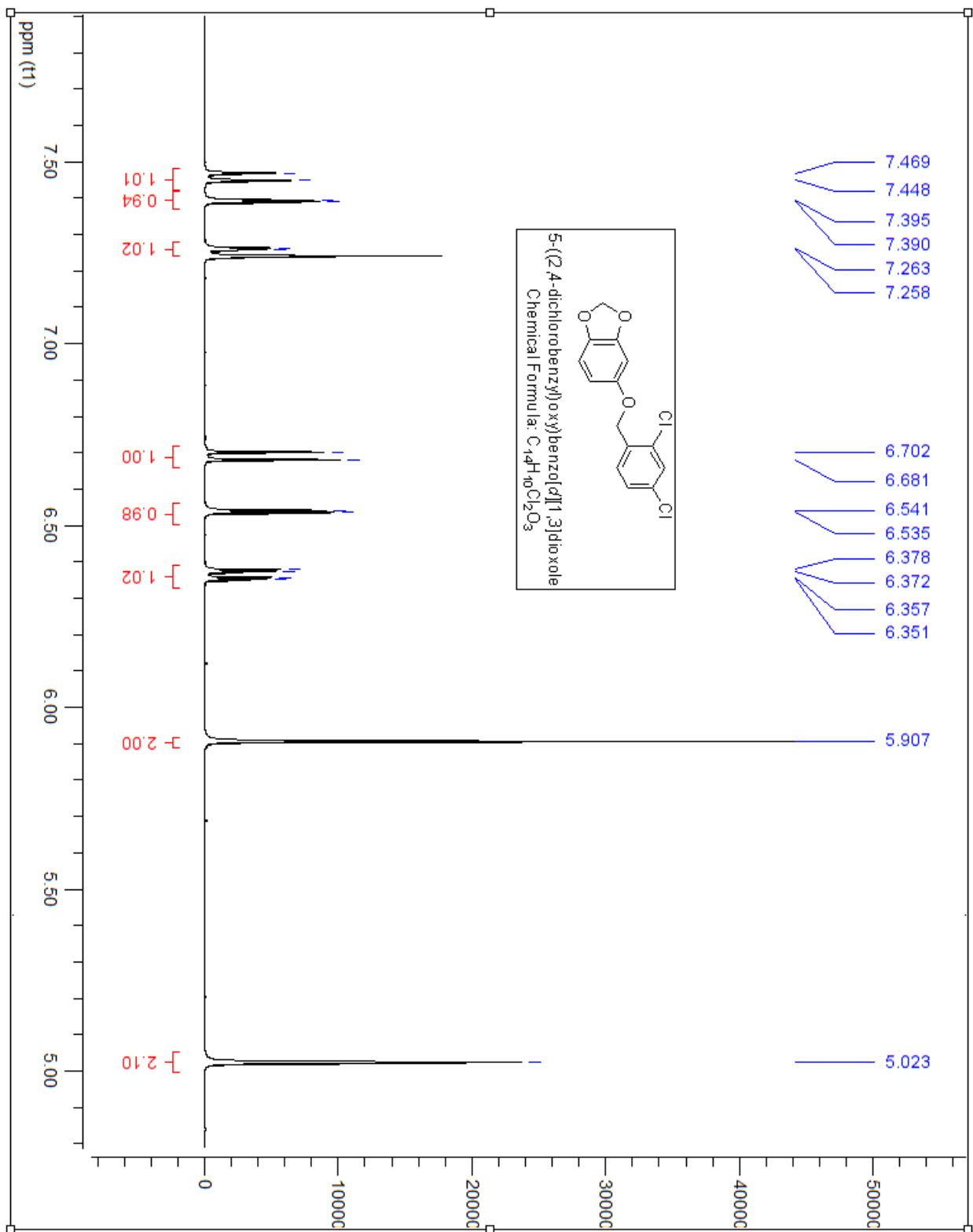
Molecular Weight: 297.13

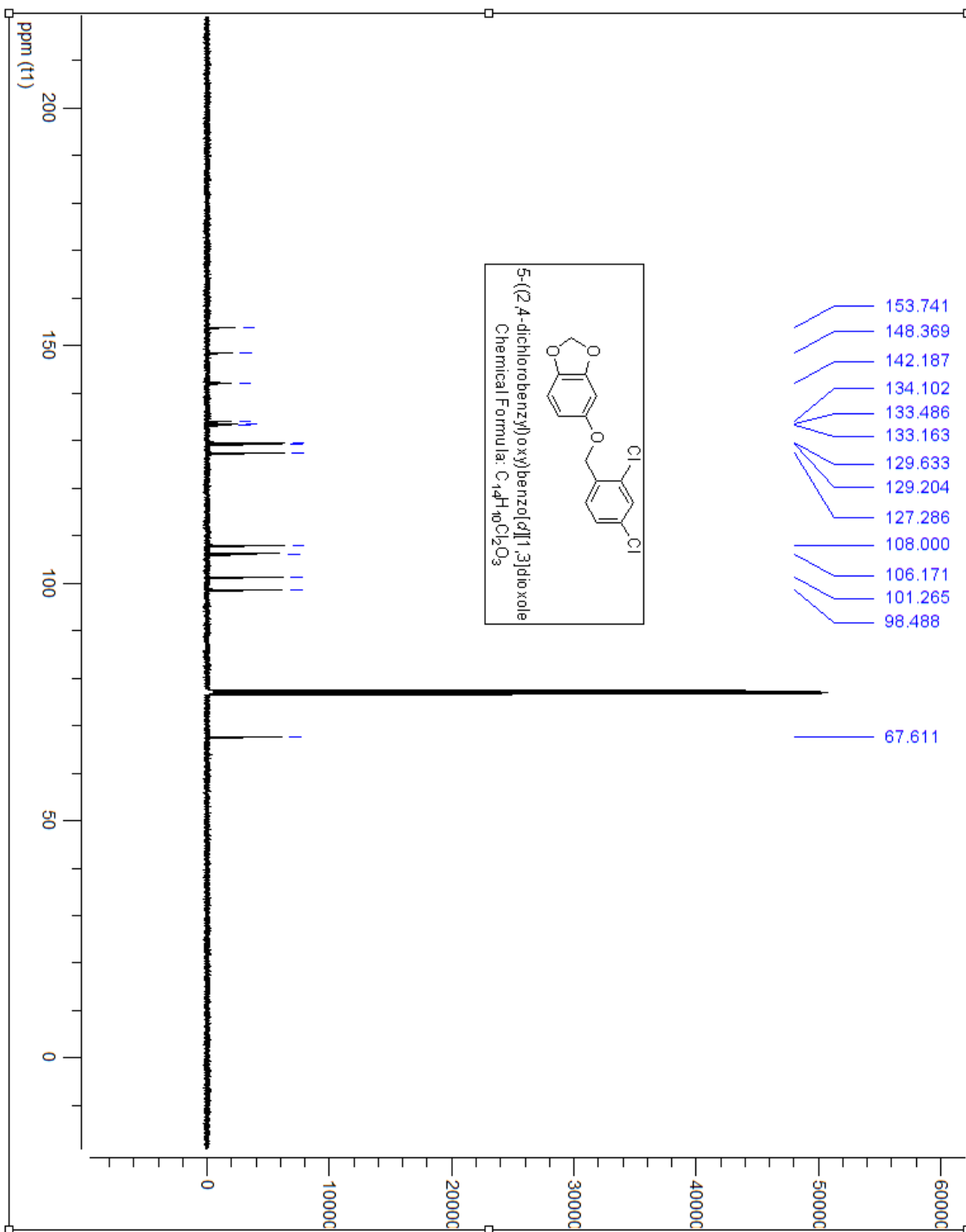
## 88

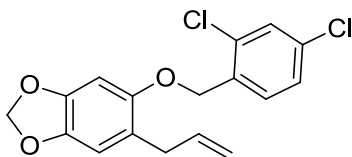
This compound was prepared using **sesamol** (0.2 g, 1.2 mmol), in 20 ml of Acetone, potassium carbonate (0.465 g, 33.7mmol) was added and stirred for 10 minutes before the addition of 2,3 dichlorobenzyl chloride (0.21ml, 1.2 mmol) and refluxed for 6 hours. The reaction mixture was extracted with EtOAc and water. The phenol was washed with 10% NaOH. The crude product was purified via gradientcolumn chromatography (2.5% EtOAc in hexanes) resulting as a brown solid (2.5g, Rf= 0.85 in 2:8 EtOAc:Hexanes).

$^1H$  NMR (400 MHz,  $CDCl_3$ )  $\delta$  ppm 7.46-7.44(d, J=8.32Hz, 1H), 7.39(d, J=2.06Hz, 1H), 7.26-7.25(m, 1H), 6.70-6.68(d, J=8.47Hz, 1H), 6.54(d, J=2.50, 1H), 6.37-6.35(dd, J=2.53, 2.53Hz, 1H), 5.91(s, 2H), 5.02(s, 2H)

$^{13}C$  NMR (100 MHz,  $CDCl_3$ )  $\delta$  ppm 153.74, 148.36, 142.18, 134.10, 133.48, 133.16, 129.63, 129.20, 127.29, 108.00, 106.17, 101.26, 98.48, 67.61







Chemical Formula: C<sub>17</sub>H<sub>14</sub>Cl<sub>2</sub>O<sub>3</sub>

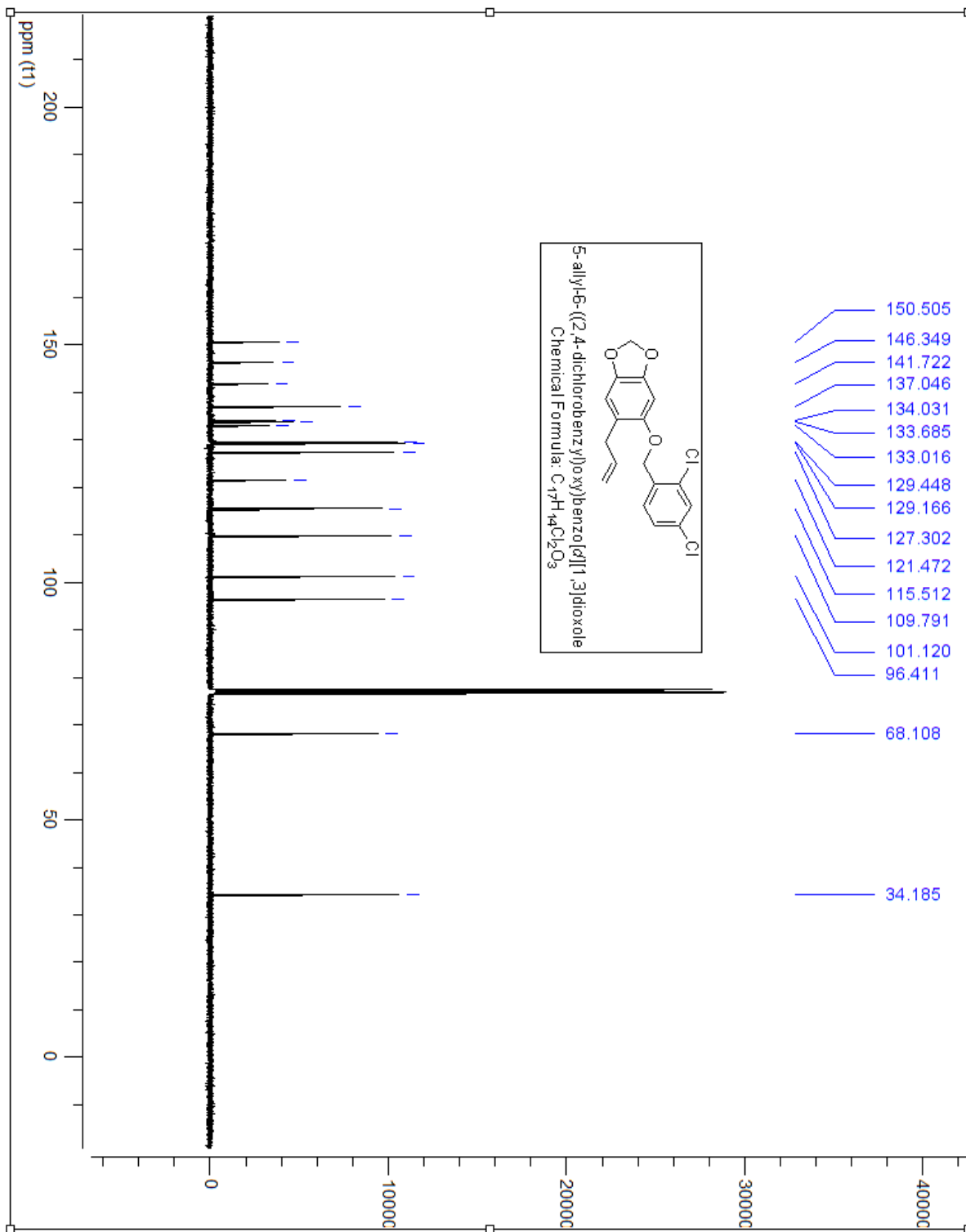
Molecular Weight: 337.20

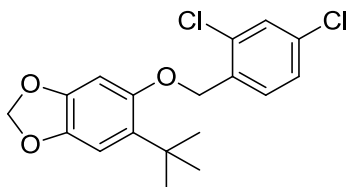
## 89

This compound was prepared using **21b** (0.2 g, 1.12 mmol), in 15 ml of Acetone, potassium carbonate (0.613 g, 4.44 mmol) was added and stirred for 10 minutes before the addition of 2,4 dichloro benzyl chloride (1.15ml, 1.11mmol) and refluxed for 6 hours. The reaction mixture was extracted with EtOAc and water. The phenol was washed with 10% NaOH. The crude product was purified via gradient column chromatography (2.5% EtOAc in hexanes) resulting as a white solid (195mg, Rf= 0.80 in 2:8 EtOAc:Hexanes).

<sup>1</sup>H NMR (400 MHz, CDCl<sub>3</sub>) δ ppm 7.48-7.46 (d, J=8.35, 1H), 7.39(d, J=2.05, 1H), 7.27-7.26(m, 1H), 6.65(s, 1H), 6.52(s, 1H), 5.88(m, 3H), 5.03-4.99(m, 4H), 3.34-3.32(dt, J=6.51, 6.51, 6.51 Hz, 2H)

<sup>13</sup>C NMR (100MHz, CDCl<sub>3</sub>) δ ppm 150.51, 146.34, 141.72, 137.04, 134.03, 133.68, 133.01, 129.44, 129.16, 127.30, 121.47, 115.51, 109.79, 101.12, 96.41, 68.10, 34.18





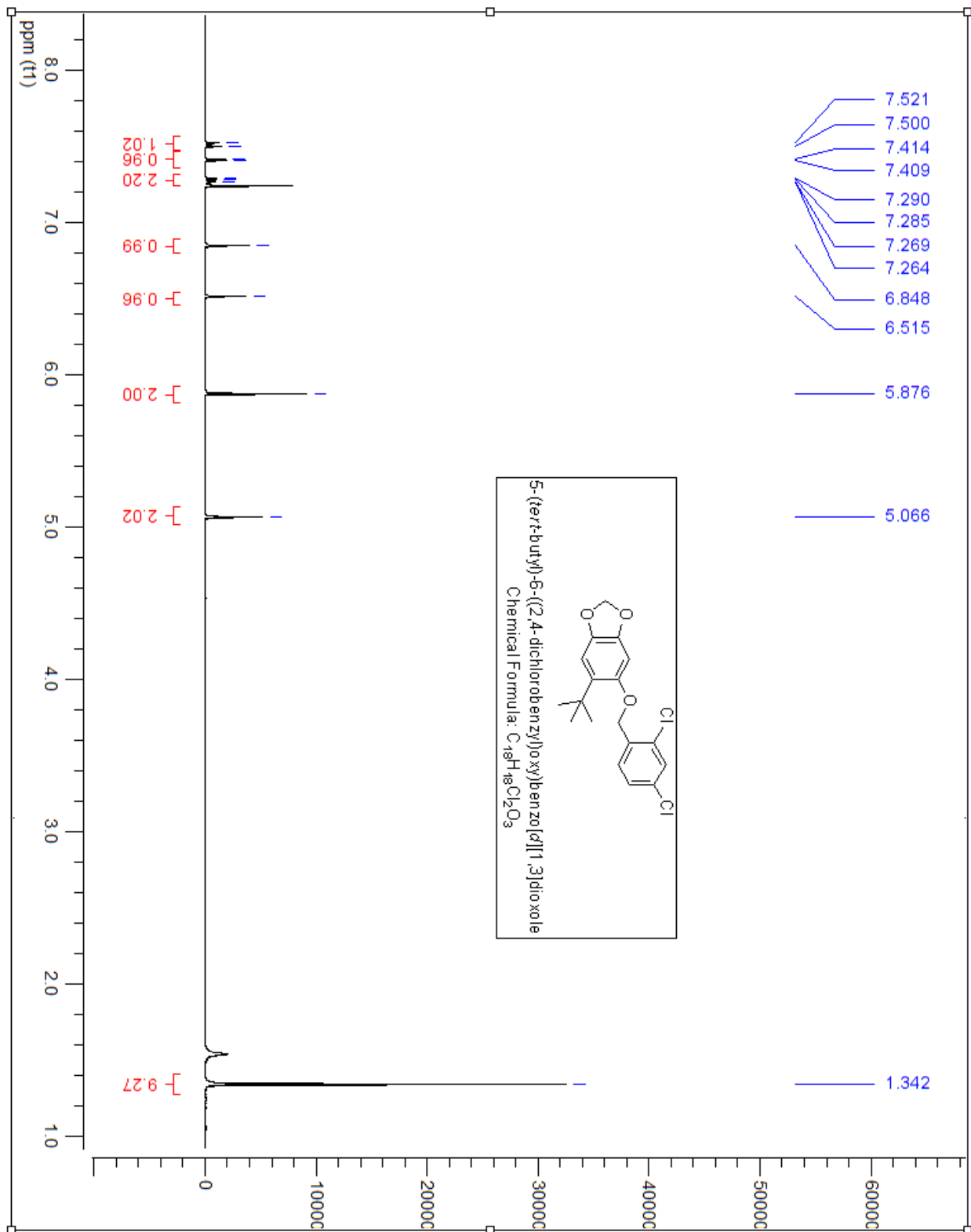
Chemical Formula:  $C_{18}H_{18}Cl_2O_3$   
Molecular Weight: 353.24

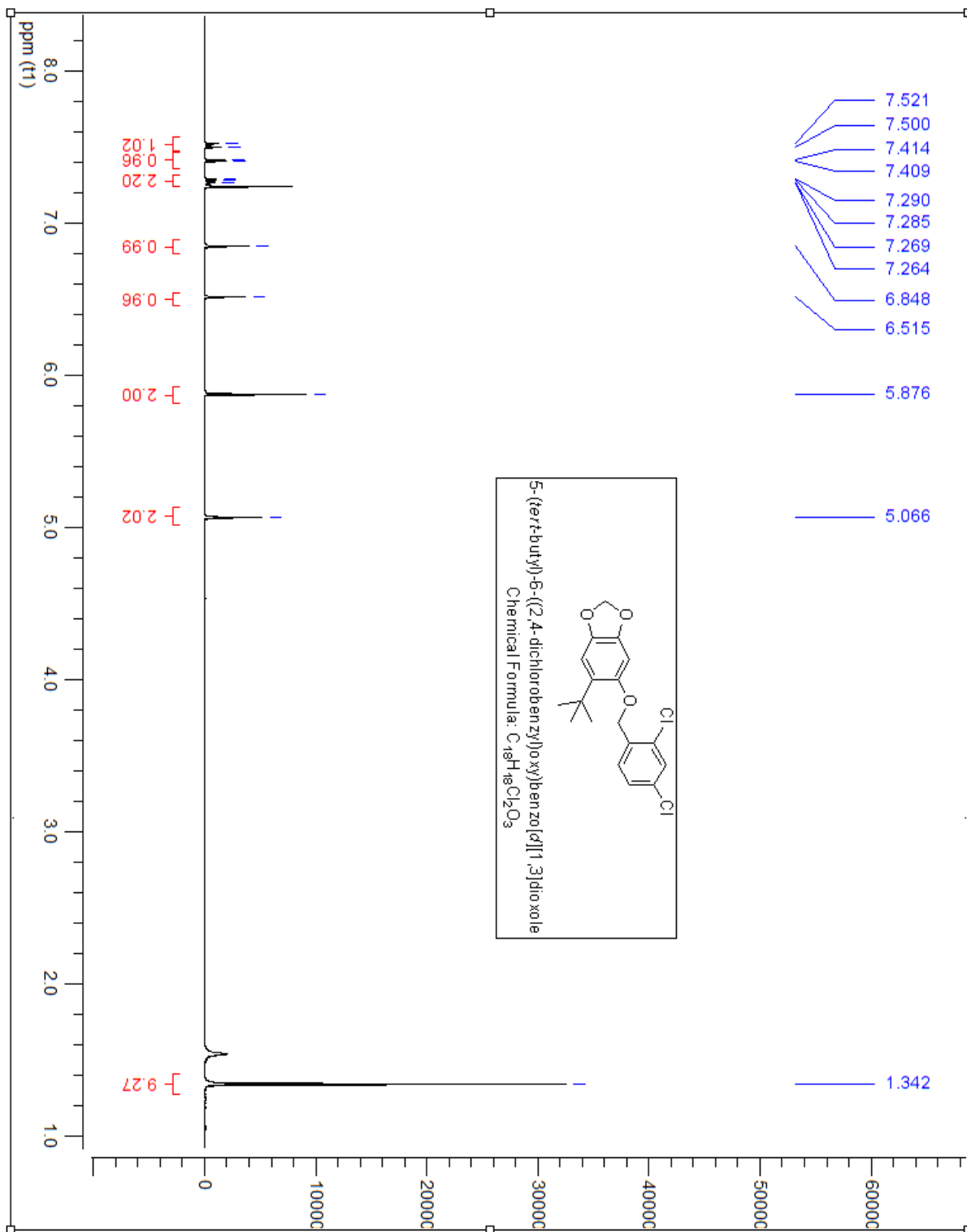
## 90

This compound was prepared using *t*-butyl allylated sesamol (0.2 g, 1.02 mmol), in 10 ml of ethanol, sodium hydroxide (0.082 g, 2.05 mmol) was added and stirred for 10 minutes before the addition of 2,4 dichloro benzyl chloride (0.14ml, 1.02mmol) and refluxed for 6 hours. The reaction mixture was extracted with EtOAc and water. The phenol was washed with 10% NaOH. The crude product was purified via gradient column chromatography (2.5% EtOAc in hexanes) resulting as a white solid (169mg, Rf= 0.80 in 2:8 EtOAc:Hexanes).

$^1H$  NMR (400 MHz,  $CDCl_3$ )  $\delta$  ppm 7.52-7.50(d, J=8.34Hz, 1H), 7.41-7.41(d, J=2.07 Hz, 1H), 7.29-7.26(m, 1H), 6.84(s, 1H), 6.51(s, 1H), 5.87(s, 2H), 5.06(s, 2H), 1.34(s, 9H)

$^{13}C$  NMR (100MHz,  $CDCl_3$ )  $\delta$  ppm 151.97, 145.73, 141.29, 134.03, 133.76, 132.94, 131.36, 129.50, 129.24, 127.37, 107.18, 101.13, 96.68, 68.21, 34.76, 30.13





## APPENDIX B. Copies of NMR spectra of Z02 Analogs.

### Experimental Section

#### *Reactions*

All reactions were monitored by TLC using aluminum backed TLC plates (EMD Chemicals, TLC Silica Gel 60 F<sub>254</sub>), which were visualized by UV lamp (254 nm – fixed wavelength). Plates were then permanently stained with Hannessian's stain. All moisture sensitive reactions were carried out under nitrogen or argon atmosphere. Anhydrous THF was prepared by distillation from sodium and benzophenone and DCM from calcium hydride.

#### *Purification*

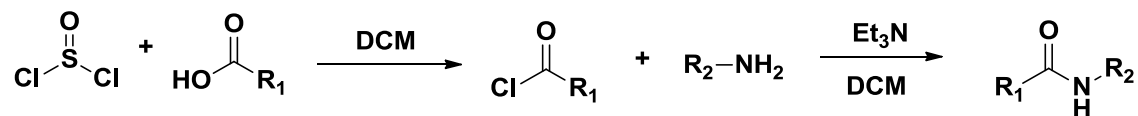
Purification by column chromatography was performed using SiliCycle SiliFlash® F60 silica gel of 230-400 mesh and glass columns fitted with a cotton piece and sand or fritted glass filter. Elutions were carried out with mixtures of hexanes and ethyl acetate.

#### *NMR*

<sup>1</sup>H NMR and <sup>13</sup>C NMR were recorded on Bruker Avance 400 spectrometer. Samples were dissolved in deuterated chloroform, methanol or acetone as indicated. All chemical shifts are reported in parts per million (ppm) and are referenced accordingly to the deuterated solvent used. Integrations are listed in parentheses along with coupling constants which are reported in Hz, where applicable.

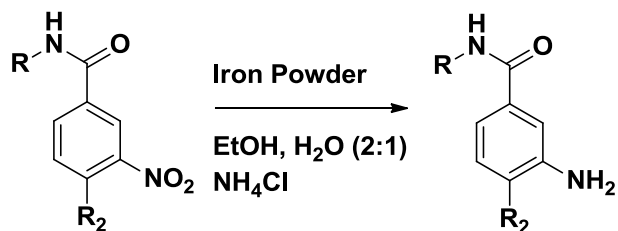
## General Procedures

### General Procedure 1: Amide Synthesis



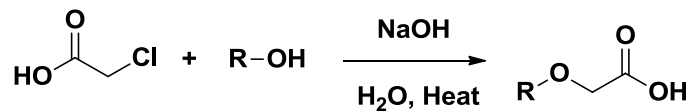
In a round bottom flask equipped with a magnetic stirrer, selected aryloxyacetic acid (1 equiv.) was dissolved in DCM. Thionyl chloride (3 equiv.) was then added to the mixture and was refluxed under nitrogen atmosphere. The mixture was then refluxed for approximately 1 hour. In a different round bottom flask equipped with a magnetic stirrer, the selected amine (1.1 equiv.) was dissolved in DCM and left to stir. Triethyl amine (4 equiv.) was then added and the reaction was placed in an ice bath. After stirring for 10 minutes the corresponding acyl chloride (1 equiv.) was added slowly, dropwise. The solution was left to stir for approximately 1 hour, or until deemed complete by TLC analysis. Workup of the reaction involved quenching with distilled water followed by base (5% NaOH) and acid (5% HCl) washes for extraction of product from starting materials. The combined organic extracts were dried (MgSO<sub>4</sub>), filtered and concentrated in vacuo. The product was purified either by recrystallization or by column chromatography and the final compound was analyzed by NMR.

## General Procedure #2: Nitro Group Reduction



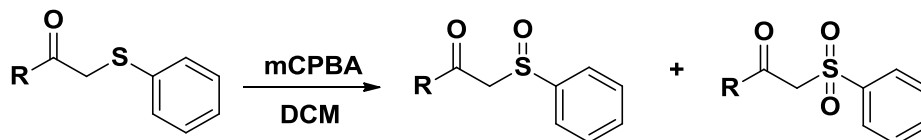
In a round bottom flask, selected nitro-group compound (1 equiv.) was dissolved in a 2:1 mixture of ethanol (EtOH) and H<sub>2</sub>O. Iron powder (5.5 equiv.) and ammonium chloride (NH<sub>4</sub>Cl) (0.58 equiv.) were added. The mixture was refluxed for approximately 1 hour. Once deemed complete by TLC analysis, the mixture was filtered through celite and extracted with DCM. The solution was dried with MgSO<sub>4</sub> which was then filtered off. The resulting solution was concentrated *in vacuo* and the product was purified either by recrystallization (ethyl acetate and hexanes) or column chromatography. The purified compound was analyzed by NMR.

### General Procedure #3: Chloroacetic Acid Coupling:

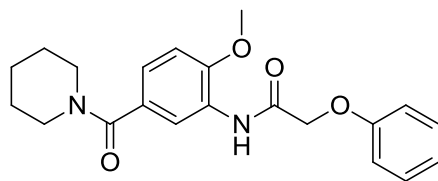


In a round bottom flask equipped with a magnetic stirrer, selected alcohol (1.1 equiv.) was dissolved in dH<sub>2</sub>O with chloroacetic acid (1 equiv.). Solid NaOH (3 equiv.) was then added to the flask and the reaction was brought to reflux. Once the reaction was deemed complete by TLC analysis, the mixture was cooled to room temperature and carefully acidified with concentrated HCl. The product was filtered off from the solvent and purified by recrystallization (Ethyl Acetate and Hexanes). The product was then characterize by NMR analysis.

#### General Procedure #4: Sulfide Oxidation:



In a round bottom flask equipped with a magnetic stirrer, selected sulfide (1 equiv.) was dissolved in approximately 8 mL of DCM and left to stir for a couple minutes. mCPBA (2 equiv.) was then added and the reaction was left to stir until deemed complete by TLC analysis. Once complete, the products were extracted with 5% NaOH. The organic extracts were combined, dried (MgSO<sub>4</sub>), filtered and evaporated in vacuo. The products were separated by column chromatography using a gradient solvent system of ethyl acetate and hexanes. Each product was analyzed by NMR.

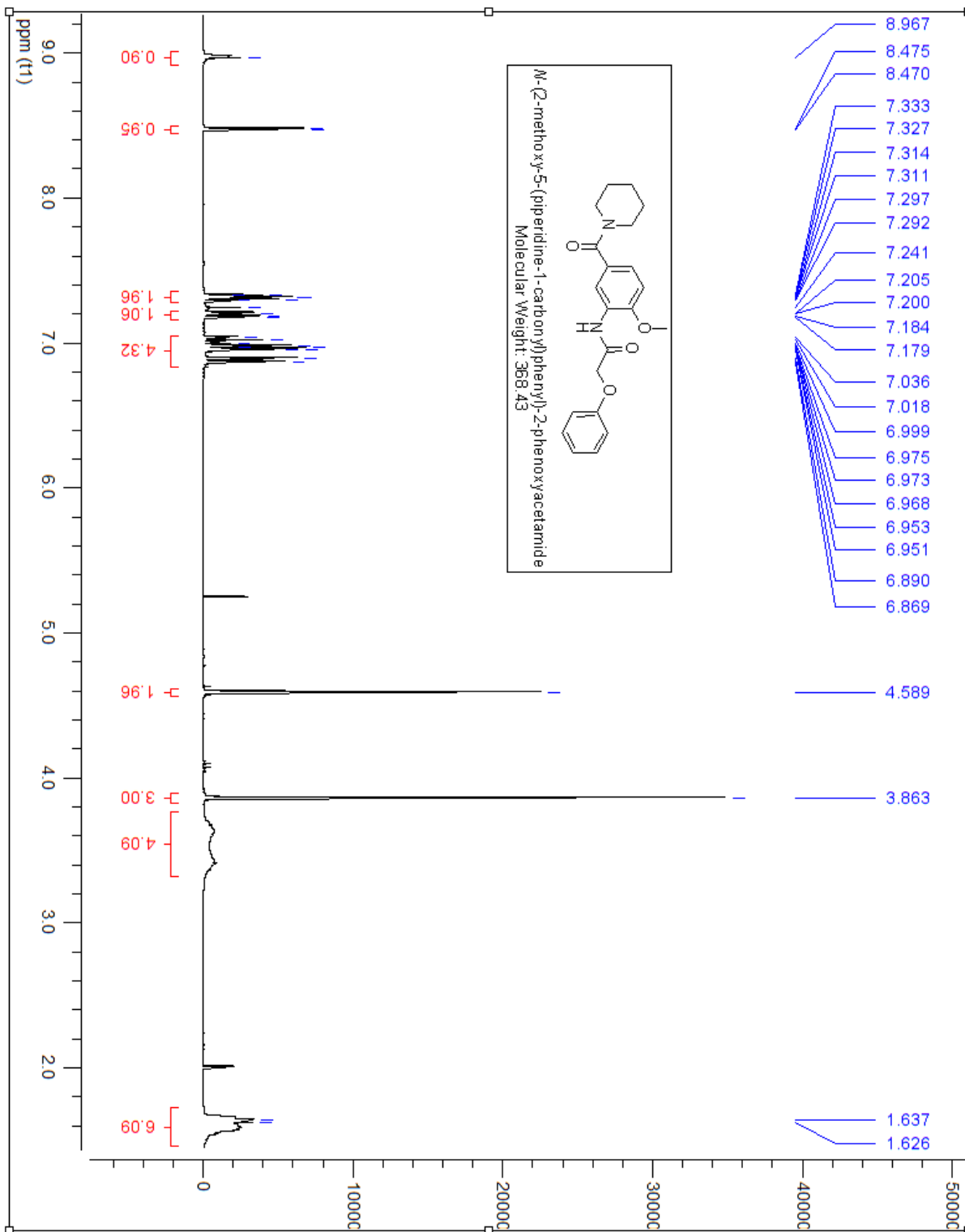


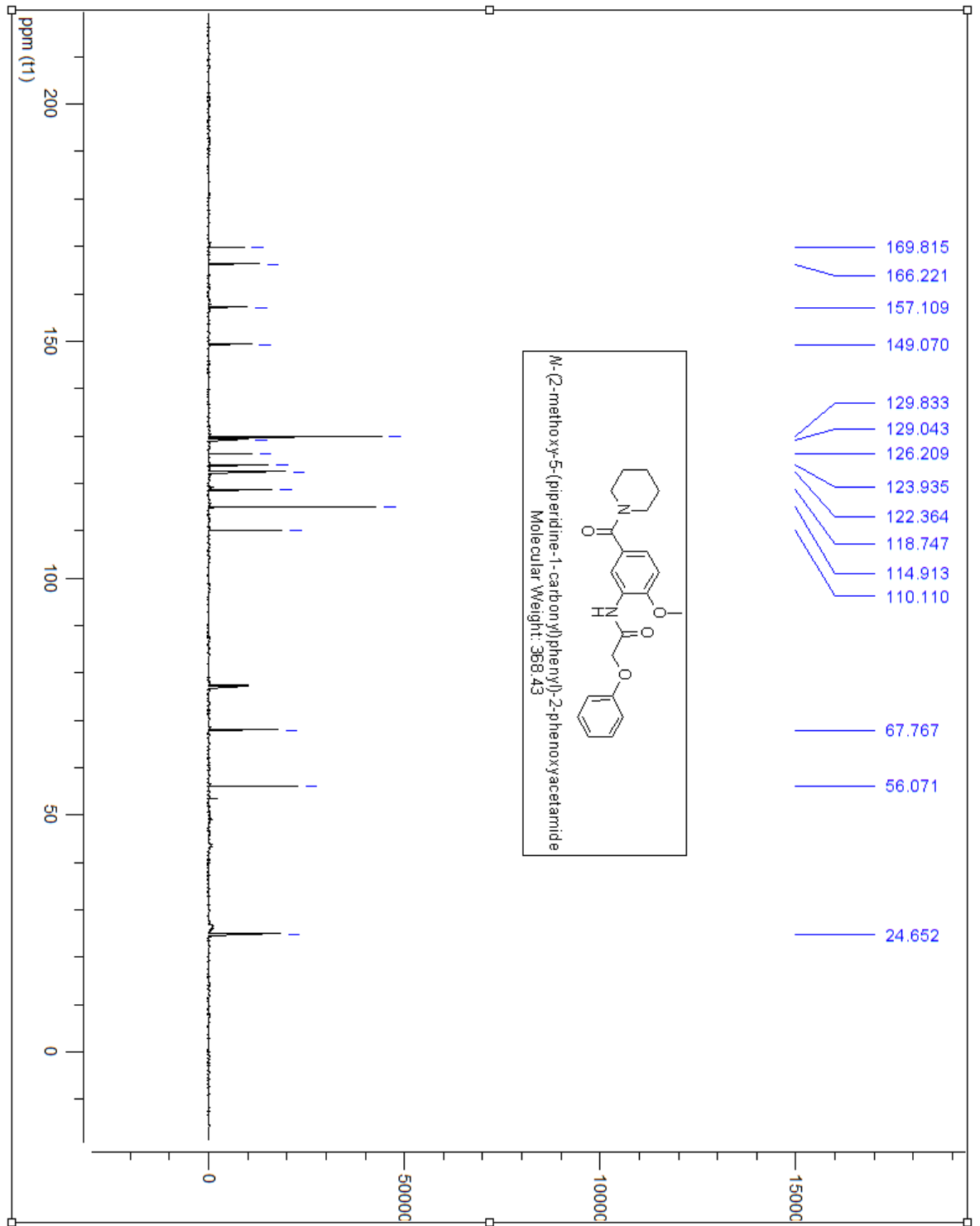
Chemical Formula:  $C_{21}H_{24}N_2O_4$   
Molecular Weight: 368.43

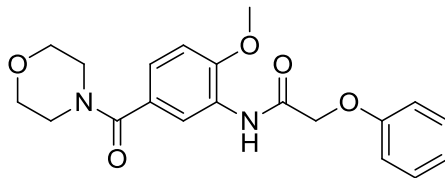
3-amino-4-methoxyphenyl)(piperidin-1-yl)methanone (0.3g, 1.28mmol) was added to DCM (10ml) followed by the addition of triethylamine (0.39ml, 3.8mmol) in a round bottom flask. Phenoxyacetyl chloride (0.18ml, 1.2mmol) was added to the reaction flask and allowed to stir at room temperature for 1 hour.  $NaHCO_3$  was added to quench the reaction followed by extraction with DCM (20ml x 3 times). The organic layers were collected and dried using  $MgSO_4$ . The mixture was filtered and concentrated in *vacuo*. The product was purified through column chromatography to form yellow oil (101mg, 21%)

$^1H$  NMR (400MHz,  $CDCl_3$ )  $\delta$  ppm 8.47 (d, 1H), 7.33-7.29 (m, 2H), 7.24-7.20 (m, 1H), 7.18-6.95 (m, 3H), 6.89-6.86 (d, 1H), 4.59 (s, 2H), 3.86 (s, 3H), 3.67-3.36 (m, 4H), 1.63-1.58 (m, 6H)

$^{13}C$  NMR (400MHz,  $CDCl_3$ )  $\delta$  ppm 170.783, 169.815, 166.221, 157.728, 157.109, 149.070, 129.833, 129.043, 126.209, 123.935, 122.364, 121.171, 118.747, 114.913, 110.110, 67.767, 56.071, 53.483, 24.652





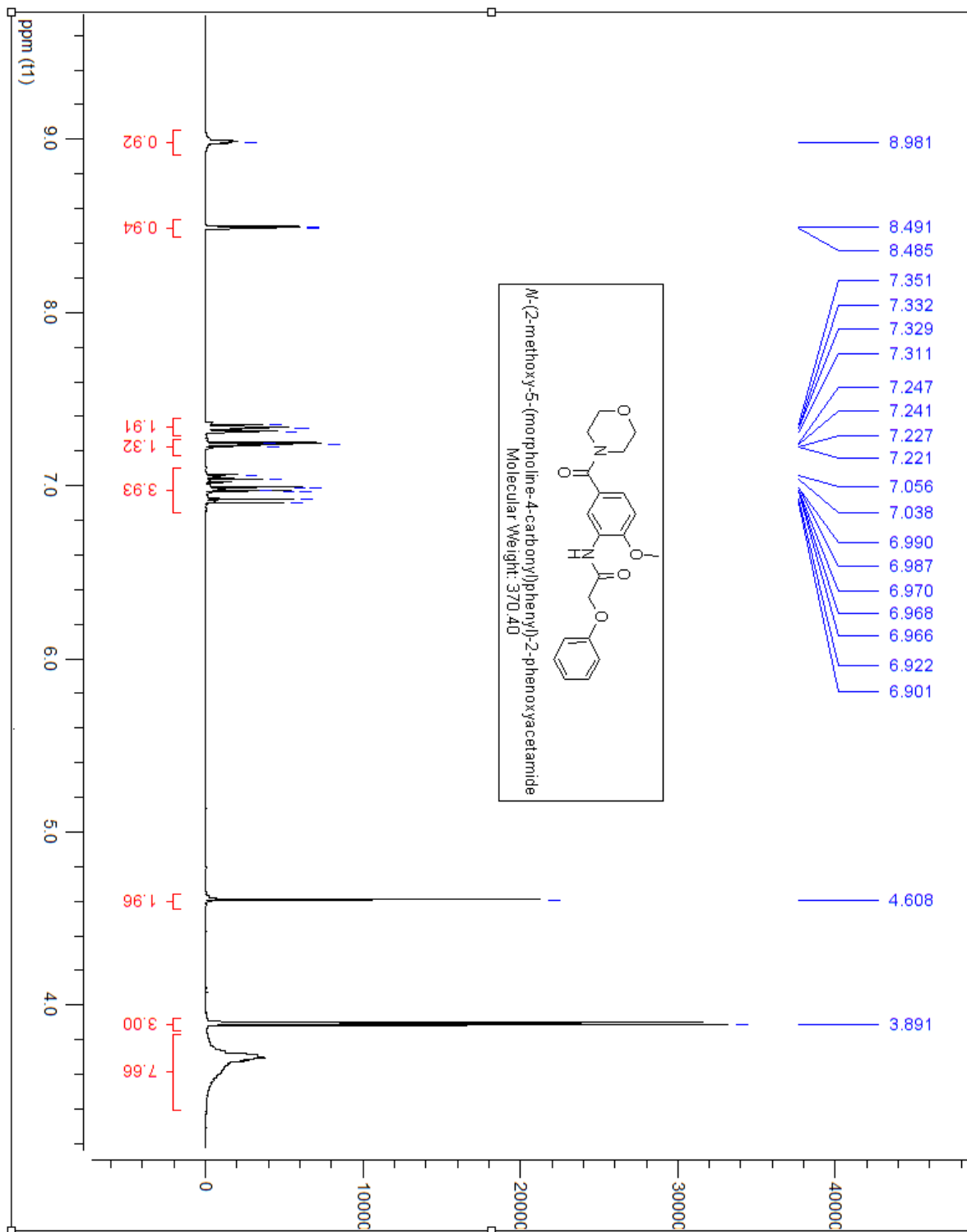


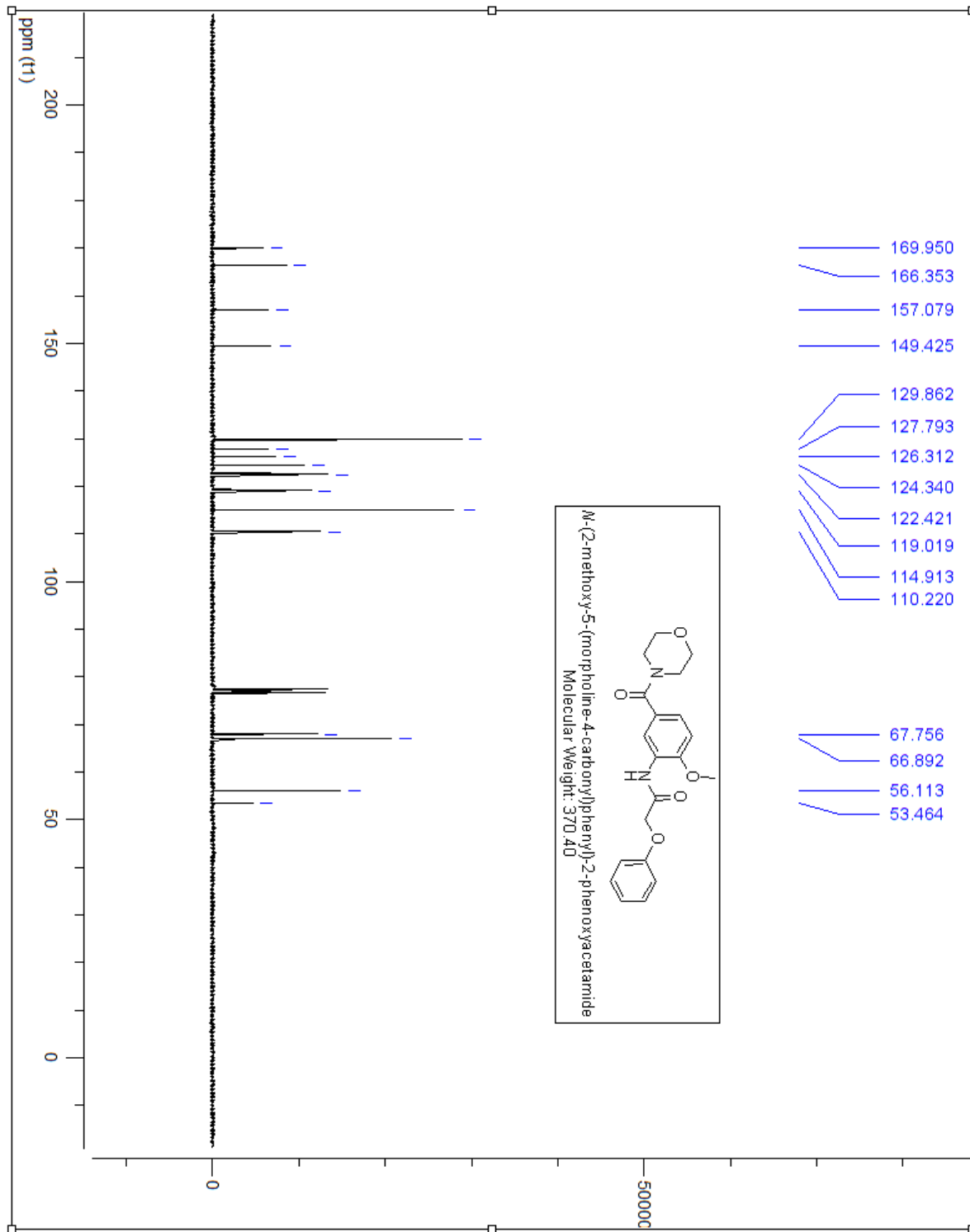
Chemical Formula:  $C_{20}H_{22}N_2O_5$   
Molecular Weight: 370.40

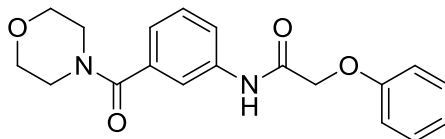
(3-amino-4-methoxyphenyl)(morpholino)methanone (0.15g, 0.73mmol) was added to DCM (10ml) followed by the addition of triethylamine (0.41ml, 2.91mmol) in a round bottom flask. Phenoxyacetyl chloride (0.1ml, 0.65mmol) was added to the reaction flask and allowed to stir at room temperature for 1 hour.  $NaHCO_3$  was added to quench the reaction followed by extraction with DCM (20ml x 3 times). The organic layers were collected and dried using  $MgSO_4$ . The mixture was filtered and concentrated in *vacuo*. The product was purified through column chromatography to form yellow crystals (112mg, 42%)

$^1H$  NMR (400MHz,  $CDCl_3$ )  $\delta$  ppm 8.98 (s, 1H), 8.49-8.48 (s, 1H), 7.35-7.31 (m, 2H), 7.24-7.22 (m, 1H), 7.05-6.90 (m, 4H), 4.61 (s, 2H), 3.89 (s, 3H), 3.69 (s, 8H)

$^{13}C$  NMR (400MHz,  $CDCl_3$ )  $\delta$  ppm 169.950, 166.353, 157.079, 149.425, 129.862, 127.793, 126.312, 124.340, 122.421, 119.019, 114.913, 110.220, 67.756, 66.892, 56.113, 53.464







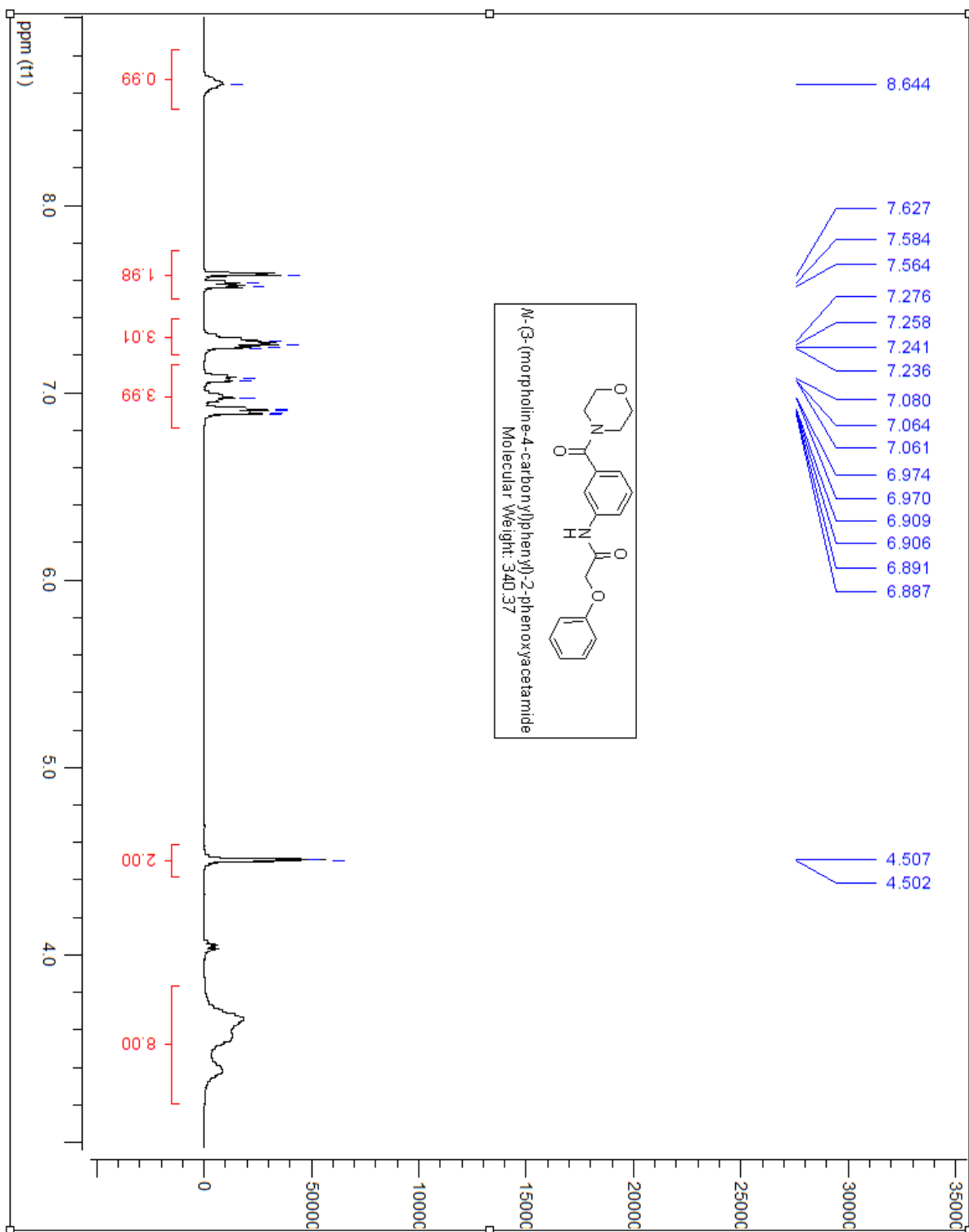
Chemical Formula:  $C_{19}H_{20}N_2O_4$

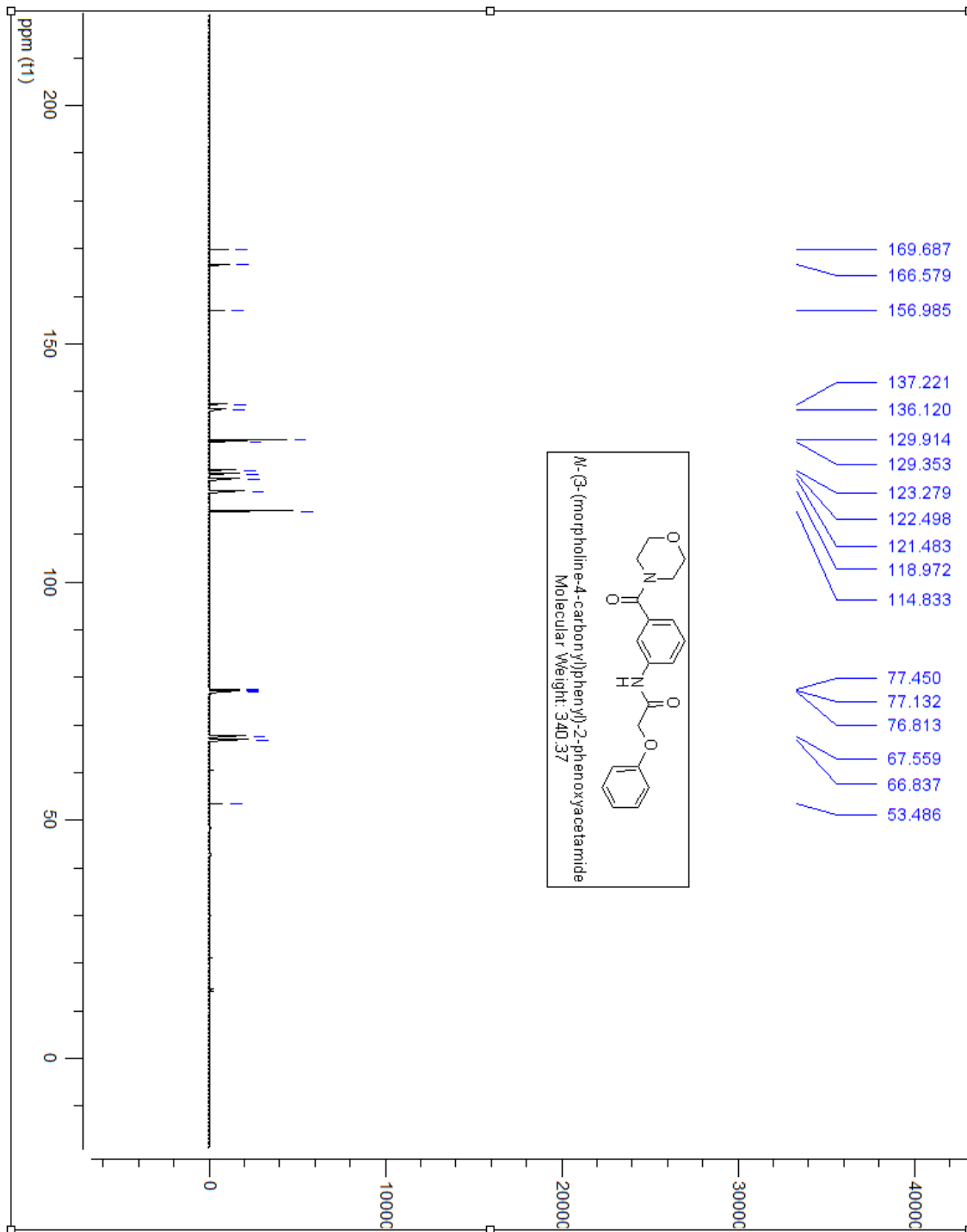
Molecular Weight: 340.37

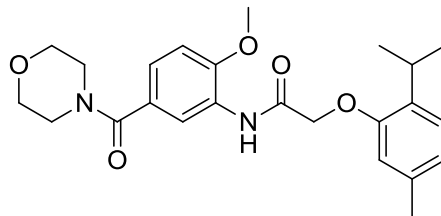
(3-aminophenyl)(morpholino)methanone (0.25g, 1.21mmol) was added to DCM (10ml) followed by the addition of triethylamine (0.61ml, 4.36mmol) in a round bottom flask. Phenoxyacetyl chloride (0.15ml, 1.09mmol) was added to the reaction flask and allowed to stir at room temperature for 1 hour.  $NaHCO_3$  was added to quench the reaction followed by extraction with DCM (20ml x 3 times). The organic layers were collected and dried using  $MgSO_4$ . The mixture was filtered and concentrated in *vacuo*. The product was purified through column chromatography to form yellow crystals (145mg, 35%)

$^1H$  NMR (400MHz,  $CDCl_3$ )  $\delta$  ppm 7.62 (s, 1H), 7.58-7.56 (d, 2H), 7.29-7.25 (t, 3H), 7.24-7.23 (d, 1H), 7.08-6.95 (m, 1H), 6.91-6.88 (dd, 2H), 4.51-4.50 (d, 2H), 3.65-3.37 (m, 8H)

$^{13}C$  NMR (400MHz,  $CDCl_3$ )  $\delta$  ppm 169.687, 166.579, 156.985, 137.221, 136.120, 129.914, 129.353, 123.279, 122.498, 121.483, 118.972, 114.833, 67.559, 66.837, 60.377, 53.486, 21.037, 14.199







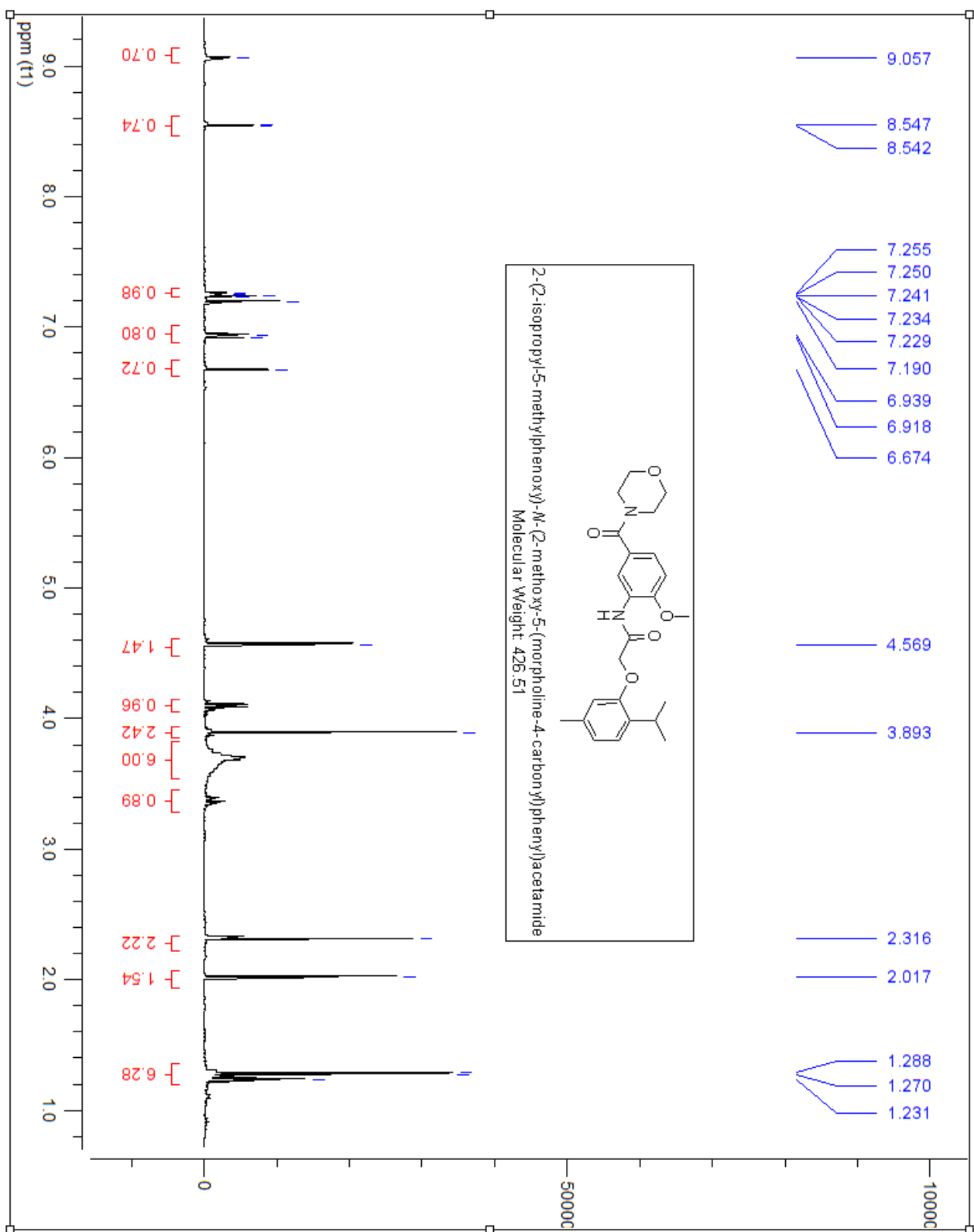
Chemical Formula:  $C_{24}H_{30}N_2O_5$

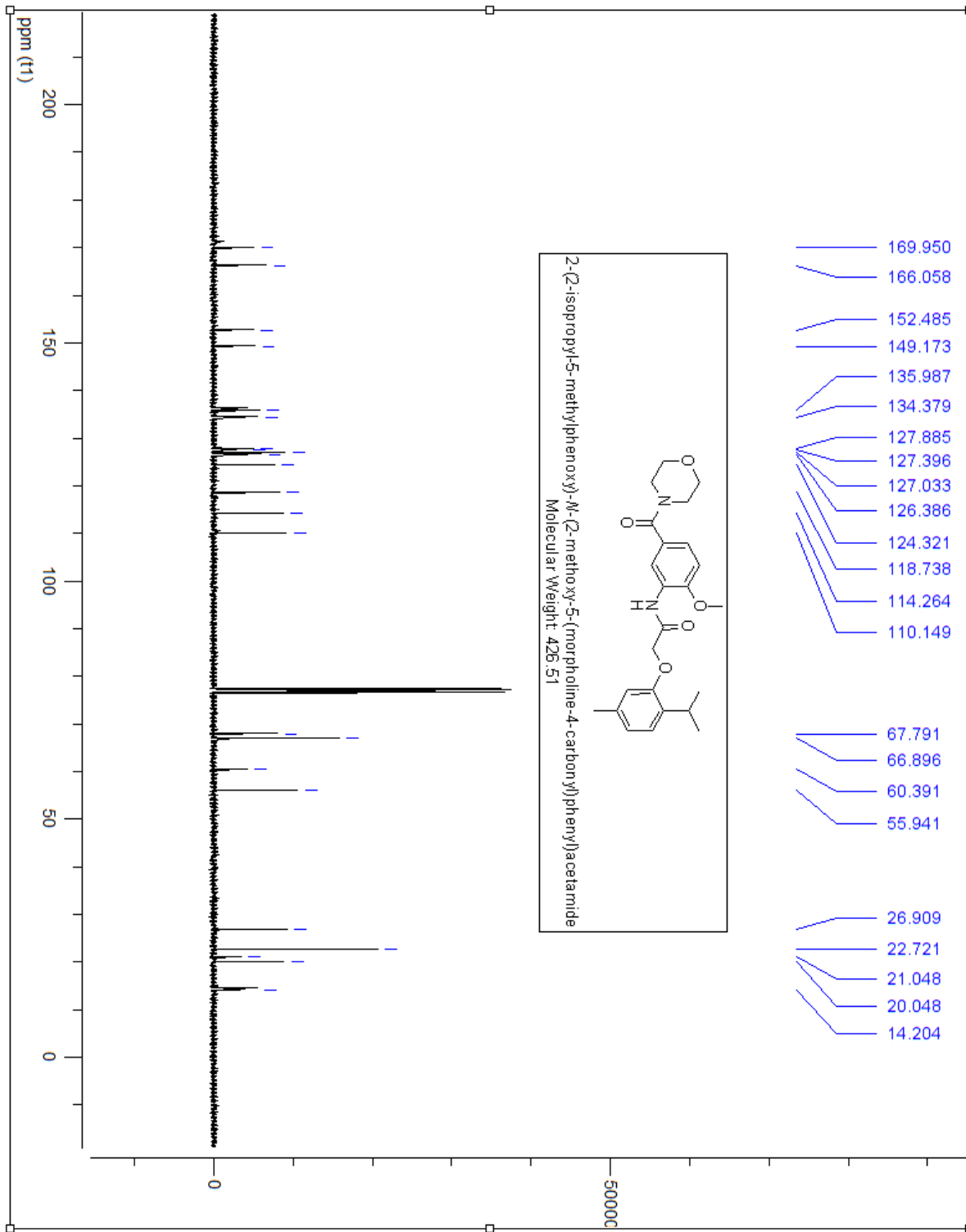
Molecular Weight: 426.51

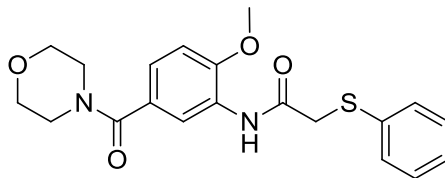
2-isopropyl-5-methylphenyl hydrogen carbonate (0.3g, 1.44mmol) was added to DCM (2ml) followed by the addition of thionyl chloride (4ml) in a round bottom flask. This solution was stirred for 4hrs, and then evaporated. The evaporated flask was then diluted with 4ml of DCM and then added to a solution of (3-amino-4-methoxyphenyl)(morpholino)methanone (0.3g, 1.45mmol) and in DCM (10ml) and triethylamine (0.8ml, 5.81mmol).  $NaHCO_3$  was added to quench the reaction followed by extraction with DCM (20ml x 3 times). The organic layers were collected and dried using  $MgSO_4$ . The mixture was filtered and concentrated in *vacuo*. The product was purified through column chromatography to form yellow oil (89mg, 14%)

$^1H$  NMR (400MHz,  $CDCl_3$ )  $\delta$  ppm 8.52 (s, 1H), 7.74-7.73 (s, 1H), 7.63-7.61 (d, 1H), 7.34-7.23 (m, 4H), 7.02-7.01 (t, 1H), 6.99-6.92(d, 2H), 4.56 (s, 2H), 3.60-3.566 (t, 2H), 3.42-3.39 (t, 2H), 1.99 (s, 1H), 1.92-1.87 (m, 4H), 1.23-1.19 (t, 1H)

$^{13}C$  NMR (400MHz,  $CDCl_3$ )  $\delta$  ppm 168.960, 166.525, 157.024, 138.026, 136.948, 129.890, 129.053, 123.355, 122.432, 121.386, 118.985, 114.822, 67.556, 60.375, 49.598, 46.250, 26.383, 24.436, 21.039, 14.199





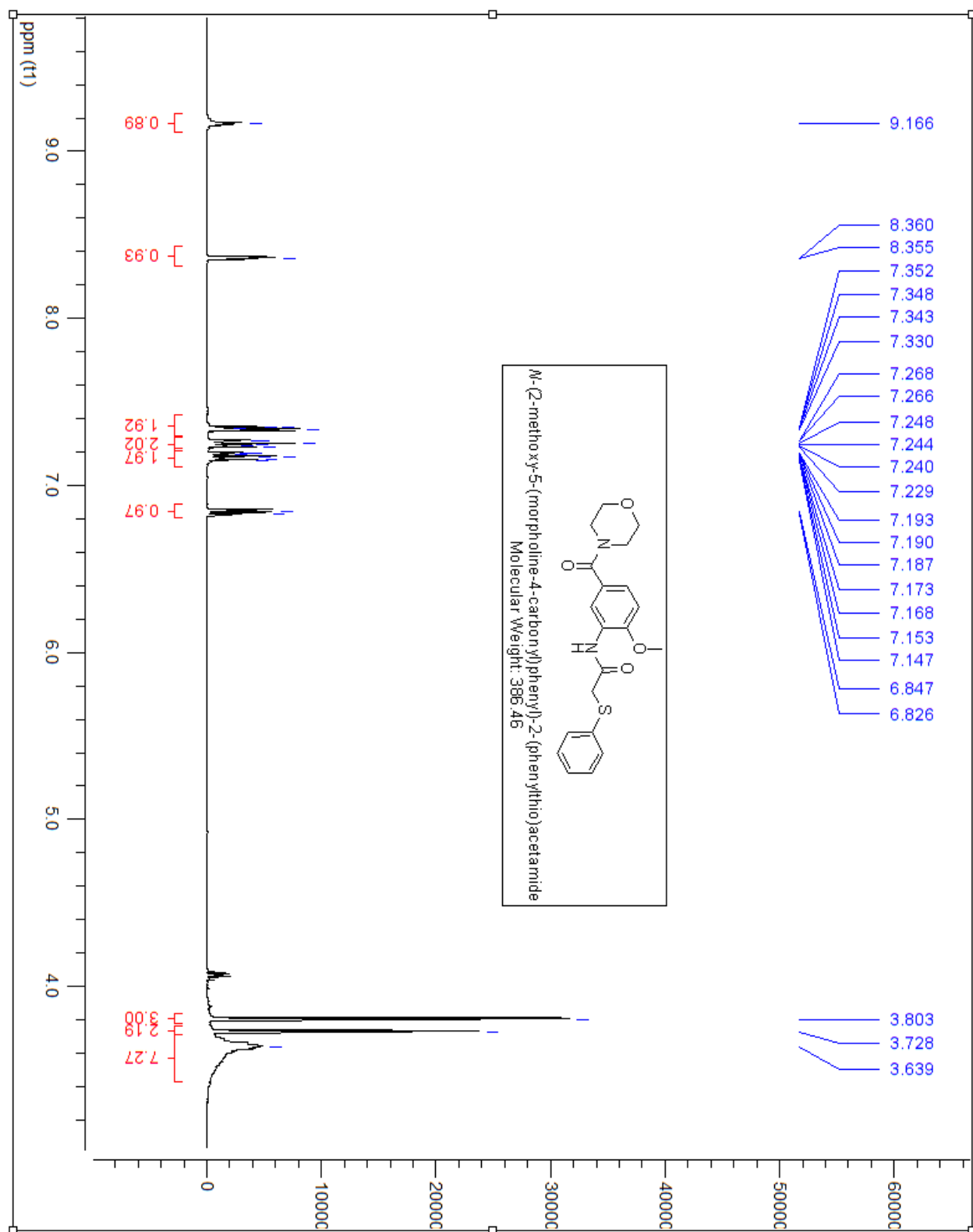


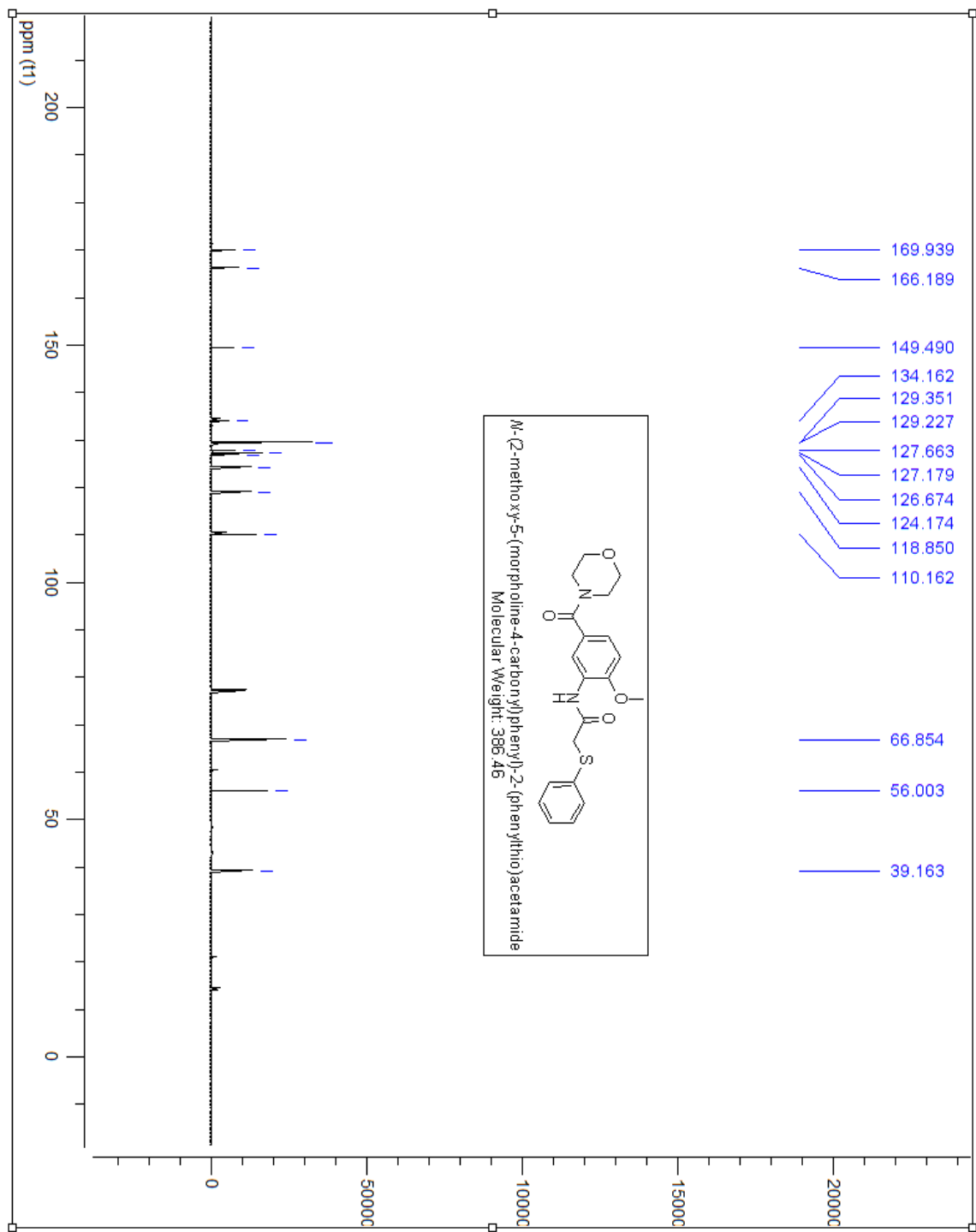
Chemical Formula: C<sub>20</sub>H<sub>22</sub>N<sub>2</sub>O<sub>4</sub>S  
Molecular Weight: 386.46

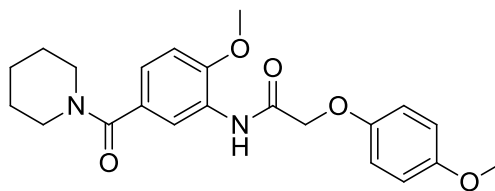
2-(phenylthio) acetic acid (0.3g, 1.44mmol) was added to DCM (2ml) followed by the addition of thionyl chloride (4ml) in a round bottom flask. This solution was stirred for 4hrs, and then evaporated. The evaporated flask was then diluted with 4ml of DCM and then added to a solution of (3-amino-4-methoxyphenyl)(morpholino)methanone (0.3g, 1.45mmol) and in DCM (10ml) and triethylamine (0.79ml, 5.64mmol). NaHCO<sub>3</sub> was added to quench the reaction followed by extraction with DCM (20ml x 3 times). The organic layers were collected and dried using MgSO<sub>4</sub>. The mixture was filtered and concentrated in *vacuo*. The product was purified through column chromatography to form brown oil (121mg, 22%)

<sup>1</sup>H NMR (400MHz, CDCl<sub>3</sub>) δ ppm 9.16 (s, 1H), 8.36 (s, 1H), 7.35-7.14 (m, 6H), 6.84-6.82 (d, 1H), 3.81 (s, 3H), 3.72 (s, 2H), 3.63 (s, 8H)

<sup>13</sup>C NMR (400MHz, CDCl<sub>3</sub>) δ ppm 169.939, 166.189, 149.490, 134.162, 129.351, 129.227, 127.663, 127.179, 126.674, 124.174, 118.850, 110.162, 66.854, 60.363, 56.003, 39.163, 39.163, 21.038, 14.203





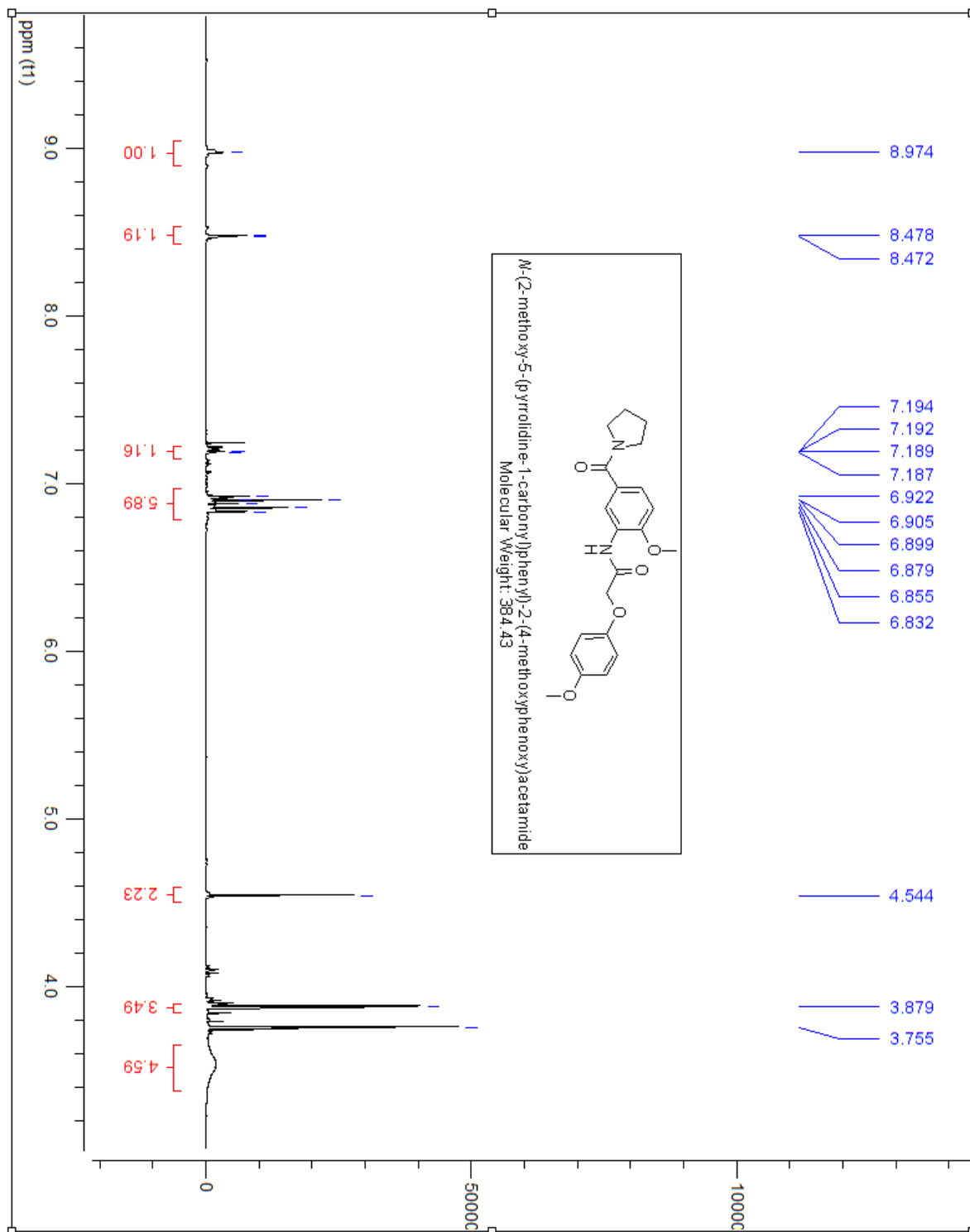


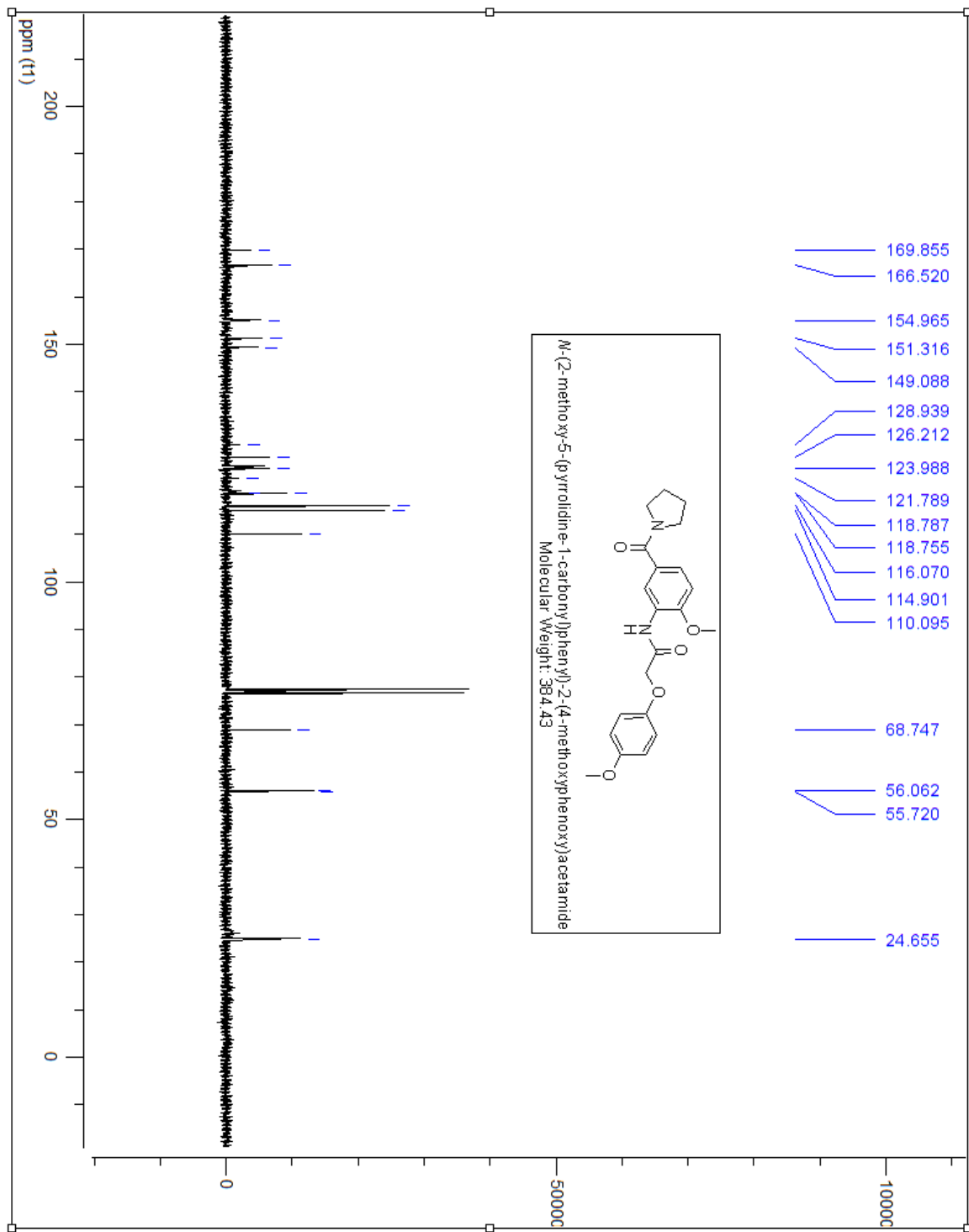
Chemical Formula: C<sub>22</sub>H<sub>26</sub>N<sub>2</sub>O<sub>5</sub>  
Molecular Weight: 398.45

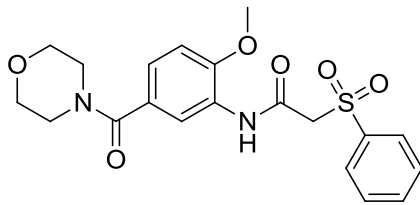
2-(4-methoxyphenoxy) acetic acid (0.3g, 1.44mmol) was added to DCM (2ml) followed by the addition of thionyl chloride (4ml) in a round bottom flask. This solution was stirred for 4hrs, and then evaporated. The evaporated flask was then diluted with 4ml of DCM and then added to a solution of 3-amino-4-methoxyphenyl(piperidin-1-yl)methanone (0.3g, 1.28mmol) and in DCM (10ml) and triethylamine (0.79ml, 5.64mmol). NaHCO<sub>3</sub> was added to quench the reaction followed by extraction with DCM (20ml x 3 times). The organic layers were collected and dried using MgSO<sub>4</sub>. The mixture was filtered and concentrated in *vacuo*. The product was purified through column chromatography to form white crystals (136mg, 12%)

<sup>1</sup>H NMR (400MHz, CDCl<sub>3</sub>) δ ppm 8.97 (s, 1H), 8.47 (s, 1H), 7.24-7.18 (m, 2H), 6.92-6.83 (m, 5H), 4.54 (s, 2H), 3.87 (s, 3H), 3.75 (s, 3H), 3.57-3.52 (s, 3H), 1.79 (s, 7H)

<sup>13</sup>C NMR (400MHz, CDCl<sub>3</sub>) δ ppm 169.855, 166.520, 154.965, 151.316, 149.088, 128.939, 126.212, 123.988, 121.789, 118.755, 116.070, 114.901, 110.095, 68.747, 56.062, 55.720, 26.045, 25.996, 25.964, 24.655





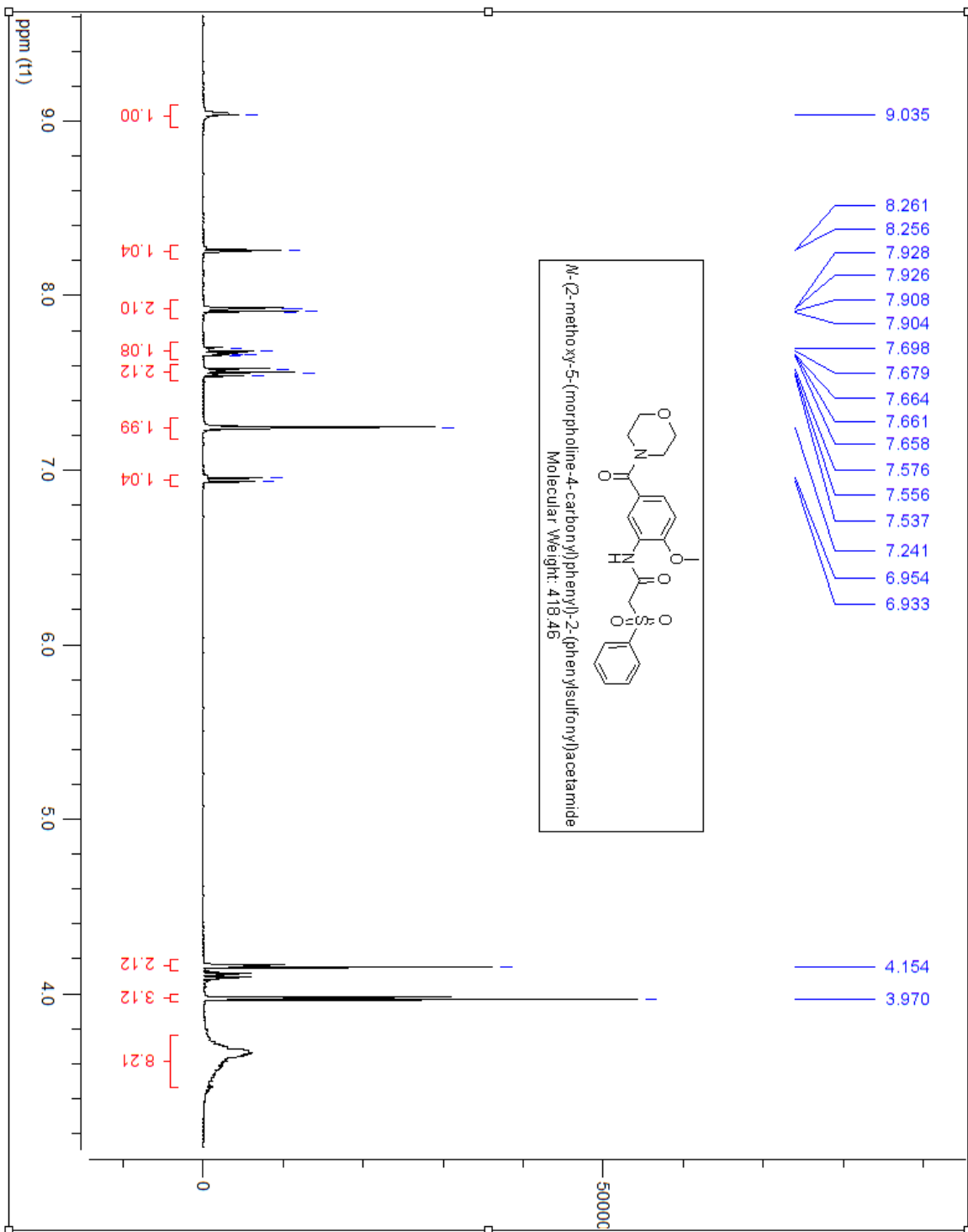


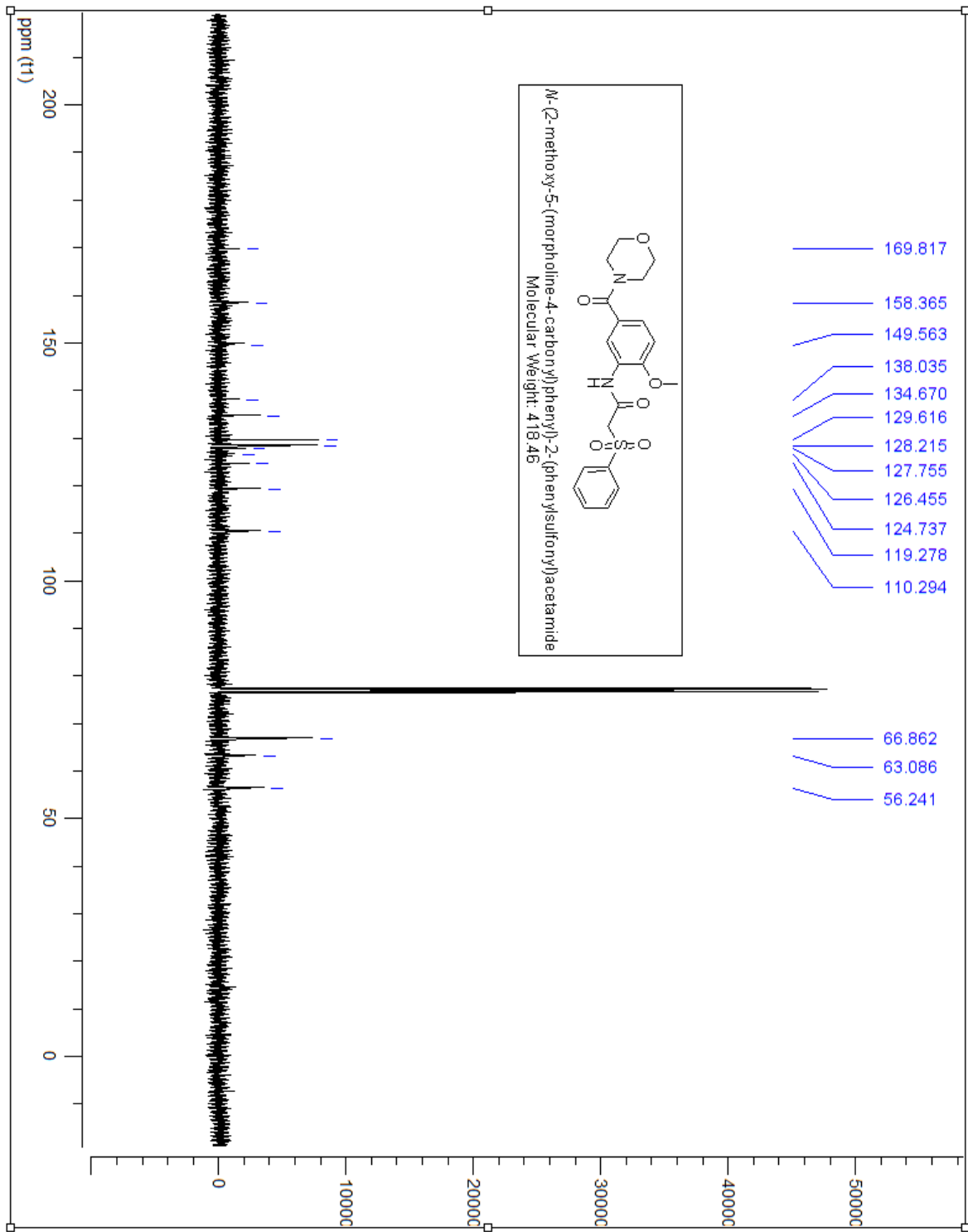
Chemical Formula: C<sub>20</sub>H<sub>22</sub>N<sub>2</sub>O<sub>6</sub>S  
Molecular Weight: 418.46

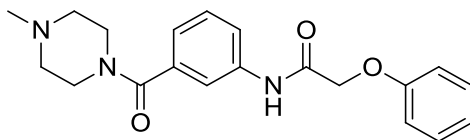
N-(2-methoxy-5-(morpholine-4-carbonyl)phenyl)-2-(phenylthio)acetamide (140mg, 0.362mmol) was dissolved in DCM (10ml). This mixture was cooled down to 0°C and MCPBA (63mg, 0.36mmol) was added slowly to the reaction vessel and allowed to stir for 3 hours. The reaction mixture was then diluted with DCM and quenched with NaHCO<sub>3</sub> (5ml). This reaction mixture was extracted with DCM (3X20ml). The organic phase was collected and combined, dried with MgSO<sub>4</sub>, filtered and concentrated in *vacuo*. The resulting mixture was purified by column chromatography to yield a beige solid (20mg, 14%)

<sup>1</sup>H NMR (400MHz, CDCl<sub>3</sub>) δ ppm 9.03 (s, 1H), 8.26 (s, 1H), 7.92-7.90 (d, 2H), 7.69-7.65 (m, 1H), 7.55-7.53 (m, 2H), 7.25-7.22 (m, 2H), 6.95-6.93 (d, 1H), 4.15 (s, 2H), 3.97 (s, 3H), 3.66-3.65 (s, 8H)

<sup>13</sup>C NMR (400MHz, CDCl<sub>3</sub>) δ ppm 169.82, 158.36, 149.56, 138.04, 134.67, 129.62, 128.22, 127.75, 126.45, 124.74, 119.28, 110.29, 66.86, 63.08, 56.24







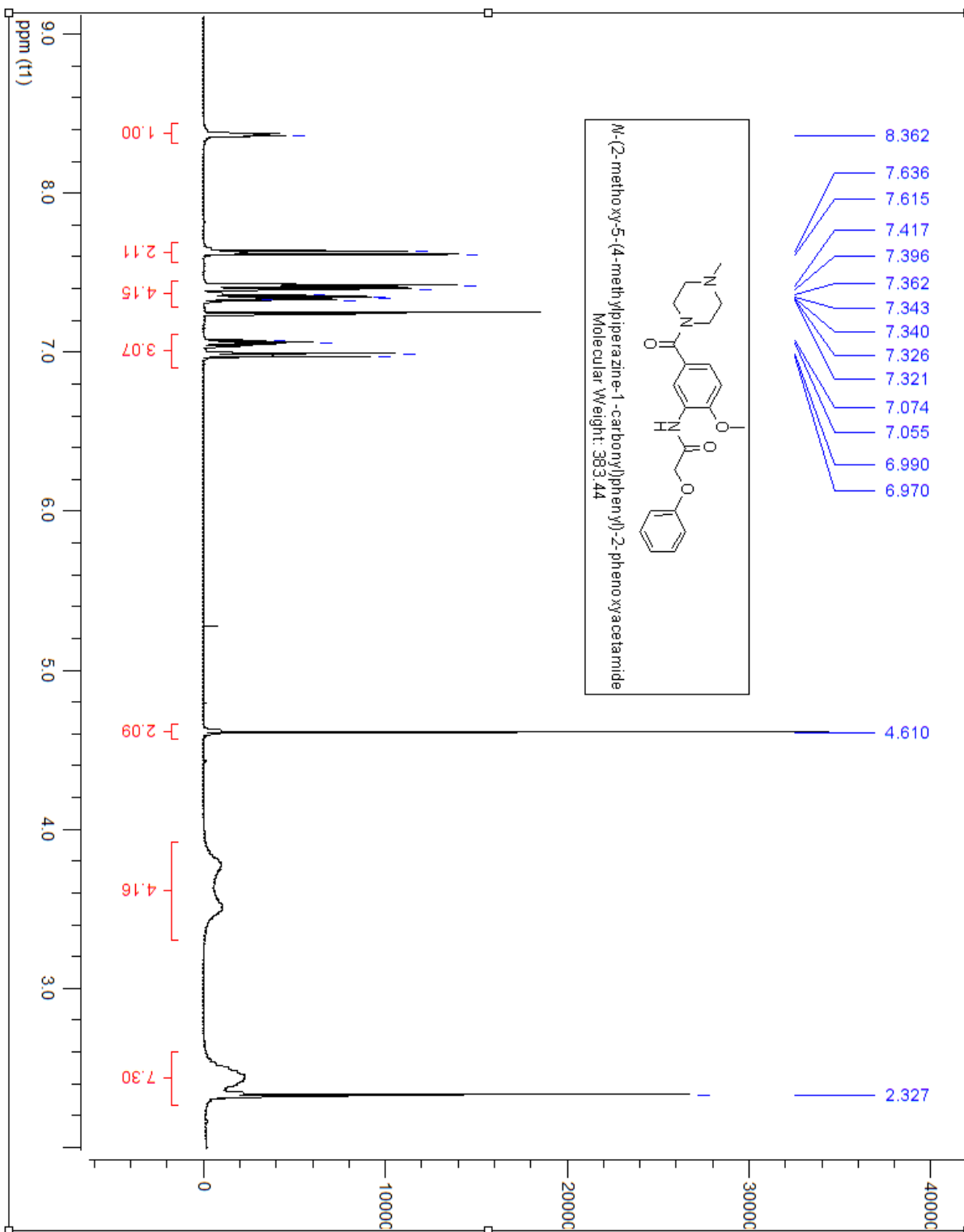
Chemical Formula:  $C_{20}H_{23}N_3O_3$

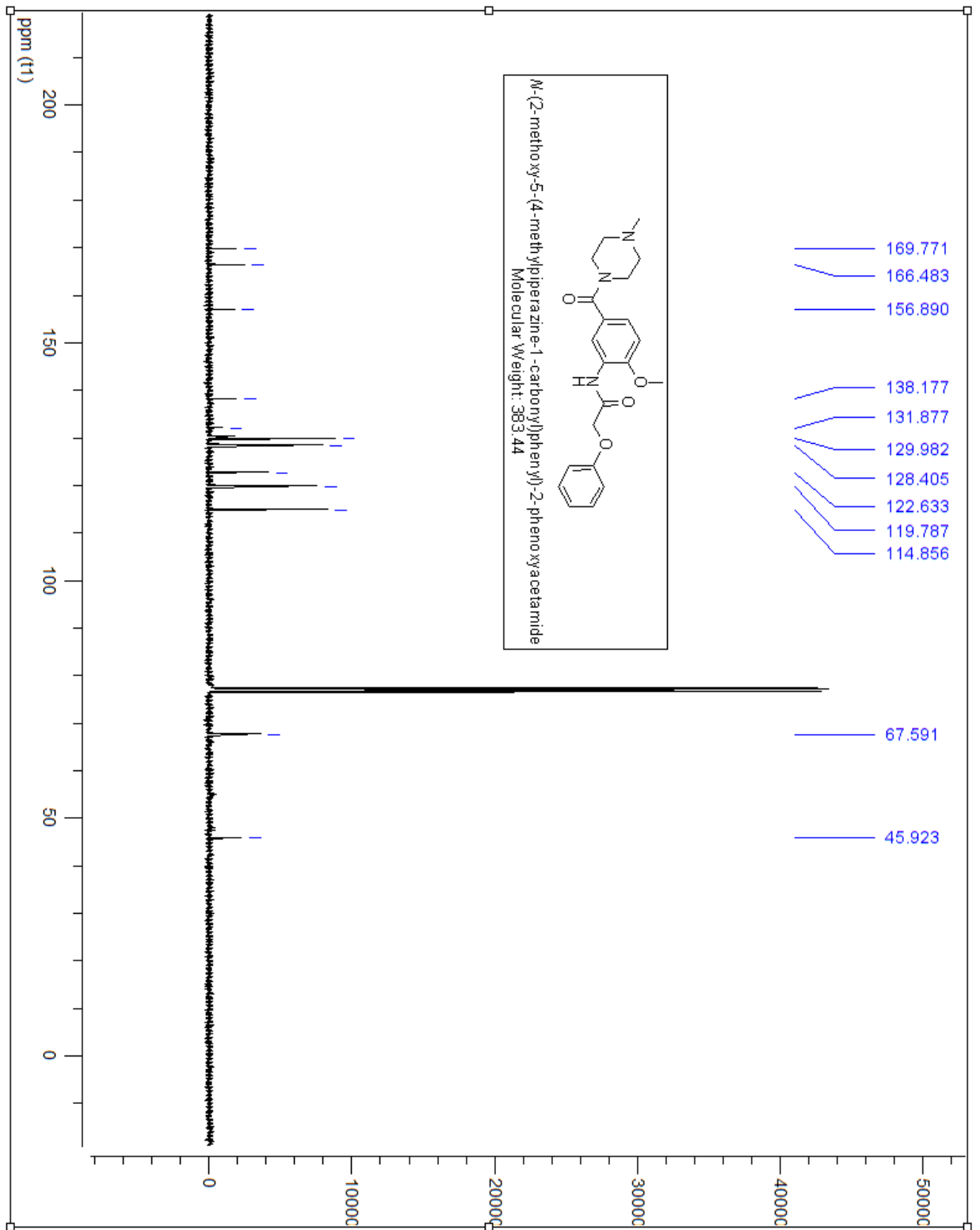
Molecular Weight: 353.41

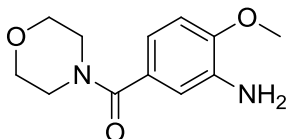
Amine (0.05g, 0.23mmol) was added to DCM (10ml) followed by the addition of triethylamine (0.13ml, 0.91mmol) in a round bottom flask. Phenoxyacetyl chloride (0.03ml, 0.21mmol) was added to the reaction flask and allowed to stir at room temperature for 1 hour.  $NaHCO_3$  was added to quench the reaction followed by extraction with DCM (20ml x 3 times). The organic layers were collected and dried using  $MgSO_4$ . The mixture was filtered and concentrated in *vacuo*. The product was purified through column chromatography to form brown oil (39mg, 49%)

$^1H$  NMR (400MHz,  $CDCl_3$ )  $\delta$  ppm 7.64-7.61 (m, 2H), 7.36-7.29 (m, 3H), 7.14-7.12 (d, 1H), 7.04-6.94 (m, 3H), 4.57 (s, 2H), 3.78-3.76 (m, 1H), 3.47 (s, 2H), 2.52-2.45 (m, 4H), 2.25 (s, 3H)

$^{13}C$  NMR (400MHz,  $CDCl_3$ )  $\delta$  ppm 169.588, 166.545, 156.939, 137.106, 136.389, 129.941, 129.363, 123.341, 122.551, 121.398, 118.877, 114.832, 67.548, 60.389, 53.433, 45.548, 29.695, 21.037, 14.194







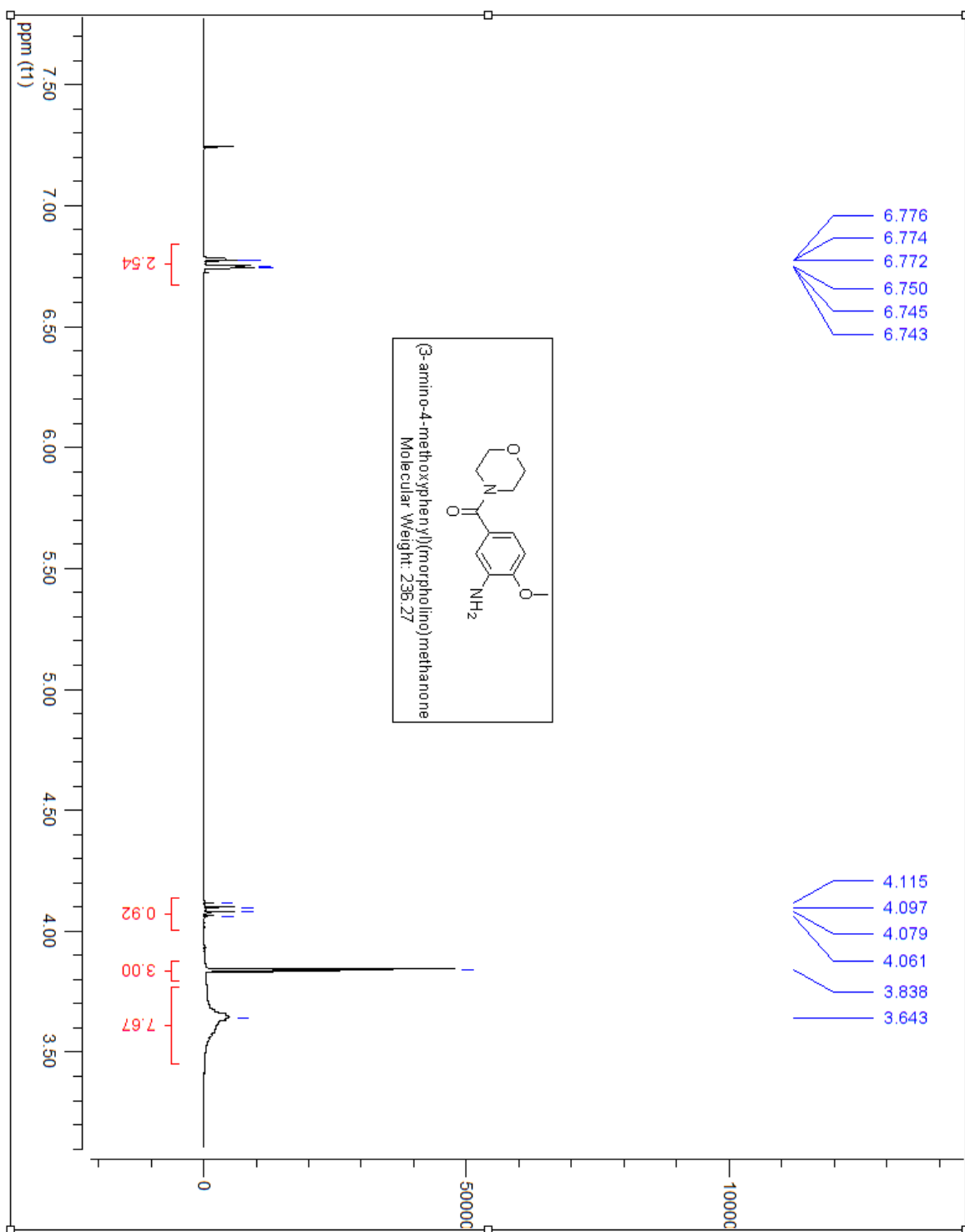
Chemical Formula:  $C_{12}H_{16}N_2O_3$

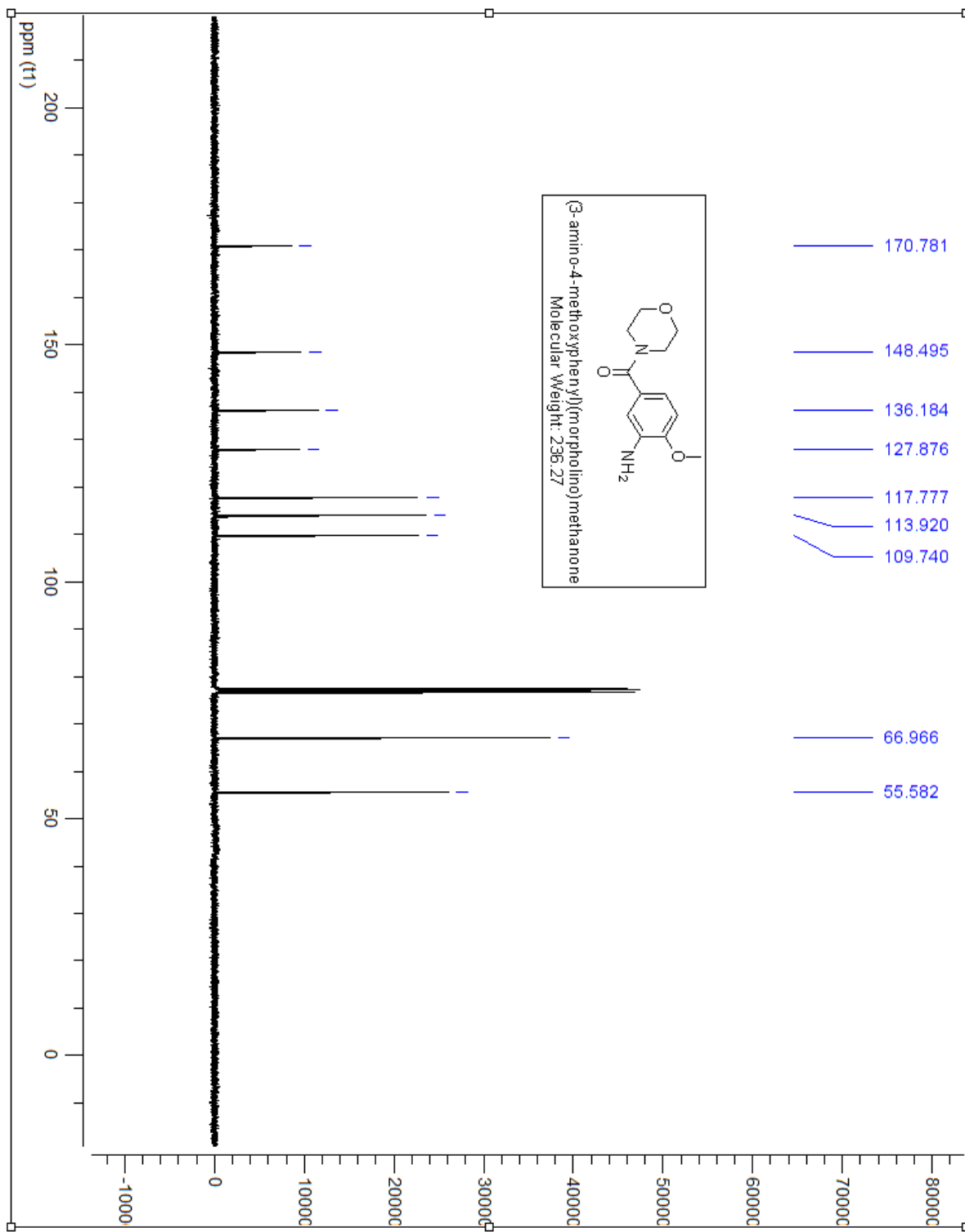
Molecular Weight: 236.27

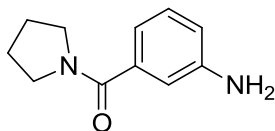
4-methoxy-3-aminobenzoic acid (2.1g, 12.7mmol) was added to DCM (15ml) followed by the addition of triethylamine (3.2ml, 23mmol) in a round bottom flask. EDCI.HCL (3.3g, 17.3mmol) was added to the reaction and the solution was allowed to stir for 40 minutes. Morpholine (1.0ml, 11.5mmol) was added to the reaction flask and allowed to stir at room temperature for 24 hours.  $NaHCO_3$  was added to quench the reaction followed by extraction with DCM (20ml x 3 times). The organic layers were collected and dried using  $MgSO_4$ . The mixture was filtered and concentrated in *vacuo*. The product was purified through column chromatography to form white crystals (1.6g, 44%)

$^1H$  NMR (400MHz,  $CDCl_3$ )  $\delta$  ppm) 6.77-6.74 (m, 3H), 3.83 (s, 3H), 3.64 (s, 8H), 2.01 (s, 1H), 1.24-1.21 (t, 1H)

$^{13}C$  NMR (400MHz,  $CDCl_3$ )  $\delta$  ppm) 170.781, 148.495, 136.184, 127.876, 117.777, 113.920, 109.740, 66.966, 55.582







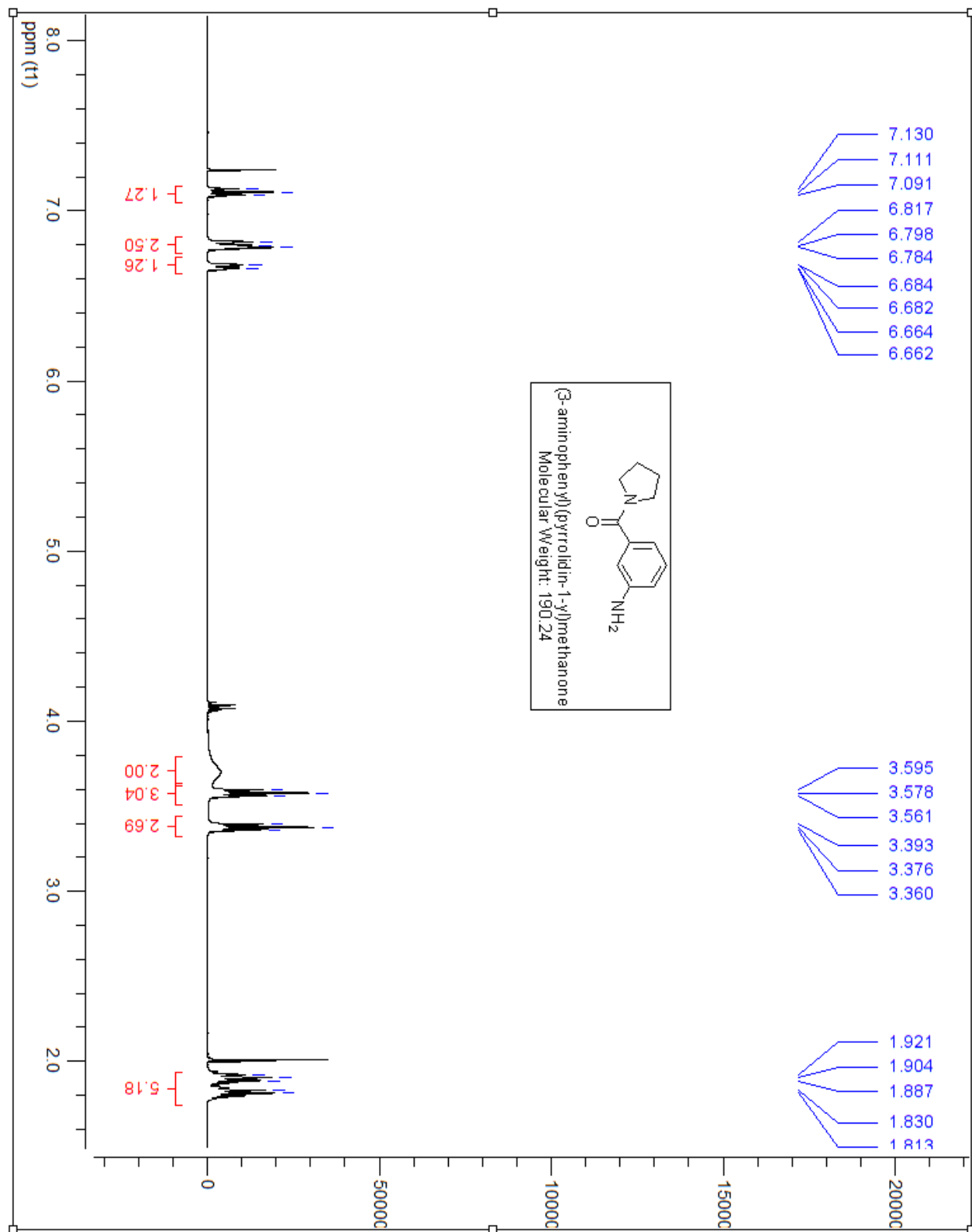
Chemical Formula: C<sub>11</sub>H<sub>14</sub>N<sub>2</sub>O

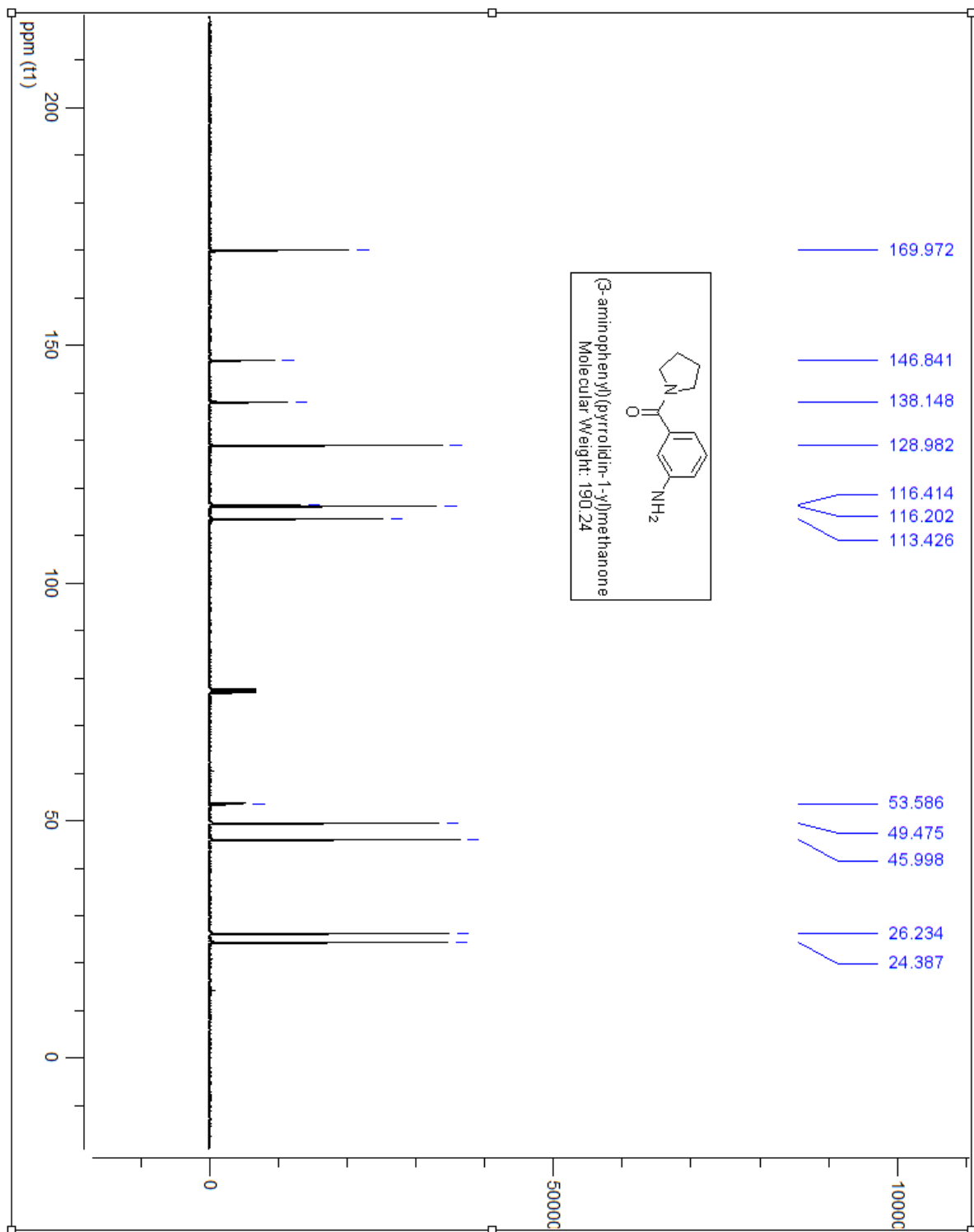
Molecular Weight: 190.24

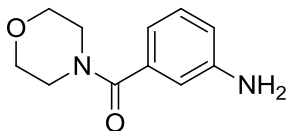
3-aminobenzoic acid (1g, 7.99mmol) was added to DCM (15ml) followed by the addition of triethylamine (4.06ml, 29.16mmol) in a round bottom flask. EDCI.HCL (1.82g, 9.47mmol) was added to the reaction and the solution was allowed to stir for 40 minutes. Pyrrolidine (0.53ml, 6.56mmol) was added to the reaction flask and allowed to stir at room temperature for 24 hours. NaHCO<sub>3</sub> was added to quench the reaction followed by extraction with DCM (20ml x 3 times). The organic layers were collected and dried using MgSO<sub>4</sub>. The mixture was filtered and concentrated in *vacuo*. The product was purified through column chromatography to form clear oil (0.645g, 57.1%)

<sup>1</sup>H NMR (400MHz, CDCl<sub>3</sub>) δ ppm 7.13-7.09 (t, 1H), 6.81-6.68 (m, 2H), 6.66-6.65 (d, 1H), 3.71-3.69 (s, 1H), 3.59-3.56 (t, 2H), 3.39-3.36 (t, 2H)

<sup>13</sup>C NMR (400MHz, CDCl<sub>3</sub>) δ ppm 169.972, 146.841, 138.148, 128.982, 116.414, 116.202, 113.428, 53.586, 49.475, 45.998, 26.234, 24.387





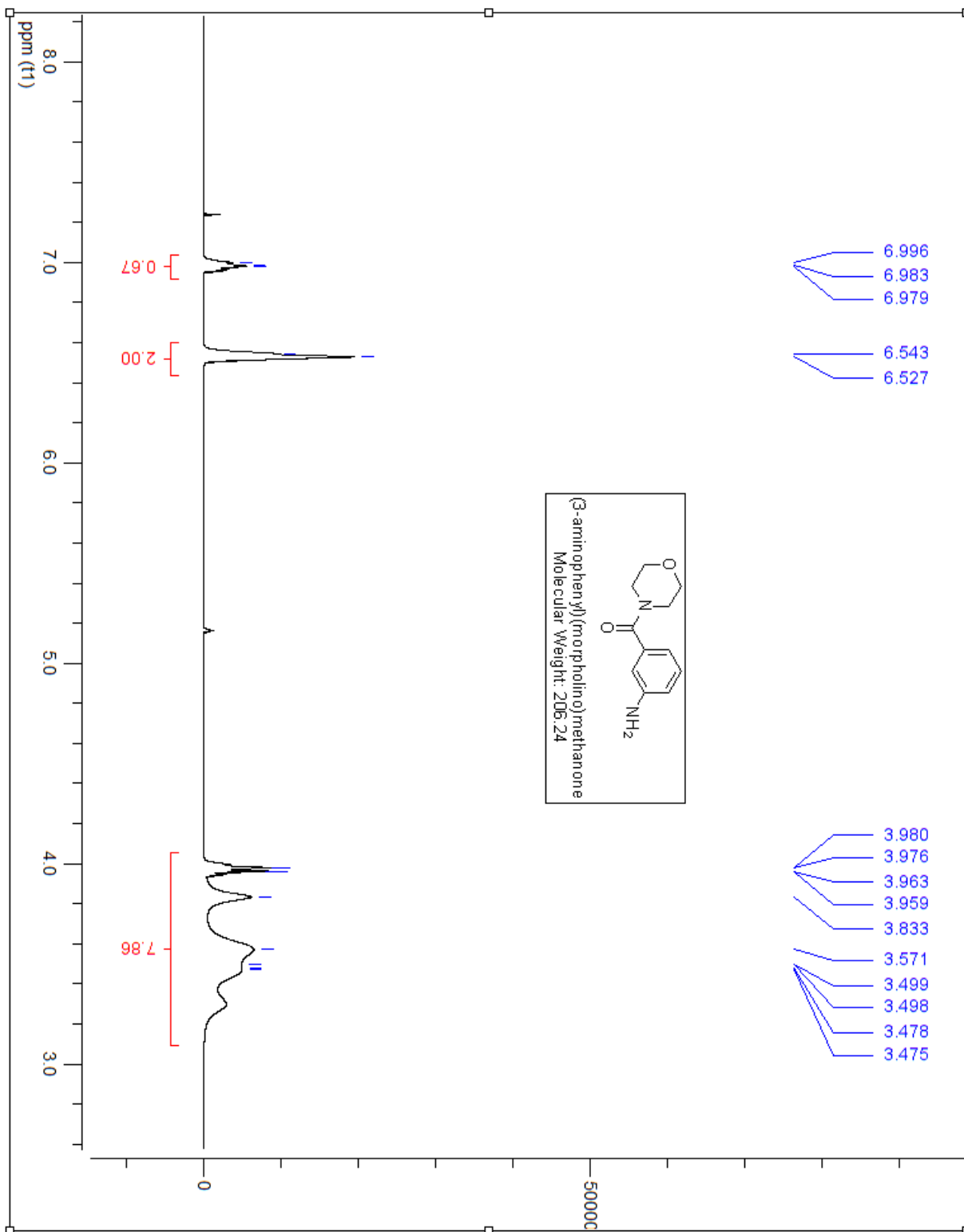


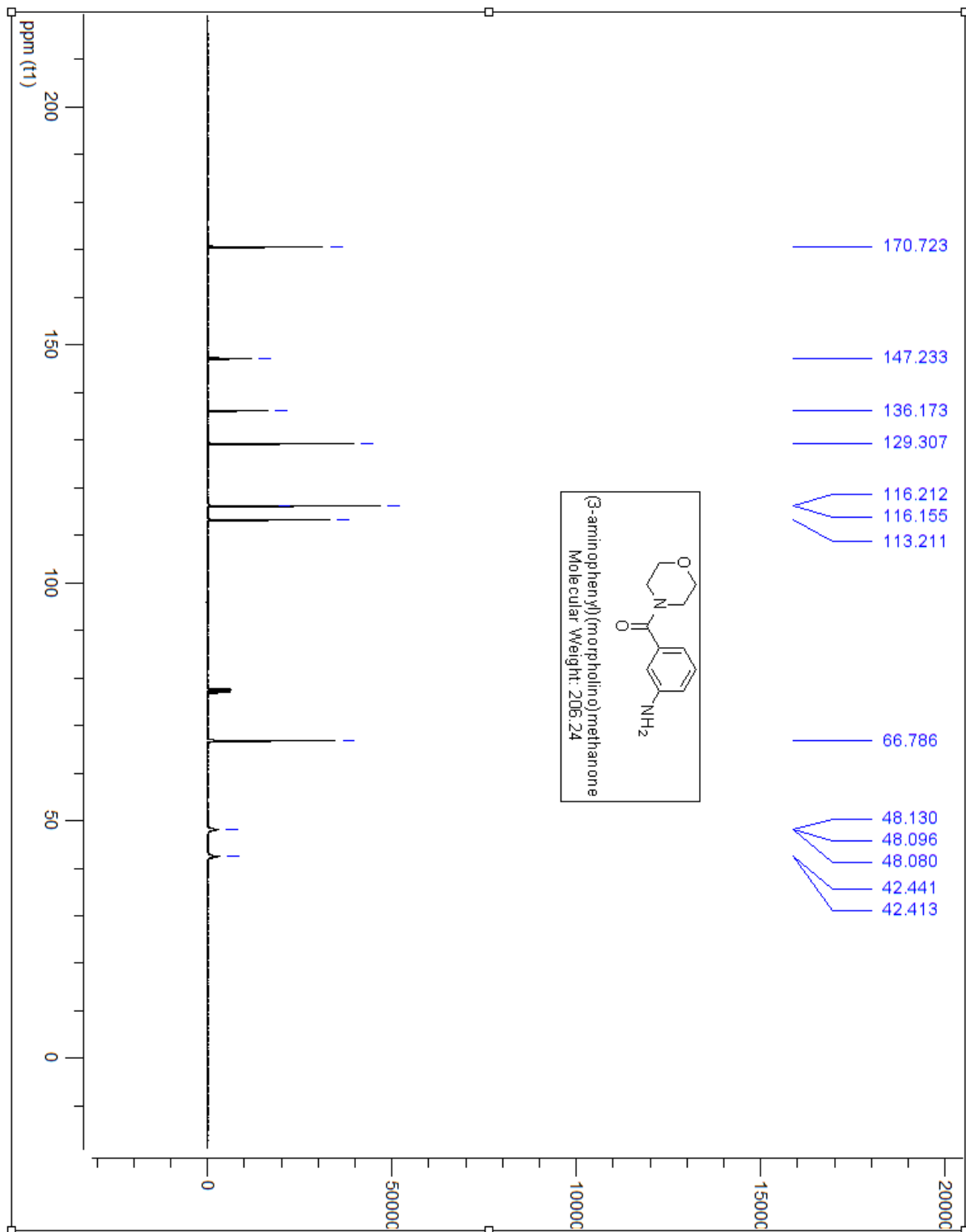
Chemical Formula: C<sub>11</sub>H<sub>14</sub>N<sub>2</sub>O<sub>2</sub>  
Molecular Weight: 206.24

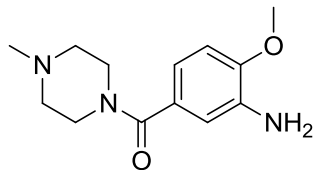
3-aminobenzoic acid (1g, 7.29mmol) was added to DCM (15ml) followed by the addition of triethylamine (3ml, 21.8mmol) in a round bottom flask. EDCI.HCL (1.7g, 10.2mmol) was added to the reaction and the solution was allowed to stir for 40 minutes. Morpholine (0.57ml, 26.6mmol) was added to the reaction flask and allowed to stir at room temperature for 24 hours. NaHCO<sub>3</sub> was added to quench the reaction followed by extraction with DCM (20ml x 3 times). The organic layers were collected and dried using MgSO<sub>4</sub>. The mixture was filtered and concentrated in *vacuo*. The product was purified through column chromatography to form white crystals (1.1g, 73%)

<sup>1</sup>H NMR (400MHz, CDCl<sub>3</sub>) δ ppm) 6.54-6.52 (s, 3H), 3.83 (s, 2H), 3.57-3.29 (m, 8H)

<sup>13</sup>C NMR (400MHz, CDCl<sub>3</sub>) δ ppm) 170.723, 147.233, 136.173, 129.307, 116.212, 116.155, 113.211, 66.786, 48.130, 48.096, 48.080, 42.441, 42.413







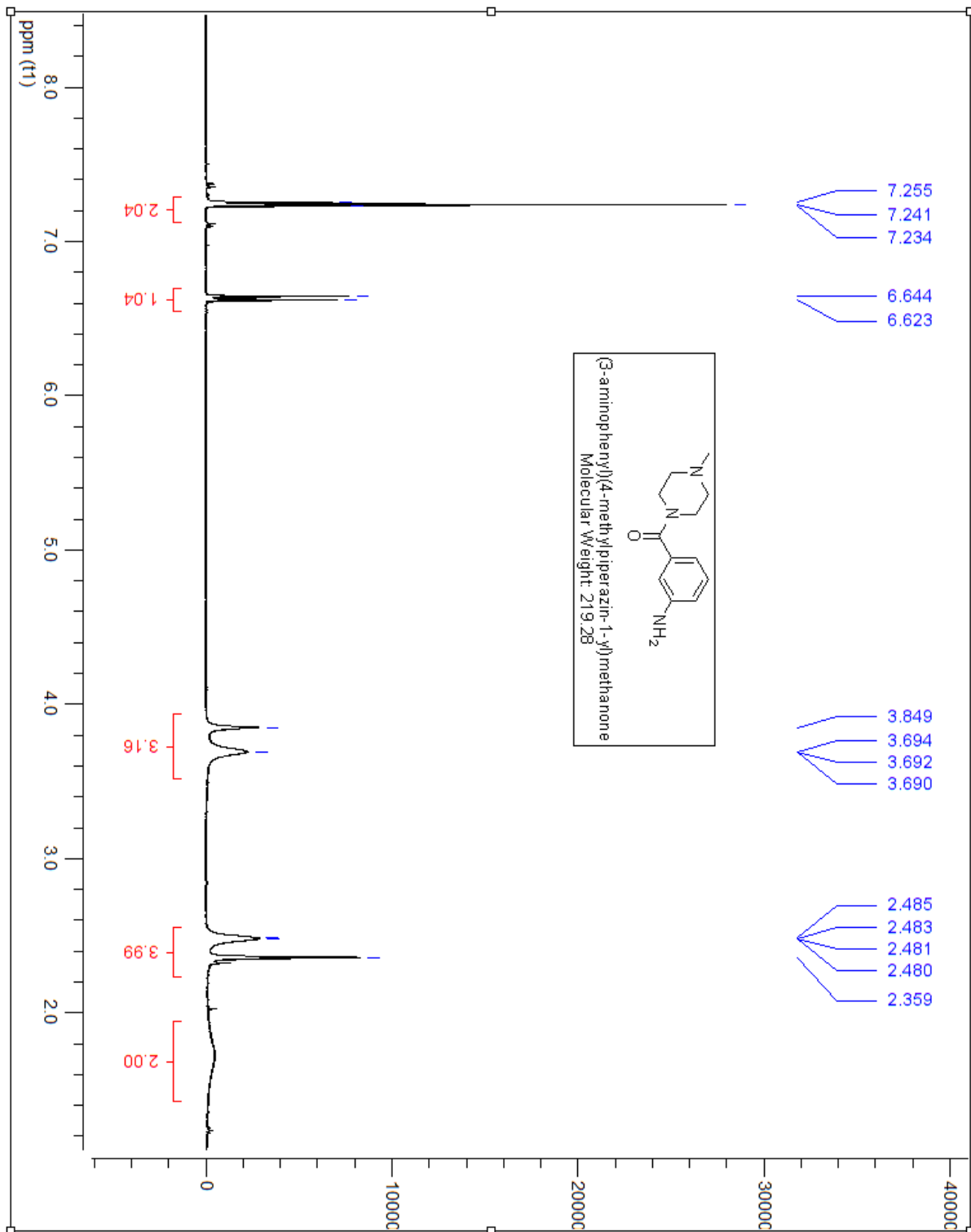
Chemical Formula:  $C_{13}H_{19}N_3O_2$

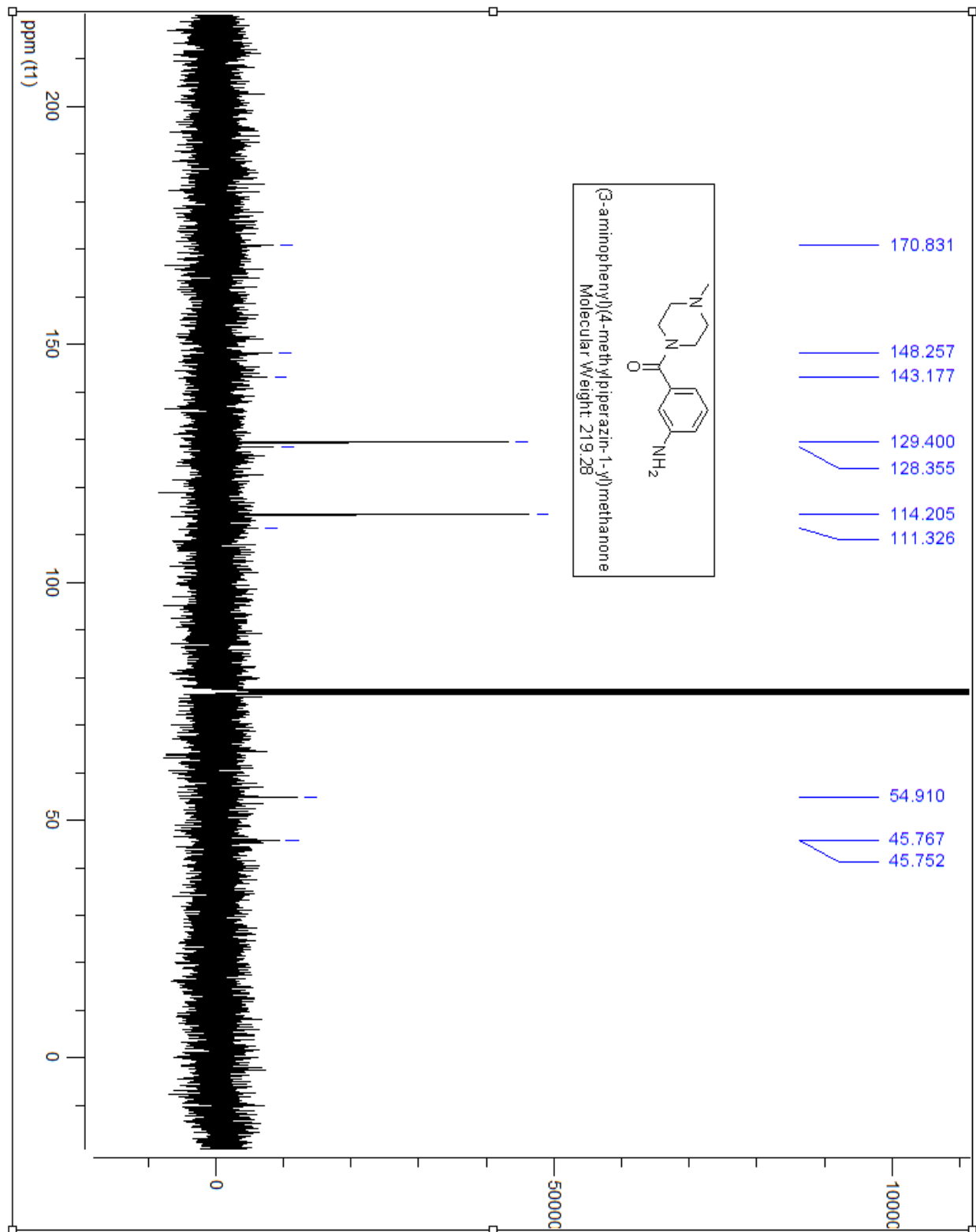
Molecular Weight: 249.31

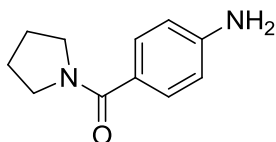
4-methoxy-3-aminobenzoic acid (1g, 5.98mmol) was added to DCM (15ml) followed by the addition of triethylamine (3.34ml, 23.93mmol) in a round bottom flask. EDCI.HCL (1.7g, 8.97mmol) was added to the reaction and the solution was allowed to stir for 40 minutes. 1-methylpiperazine (0.60ml, 5.38mmol) was added to the reaction flask and allowed to stir at room temperature for 24 hours.  $NaHCO_3$  was added to quench the reaction followed by extraction with DCM (20ml x 3 times). The organic layers were collected and dried using  $MgSO_4$ . The mixture was filtered and concentrated *in vacuo*. The product was purified through column chromatography to form beige crystals (554mg, 42.6%)

$^1H$  NMR (400MHz,  $CDCl_3$ )  $\delta$  ppm 6.63-6.60 (m, 3H), 3.85 (m, 2H), 3.73-3.7 (m, 3H), 3.51-3.48 (m, 4H), 3.26-3.25 (m, 1H), 2.26 (s, 3H), 2.18-2.17 (m, 3H)

$^{13}C$  NMR (400MHz,  $CDCl_3$ )  $\delta$  ppm 170/83, 148.25, 143.17, 129.40, 128.35, 114.21, 111.32, 54.91, 45.76, 45.75







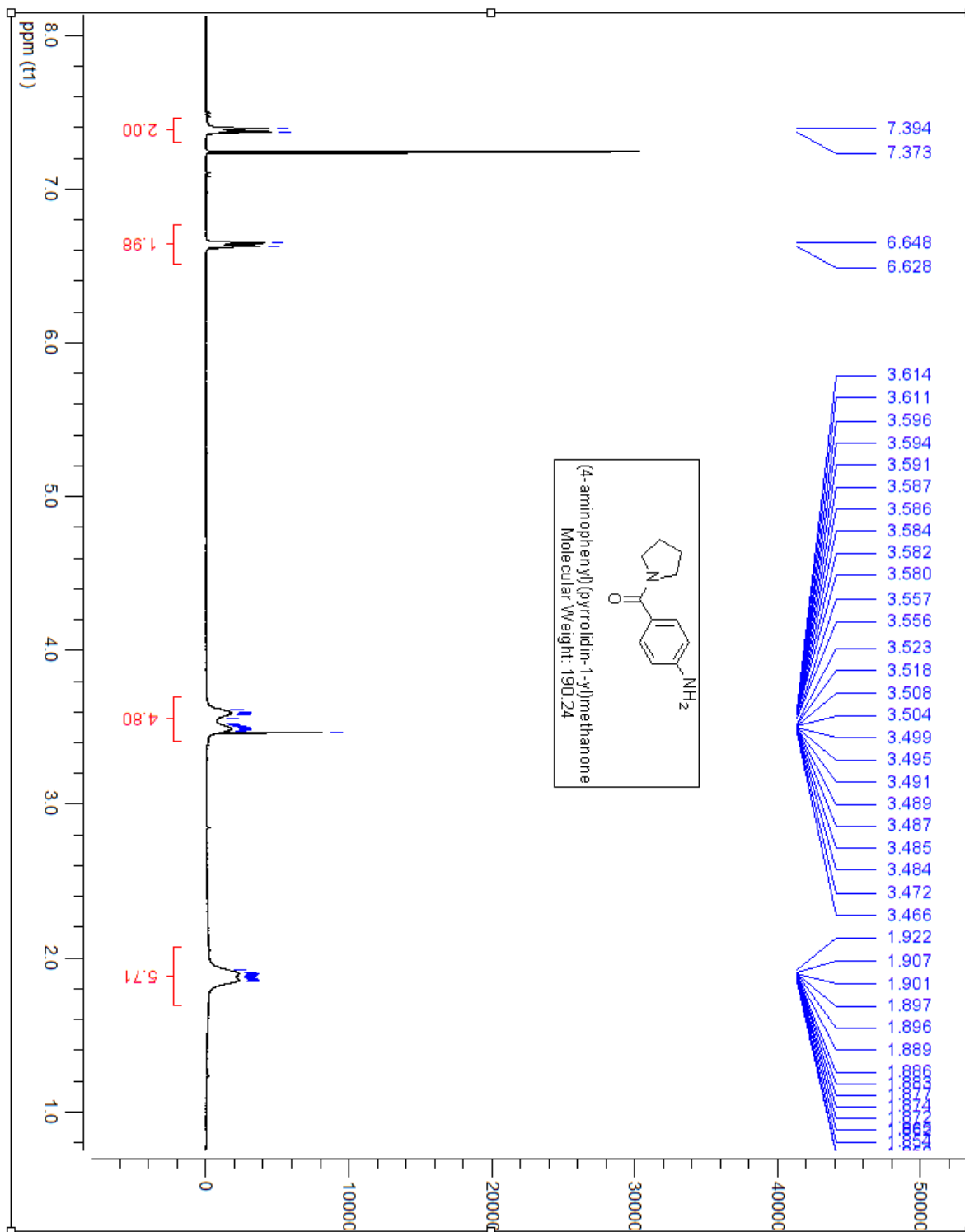
Chemical Formula: C<sub>11</sub>H<sub>14</sub>N<sub>2</sub>O

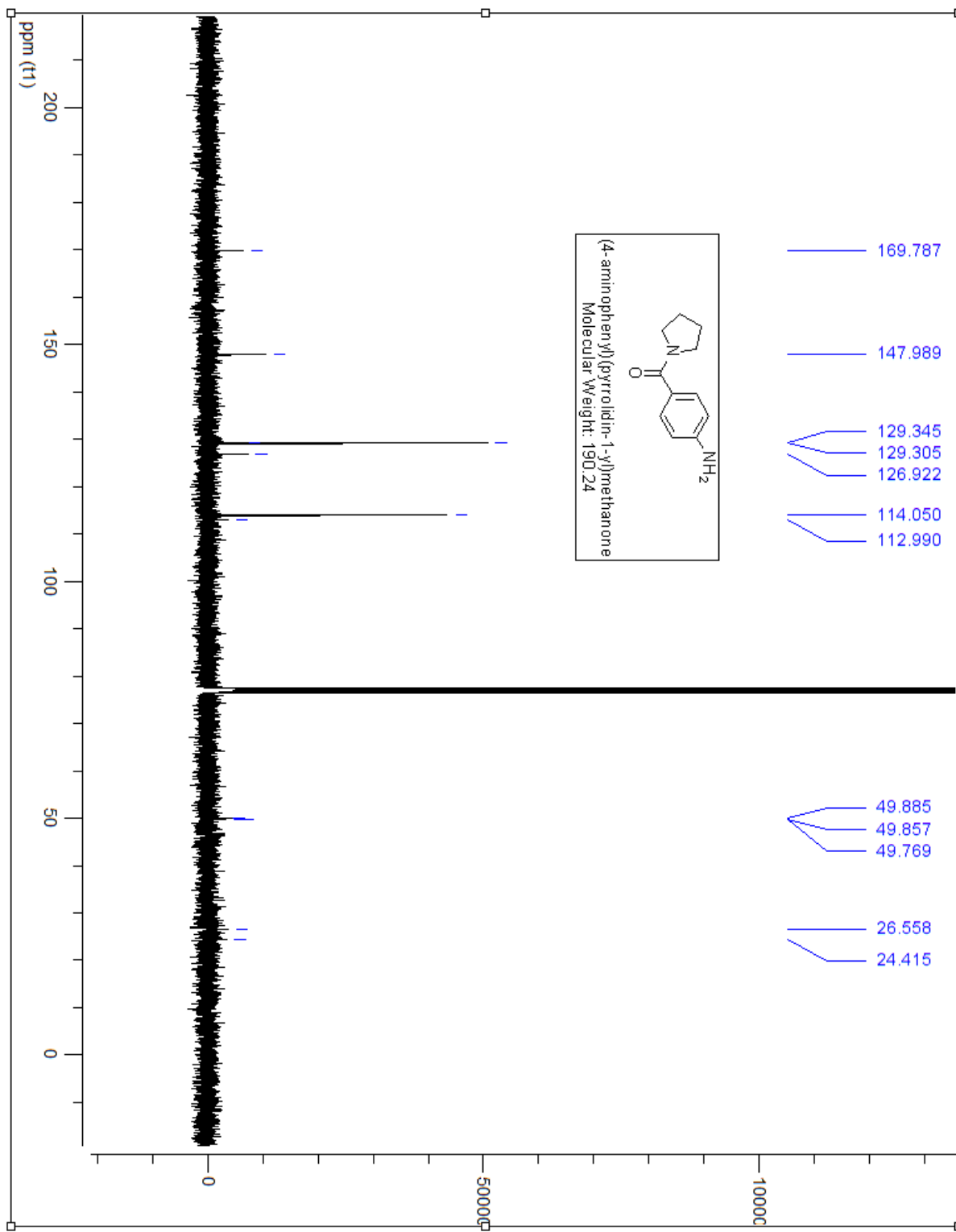
Molecular Weight: 190.24

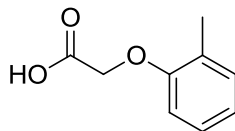
4-aminobenzoic acid (1g, 7.99mmol) was added to DCM (15ml) followed by the addition of triethylamine (4.06ml, 29.16mmol) in a round bottom flask. EDCI.HCL (1.82g, 9.47mmol) was added to the reaction and the solution was allowed to stir for 40 minutes. Pyrrolidine (0.53ml, 6.56mmol) was added to the reaction flask and allowed to stir at room temperature for 24 hours. NaHCO<sub>3</sub> was added to quench the reaction followed by extraction with DCM (20ml x 3 times). The organic layers were collected and dried using MgSO<sub>4</sub>. The mixture was filtered and concentrated in *vacuo*. The product was purified through column chromatography to form clear oil (0.645g, 57.1%)

<sup>1</sup>H NMR (400MHz, CDCl<sub>3</sub>) δ ppm 7.13-7.09 (t, 1H), 6.81-6.68 (m, 2H), 6.66-6.65 (d, 1H), 3.71-3.69 (s, 1H), 3.59-3.56 (t, 2H), 3.39-3.36 (t, 2H)

<sup>13</sup>C NMR (400MHz, CDCl<sub>3</sub>) δ ppm 169.972, 146.841, 138.148, 128.982, 116.414, 116.202, 113.428, 53.586, 49.475, 45.998, 26.234, 24.387





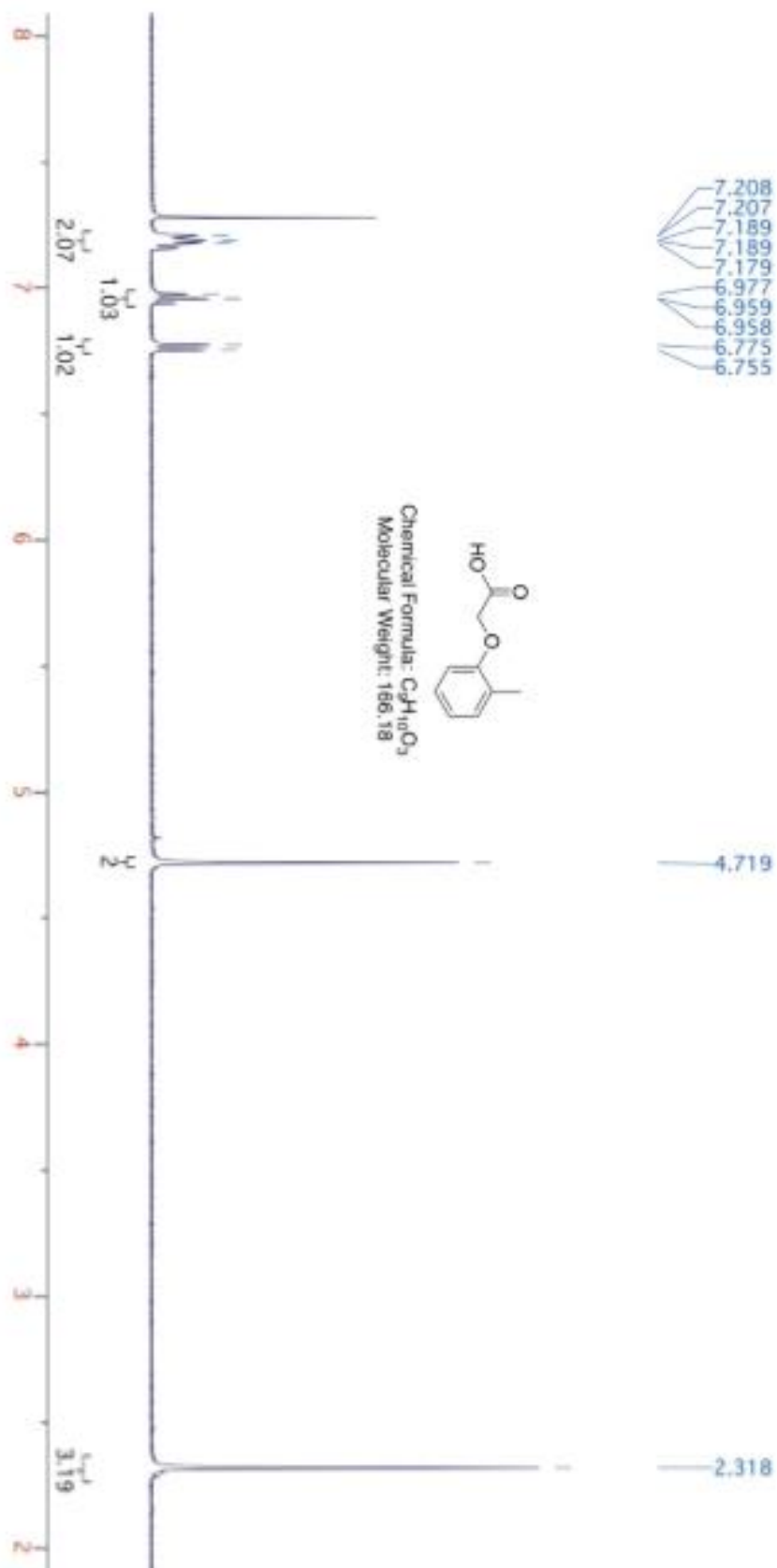


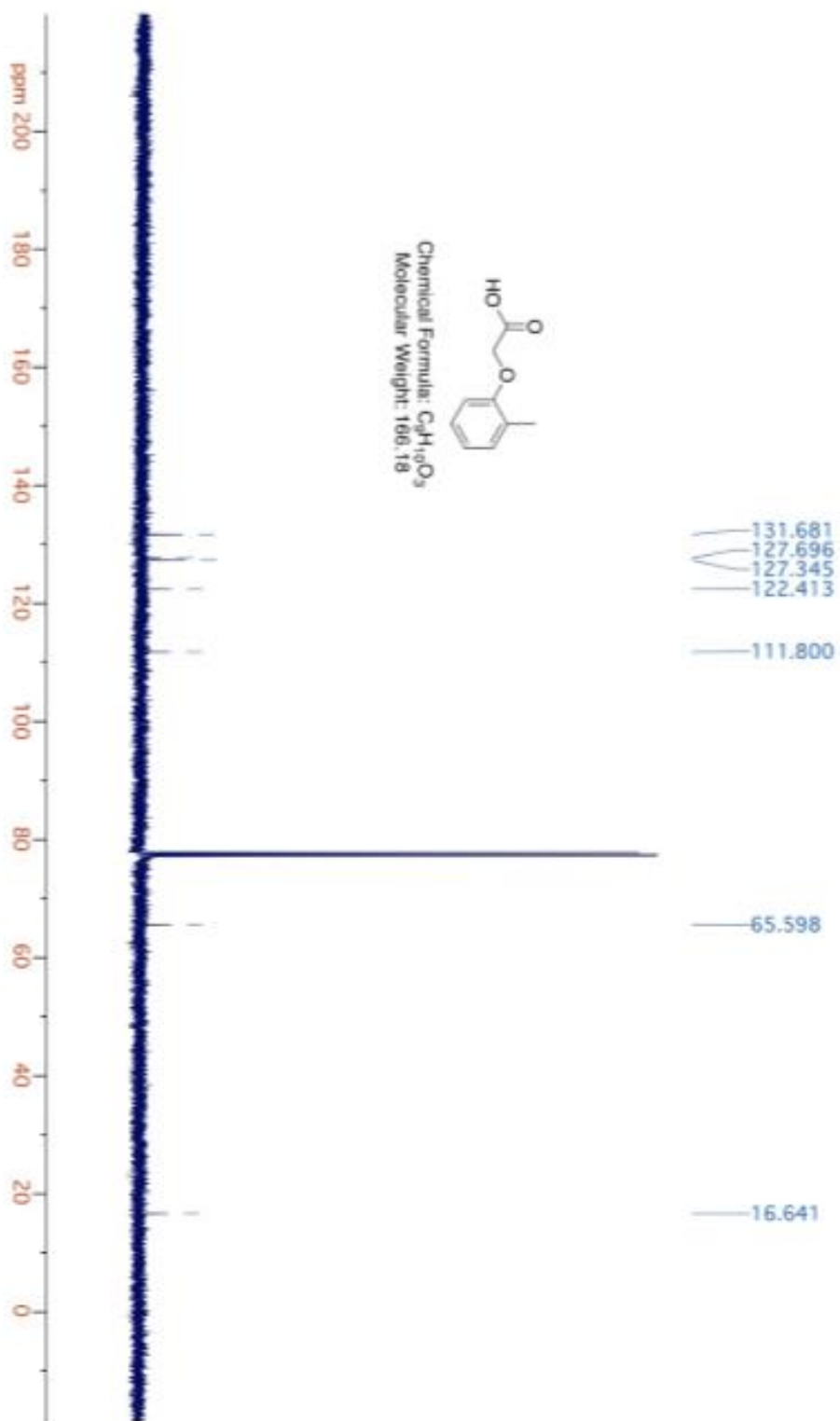
Chemical Formula:  $C_9H_{10}O_3$   
Molecular Weight: 166.17

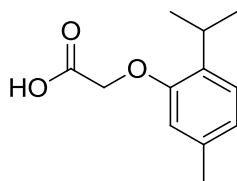
This compound was prepared following general procedure 3 using *o*-cresol (14.3g, 133 mmol), chloroacetic acid (11.5g, 121 mmol), and NaOH (14.5 g, 364 mmol) in distilled H<sub>2</sub>O (50 mL). Crude product (7 g) was purified by recrystallization using EtOAc and hexanes resulting in 2-(*o*-tolylloxy)acetic acid, a white powder (3 g, 15%, R<sub>f</sub> = 0.6 in 3:2 Hexanes : EtOAc).

<sup>1</sup>H NMR (400 MHz; CDCl<sub>3</sub>): δ 7.21-7.18 (m, 2H), 6.98-6.96 (t, J=7.2, 1H), 6.76 (d, J = 8.0, 1H), 4.72 (s, 2H), 2.32 (s, 3H)

<sup>13</sup>C NMR: (400 MHz; CDCl<sub>3</sub>): δ 131.68, 127.69, 127.35, 122.41, 111.80, 65.59, 16.64







Chemical Formula: C<sub>12</sub>H<sub>16</sub>O<sub>3</sub>

Molecular Weight: 208.25

This compound was prepared following general procedure 3 using Thymol (34.9 g, 232.8 mmol), chloroacetic acid (20 g, 211.7 mmol), and NaOH (25.4 g, 635 mmol) in distilled H<sub>2</sub>O (75 mL). No purification was required for this reaction. Pure product, 2-(2-isopropyl-5methylphenoxy)acetic acid, a beige powder (14.23 g, 32%, R<sub>f</sub> = 0.57 in 3:2 EtOAc : Hexanes).

<sup>1</sup>H NMR (400 MHz; CDCl<sub>3</sub>): δ 7.15 (d, J = 7.7, 1H), 6.83 (d, J = 7.7, 1H), 6.58 (s, 1H), 4.70 (s, 2H), 3.36 (t, J = 6.9, 1H), 2.33 (s, 3H), 1.24 (d, J = 6.9, 6H)

<sup>13</sup>C NMR: (400 MHz; CDCl<sub>3</sub>): δ 174.85, 155.01, 136.91, 135.01, 126.85, 123.12, 112.84, 65.63, 27.03, 23.25, 21.74

